Starch Metabolism in Guard Cells of *Arabidopsis thaliana*

Dissertation

zur
Erlangung der naturwissenschaftlichen Doktorwürde
(Dr. sc. nat.)

vorgelegt der
Mathematisch-naturwissenschaftlichen Fakultät
der
Universität Zürich
von

Daniel Horrer

aus
Deutschland

Promotionskomitee

Prof. Dr. Enrico Martinoia (Vorsitz)
Dr. Diana Santelia (Leitung der Dissertation)
Prof. Dr. Beat Keller
Prof. Dr. Samuel C. Zeeman

Zürich, 2016

ABSTRACT

In order to survive on land, plants evolved a diverse set of adaptations to limit water loss through transpiration. At the same time, they need to take up CO_2 for photosynthetic carbon assimilation. These two conflicting requirements for optimal plant growth are controlled through pores on the leaf surface, the stomata, which are lined by two kidney-shaped cells. These highly specialised guard cells control stomatal aperture through changes in their osmotic potential. For a long time, research primarily focused on the accumulation of potassium through the uptake from the guard cell apoplast as the primary mechanism for increasing osmolyte concentrations, ultimately leading to the opening of the stomatal pore. Although an influence of guard cell carbon metabolism and especially early morning starch breakdown for stomatal control was proposed, up until now no clear consensus or detailed insights into the relative role of starch degradation were reached. This was partially due to the lack of appropriate experimental tools, especially for guard cell starch quantification in Arabidopsis, where many genetic resources to advance our understanding of stomatal physiology are available.

In order to overcome this limitation, we initially established a new method for the precise quantification of guard cell starch content in Arabidopsis, based on confocal laser scanning microscopy of propidium iodide stained epidermal peels. This breakthrough enabled us to describe the distinct pathway of starch degradation in guard cells, including two enzymes, the β-AMYLASE1 (BAM1) and the α-AMYLASE3 (AMY3), which are usually not considered to play a major role in starch breakdown in mesophyll cells. The *amy3bam1* double mutant was unable to degrade starch in response to blue light, which led to severely impaired stomatal opening and reduced biomass accumulation. We could furthermore show that early morning breakdown of starch reserves is induced by the blue light-dependent activation of plasma membrane proton pumps. In summary, the first part of this thesis showed the importance of starch metabolism for stomatal regulation, which will inspire a more detailed analysis of guard cell carbon metabolism in general.

Furthermore, we were able to describe a role for BAM1 and AMY3 in the degradation of mesophyll cell starch reserves in response to osmotic stress. Hydroponically grown plants treated with mannitol showed an ABA-dependent induction of BAM1 transcription mediated by the ABA-RESPONSIVE ELEMENT BINDING (AREB) transcription factors. The subsequent starch degradation and carbon reallocation

leads to the accumulation of osmotic substances in the root, counteracting the effect of the high extracellular osmolyte concentration.

In order to better understand the regulation of BAM1, which acquired specific functions in starch metabolism distinct from night-time starch degradation in mesophyll cells, we focused on posttranslational protein phosphorylation as a possible regulatory mechanism. We could show that BAM1 is phosphorylated at three specific serine residues and that the GSK3-like kinase AtK4 is able to catalyse one of these modifications *in vitro*. Although preliminary, these results are a promising first step in elucidating the network underlying the control of BAM1 regulation.

Finally, we were able to gain first insights into the mechanism of guard cell starch synthesis. Here we show that glucose-6-phosphate (Glc6P) import into guard cell chloroplasts through the Glc6P/PHOSPHATE TRANSLOCATOR 1 (GPT1) is important for the accumulation of wild type starch levels, while guard cell photosynthesis seems to play only a minor, although still significant role in supplying sugars for starch synthesis. Furthermore, we suggest a specific role for the APL3 and APL4 subunits of the ADP-GLUCOSE PYROPHOSPHORYLASE (AGPase) enzyme, which catalyses the first committed step in the synthesis of the glucosyl-donor ADP-Glc and therefore controls the rate of starch synthesis.

Taken together, the data presented in this thesis extends our knowledge of starch metabolism in guard cells and provides novel insights into the specific roles and the regulation of BAM1 in both guard and mesophyll cells.

ZUSAMMENFASSUNG

Um an Land überleben zu können, entwickelten Pflanzen im Laufe der Evolution eine Vielzahl verschiedener Anpassungen, um den Verlust von Wasser durch Transpiration an der Blattoberfläche zu minimieren. Gleichzeitig sind Pflanzen darauf angewiesen Kohlenstoffdioxid (CO_2) für die CO_2-Assimilation in der Fotosynthese über die Blätter aufzunehmen. Die Balance zwischen Wasserverlust und CO_2-Aufnahme, die Voraussetzung für optimales Pflanzenwachstum ist, wird durch Poren (Stomata) auf der Blattoberfläche geregelt, die von zwei nierenförmigen Zellen begrenzt werden. Diese hochspezialisierten Schließzellen kontrollieren die Öffnungsweite der Stomata durch Veränderungen des osmotischen Potenzials. Für lange Zeit konzentrierte sich die Forschung auf die Anreicherung von Kalium, welches aus dem Interzellularraum aufgenommen wird. Durch diese Erhöhung des osmotischen Potenzials und der damit verbundenen Aufnahme von Wasser, kommt es zum Anschwellen der Schließzellen und somit zu einer Öffnung der Stomata. In vielen Publikationen wurde ein Einfluss des Kohlenstoffmetabolismus und insbesondere des Stärkeabbaus am frühen Morgen auf die Regulation der Stomata postuliert. Dennoch konnte bisher weder ein Konsens über die Bedeutung des Kohlestoffwechsels noch eine detaillierte molekulare Beschreibung desselben erarbeitet werden. Dies ist teilweise auf fehlende Methoden zurückzuführen, die es erlaubt hätten die Vielzahl der genetischen Ressourcen der Modellpflanze Arabidopsis zu nutzen, um unser Verständnis der Schließzellen-Physiologie zu erweitern.

Um diese Einschränkung zu umgehen, wurde zunächst eine neue Methode für die präzise Quantifizierung der Stärke in Arabidopsis Schließzellen entwickelt, die auf der konfokalen Laser-Mikroskopie von mit Propidium-Iodid gefärbten, epidermalen Zellschichten beruht. Dieser methodische Durchbruch erlaubte es uns anschließend den spezialisierten Abbauweg der Stärke in den Schließzellen zu beschreiben, der insbesondere zwei Amylasen, die β-AMYLASE1 (BAM1) und die α-AMYLASE3 (AMY3), einschließt, die unter normalen Wachstumsbedingungen nicht am Stärkeabbau in Mesophyllzellen beteiligt sind. Pflanzen, denen diese beiden Amylasen fehlen, können ihre Schließzell-Stärke nicht mehr abbauen, was zu einer drastischen Reduktion der Stomata-Öffnung und zu einem verringerten Wachstum führt. Weiterhin konnten wir zeigen, dass der Stärkeabbau in diesen Zellen durch die blaulichtinduzierte Aktivierung von plasmamembranständigen Protonenpumpen

kontrolliert wird. Insgesamt zeigt dieser erste Teil der vorliegenden Arbeit die Bedeutung des Stärkemetabolismus für die Regulation der Spaltöffnungen und wird zu weiteren, detaillierten Analysen des gesamten Schließzellenmetabolismus führen.
Darüber hinaus konnten wir zeigen, dass BAM1 und AMY3 eine wichtige Rolle im Stärkeabbau unter osmotischen Stressbedingungen in den Mesophyllzellen spielen. In Hydrokultur angezogene Pflanzen, die durch Mannitol-Applikation einem osmotischen Stress ausgesetzt wurden, zeigen eine Induktion der Transkription des *BAM1* Gens. Dies beruht auf der durch erhöhte ABA Konzentrationen ausgelösten Aktivierung von ABA-RESPONSIVE ELEMENT BINDING (AREB) Transkriptionsfaktoren. Der daraus folgende Stärkeabbau und die Umverteilung von Kohlenstoffverbindungen führt zur Anreicherung von osmotisch aktiven Substanzen in den Wurzeln. Dies wirkt der hohen extrazellulären Konzentration an Osmolyten entgegen.
Um nun die Regulation von BAM1 in diesen speziellen Fällen besser zu verstehen, haben wir in einem weiteren Schritt die Möglichkeit der posttranslationalen Proteinphosphorylierung dieser Amylase untersucht. Dabei konnten wir zeigen, dass BAM1 an drei spezifischen Serinen phosphoryliert wird und AtK4, eine Kinase der GSK3 Familie, für eine dieser Modifikationen *in vitro* verantwortlich ist. Zwar sind dies erst vorläufige Ergebnisse, aber sie bilden einen vielversprechenden ersten Schritt zur Aufklärung der Kontrollmechanismen, die der Regulation von BAM1 zugrunde liegen.
In einem letzten Teil konnten wir erste Einblicke in die Mechanismen der Schließzellen-Stärkesynthese gewinnen. Hier konnten wir zeigen, dass der Import von Glucose-6-Phosphat (Glc6P) in die Chloroplasten dieser Zellen durch den Glc6P/PHOSPHAT TRANSLOCATOR 1 (GPT1) wichtig für die Akkumulation von Stärke ist. Dagegen spielt die Fotosynthese in diesen Zellen eine untergeordnete, wenn auch immer noch signifikante Rolle, bei der Bereitstellung von Zuckern für die Synthese von Stärke. Des weiteren implizieren unsere Ergebnisse eine spezifische Rolle für die APL3 und APL4 Untereinheiten der ADP-GLUCOSE PYROPHOSPHORYLASE (AGPase). Dieses Enzym, welches die Bildung von ADP-Glucose katalysiert, reguliert zu einem großen Teil die Biosyntheserate von Stärke.

Insgesamt können die Daten, die in dieser Arbeit präsentiert werden, unser Verständnis des Stärkemetabolismus in den Schließzellen deutlich erweitern. Zusätzlich konnten neue Erkenntnisse über die spezifischen Funktionen, sowie über die Regulation des BAM1 Enzyms gewonnen werden.

TABLE OF CONTENT

INTRODUCTION

Context of this thesis

The increasing world population required and continues to require an increase in food production. The industrial revolution during the 18th and 19th century and the "Green Revolution" of the 20th century provided a massive increase in agricultural productivity. Despite the progress made towards food security, one in eight people are still undernourished and many more suffer from micronutrient deficiencies (Food and Agricultural Organization of the United Nations, 2013). With the world population predicted to reach a plateau at 9 to 10 billion people by the end of this century, further increase in food production will be necessary, although it will be much more difficult to achieve it than it has been in the past (Godfray et al., 2010). Recent progress relied mainly on the increased use of non-renewable resources, primarily land, water and energy (Morison et al., 2008). This intensification of agriculture can hardly be sustained given our limited resources and several interconnected challenges. Human activities and unsustainable agricultural production system lead to a net loss of arable land (e.g. urbanization, desertification). The increase in the production of first generation biofuels in some regions added pressure on food security and caused a rise in world market prices, while the transfer of natural ecosystems into agricultural land (e.g. the Amazonian rainforest) faces increasing opposition from society, insisting on the preservation of biodiversity and other natural resources. On top of these challenges, the predicted impact of climate change will make it even more difficult to reach the estimated requirement of increasing food production between 70% and 100% by 2050 (World Bank, 2008; Intergovernmental Panel on Climate Change, 2007).

The term coined "sustainable intensification" describes a model by which the crop yield per ha is increased through an optimized use of inputs, while negative influences are reduced (Godfray et al., 2010). One important factor for this precision agriculture is the use of crop plants well adapted to the climatic conditions of a certain region, which show high water- and nutrient- use efficiencies, while being able to withstand abiotic and biotic stresses (such as fungal diseases, drought conditions and high salinity of the soil). This will allow high biomass production also under unfavourable growth conditions. Therefore, a deeper understanding of plant

physiology will help to push production limits, through the identification of new targets for modern breeding approaches. This will include not only the exploitation of the natural genetic diversity of todays most important crop plants, but it will also involve genetically modified varieties at least where these are socially accepted, ultimately leading to an improved combination of traits.

Guard Cell Function and Regulation

Guard cells regulate transpiration and CO_2 uptake

Terrestrial plants take up water and nutrients from the soil and transport them via the xylem to the aboveground organs using an evapotranspiration stream. Because in most ecosystems water is the limiting determinant of growth (Boyer, 1982), the resulting loss of water needs to be minimized, while at the same time CO_2 uptake into the leaf is necessary for photosynthesis. One main target of modern breeding approaches is the water use efficiency (WUE), describing the amount of fixed carbon per unit of water lost through transpiration (Morison et al., 2008; Lawson and Blatt, 2014). Water loss through the epidermal cells is prevented by a layer of epicular waxes called the cuticle, while gas exchange is possible through the stomata, a pore in the leaf epidermis surrounded by a pair of guard cells. In contrast to the dumb-bell shaped guard cells of grasses, the Greek term stoma – meaning “mouth” – fits well to describe the stomata of dicot plant species (Franks and Farquhar, 2006).

The stomatal apparatus is present in the fossil record of mosses and hornworts, already resembling the higher plant stomata. These specialized cells are estimated to have been evolved from a single origin around 400 mio years ago (Edwards et al., 1998; Vatén and Bergmann, 2013). With the exception of petals and stamen filaments, aboveground plant tissues contain guard cells. Although more guard cells are found on the abaxial (lower) epidermis, they are also present on the adaxial (upper) epidermis of the leaves. During development several asymmetric and a final symmetric division of precursor cells give rise to the guard cell pair surrounding the stomatal pore (Pillitteri and Dong, 2013).

Guard cells need to rapidly respond to changes in the environment in order to prevent damage to the plant through abiotic and biotic stresses. Plants are generally considered to open their stomata under illumination and close them in response to high ambient CO_2 concentrations and under adverse environmental conditions (Vavasseur and Raghavendra, 2005; Shimazaki et al., 2007; Lawson, 2009), but several species evolved a divers set of adaptations in the way they regulate stomatal

aperture. One notable example is the difference between Crassulacean acid metabolic (CAM) plants, which open their stomata only in the dark, while C_3 and C_4 photosynthetic plants, including the C_3 plant *Arabidopsis thaliana*, open their stomata in the light and keep them closed during the night (Lüttge, 2002). Another interesting difference is the reaction to drought conditions. While ferns with their relatively large guard cells close their stomata passively if water becomes scarce, angiosperm species close their stomata in response to the phytohormone abscisic acid (ABA) (McAdam and Brodribb, 2013; Lind et al., 2015).

Basic principles of guard cell movements

Guard cell functionality depends on the uptake and release of water. If the water potential inside the guard cell decreases through the accumulation of osmotic substances, water flows into the cell and the turgor pressure rises. Due to the radially arrangement of cellulose fibrils, this rise in internal pressure causes the bending of guard cells leading to stomatal pore opening (Aylor et al., 1973), with a strong correlation between the turgor pressure and stomatal aperture (Franks et al., 1998). The necessary increase in the surface of the plasma membrane upon cell swelling is achieved by the recruitment of internal membranes (Shope et al., 2003). Furthermore, small vacuoles are thought to fuse to a single large vacuole during stomatal opening (Gao et al., 2005). Although guard cells react autonomously to environmental stimuli, their neighbouring cells still influence stomatal movements. Especially in grasses the subsidiary neighbouring cells of the dumb-bell shaped guard cells exert a high degree of control over stomatal movements, mechanically hindering the opening of stomata up to 50% (Franks et al., 1998; Franks and Farquhar, 2006).

Changes in the osmotic pressure as the underlying principle of guard cell regulation was first described by Hugo von Mohl in the 19th century (von Mohl, 1856), although the nature of the osmolytes involved remained unknown for a long time. American botanist Francis E. Lloyd was the first to report that guard cells, unlike other leaf cells, contain large starch granules at the end of the night (Lloyd, 1908). These granules were quickly degraded after dawn and sugars derived from starch breakdown were initially thought to act as the main osmolytes during stomatal opening (Tallman and Zeiger, 1988).

This so-called starch to sugar hypothesis was later replaced by the potassium paradigm, when several observations showed that guard cells imported high amounts of potassium upon illumination and that this K^+ accumulation correlated with increases in stomatal aperture (Fischer, 1968; Fischer and Hsiao, 1968; Humble and Raschke, 1971). Because of the positive charge of potassium, a counterion has to accumulate as well, although plants do not seem to be limited to a specific anion (Humble and Hsiao, 1969). The two major inorganic anions found in most plant species are chloride (Cl^-) and nitrate (NO_3^-), which are taken up from the apoplast. In the absence of plasma membrane permeable anions, mainly the organic acid malate is synthesised. Therefore, the amount of malate produced by guard cells seems to depend on the availability of Cl^- and NO_3^-, with a near linear relationship between the observed stomatal aperture and guard cell malate concentration under inorganic anion limited conditions (Van Kirk and Raschke, 1978a; Raschke and Schnabl, 1978). In this context, starch degradation was proposed to yield the carbon skeletons for malate synthesis (Vavasseur and Raghavendra, 2005).

In the next sections, the molecular mechanisms for ion uptake and excretion during stomatal movements will be discussed, followed by an overview of the environmental and internal stimuli leading to these changes in ion fluxes.

Potassium influx depends on membrane hyperpolarization

The activation of guard cell potassium channels depends on the hyperpolarization of the plasma membrane through the activity of P-type H^+-ATPases (Schroeder et al., 1987, 2001b). Higher plants contain between 9 and 12 plasma membrane H^+-ATPases of this specific subgroup (Palmgren, 2001). These proton pumps are around 120 kDa in size and consist of a nucleotide binding (N), an actuator (A), a C-terminal regulatory (R) and a phosphorylation (P) domain, the latter of which is phosphorylated during the transport cycle (hence P-type ATPase) (Pedersen et al., 2007; Morth et al., 2011; Figure 1). The N-domain binds and hydrolyses one ATP per proton pumped across the plasma membrane, enabling the establishment of a strong proton electrochemical gradient (Briskin and Reynolds-Niesman, 1991). Hyperpolarized membrane potentials over the guard cell plasma membrane were shown to be as negative as -120 mV in intact plants (Roelfsema et al., 2001).

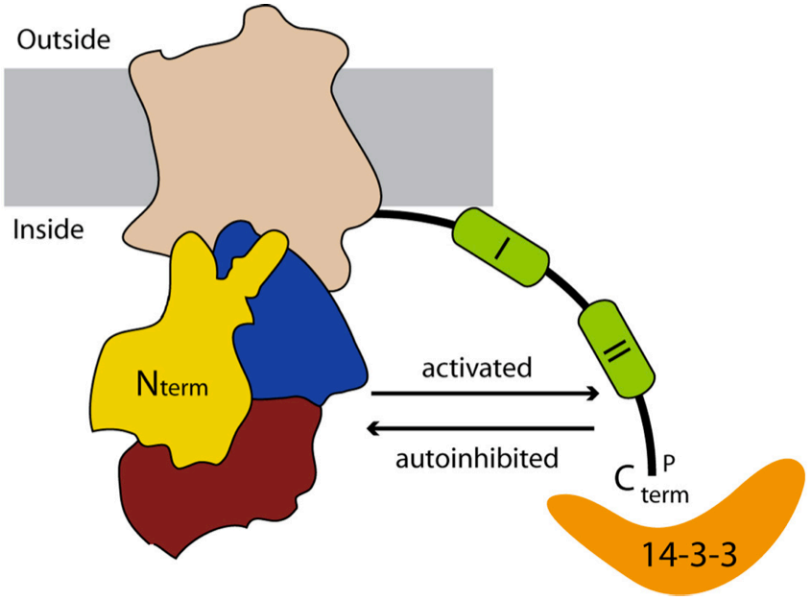

Figure 1: Structure of the plant P-type H^+-ATPase. Domains are depicted as follows: red = nucleotide-binding domain; blue = phosphorylation domain; yellow = actuator domain including the protein N-terminus. The C-terminal autoinhibitory domain can be bound by a 14-3-3 protein, which leads to the activation of the proton pump. Taken from Ekberg et al. 2010.

The R-domains formed by a C-terminal extension of many P-type ATPases such as AHA2 inhibit the proton pumping activity and are therefore referred to as autoinhibitory domains (Palmgren et al., 1991). In a later study it was shown that plant plasma membrane P-type ATPases also contain a regulatory domain in the N-terminal extension, which in addition to the C-terminal domain contributes to the autoinhibitory effect (Ekberg et al., 2010).

The activation of the guard cell proton pumps from *Vicia faba* and *Arabidopsis thaliana* require the phosphorylation of the penultimate threonine residue in the C-terminal autoinhibitory domain and the subsequent, phosphorylation-dependent binding of a 14-3-3 protein (Kinoshita and Shimazaki, 1999, 2002; Fuglsang et al., 1999). 14-3-3 proteins are known to regulate many signalling pathways in eukaryotic organisms through the formation of protein complexes by binding to specific peptide sequences after an initial phosphorylation event (Ferl, 2004). This protein-protein interaction between 14-3-3 proteins and the phosphorylated proton pump is thought to displace the autoinhibitory domain from the active site, causing the activation of the proton extrusion over the plasma membrane (Kinoshita and Shimazaki, 2002; Würtele et al., 2003; Ottmann et al., 2007; Morth et al., 2011). P-type H^+-ATPases form dimeric complexes in the inactive state. Upon activation by phosphorylation and subsequent 14-3-3 protein binding they form hexameric, wheel–like structures (Kanczewska et al., 2005; Ottmann et al., 2007).

The fungal toxin Fusicoccin, initially isolated from *Fusicoccum amygdali*, is known to activate proton pumps in very different plant species, causing a wide variety of physiological changes associated with the acidification of the extracellular space in seeds, roots and other plant tissues (Marre, 1979; De Boer and Leeuwen, 2012). Fusicoccin activates the plasma membrane H^+-ATPases in guard cells and it was initially thought that this is due to the displacement of the autoinhibitory C-terminal domain by Fusicoccin or a Fusicoccin-receptor complex (Johansson et al., 1993). Fusicoccin was indeed shown to bind to a protein of approximately 30 kDa, which was later identified as a 14-3-3 protein (Korthout and de Boer, 1994; Marra et al., 1994; Oecking et al., 1994), causing the displacement of the C-terminal autoinhibitory domain from the catalytic site (Kinoshita and Shimazaki, 2002). The crystal structure of this 14-3-3 protein together with Fusicoccin and the C-terminal phosphopeptide shows that Fusicoccin binds at the 14-3-3 protein AHA interaction surface, leading to a constitutively active proton pump (Fuglsang et al., 1999; Würtele et al., 2003).

The interaction of the 14-3-3 protein with the N-terminal autoinhibitory domain can be inhibited by the protein kinase PKS5-dependent phosphorylation of the Ser^{931} residue, independently of the phosphorylation state of the penultimate Thr (Fuglsang et al., 2007). This indicates that the activation and inactivation of the H^+-ATPase does not only depend on the single Thr phosphorylation as initially thought, and phosphorylation status seems to be controlled by several cellular signalling pathways. Indeed, further phosphorylation sites have been described, but their significance for proton pump regulation and the involved kinases and presumably phosphatases are barely known (Nühse et al., 2004; Niittylä et al., 2007). Most remarkably, the protein kinase responsible for the phosphorylation of the penultimate threonine residue Thr, which is thought to link different signalling pathways to the activation of the H^+-ATPase, is still unknown. In summary, the phosphorylation and dephosphorylation events leading to proton extrusion seem to be a complex and finely tuned mechanism controlled by different molecular pathways.

The Arabidopsis genome encodes 11 full length and a 12^{th} truncated proton pump (*AHA1* to *AHA12*) (Arango et al., 2003). The major H^+-ATPase isoform in the guard cell plasma membrane responsible for its hyperpolarization was shown to be AHA1 (Merlot et al., 2007). AHA1 and the related AHA2 and AHA5 proteins are members of the subfamily II and constitute the majority of H^+-ATPase transcripts in guard cell protoplasts, although transcripts from all eleven isogenes could be detected (Arango

et al., 2003; Ueno et al., 2005; Bates et al., 2012). It should be mentioned that it is not known which of the isoforms are present in sufficient amounts at the protein level in order to have a profound influence on the guard cell membrane potential. Interestingly, the C-terminal autoinhibitory domains of Arabidopsis H^+-ATPases are not conserved, leaving the possibility for different regulatory and kinetic properties between the isoforms. For example, AHA7, AHA9 and AHA10 lack the C-terminal motif required for the phosphorylation-dependent binding of the 14-3-3 protein (Palmgren, 2001).

The gain of function mutation *ost2-1D* in the *OPEN STOMATA 2* (*OST2*) locus encodes a constitutively active version of AHA1, which cannot close the stomata in response to ABA, but interestingly reacts towards other closing stimuli (light to dark transition, CO_2 concentration) (Merlot et al., 2002, 2007). This suggests that ABA partially acts via the inhibition of proton pump activity, while CO_2 concentration and light to dark transition might rely on other mechanisms such as the opening of anion channels (see below).

The activation of the plasma membrane proton pump leads to the generation of a strong hyperpolarized electrical potential across the guard cell membrane, from -60 mV in the depolarized state to around -120 mV in the hyperpolarized state (Roelfsema et al., 2001; Kollist et al., 2014). At the same time proton pump activity increases the proton concentration gradient up to 2 pH units, resulting in a cytosolic pH of around 7.5 and a cell wall pH of approximately 5.5 (Kollist et al., 2014). After the role of potassium during stomatal opening was described in the 1960s and 1970s, Schroeder and colleagues revealed that the potassium influx is mediated by selective channels that are opened by the hyperpolarization of the plasma membrane (Schroeder et al., 1984, 1987; Shimazaki et al., 1986) and allow the movements of potassium along its concentration gradient. The direction of the theoretically bidirectional K^+ flux depends on the electrical potential of the plasma membrane, with an influx through voltage-gated inwardly rectifying potassium channels (K^+_{in}) at hyperpolarized membrane potentials more negative than -70 mV and an outflow from outwardly rectifying K^+ channels (K^+_{out}) at depolarized potentials more positive than -70 mV (Roelfsema et al., 2001; Kollist et al., 2014). Therefore the activation of the plasma membrane H^+-ATPase leads to the influx of K^+, while the depolarization of the plasma membrane mediated by environmental stimuli such as high CO_2 and ABA (discussed below) leads to the efflux of K^+ from the guard cells (Roelfsema et al., 2002, 2004).

Several K^+_{in} channels are encoded by the voltage-gated *SHAKER*-family of K^+ channels, with K^+ CHANNEL OF ARABIDOPSIS THALIANA 1 (KAT1) being the major channel for K^+ influx in Arabidopsis guard cells (Schachtman et al., 1992; Kwak et al., 2001). Besides KAT1, its homologue KAT2 and other members of the *SHAKER*-family such as ARABIDOPSIS K^+ TRANSPORTER 1 (AKT1) and AKT2/3 channels might contribute as well to the K^+ influx into guard cells (Szyroki et al., 2001; Ivashikina et al., 2005). Furthermore, functional K^+_{in} channels can be formed by the dimerization of two subunits coded by different genes, such as KAT1-KAT2 heterodimers (Lebaudy et al., 2010).

Vacuolar uptake of potassium occurs against the concentration gradient, suggesting an H^+/K^+ antiport mechanism. At the vacuolar membrane, potassium transporters are energized by a proton gradient of approximately 2 pH values, while the electrical potential across the vacuolar membrane stays relatively small, presumably because V-type ATPases responsible for this high ΔpH can be inactivated by electrical potentials (Walker et al., 1996; Rienmüller et al., 2012). V-type ATPases of the vacuolar membrane are large protein complexes formed by several subunits (Schumacher and Krebs, 2010). Besides V-type ATPases, pyrophosphatases are also known to pump protons across the vacuolar membrane of guard cells (Gaxiola et al., 2007). The transporters responsible for the uptake of K^+ at the vacuolar membrane were shown to be two members of the $Na^+,K^+/H^+$ antiporter, NHX1 and NHX2 (Venema et al., 2002; Barragán et al., 2012).

Uptake of anions is required to balance the K^+ charge

Uptake of anions from the apoplast requires active transport against a concentration gradient as well as against the plasma membrane potential. One identified transporter is the NO^{3-}/H^+ SYMPORTER 1 (NRT1.1), which imports nitrate from the apoplast into Arabidopsis guard cells (Guo et al., 2003). Until now no importer for chloride was identified at the plasma membrane (Kollist et al., 2014), but an import of malate via the AtABCB14 transporter of the ATP-BINDING CASSETTE TRANSPORTER family was postulated, although no obvious phenotype was observed under normal growth conditions for the *atabcb14* mutant (Lee et al., 2008). Rather, it was suggested that malate import was induced under high CO_2 concentrations, when malate accumulates in the guard cell apoplast (Hedrich et al., 1994). This malate accumulation is thought to originate from mesophyll

photosynthesis and to participate in modulating stomatal responses to changes in ambient CO_2 concentrations (Hedrich et al., 1994; Lawson et al., 2014).

At the tonoplast one member of the ALUMINIUM-ACTIVATED MALATE TRANSPORTER (ALMT) anion channel family, ALMT9, was shown to enable Cl^- influx into guard cell vacuoles upon activation by cytosolic malate (De Angeli et al., 2013). The loss of ALMT9 resulted in reduced stomatal opening upon illumination and a drought insensitive phenotype. Besides ALMT9, one member of the family of chloride channels (CLCs), AtCLCc was also shown to import Cl^- into guard cell vacuoles, probably via a H^+/Cl^- antiport mechanism (Jossier et al., 2010). Furthermore, another member of this family, AtCLCa, which is expressed in guard cells, could import NO^{3-} into guard cell vacuoles (De Angeli et al., 2006; Jossier et al., 2010). Finally, malate can be taken up into guard cell vacuoles by the ALMT6 channel, although the lack of a stomatal phenotype in the knock-out mutant suggests further players in malate translocation (Meyer et al., 2011).

Efflux of anions causes K^+ efflux during stomatal closure

During stomatal closure plasma membrane anion channels not only release osmolytes, but also causes the depolarization of the plasma membrane potential (Kollist et al., 2011; Roelfsema et al., 2012). This is necessary for the opening of K^+_{out} channels and the release of potassium from the guard cells. Guard cells contain two different types of plasma membrane localized anion channels, which show differences in the voltage dependency and in their activation kinetics. While the rapid (R)-type channels open in milliseconds, slow (S)-type channels open in the range of seconds (Linder and Raschke, 1992; Hedrich, 2012). The loss of the (S)-type anion channel SLOW ANION CHANNEL-ASSOCIATED 1 (SLAC1) leads to a strong increase in guard cell Cl^- and malate concentrations, resulting in opened stomata with severely reduced responses to several environmental stimuli such as high CO_2 concentrations and ABA (Negi et al., 2008; Vahisalu et al., 2008). One of the closest related genes to *SLAC1*, *SLAC1 HOMOLOG 3* (*SLAH3*) was also found to be important for the extrusion of anions, with a strong preference for NO^{3-} (Geiger et al., 2011). (R)-type anion channels belong to the ALMT family, with ALMT12, also referred to as QUICK ANION CHANNEL 1 (QUAC1), being responsible for the fast closure of stomata in response to darkness and high ambient CO_2 concentration, most likely through the release of organic acids such as malate (Meyer et al., 2010).

While these channels facilitate the extrusion of anions over the guard cell plasma membrane, channels and regulatory components controlling their efflux from the vacuole into the cytosol are not known (Kollist et al., 2014; Figure 2).

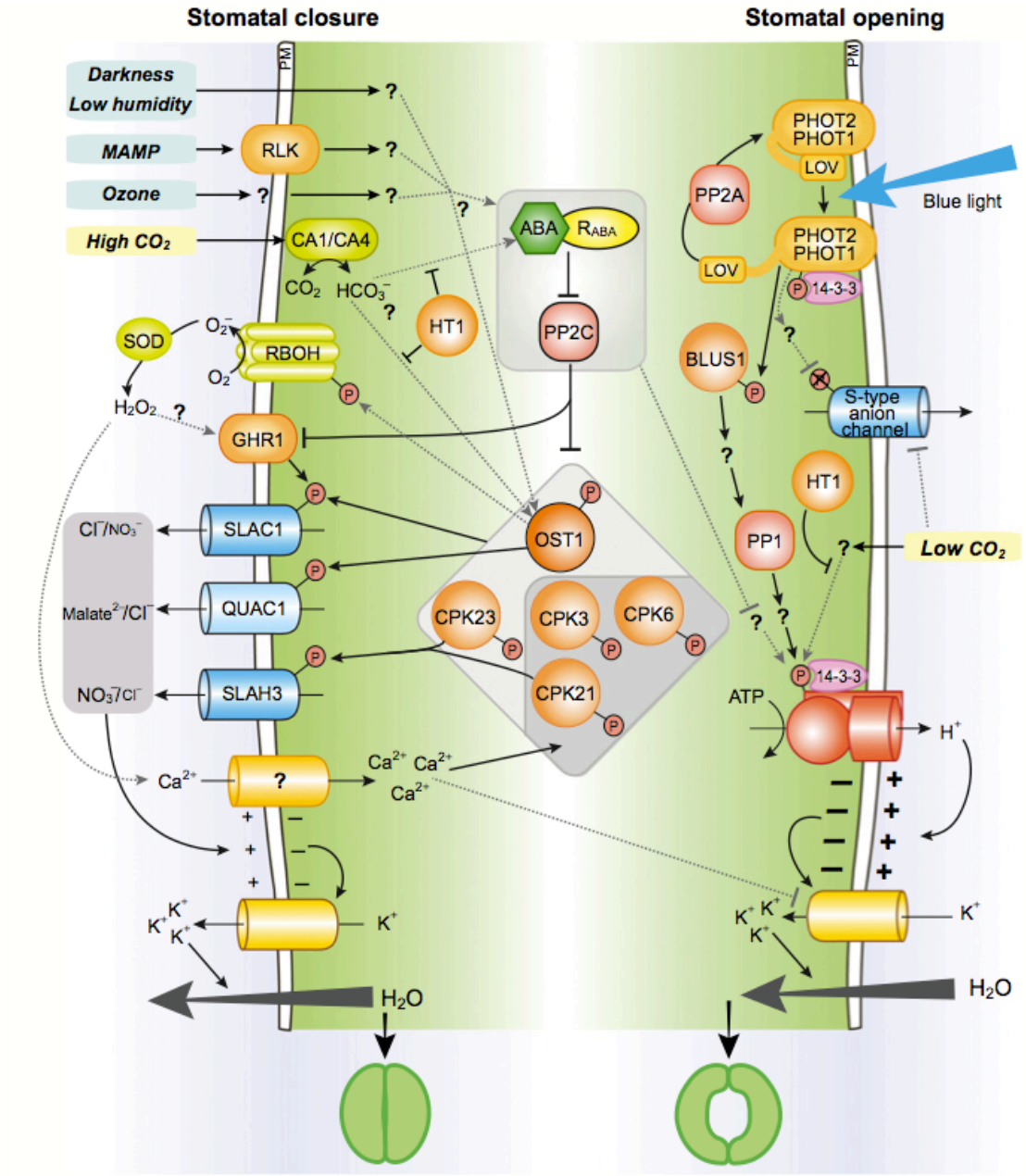

Figure 2: Summary of known plasma membrane ion transporter and channels and the regulatory network controlling their activation during stomatal closure (left) and opening (right). Taken from Kollist et al. 2014. See text for details.

The depolarization of the plasma membrane caused by the activation of the plasma membrane anion channels inactivates the voltage-gated K^+_{in} channels (Roelfsema et al., 2001; Kollist et al., 2014; Figure 2). The K^+ stored in the guard cell vacuole is at the same time removed by the voltage-insensitive Arabidopsis TANDEM PORE K^+ 1

(TPK1) channel, which might act together with the related TPK3 and the K_{ir}-like potassium channel KCO3 (Voelker et al., 2006; Gobert et al., 2007; Voelker et al., 2010). Finally, K^+ efflux from the guard cell cytosol is mediated by the GUARD CELL OUTWARD RECTIFYING K^+ (GORK) channel (Ache et al., 2000; Hosy et al., 2003) and the synergistic activities of the K^+ UPTAKE TRANSPORTER 6 (KUP6) and KUP8 K^+/H^+ symporter (Osakabe et al., 2013).

The network controlling stomatal aperture is complex

Many different environmental factors influence stomatal movement (Figure 2). During the last decades it became clear that many different signalling pathways act together in a complex network (Hetherington and Woodward, 2003). This organizational form allows guard cells to respond simultaneously to multiple and sometimes contradicting signals in a robust but flexible way. One example which indicates this fact is the observation that Arabidopsis plants grown at elevated CO_2 levels show an enhanced response to ABA or osmotic stress (Leymarie et al., 1999). This integrative approach allows single or small groups of guard cells to react autonomously to localized changes in environmental factors, resulting in strong heterogeneity in stomatal apertures even within a small area of a single leaf (Lawson and Weyers, 1999; Mott and Buckley, 2000; Lawson and Blatt, 2014). The different environmental factors influencing stomatal aperture will be described below and the interconnections in their signalling pathways will be mentioned where known.

Blue-light induced stomatal opening

One of the most potent environmental signals inducing stomatal opening is blue light (Shimazaki et al., 2007; Figure 2), although a background red light illumination is needed for the response to low rates of blue light (see below for a reasoning behind this effect of red light). Under background red light illumination, already a fluence rate of 5 to 10 µmol photons m^{-2} s^{-1} in the range of 430 to 460 nm, corresponding to approximately 1% of the light intensity under full day light, is sufficient to induce the blue-light specific response of guard cells (Sharkey and Raschke, 1981; Kinoshita et al., 2001; Shimazaki et al., 2007). The high sensitivity of stomatal opening to low blue light illumination might play a role during early dawn, preparing the plant for the coming sunrise (Zeiger and Field, 1982). Blue light induces guard cell movements through the activation of the plasma membrane proton pumps (Assmann et al., 1985;

Shimazaki et al., 1986), which leads to the influx of potassium into the guard cells as described above (Schroeder et al., 1984, 1987).

Arabidopsis thaliana contains two classes of blue light photoreceptors, cryptochromes, encoded by the *CRYPTOCHROME 1* (*CRY1*) and *CRY2* genes and phototropins, which are encoded by the *PHOT1* and *PHOT2* genes (Christie, 2007). The plasma membrane localized Ser/Thr kinases PHOT1 and PHOT2 (Sakamoto and Briggs, 2002) induce blue-light specific effects generally related to an optimization of photosynthesis and growth (Takemiya et al., 2005; Christie, 2007; Boccalandro et al., 2012). They were first identified as phosphorylated proteins in *Pisum sativa* under blue light illumination, responsible for the inhibition of hypocotyl elongation (Gallagher et al., 1988). Additional roles were later described, as it became evident that phototropins also play important roles in the regulation of phototropism and chloroplast movement (Sakai et al., 2001), as well as during leaf expansion (Sakamoto and Briggs, 2002) and stomatal opening (Kinoshita et al., 2001). The Arabidopsis genes were identified in the 90s as *NONPHOTOTROPIC HYPOCOTYL 1* (*NPH1*) and *NPH-LIKE 1* (*NPL1*) (Huala et al., 1997; Kagawa et al., 2001), but later renamed *PHOT1* and *PHOT2* for their prominent role in light-induced tropic responses (Briggs et al., 2001). Dark grown seedlings of the *phot1* single mutant do not show a rapid inhibition of their hypocotyl elongation under blue light, while *phot2* seems to lack the ability to move chloroplasts in response to adverse high light conditions (Folta and Spalding, 2001; Kagawa et al., 2001; Sakai et al., 2001), indicating some degree of functional specialization. On the other side, responses such as leaf expansion and stomatal opening are mediated by both PHOT1 and PHOT2 (Kinoshita et al., 2001; Sakamoto and Briggs, 2002). In the case of stomatal opening, the *phot1phot2* double mutant did not respond to 50 µmol m^{-2} s^{-1} of blue light under a red light background illumination (50 µmol m^{-2} s^{-1}), while the wild type response saturated already at 5 µmol m^{-2} s^{-1} blue plus red light, with the two single mutants showing an intermediate phenotype (Kinoshita et al., 2001).

Phototropins perceive blue light with a flavin mononucleotide (FMN) chromophore bound to the LOV1 (light, oxygen or voltage) and LOV2 domains of the N-terminal part, while the C-terminal part consists of a Ser/Thr kinase domain (Huala et al., 1997; Christie et al., 1998; Harper et al., 2003; Figure 3). In darkness the FMN is noncovalently bound to the LOV domain, while blue light illumination causes the formation of a cysteinyl adduct with the receptor protein (Christie et al., 1999; Salomon et al., 2000; Crosson and Moffat, 2001). The adduct formation leads to

conformational changes in the position of LOV2, which is thought to bind and thereby inhibit the kinase domain in the dark (Matsuoka and Tokutomi, 2005). This domain rearrangement leads to the autophosphorylation at several amino acids, including two serine residues in the activation loop of the kinase domain (Salomon et al., 2003; Matsuoka and Tokutomi, 2005; Inoue et al., 2008). Following autophosphorylation of PHOT1 and PHOT2 in guard cells, a 14-3-3 protein binds to the hinge region between the LOV1 and LOV2 domains in a phosphorylation-dependent manner, presumably stabilizing the active state and enabling the phosphorylation of downstream targets (Kinoshita et al., 2003; Sullivan et al., 2009; Tseng et al., 2012). In the absence of light, phototropins are known to become rapidly dephosphorylated, which is one important step for dark recovery and the inhibition of the signalling cascade (Salomon et al., 2000). Dephosphorylation occurs presumably through the activity of one or several protein phosphatases. In the case of PHOT2, the PP2A Ser/Thr protein phosphatase, a holoenzyme consisting of three subunits, was shown to catalyse this dephosphorylation step (Tseng and Briggs, 2010). PHOT1 was not dephosphorylated by the same PP2A enzyme containing the regulatory subunit A1, but might require another phosphatase or a specific subunit combination of the PP2A holoenzyme.

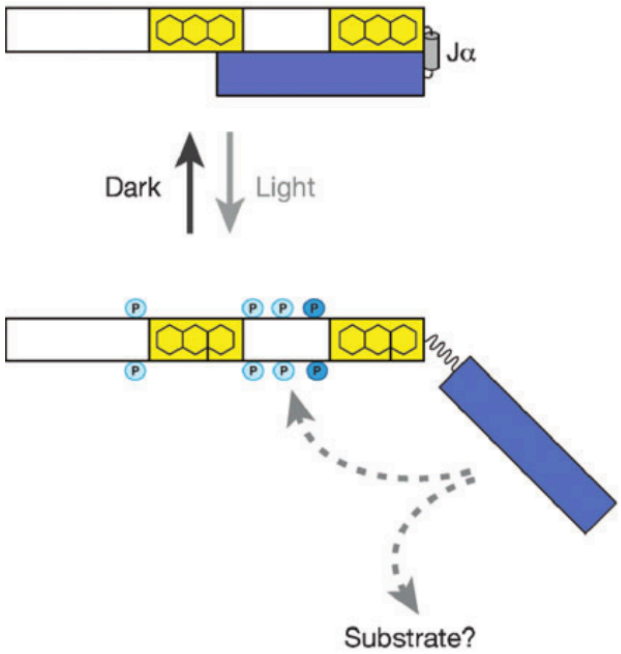

Figure 3: Schematic representation of phototropin activation by light. Blue light illumination leads to the adduct formation between FMN and a cysteine residue of the LOV domain. The subsequent structural rearrangements leads to the activation of the kinase domain. Taken from Christie 2007.

The identification of direct targets of the PHOT kinase domain in guard cell blue light signalling proofed to be difficult. The coiled-coil domain containing ROOT PHOTOTROPISM 2 (RPT2) protein was implicated in phototropin-mediated regulation of hypocotyl and root phototropism as well as in stomatal regulation (Sakai et al., 2000). Furthermore, yeast-two-hybrid screens found the RPT2-like NONPHOTOTROPIC HYPOCOTYL 3 (NPH3) and PHYTOCHROME KINASE SUBSTRATE (PKS) proteins to interact with PHOT1. But in depth analysis of these proteins and the corresponding mutants showed that neither of them is involved in the phototropin-mediated blue light signalling cascade in guard cells (de Carbonnel et al., 2010; Tsutsumi et al., 2013).

Only recently Takemiya and colleagues showed that the Ser/Thr protein kinase BLUE LIGHT SIGNALING 1 (BLUS1) is a direct substrate of PHOT1 and PHOT2 (Takemiya et al., 2013a). The *blus1* mutant of Arabidopsis showed impaired stomatal opening, while other phototropin-mediated processes were not altered, suggesting a guard cell specific role for BLUS1 in the blue light signalling cascade.
The following steps leading to the activation of the H^+-ATPase are not well understood, but were shown to involve a type 1 protein phosphatase (PP1) (Takemiya et al., 2006). This major eukaryotic serine/threonine protein phosphatase is formed in Arabidopsis as a holoenzyme consisting of the catalytic subunit PP1c and the regulatory subunit PP1 REGULATORY SUBUNIT2-LIKE PROTEIN 1 (PRSL1). PRSL1 is able to bind the catalytic subunit, leading to the localization of the complex to the cytoplasm, while in the absence of PRSL1 a strong PP1c-RFP signal was found in the nucleus, where it would be unable to participate in the cytoplasmic localized signalling cascade (Takemiya et al., 2006, 2013b). Tautomycin, a potent inhibitor of PP1c phosphatases, is able to inhibit blue light induced activation of the plasma membrane proton pump, suggesting that PP1 works upstream of the H^+-ATPase (Takemiya et al., 2006). Similarly, the treatment of guard cells of the *prsl1* mutant with fusicoccin overcomes the inhibition of stomatal opening, again placing PP1 upstream of the activation of the H^+-ATPase (Takemiya et al., 2013b). The molecular pathway connecting the PP1 phosphatase with the phosphorylation-dependent activation of the H^+-ATPase is not known. Several mechanisms seem possible. Firstly, PP1 could activate a yet to be described protein kinase, which in turn acts on the C-terminal threonine residue of H^+-ATPases. Alternatively, they could inhibit phosphatases, which constitutively remove this phosphate groups (Kinoshita and Shimazaki, 1999; Svennelid et al., 1999). Finally, PP1 could inactivate Arabidopsis Ser/Thr protein kinase PKS5, which is able to phosphorylate Ser^{931} of

AHA2 leading to the inhibition of 14-3-3 protein binding necessary for proton extrusion (Fuglsang et al., 2007), although PKS5 was suggested to be involved in a novel Ca^{2+}-dependent singaling pathway (Fuglsang et al., 2007). In any case, the exact mechanism of H^+-ATPase activation through the blue light signalling cascade is still not known and needs further investigation.

Besides the H^+-ATPase, blue light signalling in guard cells mediated by phototropins might have additional targets. It is obvious that the activation of the plasma membrane proton pump alone would not be sufficient for the necessary degree of hyperpolarization, if at the same time anion channels would be open. Indeed, blue light was shown to cause the inactivation of S-type anion channels in the plasma membrane in a phototropin-dependent manner, although the exact mechanism is still not known (Marten et al., 2007).

Cryptochromes influence stomatal behaviour

Besides PHOTs, cryptochromes (CRY1 and CRY2) were also implicated in the response of guard cells to blue light illumination, although they are best known for their role in photomorphogenic responses (Mao et al., 2005). Epidermal peels of *cry1cry2* double mutants illuminated with 5 µmol m^{-2} s^{-1} blue light under a 50 µmol m^{-2} s^{-1} red light background showed a reduced stomatal opening response. It was also reported that guard cells of the *phot1phot2* double mutant still respond to relatively high fluence rates of blue light (20 – 50 µmol m^{-2} s^{-1} under a 100 µmol m^{-2} s^{-1} red light background), presumably as a result of a cryptochrome-dependent response (Talbott et al., 2003). On the other hand, some doubts about a direct, guard cell specific signalling function of cryptochromes were raised (Ohgishi et al., 2004; Shimazaki et al., 2007). In contrast to the *phot1phot2* double mutant, the *cry1cry2* mutant guard cells showed the same defect in stomatal regulation under both high blue and high red light illumination as well as already reduced apertures in the dark compared to wild type plants (Boccalandro et al., 2012). Further experiments showed that the underlying reason for reduced stomatal aperture in *cry1cry2* under relatively high blue light illumination, which changed transpiration rates and photosynthetic capacity, were largely indirect (Boccalandro et al., 2012). The effect of *cry1cry2* was mainly attributed to elevated levels of ABA in the *cry1cry2* mutant leaves compared to the wild type (Boccalandro et al., 2012), although the link between cryptochrome signalling and ABA synthesis is not clear at the moment. Higher ABA levels in the

cry1cry2 plants would inhibit phototropin-induced blue light dependent opening of stomata as will be discussed below. Furthermore, differences in the stomatal index (number of stomata relative to the number of epidermal cells) and alterations in the development of stomatal pores were observed in *cry1cry2* plants (Kang et al., 2009). CRYs were shown to be important for the entrainment of the circadian clock to a precise 24 h periodicity (Harmer, 2009), as well as controlling the flowering time regulator CONSTANS (CO) (Turck et al., 2008). Recently the influence of the circadian clock and CO on stomatal regulation was established and will be discussed below.

Taken together, it seems that both double mutants, *phot1phot2* and *cry1cry2*, influence photosynthetic rates and therefore indirectly stomatal aperture in a non-stomatic way under high irradiance, through long-term adaptive changes such as phototropin mediated leaf flattening and cryptochrome dependent control of ABA levels, while only phototropins are involved in the guard cell specific, direct perception of low levels of blue light and the following rapid stomatal opening.

Photosynthesis-dependent stomatal opening

Continuous red light illumination at relatively high fluence rates is known to induce stomatal opening, although with a ten times lower sensitivity then blue light (Sharkey and Raschke, 1981).

The fact that relatively high fluence rates of blue light can induce stomatal opening in the *phot1phot2* double mutant to a similar extend as high fluence rate of red light (Talbott et al., 2003) does hint towards a more general influence of photosynthetically active radiation (PAR). It was therefore proposed that the red light-induced opening depends either on the stimulation of the plasma membrane proton pump through the photophosphorylation-dependent production of ATP (Serrano et al., 1988) or on the photosynthesis driven accumulation of sugars in red light illuminated guard cells (Gotow et al., 1988; Talbott and Zeiger, 1993). Later patch clamp studies could not find a red light specific activation of the H^+-ATPase (Roelfsema et al., 2001; Taylor and Assmann, 2001) and illumination of single guard cells with red light did not induce an opening response or induced sufficient accumulation of sugars (Reckmann et al., 1990; Roelfsema et al., 2002), arguing against a role of guard cell CO_2 fixation. Furthermore, guard cell starch breakdown is not observed under red light illumination (Tallman and Zeiger, 1988). Although the uptake of sugars from the apoplast in response to red light could still contribute significantly to the initial opening reaction

(discussed below), the red light induced stomatal opening is often attributed to a drop in the internal leaf CO_2 concentration (C_i) during mesophyll carbon fixation, which requires the constant illumination of a larger part of the leaf (Roelfsema et al., 2002; Shimazaki et al., 2007). Indeed, CO_2 insensitive mutants were also shown to be insensitive to PAR (Hashimoto et al., 2006; Marten et al., 2008), further hinting to a connection between C_i and light signalling. Guard cells are known to react autonomously to changes in C_i as will be discussed below and changes in C_i seem to contribute a large part to PAR-responses in intact leaves.

On the other hand, Messinger and colleagues reported that guard cells still responded to PAR illumination even when the C_i was kept constant via manipulations of the ambient CO_2 concentration (Messinger et al., 2006). Furthermore, several reports on experiments with isolated epidermal peels showed a guard cell autonomous response to red light. This red light-induced opening under high light intensities depends on the electron transport chain and was inhibited by the addition of the photosystem II (PSII) inhibitor 3-(3,4-dichlorophenyl)-1,1-dimethylurea (DCMU) (Schwartz and Zeiger, 1984). A red light-dependent opening response could not be observed in epidermal peels of the orchids belonging to the *Paphiopedilum* genus, whose guard cells do not contain chloroplasts (Zeiger et al., 1983).

One mechanism by which guard cells could sense PAR was proposed to involve the PHYTOCHROME (PHY) photoreceptors (Talbott et al., 2003; Wang et al., 2010a). PHYs are known to regulate photomorphogenic processes together with cryptochromes (Kami et al., 2010). As discussed above for CRY1/CRY2, PHYB and the PHYTOCHROME INTERACTING FACTOR 4 (PIF4) were shown to play a role in stomatal development and are influencing the guard cell transcriptional network (Boccalandro et al., 2009; Casson et al., 2009; Wang and Wang, 2015). Genes altered in the *phyB* mutant include the guard cell specific transcription factor *MYB60* (Wang et al., 2010a), as well as the guard cell development regulators *FAMA* and *TOO MANY MOUTHS* (Boccalandro et al., 2009). It seems therefore likely that PHYs have only a small contribution to the immediate opening response upon illumination, probably through the transcriptional modulation of the involved signalling cascades.

A recent review added the idea of redox changes in plastoquinone (PQ) as a possible red light sensor to the debate about the exact mechanism by which red light induces stomatal movements (Busch, 2014). Because DCMU inhibits the transfer of electrons from PSII to the primary electron acceptor PQ, the ratio of PQ_{red} to PQ_{ox} could act as a signal. So far no downstream targets of PQ in the red light response of

stomata were described and further work has to be conducted to clearly establish a photoreceptor for the guard cell autonomous red light induced opening response.

Synergistic effects of blue and red light

Low intensities of blue light illumination have a higher impact on stomatal opening under a background illumination of red light (Iino et al., 1985; Assmann, 1988; Kinoshita et al., 2001). This could be explained with the drop in the internal CO_2 concentration (C_i), which is caused by red light driven mesophyll photosynthesis (see below). Subsequently, S-type anion channels are inhibited through the CO_2 signaling pathway (Tian et al., 2015), thereby increasing the effect of the blue light activation of K^+_{in} channels. This effect of red light on S-type anion channels is thought to be indirect through its influence on C_i in intact leaves, although a direct influence of red light signalling on these channels cant be excluded at the moment.

In contrast to this idea, the synergistic effect of red and blue light can also be observed in epidermal peels, where the background red light increases stomatal opening as well as malate formation (Ogawa et al., 1978; Schwartz and Zeiger, 1984) and can therefore not be attributed solely to lowered CO_2 concentrations caused by the underlying mesophyll cell photosynthesis as described above. Shimazaki and colleagues proposed that the synergism is related to the production of malate (Shimazaki et al., 2007). Blue light activates proton extrusion from guard cells causing subsequent K^+ influx, while red light provides reducing equivalents and ATP through guard cell photophosphorylation for the generation of malate as the counterion (Shimazaki et al., 2007). This would also explain why red light needs to be applied continuously, while a blue light pulse of a few seconds is already sufficient to induce stomatal opening (Kinoshita et al., 2001).
Besides malate synthesis another effect of the background red light illumination can be imagined. As described above, red light was initially postulated to cause stomatal opening by generating a large supply of ATP for proton pumping. Although red light alone was shown to be unable to drive efficient proton pumping (Roelfsema et al., 2001; Taylor and Assmann, 2001), a recent report showed that blue-light induced H^+-ATPase activity was elevated under a background of red light in Arabidopsis guard cell protoplasts and this effect was eliminated when DCMU was added to the cell suspension (Suetsugu et al., 2014). This also explains earlier reports, where the blue

light induced stomatal opening under a red light background was inhibited using DCMU (Tominaga et al., 2001).

In summary, blue light induces quick opening and might be important for adaptations to changing light conditions under natural growth conditions, e.g. responding to sun flecks (Way and Pearcy, 2012). Red light is necessary for the rapid blue light responses for efficient photosynthetic capacity (Suetsugu et al., 2014) and links mesophyll photosynthesis via changes in C_i to stomatal regulation. The guard cell autonomous, red light dependent signalling pathway seen in isolated epidermal peels remains controversial and its actual contribution to PAR-induced stomatal opening in intact leaves is not completely understood.

Light to darkness transition

Many plant species, with the notable exception of CAM plants, close their stomata in the evening and maintain a low conductance during the dark period in order to save water and improve plant fitness. It is not clear if this stomatal behaviour is simply a passive effect of the absence of light or under specific genetic control (Kollist et al., 2014; Costa et al., 2015). The recent isolation of the *OPEN ALL NIGHT LONG* (*opal*) mutants, which exhibit open stomata throughout the night, but close normally in response to ABA and high CO_2 concentrations, might shed some light on this long debated question (Darwin, 1898; Costa et al., 2015).

Influence and perception of CO_2

Under elevated CO_2 concentrations stomata of most land plants close or show only a mild increase in the aperture upon illumination, while low carbon dioxide concentrations induce an increase in stomatal aperture (Vavasseur and Raghavendra, 2005). It seems that guard cells react primarily to the internal leaf CO_2 concentration (C_i), which is influenced by stomatal conductance (g_s), ambient CO_2 concentration (C_a) and CO_2 consumption primarily in the mesophyll cell Calvin cycle (Roelfsema et al., 2002). Therefore, as discussed above, C_i links red light induced photosynthetic activity in the mesophyll cells with the regulation of stomatal aperture. It was debated for a long time if guard cells are able to respond autonomously to changes in C_i or if they require a photosynthesis-dependent signal from the underlying mesophyll (sometimes referred to as ‘stomatin’) (Lawson et al., 2014).

The observation that stomata react to changes in C_a in albino leaves without mesophyll photosynthetic carbon fixation, indicates that the pathway of CO_2 perception and signalling is located solely in guard cells and does not require a mesophyll signal (Roelfsema et al., 2006), although this is sometimes questioned (Mott et al., 2008; Mott, 2009). Guard cells are well known to respond to changes in C_a in darkness (Hedrich et al., 2001), indicating that the guard cell CO_2 response is independent from mesophyll photosynthesis. Furthermore, plants with strongly reduced levels of Rubisco or the Rieske FeS protein still responded to changes in C_i, although photosynthesis was strongly inhibited in both guard cells and mesophyll cells (Price et al., 1998; von Caemmerer et al., 2004). The recent elucidation of the molecular pathway of guard cell CO_2 signalling further proves the ability of guard cells to respond autonomously to changes in C_i.

This signalling pathway was initially shown to depend on the subclass III kinase OPEN STOMATA 1 (OST1), also referred to as SNF1-RELATED PROTEIN KINASE 2.6 (SnRK2.6) and SLAC1, with both mutants being insensitive to changes in either ABA (discussed below) or C_i (Negi et al., 2008; Vahisalu et al., 2008; Merilo et al., 2013). Recently, the molecular mechanism linking the perception of C_i in guard cells to the activation of OST1 was elucidated (Figure 4).

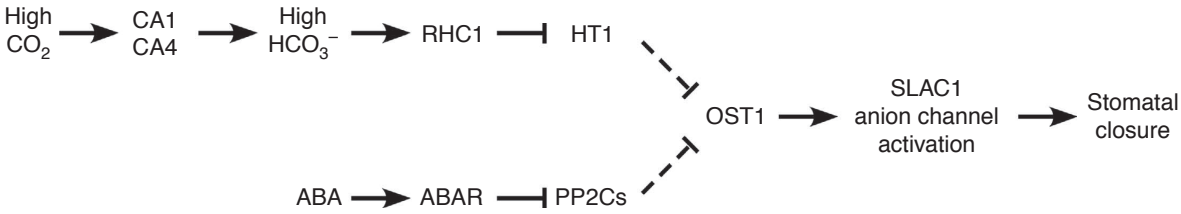

Figure 4: Updated model of CO_2 signaling pathway in guard cells and its point of integration with ABA signalling components. Taken from Tian et al. 2015, see text for details.

β-CARBONIC ANHYDRASE1 and 4 (βCA1/ βCA4) were shown to act as positive regulators for CO_2 mediated stomatal closure by converting CO_2 into bicarbonate (HCO_3^-) (Hu et al., 2010; Xue et al., 2011). Additionally, an influence of aquaporin was proposed, which seem to increase CO_2 flux over the plasma and plastidial membranes by increasing their permeability (Uehlein et al., 2003; Heckwolf et al., 2011). Elevated HCO_3^- concentrations in the vicinity of βCAs are perceived by the βCA-interacting MULTIDRUG AND TOXIC COMPOUND EXTRUSION (MATE)-like protein RESISTANT TO HIGH CARBON DIOXIDE (RHC1) (Tian et al., 2015). The *rhc1* mutant was initially shown to be impaired in high CO_2 induced growth inhibition

found in wild-type plants, which rapidly close their stomata under a 700 ppm CO_2 atmosphere. In contrast, *rhc1* mutants showed a slower and weaker stomatal closure response to high CO_2 (Tian et al., 2015). The exact molecular mechanism for HCO_3^- perception by RHC1 is not yet known, but the signal is further transduced through the inactivation of the negative OST1 regulator HIGH TEMPERATURE 1 (HT1) (Hashimoto et al., 2006; Tian et al., 2015). Under normal or low CO_2 concentrations HT1 protein kinase phosphorylates OST1, keeping the anion channel activator in an inactive state (Tian et al., 2015). In contrast, the negative regulators of the ABA specific signalling pathway, the type 2C protein phosphatases (PP2Cs), inactivate OST1 through dephosphorylation of Ser/Thr residues in its activation loop (Umezawa et al., 2009; Xie et al., 2012). Upon bicarbonate perception RHC1 is thought to recruit HT1 to the plasma membrane, inactivating its OST1 phosphorylation activity and thereby inducing OST1-mediated stomatal closure (Tian et al., 2015). This clearly establishes OST1 as a central integrator of ABA and CO_2 signals, with high CO_2 as well as ABA activating S-type anion channels via OST1 activation, leading to the efflux of anions (Brearley et al., 1997; Hanstein and Felle, 2002). High C_i concentrations and blue light have therefore antagonistic effects on these channels. In contrast, low C_i, which occurs mainly at the onset of illumination through the depletion of internal CO_2 via the mesophyll Calvin cycle induces stomatal opening.

ABA causes stomatal closure

The plant hormone abscisic acid (ABA) is the most potent antagonist to blue light induced stomatal opening. In its role as a stomatal regulator, ABA is usually synthesized in response to plant water deficit, causing stomata to close and preventing further water loss (Jones and Mansfield, 1970; Schroeder et al., 2001b). Bauer and colleagues showed recently that a guard cell autonomous pathway for ABA synthesis exists and that it is sufficient for stomatal closure (Bauer et al., 2013). Despite being described as an anti-stress hormone in plant defence against abiotic stresses as early as the 1960s, the core signalling pathway was established only recently (Cutler et al., 2010).

In guard cells ABA leads to the activation of the (S)-type and (R)-type anion channels in the plasma membrane, causing the efflux of anions and subsequently the depolarization of the plasma membrane potential and finally the activation of the K^+_{out} channels (Roelfsema et al., 2004; Levchenko et al., 2005; Figure 2).

In the absence of ABA, members of the SNF1-related kinase subgroup 2 (SnRK2) protein family are inactivated through dephosphorylation by several type 2C protein phosphatases (PP2Cs), such as ABA-INSENSITIVE 1 (ABI1) and ABI2 (Gosti et al., 1999; Rubio et al., 2009; Vlad et al., 2009; Umezawa et al., 2009). ABA induces the formation of a protein complex of PYRABACTIN RESISTANCE 1 / PYR-LIKE / REGULATORY COMPONENTS OF ABA RECEPTOR (PYR/PYL/RCAR) proteins with PP2Cs, thereby inactivating their phosphatase activity (Ma et al., 2009; Park et al., 2009; Santiago et al., 2009; Nishimura et al., 2010). This leads to the subsequent release of the SnRK2 kinases from PP2C mediated inhibition and to their activation through autophosphorylation.

OPEN STOMATA 1 (OST1), also referred to as SnRK2.6, was shown to be the most important SnRK2 kinase family member in guard cells (Mustilli et al., 2002; Fujii and Zhu, 2009). In response to ABA, OST1 activates the anion channels SLAC1 and ALMT12 (Geiger et al., 2009; Lee et al., 2009; Vahisalu et al., 2010; Imes et al., 2013) and inhibits the activities of KAT1 and KUP6 (Sato et al., 2009; Osakabe et al., 2013; Figure 2).
Additionally, ABA triggers via the activation of OST1 the opening of Ca^{2+} permeable channels through the production of ROS in the apoplast (Pei et al., 2000; Sirichandra et al., 2009), leading to elevated cytosolic concentrations of Ca^{2+}. This leads together with the inactivation of PP2Cs to the activation of Ca^{2+}-dependent protein kinases (CPKs). CPKs are also able to activate anion channels, particularly SLAC1 and SLAH3, via phosphorylation (Geiger et al., 2010, 2011; Brandt et al., 2012). Furthermore, CPKs they were recently shown to activate the vacuolar K^+ channel TPK1 (Latz et al., 2013). Therefore, the concerted action of these protein kinases leads to the activation of anion efflux from guard cells causing the depolarization of the plasma membrane, inactivation of K^+_{in} channels as well as the activation of K^+_{out} channels. The massive efflux of osmolytes results in turgor loss and the closing of the stomatal pore.

Besides the activation of outward rectifying K^+ channels, the inhibition of the H^+-ATPase activity by an early response pathway was shown to be important for ABA induced stomatal closure (Shimazaki et al., 1986; Goh et al., 1996; Hayashi and Kinoshita, 2011). Merlot et al. 2007 proposed that the proton pump AHA1 is a target of an ABA-directed pathway to close stomata under drought conditions, as indicated by the fact that the constitutively active *ost2-1D* gain of function mutation of AHA1 was insensitive to ABA (Merlot et al., 2007). Subsequent experiments showed that

epidermal peels of Arabidopsis treated with physiological concentrations of ABA did not phosphorylate the penultimate amino acid in the H^+-ATPase upon blue light illumination (Zhang et al., 2004). In contrast, ABA had no effect on blue light induced H^+-ATPase phosphorylation in the ABA-insensitive mutants *abi1-1*, *abi2-1* or *ost1-2* (Hayashi et al., 2011). This inhibitory effect of ABA is thought to be mediated by the induction of the synthesis of the lipid signalling molecule phosphatidic acid (PA), presumably by PHOSPHOLIPASE D. PA directly binds to the catalytic subunit PP1c and therefore inhibits blue light induced stomatal opening at the level of PP1 (Takemiya and Shimazaki, 2010). This results in the inhibition of ATPase phosphorylation and therefore activation, even under blue light illumination (Takemiya and Shimazaki, 2010), establishing the PP1 enzyme as an important integration point of blue light and ABA signalling cascades and at the same time explains the mechanism of ABA induced daytime stomatal closure under drought stress conditions. Conversely, it is thought that blue light has an influence on ABA induced activation of stomatal closure, namely the inhibition of the plasma membrane S-type anion channels (Marten et al., 2007).

Circadian gating influences the guard cell regulatory network

An inherent periodicity of stomatal response was already described by Francis Darwin in 1898, who observed that stomata opened in the morning under continuous darkness and that the opening response to light was greater during the day than during the night (Darwin, 1898; Martin and Meidner, 1971). This latter effect is generally known as circadian gating, where the oscillator of the circadian clock rhythmically enhances the sensitivity towards a regulatory stimulus (Harmer, 2009). Additionally, many plant species close their stomata already long before dusk in order to prevent excessive transpiration in the afternoon, when temperatures tend to be highest, further suggesting a circadian component in stomatal regulation. Finally, the circadian clock seems also to control pre-dawn opening, which occurs at the end of the night (Lebaudy et al., 2008). All these observations suggest a strong influence of the circadian clock on stomatal regulation in order to maximize photosynthetic capacity during times of illumination (Webb, 2003; Dodd et al., 2005).

Indeed, the *toc1-1* mutant, which shows circadian rhythms that are shortened by 3 h compared to wild type plants, also shows shortened rhythmicity in changes in its stomatal aperture (Somers et al., 1998). Similarly, the *ztl-1* mutant shows a longer free-running circadian rhythm, which causes the changes in the stomatal aperture to

cycle with a periodicity approximately 5 h longer than in wild type plants (Dodd et al., 2004). This, together with the observation that guard cells in isolated epidermal peels still show circadian rhythms, strongly argues for the presence of a cell autonomous circadian clock in guard cells (Gorton et al., 1989; Webb, 2003).

Recent investigations into stomatal regulation found that the circadian clock influences the sensitivity of the blue-light signalling cascade during the early morning hours (Kinoshita et al., 2011; Ando et al., 2013; Kimura et al., 2015). The molecular link between the clock and blue light signalling was shown to depend on components of the photoperiodic pathway controlling flowering. Kinoshita and colleagues found that FLOWERING LOCUS T (FT), which was first described as the “florigen”, a small protein which travels from the vasculature to the shoot meristem to induce flowering (Corbesier et al., 2007; Mathieu et al., 2007), can have an influence on the signalling cascade in guard cells (Kinoshita et al., 2011). Because guard cells are symplastically isolated it seems possible that FT and other regulators of flowering time are also involved in this very distinct process. As in the regulation of flowering induction, *FT* expression in guard cells was shown to be under the control of the circadian clock. In the *early flowering 3* (*elf3*) mutant the repressive effect of the circadian clock on *FT* expression was released, which led to an early flowering phenotype (Kim et al., 2005) and at the same time to an increase in stomatal aperture, correlated with high activity of the plasma membrane H^+-ATPase (Kinoshita et al., 2011). This elevated H^+-ATPase activity was independent of light and was suggested to depend on the increased binding of 14-3-3 proteins to the proton pump. The exact molecular mechanism by which FT influences the activity of the proton pump is not known, but it should be mentioned that FT was shown to bind to 14-3-3 proteins during the activation of flowering at the shoot apex (Taoka et al., 2011). It seems possible that FT interacts with the 14-3-3 proteins involved in binding to the phototropins or to the H^+-ATPase, therefore priming the blue-light signalling cascade. Alternatively, FT could alter transcription in guard cells, influencing the abundance of the yet to be described kinase responsible for H^+-ATPase phosphorylation in response to blue light.

In subsequent studies additional components of the flowering regulatory network (Srikanth and Schmid, 2011), such as the *FT*-paralog TWIN SISTER OF FT (TSF) (Yamaguchi et al., 2005) and SUPPRESSOR OF OVEREXPRESSION OF CO 1 (SOC1), a MADS-box transcription factor (Hepworth et al., 2002), were shown to act together with FT in the regulation of stomatal aperture (Kinoshita et al., 2011; Ando et al., 2013; Kimura et al., 2015). Guard cell protoplasts of *soc1-10* mutants showed

reduced expression levels of blue-light signalling components such as *BLUS1*, *PRSL1* and several H^+-ATPases, suggesting an influence on the transcriptional regulation of blue light signalling components, leading to an increase in their sensitivity (Kimura et al., 2015). Fusicoccin treatment could rescue the stomatal aperture phenotype in the *ft-2*, *tsf-1* and *soc1-10* mutants, suggesting that the photoperiodic flowering pathway in guard cells does not influence targets downstream of the H^+-ATPases (Ando et al., 2013; Kimura et al., 2015). Additionally, overexpression of GIGANTEA (GI) and CONSTANS (CO), known regulators of *FT* expression linking the output of the circadian clock to flower induction (Turck et al., 2008), showed a constitutive open stomatal phenotype, while the *co-1* and *gi-1* mutants had an inhibited response to light (Ando et al., 2013).
Further proof of the involvement of the circadian clock in stomatal regulation through FT comes from the investigation of cryptochrome mutants, which are important for the correct entrainment of the circadian clock to a 24 h periodicity (Mockler et al., 2003) and are involved in the stabilization of GI and CO proteins (Liu et al., 2008; Yu et al., 2008) In the *cry1cry2* mutant *FT* and *TSF* transcripts were reduced, which together with the above discussed regulation of ABA levels can explain the impaired stomatal aperture phenotype of *cry1cry2* (Boccalandro et al., 2012; Ando et al., 2013). Cryptochromes are therefore involved in the sensing of the photoperiod and increase the phototropin mediated blue light opening response through the regulation of FT and TSF expression under long day photoperiods.

Interestingly, in addition to the photoperiodic pathway, the vernalization pathway of flowering control seems to play a role in stomatal regulation of Arabidopsis ecotypes containing a functional FRIGIDA (FRI) allele, which showed a reduced stomatal aperture compared to Col-0 (Kimura et al., 2015). The common Arabidopsis lab strain Col-0 contains a null allele for the floral repressor FRI (Johanson et al., 2000), which normally increases the expression of FLOWERING LOCUS C (FLC), a potent repressor of FT, TSF and SOC1 in winter annual accessions of Arabidopsis (Koornneef et al., 1994; Helliwell et al., 2006; Choi et al., 2011). Therefore the necessity of vernalization for flower induction in Col-0 and other rapid cycling ecotypes is lost (Michaels et al., 2005). In contrast, *FRI*-Col and winter annual Arabidopsis accessions require several weeks of cold temperatures before flowering is induced, ensuring the start of the reproductive phase in the spring (Lee and Amasino, 1995). Cold temperatures are known to reduce FRI content (Sung and Amasino, 2005), therefore releasing the repression of the expression of the floral integrator genes FT, TSF and SOC1 (Johanson et al., 2000). Vernalization was also

shown to eliminate the reduced stomatal aperture phenotype of FRI-Col compared to Col-0 in response to light (Kimura et al., 2015). This mechanism would enable winter annual Arabidopsis accessions to increase stomatal aperture in spring during the reproductive phase, while limiting the aperture (and with this photosynthetic rate and transpiration) during the vegetative growth phase before the onset of winter.

In summary, the vernalization pathway has a negative effect on stomatal aperture in winter annual accessions, while the photoperiodic pathway of flowering regulation seems to have a positive, but indirect, effect on blue-light induced stomatal opening. Together this would enable plants to increase their stomatal conductance and therefore photosynthetic capacity upon flower induction.

Temperature and other factors

Besides these well described pathways, other environmental factors have an influence on stomatal behaviour. One of these factors is the ambient temperature. Cold temperatures are known to close stomata via the induction of cytosolic Ca^{2+} oscillations (Allen et al., 2000) and this reaction is strongly circadian gated (Dodd et al., 2006). On the other hand, heat induces stomatal opening, which leads to an elevated transpiration rate and therefore to the cooling of the leaves. In natural environments however, heat often occurs together with drought stress, which counteracts the temperature induced stomatal opening (Schulze et al., 1973; Rizhsky et al., 2004).

Besides temperature, high ozone levels have a profound effect on guard cells. In order to restrict damaging ozone uptake into the leaves, stomata close via a signalling pathway initiated by the ozone-induced rise of ROS and the ROS perception at the plasma membrane (Hua et al., 2012; Song et al., 2014). The further signalling cascade might interact with other pathways at the level of PP2C mediated OST1 regulation and leads ultimately to the activation of plasma membrane anion channels (Kollist et al., 2007; Vahisalu et al., 2010).

Finally, stomatal closure is an important plant response to pathogen attack. Pathogens, such as fungi and bacteria use stomata as entry points to reach the underlying stomatal cavities. The detection of microbe-associated molecular patterns (MAMPs) (Boller and Felix, 2009) leads to a signalling cascade mediated through OST1-dependent activation of the S-type anion channels SLAC1 and SLAH3, finally causing stomatal closure (Guzel Deger et al., 2015; Ye et al., 2015).

Understanding of guard cell carbon metabolism for crop breeding

Already with the elucidation of the first components in the guard cell signalling network, the first approaches to improve drought resistance and biomass production under water scarcity via changes of guard cell physiology were initiated (Schroeder et al., 2001b; Lawson et al., 2014). When altering the guard cell regulatory network it is often observed that the reduction in water loss results also in a reduction of carbon assimilation and subsequently in growth (Eisenach et al., 2012; Antunes et al., 2012; Lawson et al., 2014). Therefore it is important to optimize water use efficiency (WUE), while at the same time avoiding the restriction of photosynthetic rates (Lawson and Blatt, 2014). A better understanding of guard cell metabolism can contribute in finding new targets for the manipulation and breeding of drought tolerant and high yielding crop species.

Guard cell carbon metabolism and especially starch degradation is implicated since a long time in guard cell movement (Lloyd, 1908; Outlaw, Jr., 2003; Lawson et al., 2014). Despite great efforts of the research community not much about the molecular regulation of starch breakdown in guard cells is known. Many studies relied on model species such as *Vicia faba*, where the tools for elucidating the genetic basis of guard cell carbon metabolism are limited. Therefore, the use of the genetic resources available for Arabidopsis is promising to unravel the role of starch in guard cells.

The current state of the field of starch metabolism research with a focus on Arabidopsis transitory starch will be discussed in the next section, followed by a summary of our current understanding of guard cell carbon metabolism.

Starch metabolism

Starch is an important biopolymer

Starch is found in all chlorophyta (land plants and green algae), where it is thought to have evolved soon after the endosymbiosis event which led to the development of chloroplasts (Ball et al., 2011). Transitory or primary starch of land plants is synthesized and stored in the chloroplasts of leaf cells during the day and is almost fully degraded during the night, when the derived sugars are needed for cellular respiration and as building blocks for the synthesis of biomolecules (Smith et al., 2005). In contrast, storage or secondary starch is synthesized over the course of several days or weeks in storage tissue like the endosperm of wheat, rice and maize and in the tubers of cassava and potato, which all serve as important food sources

for humans and animals. Furthermore, the physico-chemical properties of starch granules can be employed in a wide range of industrial applications and developing different kinds of starch could yield biopolymers with novel traits and applications (Santelia and Zeeman, 2011).

Starch is composed of the highly branched molecule amylopectin formed by up to 1 mio glucose units and containing branch points at every 20 to 25 glucosyl residues and smaller amylose molecules, which contain only very few branch points. Depending on the plant specie, amylose content varies between 6% in Arabidopsis and up to 60% in kernels of certain varieties of maize (Zeeman et al., 2002; Glaring et al., 2006) and is one important determinant of the physico-chemical properties of starch. The glucose units of both molecules are linked via linear α-1,4-glycosidic bonds, while α-1,6-glycosidic bonds form the branch points. The shorter branches of amylopectin form double helical structures, which cluster together forming a crystalline matrix, responsible for the insoluble nature of starch granules. In contrast, the branch points form amorphous lamellae, which alternate with the crystalline regions of the granules at a periodicity of approximately 9 nm (Zeeman et al., 2002). Amylose is mainly synthesized as a helical structure within the amorphous lamellae (Denyer et al., 2001). Depending on the plant species and tissue types amylopectin and amylose form together granules between 0.1 and 200 µm in diameter, which can have very different morphologies (Jane et al., 1994; Pérez and Bertoft, 2010).

Synthesis of starch

During the day plants fix CO_2 in photosynthetically active tissues such as palisade and mesophyll cells of the leaves through the Calvin cycle, using ATP and reducing equivalents produced in the light reaction of photosynthesis (Figure 5). The resulting photoassimilates are either used for the synthesis of starch or exported from the chloroplast, mainly for sucrose synthesis and subsequent transport to heterotrophic tissues. In Arabidopsis, almost half of the photoassimilates are used for the synthesis of transitory starch (Zeeman and Ap Rees, 1999).

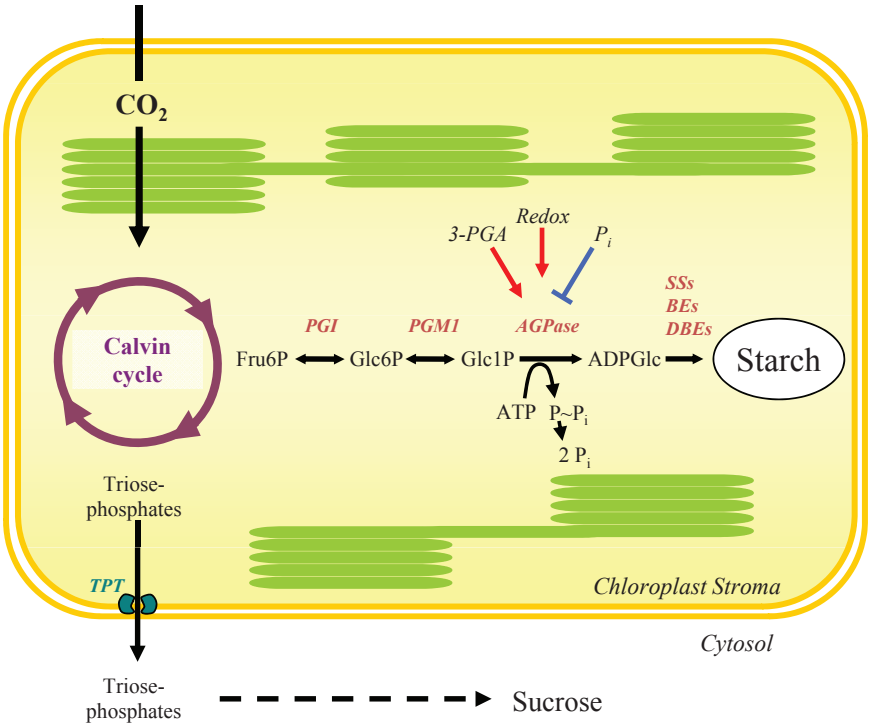

Figure 5: The pathway of leaf starch biosynthesis. Figure is taken from Streb & Zeeman 2012. See text for details.

Chloroplast contain TRIOSE PHOSPHATE/PHOSPHATE TRANSLOCATORs (TPTs), which export triose phosphates and the Calvin cycle intermediate 3-phosphoglycerate (3PGA) to the cytosol (Schneider et al., 2002), while a certain fraction of the Calvin cycle intermediate Fructose-6-P (Fru6P) is converted in a series of reactions to yield the glucosyl donor ADP-Glucose (ADP-Glc) for starch synthesis (Zeeman and Ap Rees, 1999). The initial step is catalysed by plastidial PHOSPHOGLUCOSE ISOMERASE (PGI), which converts Fru6P into Glucose-6-phosphate (Glc6P) (Caspar et al., 1985). A point mutation in the *PGI* coding sequence leads to an almost complete loss of plastidial PGI activity in the *pgi1-1* mutant and to a strong decrease in leaf starch accumulation (Yu et al., 2000). Interestingly, the accumulation of starch granules in the root cap is not affected (Yu et al., 2000), which can be explained with the activity of GLUCOSE-6-PHOSPHATE/PHOSPHATE TRANSLOCATORs (GPT1 and GPT2) in heterotrophic tissues like roots, flower organs and seeds (Borchert et al., 1989; Kammerer et al., 1998; Niewiadomski et al., 2005). GPT1 and GPT2 were shown to be functional Glc6P importers located in the plastidial envelope (Kammerer et al., 1998). Due to the tissue specific expression pattern of *GPT1* and *GPT2*, which are hardly found in photosynthetically active cells (Niewiadomski et al., 2005), the import capacity of Glc6P into chloroplasts of mesophyll cells of the *pgi1-1* mutant is too low to

compensate for the loss of plastidial PGI activity, while starch synthesis is not affected in roots and other heterotrophic tissues. In the subsequent step, the plastidial isoform of PHOSPHOGLUCOMUTASE (PGM1) catalyses the conversion of Glc6P into Glucose-1-phosphate (Glc1P) (Caspar et al., 1985).

Finally, ADP-glucose pyrophosphorylase (AGPase) synthesizes ADPGlc and inorganic pyrophosphate (PP_i) from Glc1P and ATP. Although this reaction is theoretically reversible, the rapid cleavage of PP_i by plastidial pyrophosphatases into two orthophosphates (P_i) (George et al., 2010) strongly favours the synthesis of ADP-Glc. The AGPase enzyme is a heterotetramer consisting of two catalytic and two regulatory subunits. The catalytically active small subunit is encoded by the ubiquitously expressed *AGPase SMALL SUBUNIT 1* (*APS1*), with the closely related *APS2* gene likely encoding a non-functional isoform (Lin et al., 1988a; Crevillén et al., 2003). The regulatory subunits in Arabidopsis are encoded by four genes (*APL1-4*) (Lin et al., 1988b; Ventriglia et al., 2008), which show a differential expression pattern.

AGPase is tightly regulated in order to ensure a connection between the activity of the photosystems and the Calvin cycle with the rate of starch synthesis and is considered to be the rate limiting step. The allosteric effectors 3-phosphoglycerate (3PGA), an indicator of CO_2 fixation in the Calvin cycle, and P_i are known to bind to the regulatory subunits leading to the activation or inhibition of enzyme activity, respectively (Crevillén et al., 2003).

The combinations of APS1 with the different large subunits can change the kinetic properties of the enzyme complex, enabling the fine tuning of the rate of starch synthesis. In photosynthetic tissues the AGPase enzyme shows high substrate affinity and high sensitivity towards allosteric effectors and is usually formed by APS1 and APL1 (Crevillén et al., 2003; Mugford et al., 2014). In contrast, APL3 and APL4 are thought to be involved in the synthesis of starch in heterotrophic tissues, forming proteins with reduced sensitivity to allosteric effectors and also lower substrate affinity (Crevillen et al., 2005; Ventriglia et al., 2008).

Sugars can induce the gene expression of *APL3* and *APL4*, but not *APL1* or *APL2*, in leaves (Crevillen et al., 2005). The kinetic properties of AGPase can therefore be changed under conditions of high sugar availability. A second level of regulation is based on the opening of an intermolecular disulphide bridge between the two small subunits of the heterotetrameric enzyme through thioredoxin-mediated reduction (Fu et al., 1998; Tiessen et al., 2002; Hendriks et al., 2003). In illuminated mesophyll chloroplasts, THIOREDOXIN *f*1 (Trx*f*1) links the activity of photosystem I (PSI) via

the reduction of AGPase to the activation of starch synthesis (Thormählen et al., 2013). Furthermore, sugars are able to induce the reductive activation of AGPase in illuminated and darkened leaves as well as in non-photosynthetic tissues like root cap cells and potato tubers (Hendriks et al., 2003; Kolbe et al., 2005). This mechanism involves sugar sensing via Trehalose-6-phosphate (T6P), which is a readout for cytosolic sucrose levels, as well as hexokinase-dependent glucose signalling (Tiessen et al., 2003; Kolbe et al., 2005). It is clear that redox activation of AGPase in response to high sugar concentrations in non-photosynthetic tissue and in darkened leaf cells can not be mediated by Trx*f*1, which is under these conditions in its inactive, oxidized state. It was rather shown to be dependent on a plastidial NADP-THIOREDOXIN REDUCTASE C (NTRC) (Michalska et al., 2009). Instead of electrons transferred from PSI via ferredoxins, NTRC uses NADP generated through metabolic processes, mainly respiration and oxidative pentose phosphate pathway and can therefore operate in darkened leaves as well as in non-photosynthetic tissues (Serrato et al., 2004).

The synthesis of correctly structured amylopectin requires the presence of four soluble STARCH SYNTHASES (SS1-4) (Szydlowski et al., 2009, 2011). SSs transfer the glucose from ADP-Glc onto the non-reducing end of a preformed glucosyl-chain, establishing a new α-1,4-link. The enzymes differ mainly in their preference to elongate chains of a certain length, with SS1 preferring to transfer a new glucose unit to chains of 9-10 units, SS2 to intermediate chains of 13-22 units and SS3 transfers glucose units preferentially to long chains with over 25 units in length (Delvallé et al., 2005; Zhang et al., 2008)

Furthermore, SS3 and SS4 were implicated in starch granule formation. Depending on species and organs starch granules can differ in number per plastid as well as in morphology, with Arabidopsis wild-type chloroplasts in the leaves typically containing three to five granules (Jane et al., 1994; Crumpton-Taylor et al., 2012). In contrast to mammals, where the initiation of glycogen synthesis by the self-glycosylating protein glycogenin is well described, the initiation mechanism in plants remains elusive. Plants contain proteins similar to mammalian glycogenin proteins and might therefore rely on a similar mechanism, although no clear evidence was presented so far (Chatterjee et al., 2005). Interestingly, *ss4* mutants have only one large granule, while the *ss3ss4* double mutant did not synthesise starch at all, suggesting a possible role of SS3 and SS4 in granule initiation (Roldán et al., 2007; Szydlowski et al., 2009).

New α-1,6-linked branches are introduced by the glucanotransferases STARCH BRANCHING ENZYME 2 and 3 (BE2, BE3), through the transfer of an approximately 6 glycosidic unit long fragments removed from the non-reducing end to another chain (Dumez et al., 2006). The loss of both enzyme activities in the *be2be3* double mutant abolishes starch synthesis and leads to the accumulation of high concentrations of maltose. A third predicted gene initially thought to code for another starch branching enzyme (*BE1*) has no detectable branching activity on amylopectin, but rather seems to play a role in embryo development (Dumez et al., 2006; Wang et al., 2010b).
Interestingly, two of the four debranching enzymes (DBEs) from Arabidopsis, ISOAMYLASE1 (ISA1) and the catalytically inactive ISOAMYLASE2 (ISA2), are also important for the correct synthesis of starch granules (Wattebled et al., 2005; Delatte et al., 2005; Streb et al., 2012). Active DBEs can hydrolyse the α-1,6-branchpoints and release linear oligosaccharides into the plastid stroma. The loss of either ISA1 or ISA2 leads to a strong inhibition of starch synthesis and the accumulation of glycogen-like, water-soluble polysaccharides called phytoglycogen (Wattebled et al., 2005). It is thought that the two Arabidopsis isoamylases act together as a heteromultimeric enzyme, necessary for the removal of surplus branches, which is a requirement for the correct folding of glucan chains into helical structures (Delatte et al., 2005; Sundberg et al., 2013). If ISA1 or ISA2 is missing, the establishment of the semi-crystalline lamellae takes more time, caused by small, misplaced or surplus branches introduced by branching enzymes (O'Sullivan and Perez, 1999). This gives amylolytic enzymes access to shorten or remove branches, thereby further inhibiting the proper formation of starch granules, although DBEs are not absolutely required for starch synthesis (Streb et al., 2008). It was therefore suggested that once crystallized, amylopectin is protected from further amylolytic modifications until the structure is disrupted at the onset of starch degradation (Streb et al., 2008).

Amylose is synthesized by GRANULE-BOUND STARCH SYNTHASE (GBSS), which is targeted to the starch granule surface by PROTEIN TARGETING TO STARCH (PTST) and becomes subsequently enclosed in the amylopectin matrix (Tatge et al., 1999; Denyer et al., 2001; Seung et al., 2015). Plants lacking GBSS synthesise starch that consists solely of amylopectin (so called *waxy* starches), indicating that amylose is not absolutely required for granule formation (Denyer et al., 2001; Ovecka et al., 2012). GBSS uses ADP-Glucose, which is able to diffuse through the amylopectin matrix, to processively elongate glucan chains. This is in contrast to the amylopectin synthesizing soluble SSs, which add one glucose unit to a glucan chain and then diffuse off again (Denyer et al., 1999). The linear glucan chains synthesized

by GBSS are inaccessible to branching enzymes located in the stroma and can therefore not be modified, but rather form single helical structures (Denyer et al., 2001).

Starch degradation

Night-time starch degradation of transitory leaf starch (Figure 6) occurs at a near linear rate, until almost all reserves are transformed into sugars by the end of the dark phase. Sugars, primarily maltose and to a lesser extend glucose and Glc1P, are further metabolised in the cytosol for energy production and biosynthetic processes. The precise coordination of the rate of starch degradation with the photoperiod is important to ensure optimal growth (Stitt and Zeeman, 2012). If starch reserves are depleted prematurely, plants enter a transient phase of starvation, while residual starch at the end of the night is non-productive and growth is inhibited in both cases. Starch degradation stops soon after sunrise and there is presumably no breakdown occurring during times of starch synthesis (Zeeman et al., 2002).

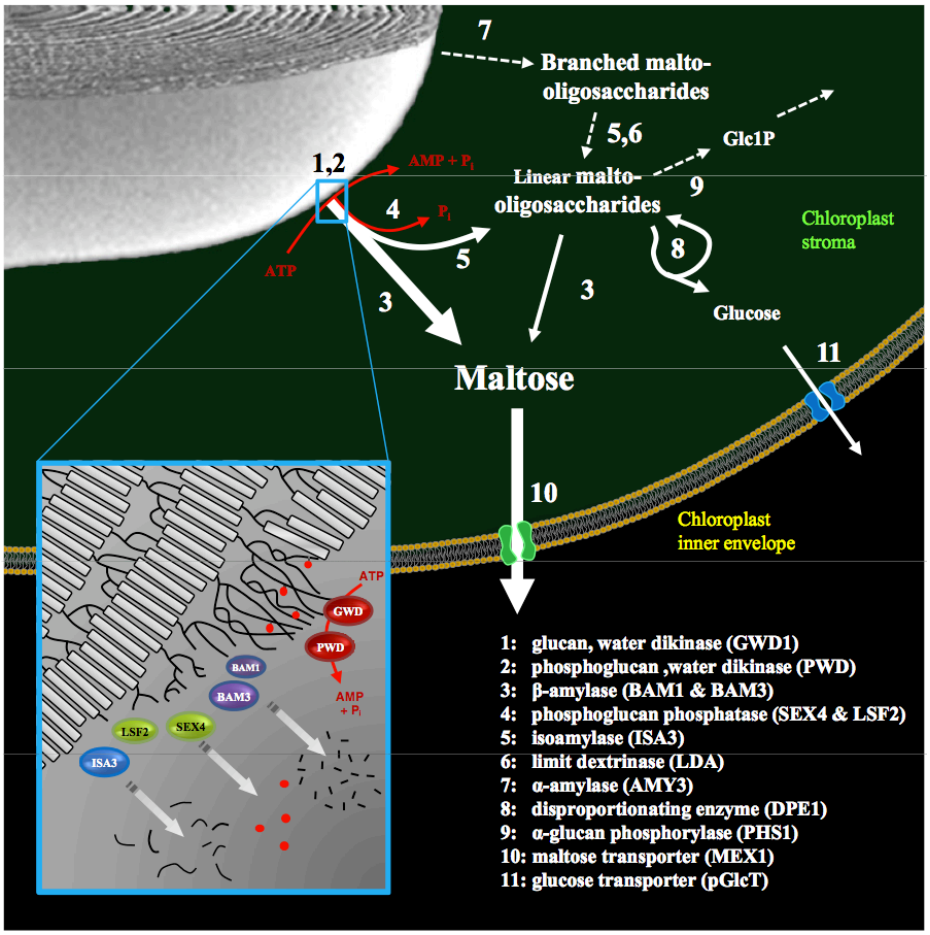

Figure 6: The pathway of leaf starch degradation in Arabidopsis during the night. Taken from Streb & Zeeman 2012. See text for details.

It was suggested that in leaves of Arabidopsis fully crystallized granules are protected from amylolytic enzymes, unless the surface is disrupted (Streb et al., 2008), preventing starch degradation during the day. This disruption of the amylopectin structure is achieved by reversible phosphorylation of the glucan chains through the activity of several α-glucan water dikinase enzymes (Streb and Zeeman, 2012). During times of net degradation, approximately 1 in 2000 glucosyl residues are phosphorylated at the C6 and to a lesser extend at the C3 position (Ritte et al., 2006; Santelia et al., 2011). This phosphorylation is thought to disrupt the helical structure of neighbouring amylopectin glucan chains, thereby solubilizing the granule surface, enabling the attack by amylolytic enzymes (Blennow and Engelsen, 2010). Investigations into the strong starch excess mutant *sex1* of Arabidopsis plants revealed a reduced level of starch phosphorylation, attributable to the loss of an enzyme termed α-GLUCAN, WATER DIKINASE 1 (GWD1) (Yu et al., 2001; Ritte et al., 2002). GWD1 phosphorylates glucosyl units at the C6 position, enabling a second glucan kinase, PHOSPHOGLUCAN, WATER DIKINASE (PWD) to transfer a phosphate group to the C3 position of another glucose molecule (Baunsgaard et al., 2005; Kötting et al., 2005). The C6 phosphorylation by GWD is thought to be a signal and a pre-requisite for the PWD catalysed phosphorylation of C3 sites, which then cause the actual disruption of the helices, followed by the hydration and degradation by amylolytic enzymes, especially β-amylases (Edner et al., 2007; Blennow and Engelsen, 2010).

Interestingly, another Arabidopsis mutant with a strong starch excess phenotype, *sex4*, was shown to be impaired in a phosphoglucan phosphatase (Zeeman et al., 1998; Niittylä et al., 2006; Kötting et al., 2009). The SEX4 enzyme releases both C6 and C3 phosphate groups from phosphoglucans during starch degradation (Hejazi et al., 2010). This seemingly contradictory process is important for the complete degradation of glucan chains by β-amylases, which are unable to release maltose from chains containing phosphate groups (Takeda and Hizukuri, 1981). Besides SEX4, two additional phosphoglucan phosphatases, LIKE SEX FOUR1 (LSF1) and LIKE SEX FOUR2 (LSF2) have been identified in Arabidopsis. LSF2 was shown to be catalytically active preferentially on C3 phosphorylated glucosyl units (Santelia et al., 2011), while the LSF1 protein might be catalytically inactive, although the *lsf1* mutant plants show a sex phenotype in the leaves (Comparot-Moss et al., 2010). It is therefore possible that LSF1 has a regulatory role during starch degradation.

Following granule surface solubilisation, α-1,4- and α-1,6-bonds of the glucan chains can be hydrolysed by several classes of proteins of which the exoamylases of the β-AMYLASE (BAM) family can be considered as key enzymes (Streb and Zeeman, 2012). Arabidopsis contains nine genes that encode proteins of the β-amylase family (BAM1-9) according to the presence of the conserved β-amylase domain, several of which show catalytic activity towards the release of maltose from the non-reducing ends of polyglucan chains (Fulton et al., 2008). Of these nine BAMs, only four (BAM1-4) are targeted to the chloroplast (Lao et al., 1999; Sparla et al., 2006; Fulton et al., 2008). While BAM2 has only a very low enzymatic activity and BAM4 activity is not detectable at all, recombinant BAM1 and BAM3 proteins are highly active against polyglucan substrates (Fulton et al., 2008). Mutants deficient in active BAM3 show a mild *sex* phenotype, which is much more pronounced in the *bam1bam3* double mutant, although the single *bam1* mutant does not depict higher starch contents in the leaves, indicating that the two BAMs have partially overlapping roles and that BAM1 can partially complement the *bam3* phenotype (Fulton et al., 2008). Under normal growth conditions BAM1 seems to be preferentially expressed in guard cells and root cap cells, while its transcription can be induced in the full leaf upon osmotic stress treatment (Sparla et al., 2006; Valerio et al., 2011). This suggests a specialized role in certain cell types and under non-standard growth conditions such as abiotic stress as well as in mutants lacking *bam3* enzymatic activity. It should be mentioned that under cold stress conditions a specific role for BAM3-dependent starch degradation was shown, indicating a further specialization between the two β-amylase isoforms (Kaplan and Guy, 2005). In addition, BAM1 activity, but not the activity of BAM3, is redox sensitive and can be induced by the reduction of an intramolecular disulphide bridge by chloroplastic thioredoxins (Sparla et al., 2006; Valerio et al., 2011). This suggests, together with the higher activity of BAM1 at elevated pH and temperatures compared to the BAM3 protein, a role in day time starch degradation in guard cells (Sparla et al., 2006; Valerio et al., 2011; Monroe et al., 2014).

While the role of BAM2 is not known, the strong starch excess phenotype of the *bam4* mutant, despite its lack of enzymatic activity, suggests a regulatory role for BAM4, although its function is unknown (Fulton et al., 2008). Interestingly, two other non-plastidial isoforms, BAM7 and BAM8, were shown to have acquired a completely new function as nuclear localized transcription factors able to bind to DNA (Reinhold et al., 2011; Soyk et al., 2014). They were shown to play a role in the regulation of leaf growth and development, probably via a crosstalk with the brassinosteriod signalling pathway (Reinhold et al., 2011). Furthermore, BAM5, which is localized in

the cytosol of phloem tissue, shows an extremely strong catalytic activity towards polyglucans *in vitro* using crude plant extracts, although its roles *in vivo* remain unknown (Laby et al., 2001; Monroe et al., 2014). Similarly, the physiological role of BAM6 and BAM9 need further investigation.

BAMs are not only inhibited by phosphorylated glucan chains, but also cannot release maltose after α-1,6-branch points. Complete starch degradation requires therefore the presence of debranching enzymes. The major isoform of DBEs during night-time leaf starch degradation is ISOAMYLASE 3 (ISA3). Another DBE, LIMIT DEXTRINASE (LDA), which belongs to the pullulanase-like class of debranching enzymes, seems to have a minor, but still significant, role in leaf starch degradation (Wattebled et al., 2005; Delatte et al., 2006). Similarly to BAM1 and BAM3, the *isa3lda* double mutant shows a stronger starch excess phenotype compared to the *isa3* single mutant and the mild *lda sex* phenotypes (Delatte et al., 2006). Both DBEs remove α-1,6-branch points preferentially of short side chains (3-5 glucose units), which are produced by the activity of β-amylases at the starch granule surface, in contrast to the longer branches produced by branching enzymes during starch synthesis (Streb et al., 2008).

The described role of BAMs during degradation of transitory leaf starch differs from the well described mechanism of storage starch breakdown in cereal endosperm, which is required for fuelling the germination and initial growth of the embryo. In cereals the endoamylolytic α-AMYLASEs (AMYs) are secreted by aleuron cells in the endosperm, while BAMs do not seem to play a major role (Fincher, 1989; Ziegler, 1999). AMYs are able to hydrolyse α-1,4-glycosidic linkages of starch in order to release short oligosaccharides, which can contain branch points. Because Arabidopsis and other members of the Brassicaceae family store primarily fatty acids as a carbon source in their seeds, an involvement of α-Amylases in seed germination seems unlikely. Nevertheless, AMYs are encoded in the Arabidopsis genome by three genes (*AMY1*, *AMY2*, *AMY3*) (Stanley et al., 2002; Yu et al., 2005). Of these three, only AMY3 is located to the chloroplast, but although this points to an involvement of AMY3 in starch breakdown, the single *amy3* mutant as well as the *amy1amy2amy3* triple mutant do not show a starch excess phenotype (Yu et al., 2005). It was therefore proposed that *amy3* is not necessary for transitory starch breakdown in mesophyll cells during the night (Yu et al., 2005). Later it was found that AMY3 does contribute to starch degradation and that only the loss of AMY3 in the *isa3lda* double mutant completely blocks starch degradation, while small

branched soluble oligosaccharides produced by the AMY3 enzyme are found in *isa3lda* mutants (Delatte et al., 2006; Streb et al., 2008, 2012). Interestingly, AMY3 activity was recently shown to be redox-regulated (Seung et al., 2013). The roles for AMY1 and AMY2 are not entirely clear, as they are not localized in the chloroplast. AMY1 shows catalytic activity and is most likely secreted from cells (Stanley et al., 2002; Doyle et al., 2007), while no specific function is published for AMY2.

Besides maltose, the end products of the concerted action of β-amylases and DBEs are maltotriose and maltotetraose, which can not be further processed by BAMs. Rather, another enzyme, the α-1,4-glucanotransferase DISPROPORTIONATING ENZYME 1 (DPE1) localized in the chloroplast stroma is able to transfer a single glucose unit from maltotriose to a longer chain of soluble oligosaccharides, while releasing maltose (Critchley et al., 2001). The accumulation of maltotriose in the *dpe1-1* mutant was shown to cause a *sex* phenotype, most likely through a feedback inhibition on starch degradation (Critchley et al., 2001). Besides DPE1, Arabidopsis also contains a cytosolic localized isozyme, DPE2, which is important for the maltose metabolism after its export from the plastid. DPE2 is thought to transfer one glucose unit of maltose to a cytosolic heteroglycan molecule, releasing the second glucose unit for further metabolism (Lu and Sharkey, 2004; Fettke et al., 2006).

Besides the above described hydrolytic enzymes, the α-GLUCAN PHOSPHORYLASE 1 (PHS1) enzyme is able to degrade polyglucan chains releasing Glc1P through phosphorolytic cleavage of the α-1,4-glycosidic bonds (Zeeman et al., 2004). The reaction is intrinsically reversible, with a possible role of PHS1 in both starch synthesis and degradation. The direction is dependent on the cellular concentrations of Glc1P and P_i, which under physiological conditions (low Glc1P content) will favour the degradation over the synthesis direction in Arabidopsis leaves (Kruger and ap Rees, 1983; Rathore et al., 2009). Interestingly, the Arabidopsis *phs1* mutant shows no overall alterations in starch content, but shows lesions on its leaves and was reported to be more sensitive to a rapid decrease in relative humidity and salt stress compared to the wild type plants (Zeeman et al., 2004). It is possible that PHS1 releases Glc1P under abiotic stress conditions such as drought, which is directly used in plastidial metabolism, most notably the generation of NADPH in the plastidial oxidative pentose phosphate pathway. Therefore, the generation of Glc1P could be induced under stress conditions in order to provide reducing power for the scavenging mechanism against reactive oxygen species, which would explain the lesions observed on *phs1* mutant leaves (Zeeman

et al., 2004). The exact physiological role of PHS1 needs further investigation (see Chapter 2).
Another Arabidopsis gene encodes the cytoplasmic localized isoform PHS2 with a proposed role in cytosolic heteroglycan metabolism. Here, PHS2 is thought to release Glc1P (Lu et al., 2006), presumably from glucose units previously added by DPE2 during maltose cleavage (Fettke et al., 2004, 2006).

Products from starch degradation, maltose, glucose and presumably Glc1P are exported from the plastid by specific transporters. MALTOSE EXPORTER 1 (MEX1) is responsible for the export of the largest proportion of sugars released during starch breakdown (Niittyla et al., 2004), while glucose is exported by the GLT1 transporter (Cho et al., 2011). Blocking the major export route in the *mex1* mutant causes a severe growth phenotype with high maltose levels in the plastid as well as a *sex* phenotype (Niittyla et al., 2004; Lu and Sharkey, 2004). In contrast, the single *glt1* mutant displayed no obvious phenotype, but enhances the impaired growth phenotype of the *mex1* mutant in the *glt1mex1* double mutant (Cho et al., 2011). Glc1P produced by PHS1 can be used either in chloroplast metabolism (see above) or might be exported by a yet unknown transporter (Fettke et al., 2011).

Regulation of diurnal leaf starch metabolism

Starch synthesis and starch degradation are not just induced by illumination and darkness, respectively, but are rather tightly coordinated with the length of the photoperiod (Scialdone et al., 2013; Mugford et al., 2014). Under short photoperiods (e.g. 8 h light, 16 h dark), starch synthesis occurs at a higher rate and degradation is slowed down to avoid carbon starvation at the end of the night (Gibon et al., 2009). In order to achieve this plants seem to track the amount of starch reserves as well as predict the time until sunrise, using the internal circadian clock, adjusting rates of starch degradation accordingly (Graf et al., 2010; Scialdone et al., 2013). This immediate adjustment of starch breakdown in order to prevent carbon starvation at the end of the night can be observed for example when the dark phase sets in unexpectedly early (e.g. after 8 h instead of 12 h of illumination) (Graf et al., 2010). Although transcript abundance for many starch metabolism related genes show strong oscillations over the diurnal cycle, which is under circadian control (Smith et al., 2004), this is often not translated into changes in protein abundance and the control of starch degradation rates is therefore considered to occur mostly at the

posttranslational level (Lu et al., 2005; Yu et al., 2005; Skeffington et al., 2014). How and at which step of the pathway the information of the circadian clock about the expected night length is integrated with information about starch reserves is not known. Because glucan phosphorylation is the initial step in the induction of starch degradation, GWD1 and PWD are possible targets of the regulatory mechanism underlying these observations. Indeed, PWD was shown to be crucial for setting the correct rate of starch degradation during the night, while GWD1 was not (Scialdone et al., 2013; Skeffington et al., 2014). For starch synthesis rates the control seems to be at the level of AGPase, depending on changes in its allosteric properties, as well as on the circadian clock components GIGANTEA and FLAVIN-BINDING, KELCH REPEAT, F BOX1 protein (Gibon et al., 2004; Mugford et al., 2014). If and to what extend redox regulation of other enzymes play a role in the modulation of starch synthesis rates is unknown, although several enzymes were shown to be activated under reducing environments *in vitro* (Kötting et al., 2010; Glaring et al., 2012). Interestingly, several enzymes associated with starch degradation were also shown to be redox sensitive (Santelia et al., 2015). Further posttranslational modifications such as protein phosphorylation could play a role as well and several phosphopeptides have been described for PGI, PGM1, APL1, APS1 and SS3 of the starch synthesis pathway, as well as for GWD1, GWD2, DPE2, AMY3, BAM1, BAM3, LDA, GLT1, MEX1 associated with starch breakdown (Heazlewood et al., 2008; Kötting et al., 2010). Finally, enzyme activities as well as localization could be influenced through protein complexes. The first identified protein-protein interaction in Arabidopsis was published recently and involves the GBSS and the PTST proteins important for amylose synthesis as described above (Seung et al., 2015). Furthermore, wheat and maize endosperm BEs and SSs are known to interact *in vivo* (Hennen-Bierwagen et al., 2008; Tetlow et al., 2008).

Role of guard cell carbon metabolism

Guard cell starch degradation

Although the presence of guard cell starch granules during the night and their rapid degradation in the morning was reported more than 100 years ago (Lloyd, 1908), our knowledge about the involved enzymes and their unique regulatory properties as well as the exact function of early morning starch degradation in these specialized cells for plant physiology is scarce (Outlaw, Jr., 2003; Lawson et al., 2014). In model

plants for guard cell physiology, such as *Vicia faba*, guard cells contain starch granules at the end of the night, which are rapidly degraded in the morning. Starch breakdown is negatively correlated with stomatal aperture and potassium concentration, and is proposed to provide carbon skeletons for organic anion synthesis (Fischer and Hsiao, 1968; Outlaw and Manchester, 1979; Kang et al., 2007). In contrast to these observations, Stadler and colleagues reported that Arabidopsis guard cells contain only little starch at the end of the night (Stadler et al., 2003), although it should be noted that they showed only electron microscopy pictures and no quantitative analysis. Nevertheless, it is not clear if light-dependent starch degradation is a common feature of all plant guard cell chloroplasts (Lawson et al., 2014). Furthermore, the investigation of starch degradation in guard cells was so far mostly limited to establishing simple correlations between stomatal aperture and starch content. Therefore the characterization of guard cell carbon metabolism was described as “an important frontier in future research” by several researchers (Schroeder et al., 2001a; Outlaw, Jr., 2003).

In an earlier study using the genetic resources from Arabidopsis, Lasceve and colleagues showed that guard cell starch is especially important for blue light-induced stomatal opening (Lasceve et al., 1997). In the starchless *pgm* mutant, stomatal aperture was severely impaired under blue light, but not red light illumination, providing indirect evidence for a role of starch breakdown products during the initial early morning increase in guard cell osmolytes. Additionally, the observation in this study that a high concentration of chloride in the buffer medium could complemented the reduced opening in the *pgm* mutant plants is in accordance with the idea that guard cells can use either malate, presumably synthesized from starch breakdown products, or inorganic anions taken up from the apoplast as counterions to balance the positive charge of the accumulating K^+ (Raschke and Schnabl, 1978). The specificity of guard cell starch degradation under blue, but not under red light, was further supported by other researchers (Tallman and Zeiger, 1988; Olsen et al., 2002; Vavasseur and Raghavendra, 2005).

The first enzyme reported indicated to have a role in guard cell specific starch degradation was BAM1 (Valerio et al., 2011). Under normal growth conditions the expression of *BAM1* was restricted to guard cells and while the *bam1* mutant plants did not show an obvious overall *sex* phenotype, *bam1* guard cells had a higher starch content as well as reduced stomatal aperture. Interestingly, *BAM1* expression was induced under mannitol stress in the full leaves, indicating a role of BAM1 not

only in guard cells, but also in mesophyll cells in response to stress, where it could degrade starch reserves during the day for the synthesis of osmoprotectants. Both proposed roles of BAM1 are in agreement with the earlier observation that the BAM1 enzyme can be activated through thioredoxin-mediated opening of an intramolecular disulphide bridge (Sparla et al., 2006; Valerio et al., 2011). Moreover, the BAM1 enzymatic properties seem to suggest a daytime role when compared to BAM3, with BAM1 showing the higher temperature optimum as well as higher activity under more alkaline pH values, which are predominant in the chloroplasts during the day (Monroe et al., 2014).
In a recent publication, Prasch and colleagues observed the downregulation of BAM1 transcripts in wild-type plants under drought stress conditions, confirmed the starch excess phenotype of *bam1* guard cells and showed that these plants are indeed less drought sensitive (Prasch et al., 2015).

Interestingly, BAM1 is not the only enzyme involved in starch degradation that was shown to be redoxsensitive (Glaring et al., 2012; Santelia et al., 2015). The α-amylase AMY3, which is thought to be dispensable for transitory starch breakdown during the night, was also reported to be activated by thioredoxins (Yu et al., 2005; Seung et al., 2013). In an *in vitro* assay, Seung and colleagues showed that the simultaneous action of BAM1 and AMY3 had an additional effect on the rate of starch degradation with AMY3 releasing additional substrates in the form of small oligosaccharides for the action of BAM1. This lead us to the hypothesis that BAM1 and AMY3 function together in the early morning degradation of starch granules in guard cells as well as in the daytime degradation of transitory starch in response to stress (see Chapter 1 and Chapter 3).

Starch malate interconversion

With the increasing focus of the research community on the role of potassium in guard cell regulation, the starch to sugar hypothesis was replaced by the idea that guard cell starch breakdown is important for supplying carbon skeletons for malate biosynthesis (Outlaw, Jr., 2003; Lawson, 2009). Several observations, including the work on the *pgm* mutant described above (Lasceve et al., 1997), support this starch malate interconversion hypothesis.
Furthermore, a quantitative relationship between starch breakdown, malate synthesis and stomatal aperture was observed in *Vicia faba* (Outlaw and Lowry, 1977; Outlaw

and Manchester, 1979). A role of organic anions was also proposed by the observation that Cl^- uptake in *Vicia faba* is not absolutely necessary for balancing K^+ accumulation (Raschke and Humble, 1973). It was therefore concluded that the contribution of malate as a counterion for K^+ can be between 50% and up to 90%, depending on the availability of chloride (Raschke and Schnabl, 1978). Interestingly, guard cells of onion and related species do not contain any starch granules and they seem to exclusively use Cl^- as a counterion for K^+, while no malate accumulates in the early phase of stomatal opening (Schnabl and Raschke, 1980; Amodeo et al., 1996). Lastly, light or fusicoccin treatment are able to induce the activity of the guard cell isoform of PEP Carboxylase, which is necessary for malate formation (Meinhard and Schnabl, 2001; Outlaw et al., 2002).

It is generally assumed that malate is exported together with K^+ to the apoplast during stomatal closure (Van Kirk and Raschke, 1978b; Meyer et al., 2010), although early reports suggested the incorporation of malate into starch via gluconeogenesis (Schnabl, 1980). In a recent publication, Penfield and colleagues showed that malate metabolism is at least partially required for normal stomatal closure (Penfield et al., 2012). This suggests that malate is either converted into phosphoenolpyruvate (PEP) and subsequently into sugars via gluconeogenesis, which could be used for the synthesis of starch, or that malate is used to fuel cellular respiration in mitochondria.

Together, these observations strongly argue for starch breakdown for malate synthesis, induced by blue light illumination to counteract the charge of K^+ accumulation as well as to reduce the changes in cytosolic pH caused by the activation of H^+-ATPase. The fate of malate during stomatal closure on the other hand remains vague, but might depend on both excretion and metabolism. The molecular pathway of malate synthesis and the mechanism of malate removal during stomatal closure will be discussed in Chapter 2.

Role and mechanism of sucrose accumulation

Besides the accumulation of K^+ and its counterions, vacuolar sucrose concentrations were also show to increase over the day, possibly replacing the ions as the major osmolytes (Tallman and Zeiger, 1988; Poffenroth et al., 1992; Talbott and Zeiger, 1998). While the rapid opening in the morning can be attributed to the influx of potassium and the accumulation of its counter ions chloride and malate, the

concentrations of sucrose, but not glucose or other monosaccharides, was shown to increase in the afternoon, presumably to compensate for the decrease of potassium ions (Talbott and Zeiger, 1996).

Three mechanisms for sucrose accumulation are possible. Firstly, guard cell photosynthesis could supply sugars for the accumulation in guard cell vacuoles. Secondly, starch breakdown could yield sugars for sucrose synthesis, Lastly, sucrose produced in mesophyll cells could be taken up from the guard cell apoplast, where it accumulates during the day. The three possibilities are discussed briefly below.

Most plant species contain chloroplasts in their guard cells, which are able to perform the light reaction of photosynthesis, synthesizing ATP and reducing equivalents (Vaughn and Outlaw, 1983; Shimazaki and Zeiger, 1985). Although initially debated, guard cells do possess the ability for photosynthetic carbon fixation through Ribulose bisphosphate Carboxylase/Oxygenase (Rubisco) in the Calvin cycle (Zemel and Gepstein, 1985; Gotow et al., 1988; Lawson, 2009) and a significant contribution of photosynthetically produced sucrose was proposed (Poffenroth et al., 1992; Talbott and Zeiger, 1993).
In contrast, other research groups proposed that CO_2 fixation in guard cells through the Calvin cycle occurs at rates which are not sufficient to supply significant amounts of osmotically active sugars such as sucrose (Tarczynski et al., 1989; Shimazaki, 1989). For example, Reckmann and colleagues estimated that CO_2 fixation through Rubisco would supply only 2% of the required osmolytes in *Pisum sativum* guard cells (Reckmann et al., 1990). Furthermore, the rate of O_2 evolution in guard cells do not match with rates of CO_2 fixation, indicating that the energy and reducing equivalents produced in the light reaction are largely used for metabolic processes other than photosynthetic carbon fixation, such as malate synthesis and energizing the plasma membrane proton pumps (Gautier et al., 1991; Tominaga et al., 2001). In this scenario, both NADPH and ATP are exported into the cytosol via the phosphoglycerate/dihydroxyacetone phosphate shuttle (Shimazaki et al., 2007).
A simple reconciliation of this controversial data is the notion that guard cell metabolism is highly plastic and it is easily imaginable, that guard cell metabolism responds to different growth conditions (Outlaw, Jr., 2003). Therefore there might be no simple black and white answer, but the general consensus is that guard cell photosynthesis does not contribute significantly to the accumulation of sugars.

Sucrose could also originate from the breakdown products of starch, but starch degradation is thought to be induced by blue light, whereas sucrose accumulation seems to play a more prominent role under red light illumination, where guard cell starch is not degraded (Tallman and Zeiger, 1988; Vavasseur and Raghavendra, 2005). Interestingly, in starchless onion guard cells sucrose accumulated in the second half of the day as described for *Vicia faba*, arguing against a role of early morning starch breakdown for the synthesis of sucrose (Schnabl and Raschke, 1980; Amodeo et al., 1996). From these observations it seemed therefore unlikely that starch degradation contributes significantly to sucrose accumulation in the afternoon. Because of the difficulties to establish metabolomic analysis on guard cell samples, the question of sucrose accumulation in the morning has never been finally resolved.

Apoplastic sucrose levels in the cell walls of guard cells increase during the day, which is thought to lead to a decrease in stomatal aperture in the afternoon through increased apoplastic water potential (Lu et al., 1997; Kang et al., 2007). It is therefore possible that guard cells simply need to accumulate sucrose in their vacuoles to compensate for the increasing strength of the apoplastic osmotic potential and to prolong the phase of opened stomata. Sugar uptake is supported by reports demonstrating the import of sucrose and hexoses into guard cell protoplasts (Reddy and Das, 1986; Ritte et al., 1999).

Finally it should be mentioned that sucrose uptake, as well as the removal of vacuolar sucrose during stomatal closure, is likely to contribute significantly to the synthesis of guard cell starch, which will be discussed in Chapter 5. In summary, it can be assumed that K^+ and its counterions are used for the rapid opening controlled by blue light, whereas the role of intercellular sucrose might be more complicated, either maintaining the turgor pressure and counteracting the effect of apoplastic sucrose accumulation or even promoting stomatal closure via hexokinase signalling as reported recently (Kelly et al., 2013) and which will be discussed in Chapter 5.

AIM OF THIS THESIS

The main focus of this thesis was the elucidation of the role and the mechanism for starch degradation in guard cells of *Arabidopsis thaliana*. In order to achieve this, a new method had to be established, allowing the accurate quantification of guard cell starch. After it became clear that an adapted pseudo-Schiff – propidium iodide (PS-PI) staining combined with high resolution confocal laser scanning microscopy allows for superior quantification of starch content compared with the usually employed Lugol staining, the pathway of starch degradation in guard cells was investigated. Furthermore, the physiological role of guard cell starch degradation was investigated using infrared gas analysis in collaboration with Prof. Zeeman at ETHZ and the group of Dr. Lawson at the University of Essex. Finally, the connection between the activation of the starch degradation pathway and the light activated molecular pathways in guard cells was investigated with the help of several mutant lines as well as chemical activators and inhibitors of guard cell signalling. The results of these investigations are shown in Chapter 1 and Chapter 2.

Because BAM1 seems to be the most important enzyme during starch degradation in guard cells, a second focus of this thesis was the investigation of possible regulatory mechanisms that allow guard cells to rapidly degrade their starch upon illumination. Besides redox-control, it was previously noted that BAM1 is posttranslational phosphorylated and we speculated that this modification plays a role in the regulation of BAM1. First insights into BAM1 protein phosphorylation are presented in Chapter 4.

Besides the regulation of starch degradation, investigations into guard cell starch synthesis, which sets in immediately after the initial rapid starch degradation and continues until the end of the night, were another important part of my work. Here, I investigated the origin of sugar precursors for starch synthesis, i.e. guard cell photosynthesis or sugar import from the cytosol. In this context the role of sucrose import from the apoplast will be discussed. Furthermore, we began to investigate the role of the different isoforms of the large subunit of AGPase, which is assumed to catalyse the key regulatory step during starch synthesis. The results are shown in Chapter 5.

Finally, as stated above, BAM1 expression can be induced by osmotic stress in mesophyll cells. Our group continued with the investigations concerning the osmotic stress induced activation of day time starch degradation in mesophyll cells with a special focus on the roles of BAM1 and AMY3. The manuscript showing the results is presented in Chapter 3.

1 – Blue light induces a distinct starch degradation pathway in guard cells for stomatal opening

Daniel Horrer, Sabrina Flütsch, Diana Pazmino, Jack SA Matthews, Matthias Thalmann, Arianna Nigro, Nathalie Leonhardt, Tracy Lawson, Diana Santelia

Accepted for publication in Current Biology

Synopsis: In this report we show a quantitative analysis of Arabidopsis guard cell starch content with unprecedented temporal resolution. Guard cell starch is broken down within the first 30 min of illumination and requires blue light-dependent activation of the H^+-ATPase. The correct regulation of this process is shown to be important for stomatal aperture and plant biomass production.

Experimental contributions: S.F. analysed stomatal aperture and guard cell starch content in epidermal peels (Figure 4 D-F and Figure SI 3D and G), analysed the leaf starch content (Figure SI 1) and contributed to the data presented in Figure 4A and SI 3A. D.P. performed the qPCR transcriptional analysis (Figure 1 D, E and Figure 2A) and measured stomatal aperture data show in Figure SI 2A and D). M.T. measured the fresh weight data shown in Figure 2D. J.S.A.M. performed all gas exchange measurements in the laboratory of T.L.

Blue light induces a distinct starch degradation pathway in guard cells for stomatal opening

Daniel Horrer[1], Sabrina Flütsch[1], Diana Pazmino[1], Jack SA Matthews[2], Matthias Thalmann[1], Arianna Nigro[1], Nathalie Leonhardt[3], Tracy Lawson[2], and Diana Santelia[1*]

[1]Institute of Plant and Microbial Biology, University of Zürich, Zollikerstrasse 107, 8008 Zürich, Switzerland

[2]School of Biological Sciences, University of Essex, Colchester, CO4 3SQ, UK

[3]Laboratoire de Biologie du Développement des Plantes (LBDP), UMR 7265 CNRS-CEA Université Aix-Marseille II. CEA Cadarache Bat 156, 13108 St Paul Lez Durance, France

*Correspondence: dsantelia@botinst.uzh.ch (D.S.)

Highlights

- Starch in guard cells is degraded within 30 min of light to promote stomatal opening
- A distinct set of hydrolytic enzymes mediates starch degradation in guard cells
- Phototropin signaling and proton pumping control starch degradation in guard cells
- Guard cell starch drives plant growth through the control of stomatal aperture

In Brief

Horrer et al. report the first quantitative analysis of starch turnover in guard cells of intact leaves, showing that *Arabidopsis* is an ideal model plant to study guard cell starch metabolism. The authors exploit *Arabidopsis* molecular genetics and demonstrate that guard cell starch degradation integrates blue light-induced proton pumping with stomatal opening to control plant growth in response to light.

GRAPHICAL ABSTRACT

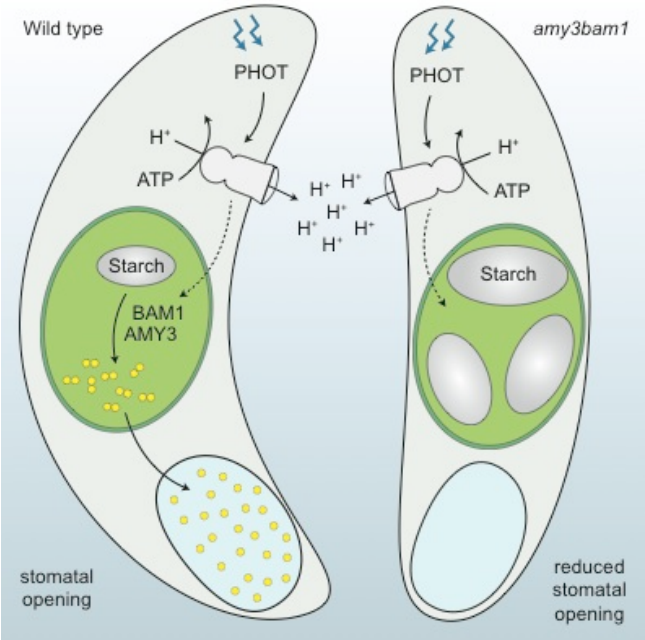

SUMMARY

Stomatal pores form a crucial interface between the leaf mesophyll and the atmosphere, controlling water and carbon balance in plants [1]. Major advances have been made in understanding the regulatory networks and ion fluxes in the guard cells surrounding the stomatal pore [2]. However, our knowledge on the role of carbon metabolism in these cells is still fragmentary [3–5]. Particularly, the contribution of starch in stomatal opening remains elusive [6]. Here, we used *Arabidopsis thaliana* as a model plant to provide the first quantitative analysis of starch turnover in guard cells of intact leaves during the diurnal cycle. Starch is present in guard cells at the end of night, unlike in the rest of the leaf, but is rapidly degraded within 30 min of light. This process is critical for the rapidity of stomatal opening and biomass production. We exploited *Arabidopsis* molecular genetics to define the mechanism and regulation of guard cell starch metabolism, showing it to be mediated by a previously uncharacterized pathway. This involves the synergistic action of β-amylase 1 (BAM1) and α-amylase 3 (AMY3) – enzymes that are normally not required for night-time starch degradation in other leaf tissues. This pathway is under the control of the phototropin-dependent blue light signalling cascade and correlated with the activity of the plasma membrane H^+-ATPase. Our results show that guard cell starch degradation has an important role in plant growth, by driving stomatal responses to light.

RESULTS

Starch dynamics in guard cells of intact *Arabidopsis* leaves

Starch is a complex glucose polymer found in plastids of higher plants [7]. In guard cell chloroplasts, starch has long been implicated in light-induced stomatal opening. Outlaw and Manchester showed 35 years ago that guard cell starch concentration was higher in leaflets of *Vicia faba* with closed stomata than with open stomata [8]. Schnabl showed a correlation between changes in volume of *Vicia faba* guard cell protoplasts and proposed the interconversion of malate and starch [9]. Talbott and Zeiger observed an increase in sucrose levels in *Vicia faba* epidermal peels throughout the light-stimulated stomatal opening concomitantly with the accumulation of the starch hydrolytic products maltose and maltotriose [10]. These observations led to the hypothesis that guard cell starch is mobilized in the light to generate malate and/or sucrose to sustain stomatal opening. After these early publications, the literature on the subject has been fragmentary and mostly correlative in nature, due to the lack of suitable methods and genetic material. Changes in guard cell starch concentrations were observed in other species (*Ocimum basilicum* and *Commelina communis),* but no details about the temporal dynamics nor the metabolic pathway were reported [4, 11]. In *Arabidopsis thaliana* – the most well studied model plant – there is no clear evidence of starch breakdown in guard cells in the light. Lasceve *et al.* showed electron micrographs of starch granules in *Arabidopsis* guard cells at the end of the night [12], suggesting that starch metabolism follows an opposite rhythm compared to mesophyll cells, where starch is degraded at night [13]. In contrast, Stadler and coworkers reported that starch was nearly absent in *Arabidopsis* guard cells at the end of the night [14]. Recently, Daloso *et al.* suggested that in tobacco guard cells changes in sugars – not starch – drive light-induced stomatal opening [15]. Due to these contradictory reports, guard cell starch metabolism is currently thought to differ between species [6] and its genetic and molecular basis remains mostly unknown.

Until now, starch content in guard cells has been mostly estimated on a relative value-scale by comparing the intensity of iodine-stained guard cell chloroplasts [11, 16–18]. A few studies have determined guard cell starch content quantitatively using the “oil well technique” on freeze-dried leaflets [8, 19], or spectrophotometrically using guard cell-enriched epidermal fragments [15]. In such cases, however, no details of temporal dynamics over the diurnal cycle were provided. Here, we developed a new method to quantify starch in guard cells of intact leaves. Epidermal peels from mature leaves were immediately fixed, treated with periodic acid, and the glucans covalently linked to the fluorophore propidium iodide. Confocal microscopy then enabled high- resolution analytical imaging to quantify the starch in guard cells over the diurnal cycle. This analysis was performed in *Arabidopsis* because this

plant is widely used as a model system for guard cell physiology, because of the contradictory literature regarding its guard cell starch metabolism, and to exploit the wealth of molecular genetic resources. As for other species [4, 8, 11], starch was present in *Arabidopsis* wild-type (WT) guard cells at the end of the night (Figures 1A-1C). In response to light, starch was rapidly degraded within an hour (Figures 1A-1C). As expected, guard cells of the *Arabidopsis* starch deficient mutant *pgm* (PHOSPHOGLUCOMUTASE 1*)* were devoid of starch (Figure 1A)[12]. Interestingly, in WT plants, starch started to decline during the latter part of the night and by dawn about half was gone. However, night-time degradation occurred slowly compared to the light-induced degradation (Figure 1B). Starch synthesis started 1 h into the light, was maintained for the rest of the photoperiod and continued into the night (Figure 1B). These results show that *Arabidopsis* guard cell starch metabolism differs markedly from the rest of the leaf, where starch is synthesized during the day and degraded at night in a near-linear manner [20].

BAM1 and BAM3 have a cell type-specific function

Next, we investigated the enzymes responsible for starch degradation in guard cells. β-amylase (BAM), which releases maltose from glucans, is the main starch-degrading enzyme [7, 13]. Mutant studies suggest that BAM3 is the major isoform in leaf mesophyll starch metabolism, while BAM1 has limited or no involvement [21]. Recently, it was shown that *bam1* mutants have more starch in illuminated guard cells and reduced stomatal opening compared to WT [18], which resulted in drought tolerance [17]. Consistently, we found that *BAM1* was preferentially and highly expressed in guard cell-enriched epidermal peels, similarly to established markers for guard cell-specific expression; the inward-rectifying *K+ CHANNEL IN ARABIDOPSIS THALIANA 1* (KAT1), *CYTOCHROME P450 86A2* (CYP86A2) and *MYB TRANSCRIPTION FACTOR 60* (MYB60) (Figures 1D and 1E)[22, 23]. Compared with WT, *bam1* mutants displayed a guard cell-specific *starch excess* (*sex*) phenotype throughout the diurnal cycle (Figures 1A-1C, and S1). To provide direct genetic evidence that the mutation in *BAM1* was responsible for the guard cell *sex* phenotype, we repressed *BAM1* in guard cells of WT using microRNA-induced gene silencing (MIGS)[24], driven by the *CYP86A2* promoter [23]. *BAM1* silencing lines showed reduced guard cell *BAM1* transcript levels and increased starch content, mimicking the *bam1* phenotype (Figures 1A, 1C and 1E). These results show that, under standard growth conditions, BAM1 functions specifically in guard cell starch metabolism. In contrast, *BAM3* transcripts were considerably less abundant in guard cells (Figure 1D) and guard cell starch levels in *bam3* were similar to WT (Figures 1A-1C). This suggests that BAM1 and BAM3 acquired different cell type-specific functions. Interestingly, *bam1bam3* double mutants had similar guard cell starch content to the *bam1* single mutants (Figures 1A and 1C). This contrasts to the situation in

mesophyll cells, where *bam1bam3* has a more severe *sex* phenotype than *bam3* single mutants (Figure S1)[21]. These data reveal that sub-functionalization amongst the chloroplastic BAMs enables the plant to adjust starch turnover to the needs of the individual cell.

A distinct pathway of starch degradation operates in guard cells during light-induced stomatal opening

Given the complex nature of starch polymers, β-amylases need to work with other glucan hydrolases to accomplish complete degradation [13, 25, 26]. We hypothesized that other enzymes that have no clear role in mesophyll starch metabolism may have a role in guard cells. As for BAM1, loss of α-AMYLASE *3* (AMY3) and the debranching enzyme *LIMIT DEXTRINASE* (LDA) do not affect starch metabolism in the leaves (Figure S1)[27, 28]. Interestingly, *AMY3* was strongly up-regulated in guard cells (Figure 2A) and the *amy3* mutant showed a slight but significant and reproducible guard cell *sex* phenotype (Figures 2B and 2C). Loss of both AMY3 and BAM1 proteins resulted in a much higher starch content than in the *bam1* mutant (Figures 2B and 2C), without affecting starch metabolism in the leaves (Figure S1). This striking *amy3bam1* phenotype indicates a role for AMY3 in guard cell starch metabolism. Unlike *AMY3* and *BAM1, LDA* was not up regulated in guard cells (Figure 2A). Mutation of *LDA* had a marginal, albeit significant and reproducible impact on guard cell starch metabolism (Figures 2B and 2C). However, transcript abundance of *ISOAMYLASE 3* (ISA3) - the major debranching enzyme in night-time leaf starch degradation – was 7-fold higher in guard cell-enriched epidermal peels relative to intact leaves (Figure 2A). Guard cells of *isa3* contained elevated starch compared with WT, even though appreciable starch degradation still occurred upon illumination (Figures 2B and 2C). The *isa3* phenotype was exacerbated by the additional mutation of LDA (isa3lda, Figures 2B and 2C), reproducing in guard cells the situation previously described in leaves (Figure S1)[28]. Collectively, these results indicate that BAM1, AMY3, LDA and ISA3 work together towards efficient guard cell starch mobilization during stomatal opening.

Mutations in the stomatal starch degradation pathway impact plant growth

To investigate the importance of starch degradation in guard cells, we examined the consequences of the absence of BAM1 and AMY3 on stomatal function and whole-plant physiology. Intact leaves of *bam1* mutants showed reduced stomatal aperture and slower increases in stomatal conductance (gs) in response to light compared with WT (Figures S2A and S2B). This correlates with the lack of light-induced starch degradation in *bam1* guard cells (Figures 1A-1C). However, CO2 assimilation (A) was generally not affected in *bam1* plants, with only subtle differences during the first 1 h of light (Figure S2C). In contrast to *bam1, bam3* mutants had normal rate of stomatal opening in response to light. Transpiration

and carbon assimilation rates were also normal (Figures S2D-S2F) indicating that BAM3 is not required for proper stomatal function.

The additional loss of AMY3 exaggerated the suppression of plant stomatal responses. Firstly, *amy3bam1* plants failed to open stomata efficiently in response to light (Figure 3A). Consequently, *amy3bam1* had lower gs (Figure 3B), decreased leaf intercellular CO_2 concentration (Ci; Figure 3C) and slightly lower CO_2 assimilation rates (Figure S2G) immediately after illumination, compared with WT. This suppression of stomatal function in the *amy3bam1* double mutant had consequences for plant growth, especially under higher light intensities. 4-week-old *amy3bam1* plants grown under 120 μmol m^{-2} s^{-1} of light were almost 30% smaller than WT, whereas there were no noticeable differences when plants were kept under low light intensities (Figure 3D and Figure S2H). These results suggest that diffusive (stomatal) limitations in *amy3bam1* plants may limit CO_2 availability for mesophyll photosynthesis upon illumination, at least under higher light intensities. Thus, we conclude that guard cell starch degradation is of major importance in plant adaptation to light through the control of stomatal aperture.

Guard cell starch degradation is specifically activated by blue light through the PHOT1/PHOT2-dependent signaling pathway

Starch degradation in guard cell chloroplasts is believed to occur mainly under blue light [5, 10], as the *Arabidopsis pgm* mutant shows a reduced rate of stomatal opening, which seems largely attributable to the inhibition of blue light-induced mechanisms [12]. Consequently, we investigated whether blue light is the actual signal for guard cell starch degradation. We found that starch was efficiently degraded and stomata opened in *Arabidopsis* WT plants illuminated with 75 μmol m^{-2} s^{-1} of blue light, a stimulus insufficient to activate photosynthesis at significant levels (Figures 4A, S3A and S3B). In contrast, illumination with 300 μmol m^{-2} s^{-1} of red light promoted efficient starch synthesis in guard cells and induced stomatal opening independently of starch (Figures 4A and S3A). Thus, distinct light qualities control synthesis and degradation of starch in guard cells, and stomatal opening triggered by red light seems to be largely independent of the breakdown of starch present in guard cell chloroplasts.

In guard cells, blue light perception by *PHOTOTROPIN 1* and *2* (PHOT1/PHOT2) [29] initiates a signal transduction cascade, involving the *BLUE LIGHT SIGNALING 1* (BLUS1) protein kinase [30] and the *PROTEIN PHOSPHATASE 1* (PP1) [31, 32]. The signal ultimately activates the plasma membrane H^+-ATPase, leading to increased inside-negative electric potential, influx of potassium and water, and opening of the stomatal pore [2, 33–35]. To determine the molecular basis of blue light-induced guard cell starch degradation, we investigated starch turnover in the *Arabidopsis* blue light-signaling mutants *phot1phot2* and

blus1. In both mutants, guard cells of intact leaves still contained high levels of starch after 1 h of light, whereas WT and the *blus1::GFP-BLUS1* complementing line efficiently degraded it (Figures 4B, 4C, S3C and S3D). In fact, WT consumed almost all the starch within 30 min of light (Figure 4B), showing that the response of guard cell starch degradation to light is extremely rapid. In contrast to guard cells, synthesis and degradation of starch in *phot1phot2* and *blus1* mesophyll cells occurred normally (Figures S3E and S3F), even though the overall starch levels in *phot1phot2* leaves were reduced compared to WT (Figure S3E). This is most likely a consequence of the impaired CO_2 assimilation rate in this mutant [36]. Tautomycin is a potent inhibitor of PP1, which mediates blue light signaling between phototropin and the plasma membrane H^+-ATPase [32]. Consistent with a role for blue light signaling in guard cell starch degradation, we found that tautomycin completely blocked starch degradation and stomatal opening (Figure 4D and S3G). Altogether, these results indicate that the effect of blue light on starch degradation is phototropin-dependent and specific to guard cells.

Proton extrusion by H^+-ATPase is required and precedes starch degradation during stomatal opening

Given that the plasma membrane H^+-ATPase is the ultimate target of the blue light signaling cascade [33], we investigated if proton pump activity was required for guard cell starch breakdown. Mutation of plasma membrane H^+-ATPase1 (*aha1*) resulted in a severe guard cell *sex* phenotype, without affecting leaf starch metabolism (Figures 4C and S3F). In contrast, mutants of H^+-ATPase2 (*aha2*) displayed a WT phenotype (Figure 4C), suggesting a major role for AHA1 in guard cells, although both isoforms are expressed [37].

The fungal toxin fusicoccin (Fc) is a well-known chemical activator of the proton pump [38]. As expected, stomata in WT isolated epidermal peels floating in a buffer containing 50 mM KCl opened to a greater extent in the presence of 10 µM Fc (Figure 4E)[29]. Starch in guard cell chloroplasts in isolated epidermal peels floating in control buffer showed a similar pattern of light-induced starch degradation and re-synthesis to that of guard cells of intact leaves (Figure 4F vs 1C). However, upon treatment with Fc, almost all guard cell starch disappeared after 1 h (Figure 4F), suggesting that enhancement of the H^+-ATPase activity correlates with enhanced starch degradation. A similar pattern of stomatal opening and guard cell starch accumulation was found in *phot1phot2* following Fc treatment (Figures 4E and 4F). On the basis of these results, we conclude that proton extrusion across the plasma membrane during stomatal opening is required for guard cell starch breakdown and that the activity of the H^+-ATPase is positively correlated with starch degradation.

Stomata in *bam1* isolated epidermal peels floating in the buffer containing 50 mM KCl opened similarly to that of WT, most likely due to the presence of high concentration of Cl^- in the medium (Figure 4E). The presence of Cl^-, however, had only little effect on *amy3bam1*

stomatal opening (Figure 4E). Exogenous application of Fc only partially rescued stomatal opening and guard cell starch degradation in *bam1,* and had little or no effect on *amy3bam1* (Figures 4E and 4F). These results indicate that H^+-ATPase functions upstream of starch degradation and that this process is ultimately required for blue light-induced stomatal opening.

DISCUSSION

It has been 100 years since the first observation that starch metabolism in guard cell chloroplasts follows a different rhythm compared to other photosynthetically active leaf tissues [39]. However, despite the increasing interest in guard cell function and regulation, our knowledge about starch metabolism in guard cells and its influence on stomatal function remains only poorly understood, especially in *Arabidopsis*. Our new protocol to quantify starch in single cells showed that starch is present in *Arabidopsis* guard cells at the end of the night, unlike the rest of the leaf. Upon illumination, the starch is very rapidly degraded and most is gone within 30 min (Figures 1B and 4B). Thus, we conclude that starch metabolism in *Arabidopsis* guard cells is similar to that of other species [4, 8, 11], overcoming the contradictions in the literature [12, 14]. By conducting *Arabidopsis* mutant analyses, we discovered that light-induced starch degradation in guard cells is surprisingly mediated by a previously uncharacterized pathway, which involves the activity of BAM1 and AMY3, which are normally not required for night-time starch degradation in the rest of the leaf (Figures 1, 2 and S1). We propose that a key mechanism underpinning such plasticity in starch mobilization is enzyme isoform specialization. In support of this, we showed that two â-amylase isoforms have acquired tissue-specific function. BAM3 has low expression in guard cells (Figure 1D) but represents the major isoform in the night-time leaf starch degradation (Figure S1)[21]. BAM1 is highly expressed in guard cells and is required for light-induced starch degradation in these cells (Figure 1 and S1)[18]. Interestingly, BAM1 is redox regulated, whereas BAM3 is not, and the cysteines involved in the disulfide formation in BAM1 are not conserved in BAM3 [40, 41]. It is therefore plausible to imagine that redox control of BAM1 may activate starch degradation in the light when the cellular environment becomes more reducing due to the activity of the electron transport chain [42]. We recently showed that, similarly to BAM1, AMY3 is also a redox regulated enzyme [26], strengthening the concept that BAM1 and AMY3 are co-regulated and work synergistically. Blocking starch degradation in guard cells by simultaneous loss of BAM1 and AMY3 proteins has severe consequences for stomatal function and a perceptible impact on plant growth, especially under high light intensities (Figure 3). This knowledge reveals the importance of starch in guard cells in driving plant growth through the control of stomatal movements.

Lastly, we provide compelling evidence that this newly discovered starch degradation pathway is under the direct control of blue light through the PHOT1/PHOT2-dependent signaling cascade. Mutation in the blue light-signaling components PHOT1/PHOT2 or BLUS1 impacted starch degradation in guard cells (Figures 4B and 4C), but not in mesophyll cells (Figures S3E and S3F), demonstrating that the influence of blue light on starch metabolism is specific to guard cells. Furthermore, we provide evidence of a direct link between proton pumping and starch degradation in guard cells. The inability of the *aha1* mutants to mobilize starch in guard cells efficiently upon illumination (Figure 4C), along with the low sensitivity of *amy3bam1* guard cells to Fc-treatment (Figures 4E and 4F), show that proton pumping is required for starch degradation during stomatal opening. Interestingly, a previous study showed a similar correlation between proton pumping and the activity of the guard cell isoform of *PHOSPHOENOLPYRUVATE CARBOXYLASE* (PEPC), which is required for the synthesis of malate [43]. This observation points towards a coordinated activation of the blue light-dependent mechanisms required for stomatal opening, whereby maltose originated from starch degradation is converted to malate in the cytosol through glycolysis and the action of PEPC, with an estimated net production of 4 molecules of malate and one molecule of ATP per molecule of maltose (S1 Data). Considering the malate concentration of open guard cells to be around 100 - 200 mM [44], we propose that approximately half of the starch broken down during early stomatal opening is sufficient for rapid malate synthesis (S1 Data). The fate of the remainder carbon skeletons is not clear, but presumably used for sucrose or other hexose sugars production as additional osmolytes or for cellular respiration to produce the ATP required for H^+ pumping.

The signal ultimately linking plasma membrane H^+-ATPase activity to starch degradation in the chloroplast is unknown. The alkalinization of the cytosol resulting from proton pumping upon illumination stimulates accumulation of H^+ through malate synthesis [45], a process requiring carbon skeletons deriving from starch degradation [9, 46]. Depletion of protons in the cytosol may therefore represent a signal for guard cell starch degradation in response to light, although it is difficult to image how changes in cytosolic pH are transferred to the chloroplast. Alternatively, changes in metabolic fluxes upon activation of stomatal opening may trigger starch degradation indirectly, through metabolic signals such as the increase in ADP:ATP ratio or the depletion of the glycolysis intermediate PEP. Lastly, both BAM1 and AMY3 are preferentially active at a slightly alkaline pH [26, 41, 47]. Thus, the reducing environment and the alkaline pH of the stroma generated by the photosynthetic electron transport chain in the light [42, 48], would favor BAM1 and AMY3 activity, promoting starch degradation.

SUPPLEMENTAL INFORMATION

Supplemental Information includes Supplemental Experimental Procedures, S1 Data file, three figures and one table.

AUTHOR CONTRIBUTIONS

D.S. conceived the project. D.S. and D.H. designed the experiments. D.H., S.F., D.P., JSA. M., M.T., and A.N. performed the experiments and analyzed the data. D.S., D.H., and T.L. interpreted the data. N.L. contributed new reagents/analytic tools. D.S. and D.H. wrote the paper.

ACKNOWLEDGEMENTS

We thank M. Coiro for help with the PS-PI staining, C. Fankhauser for providing *phot1phot2* mutant seeds, A. Takemiya for the *blus1* mutant alleles and the *blus1-1 BLUS1* complementation line, M. Galbiati for providing the pFL30 vector and D. Seung, E. Martinoia and S.C. Zeeman for helpful discussions. This work was supported by the Swiss National Science Foundation SNSF grant 31003A_147074 (to D.S.), by the Vontobel Stiftung grant F-74503-12 (to D.S), by the Agence Nationale à la Recherche, grant ANR-ENERGIZER ANR-JC09_439044 (to N.L) and by the Biotechnology and Biological Sciences Research Council BBSRC grant BB/1001187_1 (to T.L.).

REFERENCES

1. Lawson, T., and Blatt, M.R. (2014). Stomatal size, speed, and responsiveness impact on photosynthesis and water use efficiency. Plant Physiol. *164,* 1556–1570.
2. Kollist, H., Nuhkat, M., and Roelfsema, M.R.G. (2014). Closing gaps: linking elements that control stomatal movement. New Phytol. *203,* 44–62.
3. Lawson, T. (2009). Guard cell photosynthesis and stomatal function. New Phytol. *181,* 13–34.
4. Vavasseur, A., and Raghavendra, A.S. (2005). Guard cell metabolism and CO_2 sensing. New Phytol. *165,* 665–682.
5. Shimazaki, K., Doi, M., Assmann, S.M., and Kinoshita, T. (2007). Light regulation of stomatal movement. Annu. Rev. Plant Biol. *58,* 219–247.
6. Lawson, T., Simkin, A.J., Kelly, G., and Granot, D. (2014). Mesophyll photosynthesis and guard cell metabolism impacts on stomatal behaviour. New Phytol. *203,* 1064–1081.
7. Zeeman, S.C., Kossmann, J., and Smith, A.M. (2010). Starch: its metabolism, evolution, and biotechnological modification in plants. Annu. Rev. Plant Biol. *61,* 209–234.
8. Outlaw, W.H., and Manchester, J. (1979). Guard cell starch concentration quantitatively related to stomatal aperture. Plant Physiol. *64,* 79–82.

9. Schnabl, H. (1980). CO_2 and malate metabolism in starch-containing and starch lacking guard cell protoplasts. Planta *58,* 52–58.
10. Talbott, L.D., and Zeiger, E. (1993). Sugar and organic acid accumulation in guard cells of *Vicia faba* in response to red and blue light. Plant Physiol. *102,* 1163–1169.
11. Kang, Y., Outlaw, W.H., Fiore, G.B., and Riddle, K.A. (2007). Guard cell apoplastic photosynthate accumulation corresponds to a phloem-loading mechanism. J. Exp. Bot. *58,* 4061–4070.
12. Lasceve, G., Leymarie, J., and Vavasseur, A. (1997). Alterations in light-induced stomatal opening in a starch-deficient mutant of *Arabidopsis thaliana* L. deficient in chloroplast phosphoglucomutase activity. Plant Physiol. *20,* 350–358.
13. Streb, S., and Zeeman, S.C. (2012). Starch metabolism in Arabidopsis. Arabidopsis Book *10,* e0160.
14. Stadler, R., Büttner, M., Ache, P., Hedrich, R., Ivashikina, N., Melzer, M., Shearson, S.M., Smith, S.M., and Sauer, N. (2003). Diurnal and light-regulated expression of AtSTP1 in guard cells of Arabidopsis. Plant Physiol. *133,* 528–537.
15. Daloso, D.M., Antunes, W.C., Pinheiro, D.P., Waquim, J.P, Wagner, L., Araujo L., Loureiro, M.E., Fernie, A.R., and Williams, T.C.R. (2015). Tobacco guard cells fix CO_2 by both RubisCO and PEPcase whilst sucrose acts as a substrate during light induced stomatal opening. Plant Cell Environ. *38,* 2353–2371.
16. Tallman, G., and Zeiger, E. (1988). Light quality and osmoregulation in Vicia guard cells. Plant Physiol. *88,* 887–895.
17. Prasch, C.M., Ott, K.V., Bauer, H., Ache, P., Hedrich, R., and Sonnewald, U. (2015). β-amylase1 mutant Arabidopsis plants show improved drought tolerance due to reduced starch breakdown in guard cells. J. Exp. Bot. *66,* 6059–6067.
18. Valerio, C., Costa, A., Marri, L., Issakidis-Bourguet, E., Pupillo, P., Trost, P., and Sparla F. (2011). Thioredoxin-regulated β-amylase (BAM1) triggers diurnal starch degradation in guard cells, and in mesophyll cells under osmotic stress. J. Exp. Bot. *62,* 545–555.
19. Ding, Z.J., Y an, J.Y ., Xu, X.Y ., Y u, D.Q., Li, G.X, Zhang, S.Q., and Zheng, S.J. (2014). Transcription factor WRKY46 regulates osmotic stress responses and stomatal movement independently in Arabidopsis. Plant J. *79,* 13–27.
20. Stitt, M., and Zeeman, S.C. (2012). Starch turnover: pathways, regulation and role in growth. Curr. Opin. Plant Biol. *15,* 282–292.
21. Fulton, D.C., Stettler, M., Mettler, T., Vaughan, C.K., Li, J., Francisco, P., Gil, M., Reinhold, H., Eicke, S., Messerli, G., et al. (2008). Beta-AMYLASE4, a noncatalytic protein required for starch breakdown, acts upstream of three active beta-amylases in Arabidopsis chloroplasts. Plant Cell *20,* 1040–1058.

22. Bates, G.W., Rosenthal, D.M., Sun, J., Chattopadhyay, M., Peffer, E., Yang, J., Ort, D.R., and Jones, A.M. (2012). A comparative study of the *Arabidopsis thaliana* guard-cell transcriptome and its modulation by sucrose. PLoS One *7,* e49641.
23. Galbiati, M., Simoni, L., Pavesi, G., Cominelli, E., Francia, P., Vavasseur, A., Nelson, T., Bevan, M., and Tonelli, C. (2008). Gene trap lines identify Arabidopsis genes expressed in stomatal guard cells. Plant J. *53,* 750–762.
24. de Felippes, F.F., Wang, J., and Weigel, D. (2012). MIGS: miRNA-induced gene silencing. Plant J. *70,* 541–547.
25. Edner, C., Li, J., Albrecht, T., Mahlow, S., Hejazi, M., Hussain, H., Kaplan, F., Guy, C., Smith, S.M., Steup, M., et al. (2007). Glucan, water dikinase activity stimulates breakdown of starch granules by plastidial beta-amylases. Plant Physiol. *145,* 17–28.
26. Seung, D., Thalmann, M., Sparla, F., Hachem, M.A., Lee, S.K., Issakidis-Bourguet, E., Svensson, B., Zeeman, S.C., and Santelia, D. (2013). *Arabidopsis thaliana* AMY3 is a unique redox-regulated chloroplastic α-amylase. J. Biol. Chem. *288,* 33620–33633.
27. Yu, T.-S., Zeeman, S.C., Thorneycroft, D., Fulton, D.C., Dunstan, H., Lue, W.-L., Hegemann, B., Tung, S.-Y., Umemoto, T., Chapple, A., et al. (2005). α-Amylase is not required for breakdown of transitory starch in Arabidopsis leaves. J. Biol. Chem. *280,* 9773–9779.
28. Delatte, T., Umhang, M., Trevisan, M., Eicke, S., Thorneycroft, D., Smith, S.M., and Zeeman, S.C. (2006). Evidence for distinct mechanisms of starch granule breakdown in plants. J. Biol. Chem. *281,* 12050–12059.
29. Kinoshita, T., Doi, M., Suetsugu, N., Kagawa, T., Wada, M., and Shimazaki, K. (2001). *phot1* and *phot2* mediate blue light regulation of stomatal opening. Nature *414,* 656–660.
30. Takemiya, A., Sugiyama, N., Fujimoto, H., Tsutsumi, T., Yamauchi, S., Hiyama, A., Tada, Y., Christie, J.M., and Shimazaki, K. (2013). Phosphorylation of BLUS1 kinase by phototropins is a primary step in stomatal opening. Nat. Commun. *4,* 2094–2101.
31. Takemiya, A., Yamauchi, S., Yano, T., Ariyoshi, C., and Shimazaki, K. (2013). Identification of a regulatory subunit of protein phosphatase 1 which mediates blue light signaling for stomatal opening. Plant Cell. Physiol. *54,* 24–35.
32. Takemiya, A., Kinoshita, T., Asanuma, M., and Shimazaki, K. (2006). Protein phosphatase 1 positively regulates stomatal opening in response to blue light in *Vicia faba.* Proc. Natl. Acad. Sci. U S A *103,* 13549–13554.
33. Inoue, S., Takemiya, A., and Shimazaki, K. (2010). Phototropin signaling and stomatal opening as a model case. Curr. Opin. Plant. Biol. *13,* 587–593.
34. Hills, A., Chen, Z.-H., Amtmann, A., Blatt, M.R., and Lew, V.L. (2012). OnGuard, a computational platform for quantitative kinetic modeling of guard cell physiology. Plant Physiol. *159,* 1026–1042.

35. Chen, Z.-H., Hills, A., Bätz, U., Amtmann, A., Lew, V.L., and Blatt, M.R. (2012). Systems dynamic modeling of the stomatal guard cell predicts emergent behaviors in transport, signaling, and volume control. Plant Physiol. *159,* 1235–1251.
36. Takemiya, A., Inoue, S., Doi, M., Kinoshita, T., and Shimazaki, K. (2005). Phototropins promote plant growth in response to blue light in low light environments. Plant Cell *17,* 1120–1127.
37. Ueno, K., Kinoshita, T., Inoue, S.-I., Emi, T., and Shimazaki, K. (2005). Biochemical characterization of plasma membrane H^+-ATPase activation in guard cell protoplasts of *Arabidopsis thaliana* in response to blue light. Plant Cell Physiol. *46,* 955–963.
38. Ballio, A., Chain, E.B., de Leo, P., Erlanger, B.G., Mauri, M., and Tonolo, A. (1964). Fusicoccin: A new wilting toxin produced by *Fusicoccum amygdali* Del. Nature *203,* 297.
39. Lloyd, F. (1908). The behaviour of stomata. Carnegie Inst Wash Publ *82,* 1-142.
40. Sparla, F., Costa, A., Lo Schiavo, F., Pupillo, P., and Trost, P. (2006). Redox regulation of a novel plastid-targeted â-Amylase. Plant Physiol. *141,* 840–850.
41. Santelia, D., Trost, P., and Sparla, F. (2015) New insights into redox control of starch degradation. Curr. Opin. Plant Biol. *25,* 1–9.
42. Buchanan, B.B., and Balmer, Y. (2005). Redox regulation: a broadening horizon. Annu. Rev. Plant Biol. *56,* 187–220.
43. Meinhard, M., Schnabl, H. (2001). Fusicoccin- and light-induced activation and *in vivo* phosphorylation of phosphoenolpyruvate carboxylase in Vicia guard cell protoplasts. Plant Sci. *160,* 635–646.
44. Martinoia, E., and Rentsch, D. (1994). Malate compartmentation - responses to a complex metabolism. Annu. Rev. Plant. Physiol. Plant Mol. Biol. *45,* 447–467.
45. Robinson, N., and Preiss, J. (1985). Biochemical phenomena associated with stomatal function. Physiol. Plant *64,* 141–146.
46. Outlaw, W.H., Du, Z., Meng, F.X., Aghoram, K., Riddle, K.A., and Chollet, R. (2002). Requirements for activation of the signal-transduction network that leads to regulatory phosphorylation of leaf guard-cell phosphoenolpyruvate carboxylase during fusicoccin-
47. stimulated stomatal opening. Arch. Biochem. Biophys. *407,* 63–71.
48. Monroe, J.D., Storm, A.R., Badley, E.M., Lehman, M.D., Platt, S.M., Saunders, L.K., Schmitz, J.M., and Torres, C.E. (2014). â-amylase1 and â-amylase3 are plastidic starch hydrolases in Arabidopsis that seem to be adapted for different thermal, pH, and stress conditions. Plant Physiol. *166,* 1748–1763.
49. Heldt, H.W., Werdan, K., Milovancev, M., and Geller, G. (1973). Alkalization of the chloroplast stroma caused by light-dependent proton flux into the thylakoid space. Biochim. Biophys. Acta - Bioenerg *314,* 224–241.

FIGURES AND FIGURE LEGENDS

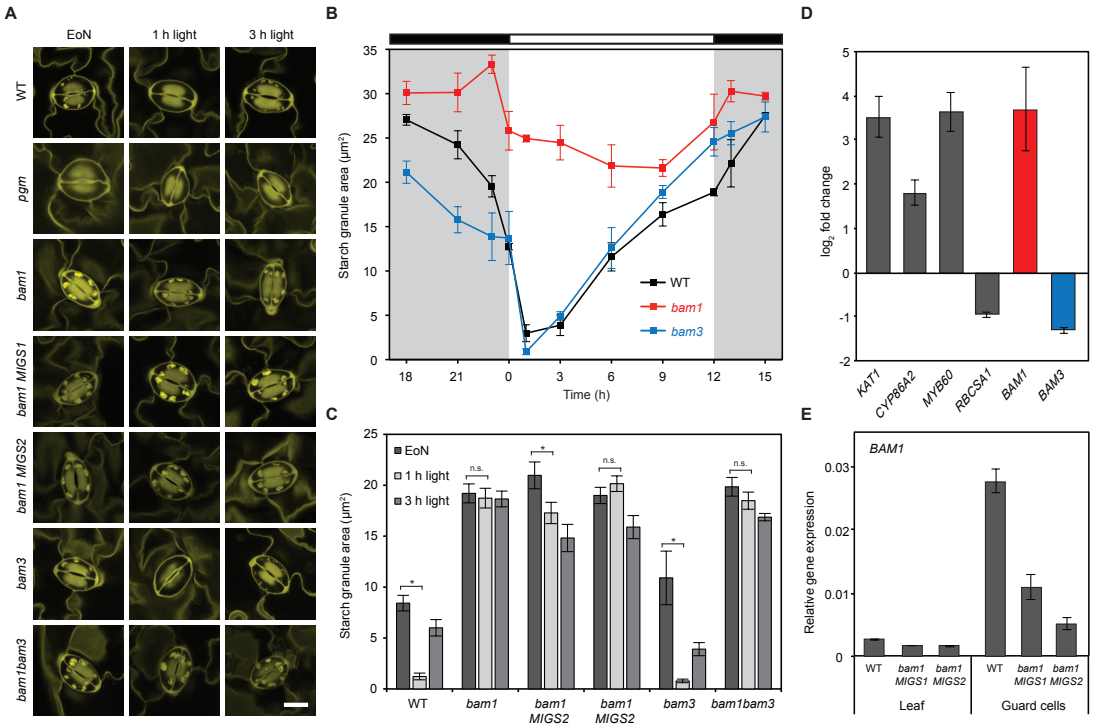

Figure 1. Starch turnover in *Arabidopsis* guard cells and isoform specialization within the β-amylase family. (A) Visualization of starch granules within *Arabidopsis* guard cells of intact leaves at the end of the night (EoN) and after 1 h and 3 h of illumination. Scale bar = 10 µm. (B) Starch accumulation in guard cells of intact leaves over the diurnal cycle (n = 110 ± sem). (C) Starch accumulation in guard cells of intact leaves at the EoN and after 1 h and 3 h of illumination (n = 100 ± sem). Unpaired Student's *t* test determined statistical significance between EoN and 1 h light (* $p < 0.05$; n.s. not significant). (D) Gene transcript abundance in guard cell-enriched epidermal peel fragments compared to leaves. Values are normalized against gene expression in the leaves (set as 0; $n = 3$ ± sem). (E) Relative expression levels of *BAM1* in leaves and guard cell-enriched epidermal peel fragments of WT and two independent *BAM1* MIGS silencing lines (n = 3 ± sem). *BAM1* transcripts in the guard cells of the two silencing lines are reduced by 60% and 80%, respectively, but are unaffected in the leaves. See also Figure S1.

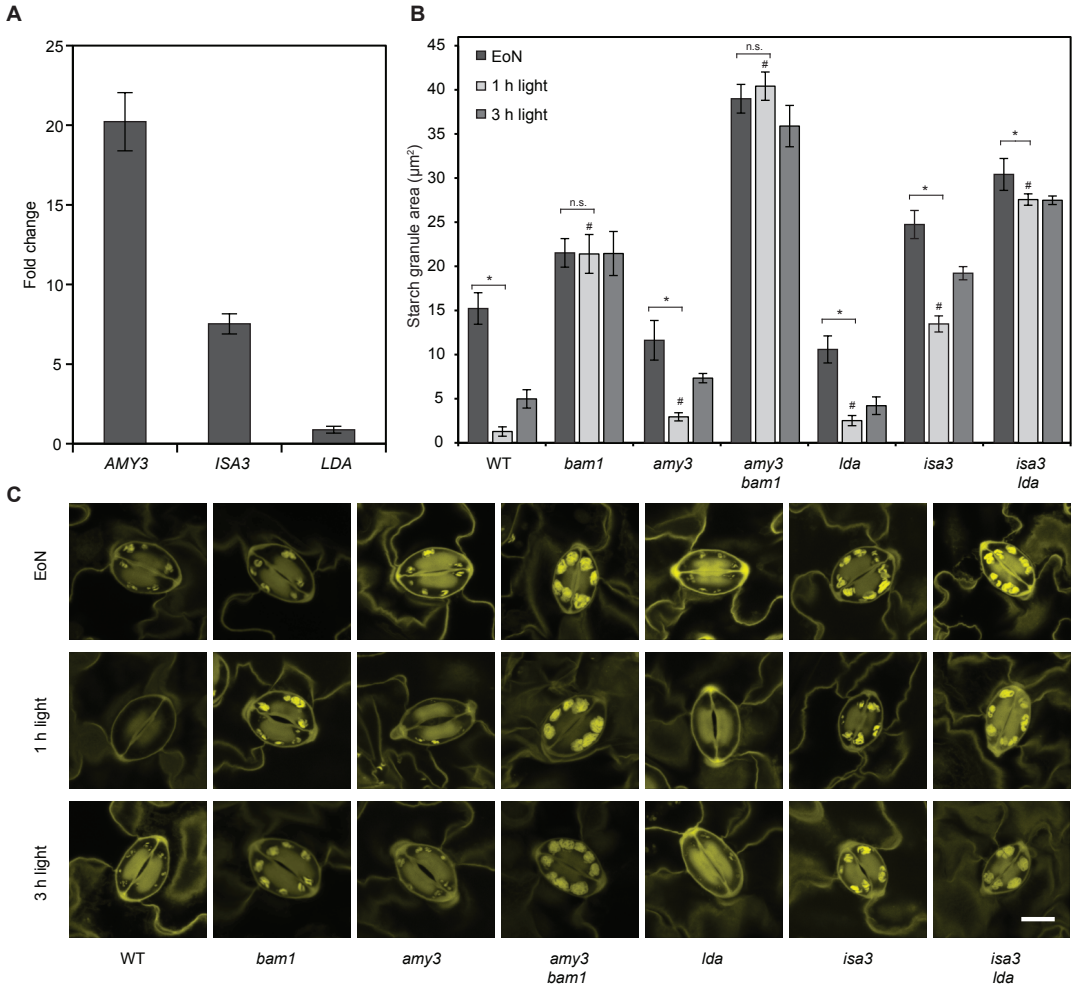

Figure 2. BAM1, AMY3, ISA3 and LDA form a distinct pathway of starch degradation in *Arabidopsis* guard cells. (A) Transcript abundance of *AMY3, ISA3* and *LDA* in guard cell-enriched epidermal peel fragments compared to leaves. Values are normalized against gene expression in the leaves (set as 1; $n = 3 \pm$ sem). (B) Quantification of starch content in guard cells of intact leaves at the EoN and after 1 h and 3 h of illumination (n = 110 ± sem). Statistical significances determined by unpaired Student's *t* tests: # denotes $p < 0.05$ mutants versus WT at the indicated time point; * denotes $p < 0.05$ for the indicated comparisons; n.s. = not significant for the indicated comparison. (C) Representative confocal images of propidium iodide-stained guard cells of intact leaves. Scale bar = 10 µm. See also Figure S1.

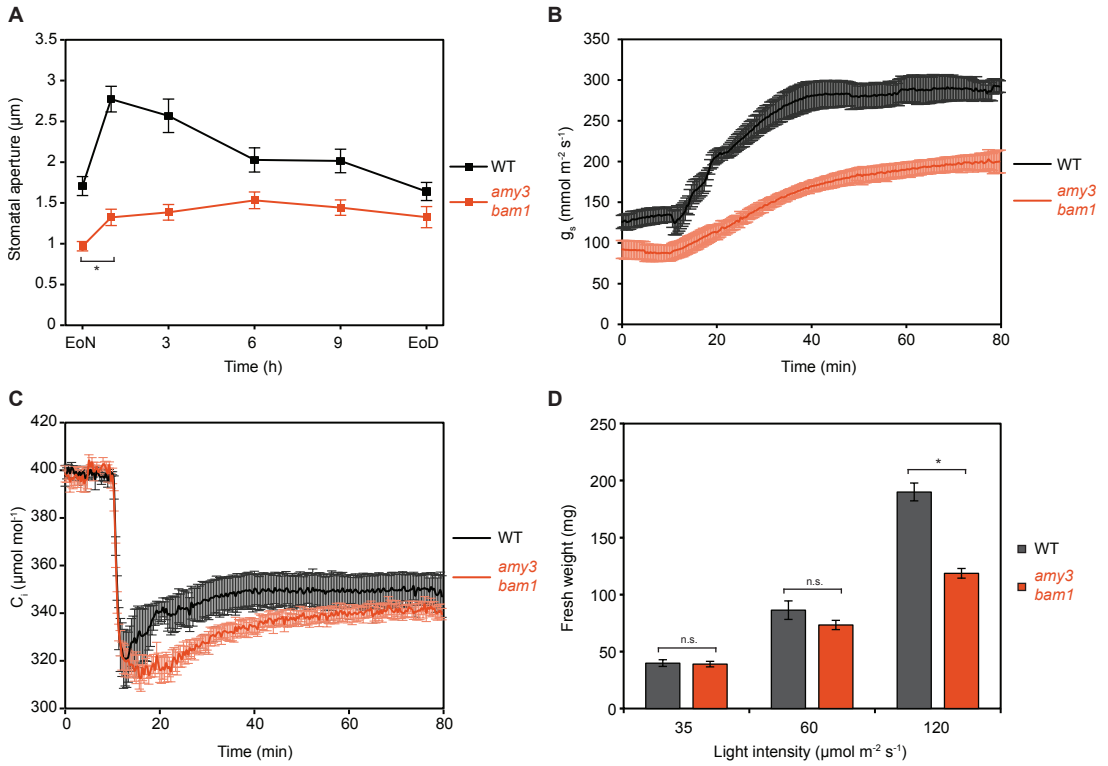

Figure 3. Stomatal function and biomass production in response to light are impaired in *amy3bam1* mutants. (A) Stomatal aperture in WT and *amy3bam1* intact leaves during the light phase, determined by light microscopy and digital image processing (n = 100 ± sem). Statistical significances determined by unpaired Student's *t* tests: * denotes $p < 0.01$ for the indicated comparison. (B, C) Single leaf measurement of WT and *amy3bam1* stomatal conductance gs (B) and internal CO_2 concentration (Ci) in 150 µmol m^{-2} s^{-1} light intensity (n ≥ 5). (D) Fresh weight of WT and *amy3bam1* rosettes of 4-week-old plants grown at different light intensities (n = 5 ± sem). Statistical significances determined by unpaired Student's *t* tests: * denotes $p < 0.01$ for the indicated comparison; n.s. = not significant for the indicated comparison. See also Figure S2.

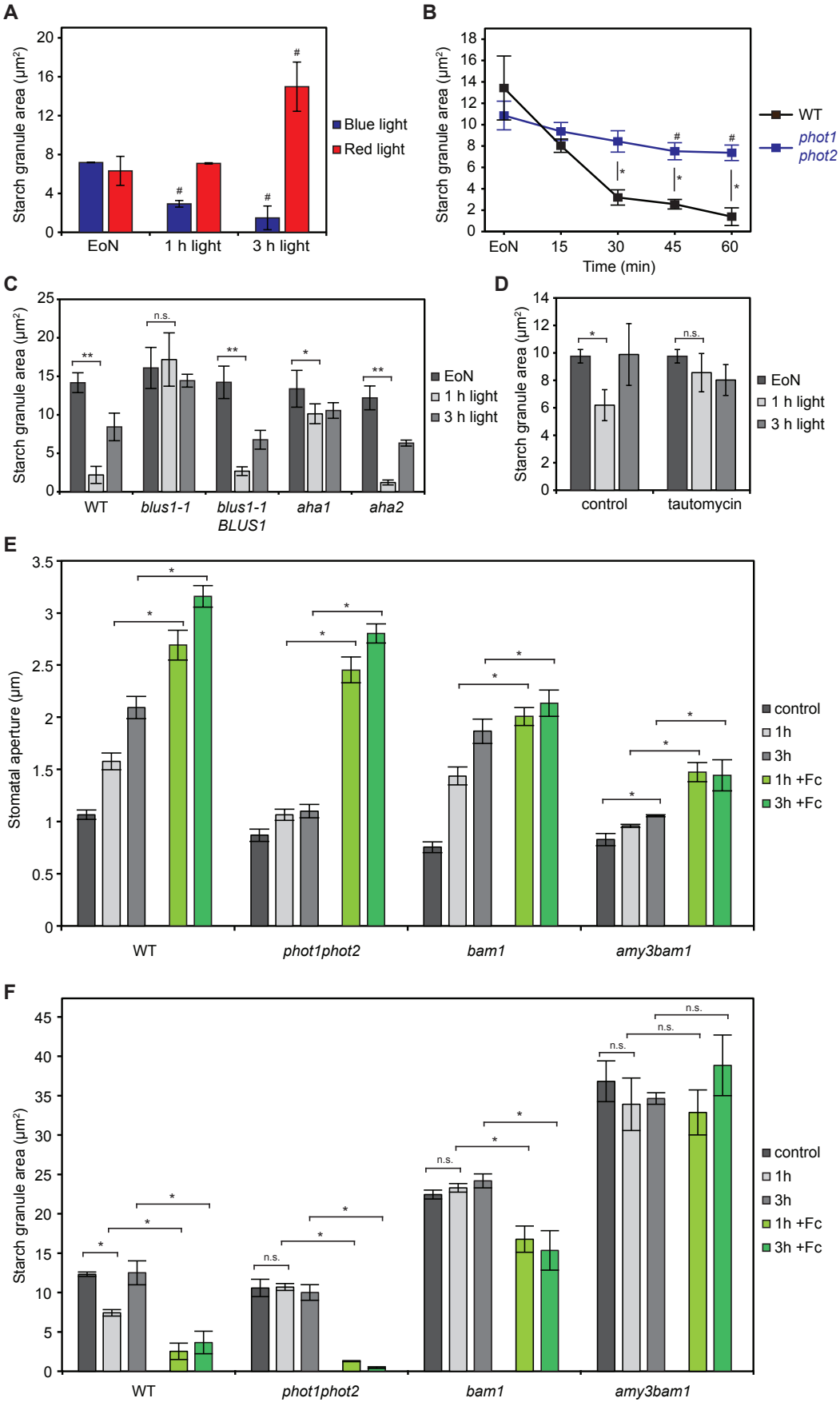
A
Starch granule area (µm²)
Blue light
Red light
EoN
1 h light
3 h light
B
Starch granule area (µm²)
WT
phot1
phot2
EoN
15
30
45
60
Time (min)
C
Starch granule area (µm²)
EoN
1 h light
3 h light
WT
blus1-1
blus1-1 BLUS1
aha1
aha2
D
Starch granule area (µm²)
EoN
1 h light
3 h light
control
tautomycin
E
Stomatal aperture (µm)
control
1h
3h
1h +Fc
3h +Fc
WT
phot1phot2
bam1
amy3bam1
F
Starch granule area (µm²)
control
1h
3h
1h +Fc
3h +Fc
WT
phot1phot2
bam1
amy3bam1

Figure 4. Blue light signaling and proton pumping activate guard cell starch degradation during stomatal opening. (A) Starch content in guard cells of WT plants illuminated with blue light (75 µmol m^{-2} s^{-1}) or red light (300 µmol m^{-2} s^{-1}) after the end of the dark period (n = 110 ± sem). Unpaired Student's *t* test determined statistical significance between EoN and 1 h and 3 h light (# $p < 0.01$). (B) Guard cell starch content of WT and *phot1phot2* intact leaves during the first hour of the light period (n = 110 ± sem). Statistical significances determined by unpaired Student's *t* tests: * denotes $p < 0.001$ for the indicated comparison; # denotes $p < 0.001$ between EoN and 45 min and 60 min of light for the *phot1phot2* mutant. (C) Starch accumulation in guard cells of intact leaves at the EoN and after 1 h and 3 h of illumination (n = 110 ± sem). Unpaired Student's *t* test determined statistical significance between the indicated comparisons (* $p < 0.01$; ** $p < 0.001$; n.s. not significant). (D) Guard cell starch content in WT epidermal peels treated for 1 h and 3 h with or without 2.5 µM tautomycin in opening buffer containing 50 mM KCl. 1 h dark-adapted peels were illuminated with 10 µmol m^{-2} s^{-1} blue light superimposed on 50 µmol m^{-2} s^{-1} red light (n = 100 ± sem). Unpaired Student's *t* test determined statistical significance between the indicated comparisons (* $p < 0.001$; n.s. not significant). (E and F) Stomatal aperture (E) and guard cell starch content (F) in epidermal peels treated for 1 h and 3 h with or without 10 µM fusicoccin (Fc) in opening buffer containing 50 mM KCl. 1 h dark-adapted peels were illuminated with 10 µmol m^{-2} s^{-1} blue light superimposed on 50 µmol m^{-2} s^{-1} red light (n = 80 ± sem). Unpaired Student's *t* test determined statistical significance between the indicated comparisons (* $p < 0.001$; n.s. not significant). See also Figure S3.

SUPPLEMENTAL INFORMATION

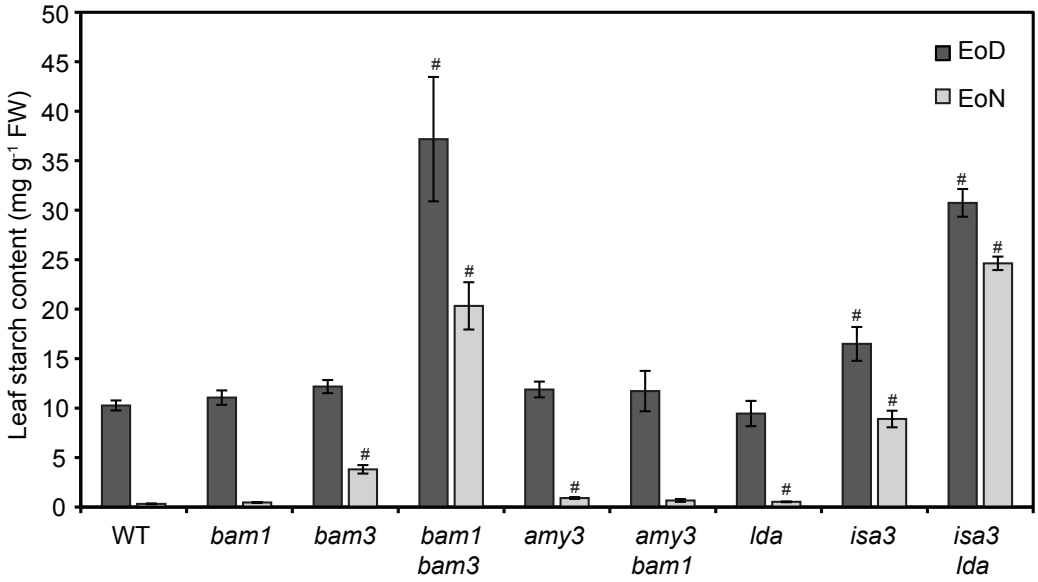

Figure S1. Related to Figure 1 and Figure 2. Leaf starch content in single and multiple starch-degrading mutants. Entire rosettes from 4-week-old plants were harvested at the end of the night (EoN) and at the end of the day (EoD), and immediately frozen in liquid nitrogen. Starch was extracted using perchloric acid and measured enzymatically by treatment with α-amylase and amyloglucosidase as described in "Supplemental Experimental Procedure". Each bar is the mean ± sem (n = 8). FW, fresh weight. Unpaired Student's *t* test determined statistical significance between mutants and WT at the indicated time points (# $p < 0.01$).

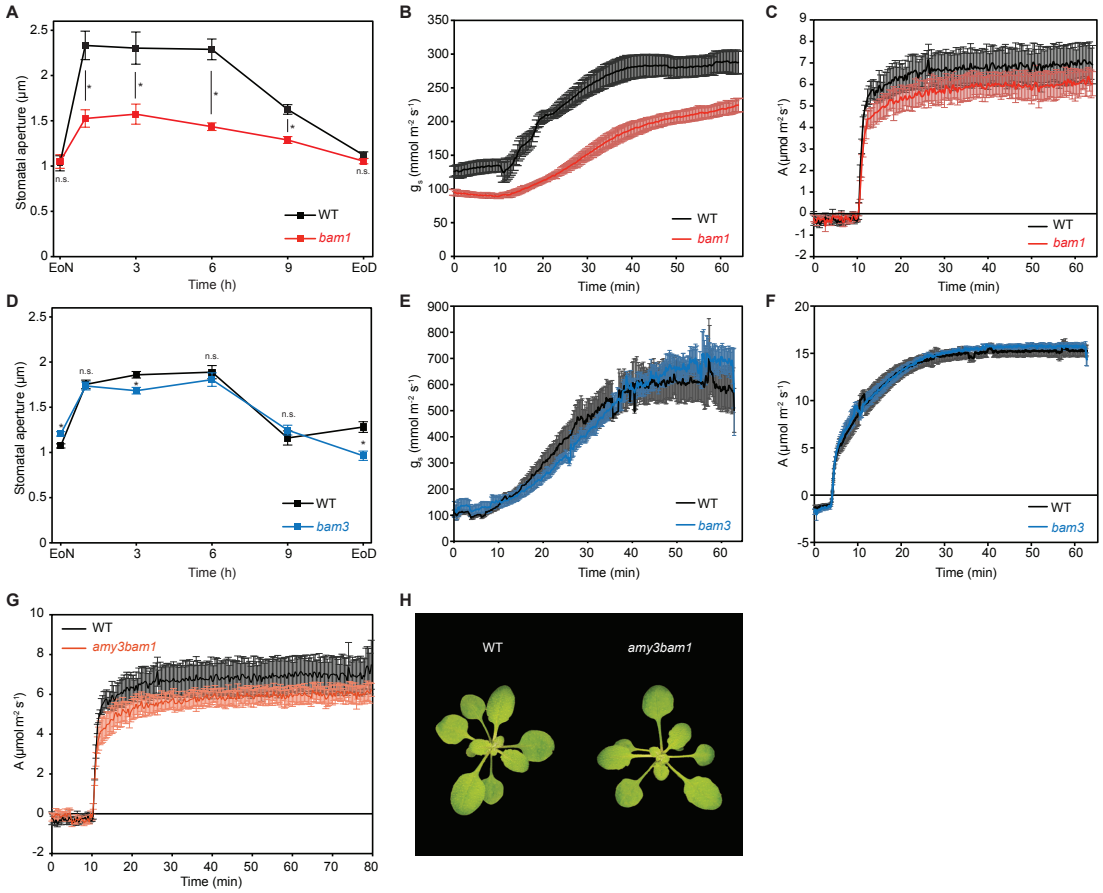

Figure S2. Related to Figure 3. Stomatal function in *bam1* and *bam3* mutants. (A and D) Stomatal aperture of WT, *bam1* and *bam3* mutant plants during the 12 h light phase, as determined by light microscopy and digital image processing. Each value is the mean of four biological replicates ± sem of more than 100 individual stomata. Similar results were obtained in two other independent experiments. Unpaired Student's *t* test determined statistical significance between the indicated comparisons (* $p < 0.01$; n.s. not significant). (B and E; C and F) Single leaf measurements of WT, *bam1* and *bam3* stomatal conductance gs (B and E) and CO_2 assimilation (C and F) under 150 µmol m^{-2} s^{-1} of white light. Shown is the mean ± sem of a representative experiment (n ≥ 5). WT control shown in (B) is the same as in Figure 3B. (G) Single leaf measurements of *amy3bam1* CO_2 assimilation. Shown is the mean ± sem of a representative experiment (n ≥ 5). WT control measurement is the same as shown in (C). (H) Representative pictures of 3-week-old plants grown under 120 µmol m^{-2} s^{-1} of light.

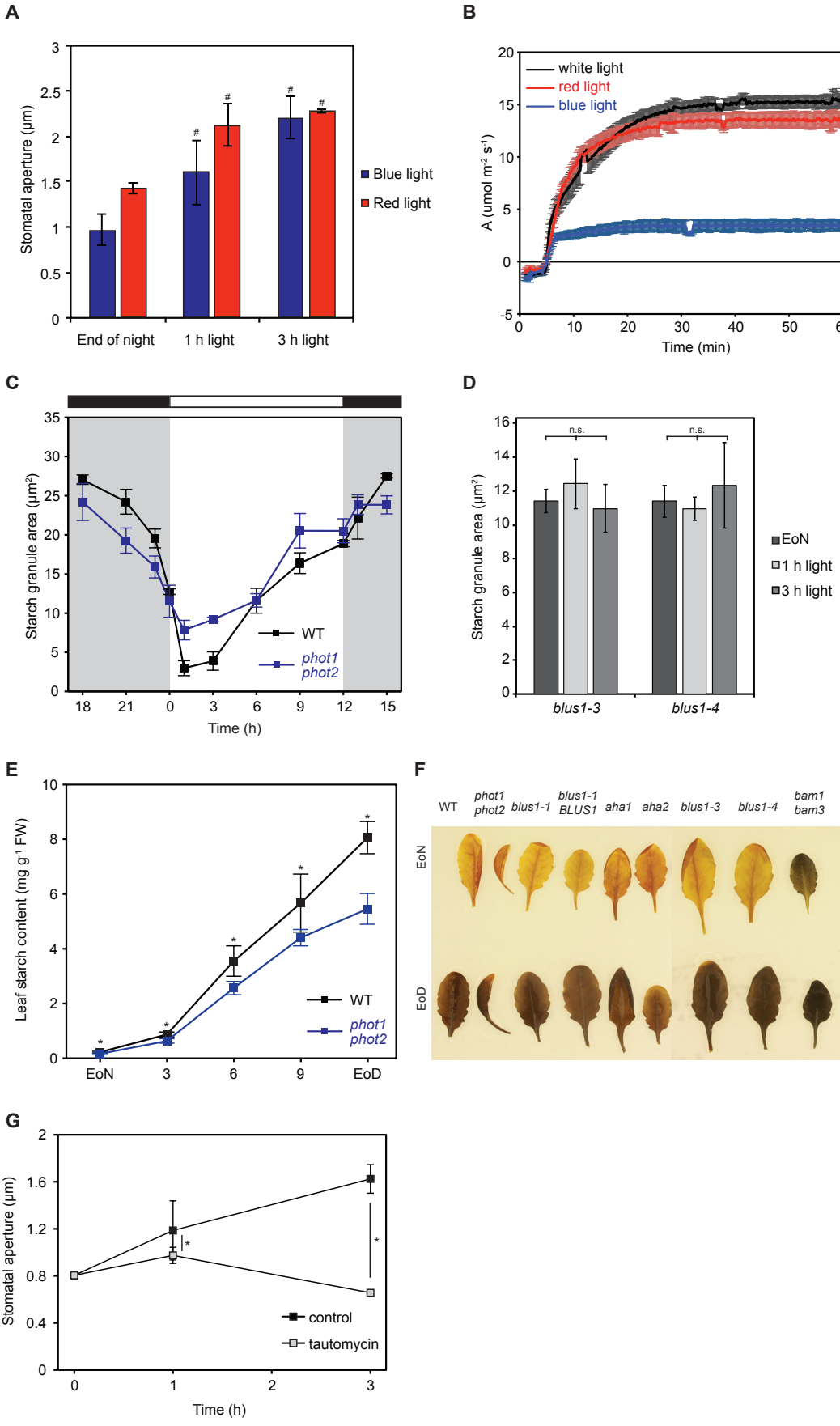
A
Stomatal aperture (µm)
Blue light
Red light
End of night
1 h light
3 h light
B
white light
red light
blue light
A (µmol m-2 s-1)
Time (min)
C
Starch granule area (µm2)
WT
phot1
phot2
Time (h)
D
Starch granule area (µm2)
n.s.
EoN
1 h light
3 h light
blus1-3
blus1-4
E
Leaf starch content (mg g-1 FW)
WT
phot1
phot2
EoN
EoD
F
WT
phot1 phot2
blus1-1
blus1-1 BLUS1
aha1
aha2
blus1-3
blus1-4
bam1 bam3
EoN
EoD
G
Stomatal aperture (µm)
control
tautomycin
Time (h)

Figure S3. Related to Figure 4. (A and B) Effect of blue and red light on stomatal function in WT. (A) WT plants were illuminated with blue light (75 µmol m^{-2} sec^{-1}) or red light (300 µmol m^{-2} sec^{-1}), after the end of the dark period. Stomatal aperture was determined at the indicated time points. Each value represents mean ± sem of at least 200 stomata from 2 independent experiments. EoN = End of night. Unpaired Student's *t* test determined statistical significance between EoN and 1 h and 3 h light (# $p < 0.01$). (B) Single leaf measurements of CO_2 assimilation in WT under white light (400 µmol m^{-2} sec^{-1}), red light (300 µmol m^{-2} sec^{-1}) or blue light (75 µmol m^{-2} s^{-1}). Shown is the mean ± sem of a representative experiment ($n \geq 5$). (C-F) Mutation of components of the guard cell blue light signal transduction cascade does not affect starch metabolism in the leaves. (C) Starch content in *phot1phot2* guard cells of intact leaves over the diurnal cycle (12-h light/12-h dark) under uniform illumination of 150 µmol m^{-2} sec^{-1}. For comparison, starch content in WT guard cells from Figure 1B is also shown. Each point is the mean ± sem of at least three independent experiments with more than 110 imaged guard cells. (D) Guard cell starch content of intact leaves in the two mutant alleles *blus1-3* and *blus1-4* at the end of the night and after 1 h and 3 h of illumination. Each point is the mean ± sem of at least three independent experiments with more than 100 imaged guard cells. n.s. = no significant differences as determined by unpaired Student's *t* test. (E) Leaf starch content of WT and *phot1phot2* mutant plants. Entire rosettes from 4-week-old plants were harvested at the indicated time points. Starch was measured enzymatically by treatment with α-amylase and amyloglucosidase as described in "Supplemental Experimental Procedure". Each point is the mean ± sem (n = 8). FW, fresh weight. Unpaired Student's *t* test determined statistical significance between the indicated comparisons (* $p < 0.01$). (F) Photographs of iodine-stained leaves of WT and several mutants of the blue light signaling cascade harvested at the end of the day (EoD) and at the end of the night (EoN) after four weeks of growth. The starch excess phenotype of *bam1bam3* is shown for comparison. (G) Tautomycin inhibits stomatal opening in WT guard cells. Stomatal aperture in epidermal peels from WT treated for 1 h and 3 h with or without 2.5 µM tautomycin in opening buffer containing 50 mM KCl. Dark-adapted peels were illuminated with 10 µmol m^{-2} sec^{-1} blue light superimposed on 50 µmol m^{-2} sec^{-1} red light. Each value is mean ± sem from two independent experiments with more than 100 guard cells analyzed. Unpaired Student's *t* test determined statistical significance between the indicated comparisons (* $p < 0.01$).

SUPPLEMENTAL DATA 1

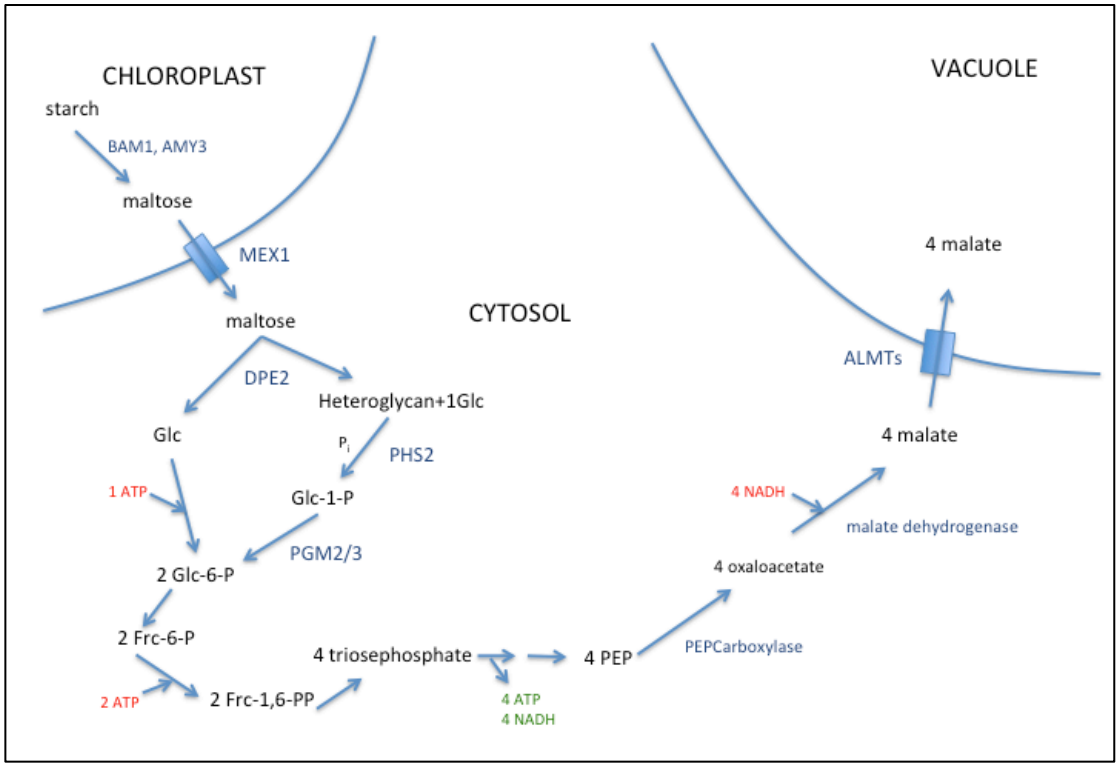

Legend: BAM1 β-amylase 1; AMY3 α-amylase 3; MEX1 maltose exporter 1; DPE2 disproportionating enzyme 2; PHS2 starch phosphorylase 2; PGM phosphoglucomutase; ALMTs aluminum-activated malate transporters; Fru fructose; PEP phosphoenolpyruvate.

Our work shows that guard cell starch is mainly degraded by the concerted action of BAM1 and AMY3, suggesting maltose as the major guard cell starch degradation product. Maltose is exported to the cytosol by the maltose exporter 1 (MEX1; Niittyla et al., 2004) where it is metabolized by the cytosolic disproportionating enzyme 2 (DPE2). DPE2 transfers one of the two glucose units of maltose to a pre-existing heteroglycans acceptor, releasing the other one as free Glc (Lu and Sharkey, 2004; Fettke et al., 2006). Glc-1-P is released from the heteroglycans by starch phosphorylase 2 (DPE2; Lu et al., 2006). Both Glc and GLc-1-P can be further metabolized through glycolysis to yield 4 molecules of phosphoenolpyruvate (PEP), with a net gain of one molecule of ATP and four molecules of NADH. PEP is subsequently converted into oxaloacetate by the action of phosphoenolpyruvate carboxylase (PEPC) and finally into malate through NAD-dependent MALATE DEHYDROGENASE (MDH) (Outlaw and Kennedy, 1978; Gotow et al., 1985; Scheibe et al., 1990; Asai et al., 2000). The NADH generated during glycolysis is used for the reduction of oxaloacetate by cytosolic NAD-MDH, which shows higher activity compared to plastidial NADP-dependent MDH in guard cells (Gotow et al., 1985). Overall, this metabolic pathway results in a net cytosolic conversion of one maltose molecule into four molecules of malate and one molecule

of ATP.

Estimation of theoretical starch to malate conversion in WT plants during early stomatal opening (first hour of light)

Starch content was calculated using the density of starch of 1.5 g / cm^3 (Dengate et al. 1978). To calculate the theoretical increase in malate concentration in guard cells a guard cell volume of opened Arabidopsis guard cells of 0.783 pl (Chen et al. 2012) was assumed. Assuming an increase in cellular malate content in guard cells of 100 to 200 mM, already less than 50% of the observed starch degradation would be sufficient.

	Starch volume per guard cell (µm3)	Starch content per guard cell (pg)	Starch degradation (End of night - 1 h light) (pg)	Glucose equivalents generated from starch degradation (pmol)	Theoretical maximum malate generated from glucose (pmol)	Theoretical increase in guard cell malate concentration (mM)
End of night	27.95	41.93				
1 h light	8.07	12.10	29.82	0.18	0.37	0.47

The high resolution of our PS-PI staining method using confocal laser scanning microscopy enabled us to determine the amount of starch that is broken down in guard cells during the initial hour of illumination. This value was used to calculate the theoretical amount of malate that can be produced in guard cells from starch during early stomatal opening (i.e. first hour of light). Using the same set of PS-PI confocal images, we measured the radius of individual granules, which we then used for the calculation of granule volume according to the equations established by Crumpton-Taylor and colleagues (Crumpton-Taylor et al., 2012), with the assumption that guard cell starch granules have a spherical shape as was shown for mesophyll granules. According to this report, granule volume equals $0.3278 * 4/3 * \pi * r^3$ with r being the radius of the granule. We calculated that on average the granule volume per guard cell is reduced from 27.95 μm^3 to 8.07 μm^3, which equals to a reduction of 29.62 pg when the starch density of approximately 1.5 g/cm^3 is taken into account (Dengate et al., 1978). Given the molecular weight of 162 g mol^{-1} for a glucosyl unit in starch and the average guard cell volume of 0.783 pl (Chen et al., 2012), we calculate a theoretical maximum of malate synthesis from starch breakdown of 470 mM per guard cell. Guard cells were reported to accumulate between 100 and 200 mM of malate on a full cell volume basis (Martinoia and Rentsch, 1994).

We therefore propose that approximately half of the guard cell starch broken down during the

initial phase of stomatal opening is sufficient for rapid malate synthesis, which is in agreement with the previous report on *Vicia faba* stating that starch breakdown is quantitatively sufficient for the synthesis of the required anions for stomatal opening (Outlaw and Manchester, 1979). The fate of the remainder carbon skeletons orginating from starch is not known. They can presumably be used for sucrose or other hexose sugars production as additional osmolytes or simply used for cellular respiration to produce the ATP required for H^+ pumping.

References

Crumpton-Taylor, M., Grandison, S., Png, K.M., Bushby, A.J., and Smith, A.M. (2012). Control of starch granule numbers in Arabidopsis chloroplasts. Plant Physiol 158: 905–916.

Dengate, H.N., Baruch, D.W., and Meredith, P. (1978). The density of wheat starch granules: a tracer dilution procedure for determining the density of an immiscible dispersed phase. Stärke 30: 80–84.

Chen, Z.-H., Eisenach, C., Xu, X.-Q., Hills, A., and Blatt, M.R. (2012). Protocol: optimised electrophyiological analysis of intact guard cells from Arabidopsis. Plant Methods 8: 15.

Martinoia, E. and Rentsch, D. (1994). Malate compartmentation - Responses to a complex metabolism. Annu. Rev. Plant Physiol. Plant Mol. Biol. 45: 447–467.

Outlaw, W.H. and Manchester, J. (1979). Guard cell starch concentration quantitatively related to stomatal aperture. Plant Physiol. 64: 79–82.

Niittyla, T., Messerli, G., Trevisan, M., Chen, J., Smith, A.M., and Zeeman, S.C. (2004). A previously unknown maltose transporter essential for starch degradation in leaves. Science 303: 87–89.

Lu, Y. and Sharkey, T.D. (2004). The role of amylomaltase in maltose metabolism in the cytosol of photosynthetic cells. Planta 218: 466–473.

Fettke, J., Chia, T., Eckermann, N., Smith, A., and Steup, M. (2006). A transglucosidase necessary for starch degradation and maltose metabolism in leaves at night acts on cytosolic heteroglycans (SHG). Plant J. 46: 668–84.

Lu, Y., Steichen, J.M., Yao, J., and Sharkey, T.D. (2006). The role of cytosolic alpha-glucan phosphorylase in maltose metabolism and the comparison of amylomaltase in Arabidopsis and *Escherichia coli*. Plant Physiol. 142: 878–889.

Outlaw, W.H. and Kennedy, J. (1978). Enzymic and substrate basis for the anaplerotic step in guard cells. Plant Physiol 62: 648–652.

Gotow, K., Tanaka, K., Kondo, N., Kobayashi, K., and Syōno, K. (1985). Light activation of NADP-malate dehydrogenase in guard cell protoplasts from *Vicia faba* L. Plant Physiol 79: 829–832.

Scheibe, R., Reckmann, U., Hedrich, R., and Raschke, K. (1990). Malate dehydrogenases in guard cells of *Pisum sativum*. Plant Physiol. 93: 1358–64.

Asai, N., Nakajima, N., Tamaoki, M., Kamada, H., and Kondo, N. (2000). Role of malate

synthesis mediated by phosphoenolpyruvate carboxylase in guard cells in the regulation of stomatal movement. Plant Cell Physiol. 41: 10–15.

SUPPLEMENTAL EXPERIMENTAL PROCEDURES

Plant growth conditions

If not stated otherwise, experiments were performed with 4-week-old, non-flowering *Arabidopsis thaliana* plants grown in soil in a controlled climate chamber (KKD Hiross, CLITEC Boulaguiem, Root, Switzerland). The temperature was kept constant at 23°C with a relative humidity of 45% under a 12-h light/12-h dark cycle and the plants were illuminated with a combination of white light (Osram Biolux) and purple light (Osram Fluora) with a total photon fluence rate of 150 µmol m^{-2} sec^{-1}. Alternatively, plants were grown in a reach in climate chamber with light-emitting diode (LED) light sources for experiments with defined light compositions (Fytoscope FS130, Photon Systems Instruments, Drasov, Czech Republic).

The two null alleles *bam1* (SALK_039895) and *amy3-2* (SAIL_613_D12) were used to generate the double mutant *amy3bam1*. All the other single and multiple mutants used in this study were described previously: *pgm-1* (CS210) [S1], *bam1* (SALK_039895), *bam3* (CS92461) and *bam1bam3* [S2], *amy3-2* (SAIL_613_D12) [S3], *lda-2* (SALK_060765), *isa3-2* (GABI_280G10) and *isa3-2lda-2* [S4], *phot1-5phot2-1* [S5], *blus1-1, blus1-3* (SALK_000221) and *blus1-4* (GABI_222H02) [S6], *aha1-8* (Salk_118350C) and *aha2-5* (Salk_022010) [S7].

Guard cell starch quantification

Epidermal peels were manually prepared from leaf number 6 at the indicated time points and immediately fixed in 50% (v/v) methanol, 10% (v/v) acetic acid. Alternatively, leaf number 6 from eight different plants were blended for 30 sec in water using an Omni Mixer (Sorvall). Epidermal peels were collected with a 200 µm mesh (Sefar), incubated floating on 1 ml of basal reaction buffer (5 mM MES-bistrispropane, pH 6.5, 50 mM KCl and 0.1 mM $CaCl_2$) and kept in the dark for 1 h. The peels were subsequently illuminated for 3 h with 10 µmol m^{-2} sec^{-1} blue light superimposed on 50 µmol m^{-2} sec^{-1} red light in the presence or absence of 10 µM fusicoccin (Sigma) or 2.5 µM tautomycin (Enzo Life Science). After the incubation period, peels were fixed in 50% (v/v) methanol, 10% (v/v) acetic acid. Starch granules were stained with a pseudo-schiff propidium iodide (PS-PI) staining [S8]. Briefly, epidermal peels were treated with 1% periodic acid to oxidize the hydroxyl groups of the glucose units to aldehyde and keton groups. After rinsing with water, samples were stained with Schiff

reagent (100 mM sodium metabisulphite, 0.15 N HCl) and propidium iodide (0.1 mg ml^{-1} (w/v) final concentration). Peels were destained in water and transferred into chloral hydrate solution on microscopy slides. After incubation in the dark for 12 h, samples were fixed using Hoyers solution. Microscopy was performed with a Leica TCS SP5 confocal laser scanning microscope (Leica Microsystems). The excitation wavelength was 488 nm and the emission was collected between 610 to 640 nm. Starch granule area was measured using ImageJ version 1.45s (NIH USA, http://rsbweb.nih.gov/ij/).

Stomatal aperture

For stomatal aperture measurement, leaf number 6 was fixed to an adhesive tape at the indicated time points. The adaxial epidermis and mesophyll layers were gently removed with a razor blade, leaving only the abaxial epidermis sticking to the tape. The cell layer was washed with 10 mM MES-KOH pH 6.15 and stomata were imaged immediately.

Alternatively, epidermal peels from leaves blended for 30 sec in water with an Omni Mixer (Sorvall) were transferred on microscopy slides at the indicated time points after treatment with or without 10 μM fusicoccin or 2.5 μM tautomycin and immediately imaged. All images were acquired with an inverted microscope (Nikon Eclipse TS100) at 40x magnification. Stomatal aperture was measured from light microscopy pictures using ImageJ. Around 16 pictures per replicate were taken and more than 100 stomatal apertures were measured per time point.

Guard cell specific gene silencing

For guard cell specific gene silencing of *BAM1,* the microRNA 173 target site was added upstream of the first 300 bp of the BAM1 coding sequence by PCR amplification, producing a microRNA induced gene silencing (MIGS) construct [S9]. The miR173_ts_BAM1 construct was sub-cloned into the pFL30 vector containing the guard cell specific promoter of *CYP86A2* [S10]. The resulting pDH12 construct was transformed into *Arabidopsis thaliana* ecotype Col-0 followed by the selection of independent, stable lines. For primer sequences see Table S1.

RNA extraction from epidermal peels and real time qPCR analysis

Fully developed leaves from 12 plants per biological replicate (3 replicates per genotype) were harvested at the end of the night and blended in water for 1.5 min with an Omni Mixer (Sorvall). The homogenate was passed through a 200 μm mesh and the retained epidermal peels were carefully rinsed. Subsequently, the epidermal peels were incubated for 1 h with 50

ml of a cellulysin cellulose enzymatic solution (0.7% cellulysin cellulase from *Trichoderma viride,* Calbiochem, 0.1% (w/v) polyvinylpyrrolidone 40000, 0.25% (w/v) BSA fraction V, 0.5 mM ascorbic acid in basic solution as described previously [S11] to digest the cell wall of the epidermal cells. At the end of the digestion step, additional 30 ml of basic solution was added to the mixture, and peels with guard cells as the only intact cell type were collected in a 200 μm mesh. Viability of guard cells was confirmed with the fluorescin diacetate (FDA) staining. The collected material was subsequently frozen in liquid nitrogen and grinded in a mortar. For comparison, 100 mg of leaf tissue from the same plant population was harvested and grinded in liquid nitrogen. RNA isolation was performed with 100 mg of tissue using the RNeasy Plant Mini Kit (Qiagen) according to manufacturers's instructions. RNA was quantified with a NanoDrop ND-1000 spectrophotometer (Thermo Scientific) and the integrity of the isolated RNA was visualized on an agarose gel. 1 μg of total RNA of each sample was used to produce cDNA using the M-MLV reverse transcriptase and oligo(dT) primers (Promega). Quantitative PCR was performed using the SYBR green master mix (Applied Biosystems) with the 7500 Fast Real-Time PCR System (Applied Biosystems). Reactions were run in triplicate with three different cDNA preparations, and the iQ5 Optical System Software (Applied Biosystems) was used to determine the threshold cycle (Ct) when fluorescence significantly increased above background. Gene-specific transcripts were normalized to *Actin2* gene (ACT2; At3g18780) and quantified by the ΔCt method (Ct of gene of interest – Ct of *ACT2* gene). Real-time SYBR green dissociation curves showed one species of amplicon for each primer combination. *KAT1* (INWARD-RECTIFYING K^+ *CHANNEL1;* At5g46240), *CYP86A2* (CYTOCHROME *P450 86A2;* At4g00360) and *MYB60* (MYB *TRANSCRIPTION FACTOR60;* At1g08810) were used as markers for guard cell-specific expression. *RBCS1A* gene (RuBisCO *SMALL SUBUNIT1A;* At1g67090) was only expressed in leaves, indicating minimal or no contamination from leaf RNA in the epidermal peel preparation. The primers for qPCR are listed in Table S1.

Mesophyll starch quantification

Mesophyll starch content was quantified enzymatically as described previously [S12]. Briefly, entire rosettes were harvested at the end of the night and at the end of the day and homogenized in 0.7 M perchloric acid. Insoluble material was pelleted and washed twice in 70% (v/v) ethanol and resuspended in water. Starch was solubilized by boiling at 95°C for 15 minutes and subsequently digested to glucose using α-amylase (Roche) and amyloglucosidase (Roche) for 2 h at 37°C. The glucose equivalents were determined through an enzymatic reaction using hexokinase (Roche) and glucose-6-phosphate dehydrogenase (Roche), which converts NAD to NADH in an equimolar ratio. The increase in the absorption spectrum at

340 nm specific for NADH was assayed in a spectrophotometer (Synergy H1, BioTek).

For visualization of starch in full rosettes, leaves were harvested at the end of the night and at the end of the day and destained in 80% (v/v) ethanol. After ethanol was removed, leaves were extensively rinsed in water and stained with iodine solution (Sigma-Aldrich). Pictures were taken after excess iodine solution was removed in water.

Gas exchange measurements

Leaf level gas exchange measurements were made on the fully expanded leaf of WT and mutant plants using a CIRAS-1 (PP systems International, Amesbury, Massachusetts, USA) with a Parkinson-type broad leaf cuvette. All measurements were made in the initial 1 h of light. Light was provided by a 600 W LED L4A-S10 lighting system (Heliospectra AB, Goteborg, Sweden). For all measurements, leaf cuvette CO_2 concentration was kept at 400 mmol mol^{-1} while vapour pressure deficit (VPDL) was maintained at 1 ± 0.05 kPa using a dew-point generator (Li-840, LI- COR) at a leaf temperature of 20°C ± 2°C and a flow rate of 200 mL min^{-1}. Leaves were initially equilibrated in the cuvette in darkness until the leaf had stabilized, about 15 – 30 min. After the reading were stable for at least 5 min, PPFD was applied at 150 ìmol m^{-2} s^{-1} white light and measurements of *A, gs* and *Ci* were recorded every 1 min.

Table S1: Oligonucleotides used in this study

Oligo ID	Atg gene code	sequence
	Primers used for qPCR experiments	
ACTIN2_fw	AT3G18780	TGGAATCCACGAGACAACCTA
ACTIN2_rev	AT3G18780	TTCTGTGAACGATTCCTGGAC
AMY3_fw	AT1G69830	TGCTTACATCCTAACTCATCC
AMY3_rev	AT1G69830	CTCTTGTCTATATTCACCTCACTC
BAM1_fw	At3g23920	CCATTGTGGAAATCCAAGTG
BAM1_rev	At3g23920	ACGAGTACTTATCATAGCACTG
BAM3_fw	At4g17090	TGATTCTGTGCCTGTCCT
BAM3_rev	At4g17090	GAATTTCCGCAATAACTCCTC
CYP86A2_fw	At4g00360	TGAATTCACCACCAGGACGT
CYP86A2_rev	At4g00360	AACCGGCTCGTAATTGTTCTG
ISA3_fw	AT4G09020	CTAGCTTTCACTCTCCATGAC
ISA3_rev	AT4G09020	GACTCGAGGTTTGTGTCAG
KAT1_fw	At5g46240	TAACGACCACGGGATATGGA
KAT1_rev	At5g46240	GAGGTAAGCTGTCAAACCGA
LDA_fw	At5g04360	CTCAGGGTATTCCATTCTTCCA
LDA_rev	At5g04360	AAGTCCAGCCTATTGAACCA
MYB60_fw	At1g08810	CATGAAGATGGTGATCATGAGG
MYB60_rev	At1g08810	TTCCATTTGACCCCCAGTAG
RBCS1A_fw	At1g67090	ACTCACCCGGATACTATGATG
RBCS1A_rev	At1g67090	CACTCTTCCACTTCCTTCAAC
	Primers used for cloning of BAM1 silencing lines	
miR173_ts-BAM1_fwd		**GTGATTTTTCTCTACAAGCGAA**ATGGCGCTTAATTTATC
BAM1_rev		TTTCTTTCCACCAATCCCTCCTTC

SUPPLEMENTAL REFERENCES

S1. Caspar, T., Huber, S.C., and Somerville, C. (1985). Alterations in growth, photosynthesis, and respiration in a starchless mutant of *Arabidopsis thaliana* (L.) deficient in chloroplast phosphoglucomutase activity. Plant Physiol. *79,* 11–17.

S2. Fulton, D.C., Stettler, M., Mettler, T., Vaughan, C.K., Li, J., Francisco, P., Gil, M., Reinhold, H., Eicke, S., Messerli, G., et al. (2008). Beta-AMYLASE4, a noncatalytic protein required for starch breakdown, acts upstream of three active beta-amylases in Arabidopsis chloroplasts. Plant Cell *20,* 1040–58.

S3. Yu, T-S., Zeeman, S.C., Thorneycroft, D., Fulton, D.C., Dunstan, H., Lue, W-L., Hegemann, B., Tung, S-Y., Umemoto, T., Chapple, A., et al. (2005). á-Amylase is not required for breakdown of transitory starch in Arabidopsis leaves. J. Biol. Chem. *280,* 9773–9779.

S4. Delatte, T., Umhang, M., Trevisan, M., Eicke, S., Thorneycroft, D., Smith, S.M., and Zeeman, S.C. (2006). Evidence for distinct mechanisms of starch granule breakdown in plants. J. Biol. Chem. *281,* 12050–12059.

S5. Kinoshita, T., Doi, M., Suetsugu, N., Kagawa, T., Wada, M., and Shimazaki, K.I. (2001). *phot1* and *phot2* mediate blue light regulation of stomatal opening. Nature *414,* 656–660.

S6. Takemiya, A., Sugiyama, N., Fujimoto, H., Tsutsumi, T., Yamauchi, S., Hiyama, A., Tada, Y., Christie, J.M., and Shimazaki, K.I. (2013). Phosphorylation of BLUS1 kinase by phototropins is a primary step in stomatal opening. Nat. Commun. *4,* 2094-2101.

S7. Haruta, M., Burch, H.L., Nelson, R.B., Barret-Wilt, G., Kline, K.G., Mohsin, S.B., Young, J.C., Otegui, M.S., and Sussman, M.R. (2010). Molecular characterization of mutant Arabidopsis plants with reduced plasma membrane proton pump activity. J. Biol. Chem. *285,* 17918–17929.

S8. Truernit, E., Bauby, H., Dubreucq, B., Grandjean, O., Runions, J., Barthélémy, J., and Palauqui J-C. (2008). High-resolution whole-mount imaging of three-dimensional tissue organization and gene expression enables the study of phloem development and structure in Arabidopsis. Plant Cell *20,* 1494–1503.

S9. de Felippes, F.F., Wang, J-W., and Weigel, D. (2012). MIGS: miRNA-induced gene silencing. Plant J *70,* 541–547.

S10. Galbiati, M., Simoni, L., Pavesi, G., Cominelli, E., Francia, P., Vavasseeur, A., Nelson, T., bevan, M., and Tonelli, C. (2008). Gene trap lines identify Arabidopsis genes expressed in stomatal guard cells. Plant J. *53,* 750–762.

S11. Pandey, S., Wang, X-Q., Coursol, S-A., and Assmann S.M. (2009). Preparation and application of *Arabidopsis thaliana* guard cell protoplasts. New Phytol. *153,* 517–526.

S12. Hostettler, C., Kölling, K., Santelia, D., Steb, S., Kötting, O., and Zeeman, S.C. (2011). Analysis of starch metabolism in chloroplasts. Methods Mol. Biol. *775,* 387–410.

2 – Addendum to Horrer et al.: Blue light induces a distinct starch degradation pathway in guard cells for stomatal opening

Daniel Horrer, Sabrina Flütsch, Diana Santelia

Supplementary data to the article Horrer *et al.*
(accepted for publication in Current Biology)
Unpublished results

Synopsis: We continued with our investigations into guard cell starch breakdown, showing that under extended nights starch degradation occurs only at very low rates. Furthermore, the role of starch degradation for malate and sucrose synthesis is discussed and several multiple mutant combinations give additional insights into the distinct metabolic pathway responsible for the observed rapid starch degradation in response to illumination.

Experimental contributions: S.F. conducted the experiment to determine the mesophyll starch data shown in Figure 2.2 B and helped with the analysis shown in Figure 2.1.

Supplementary Results and Discussion

Guard cells do not degrade starch under an extended night

As reported in Chapter 1, rapid guard cell starch degradation occurred in wild-type plants during the first hour of the day, while only little degradation was observed in the *phot1phot2* double mutant. In order to test if a circadian rhythm was involved in the control of early morning guard cell starch degradation, we determined starch content in wild type guard cells upon illumination (120 µmol m^{-2} s^{-1}) or under prolonged darkness. Under the latter condition, almost no degradation occurred, indicating that illumination is necessary for the induction of early morning starch degradation (Figure 2.1).

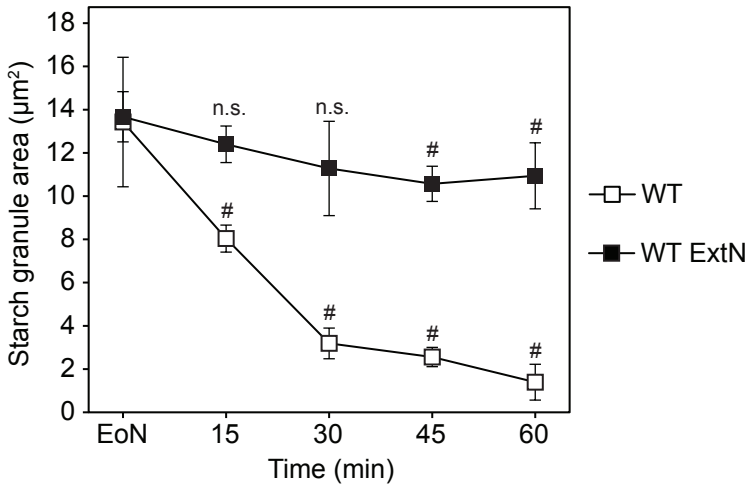

Figure 2.1: Guard cell starch degradation is strongly inhibited under an extended night. Guard cell starch content was quantified from confocal images of PS-PI stained epidermal peels of wild-type plants in the light (120 µmol m^{-2} s^{-1}) or kept in the dark for an additional hour after the end of the regular 12 h night phase (extended night, ExtN). Values represent averages of 3 independent experiments ± SE with a total of n > 110 analysed guard cells. Statistical analysis reveals significant differences in starch content compared to the end of night (EoN) (unpaired Student's t test, # denotes P < 0.01; n.s. = not significant). Wild type control data is the same as shown in Horrer *et al*. Figure 4 B.

In contrast to this observation, we reproducibly detected slow rates of starch degradation during the night, at a time when predawn opening of stomata was reported to occur in Arabidopsis (Lebaudy et al., 2008). Interestingly, this predawn opening, which seems to be circadian regulated (Gorton et al., 1989), was dependent on the presence of K^+_{in} channels (Lebaudy et al., 2008). Furthermore, malate can be synthesised in guard cells in darkness (Gotow et al., 1985; Scheibe et al., 1990). This suggests that the predawn degradation of starch observed in our experiments

may contribute to the slight stomatal opening during the night via the synthesis of malate. This priming of the guard cells for the coming day is thought to promote rapid opening at dawn, when light quantity and air humidity are relatively high, while at the same time ambient temperature is still rather low. A role of predawn starch degradation is furthermore supported by the observation that predawn increases in transpiration rates occurred in wild-type plants but not in the starchless *pgm* mutants (Lasceve et al., 1997).

Predawn starch degradation was also inhibited in the *bam1* mutant, where only a slight decrease in guard cell starch content was observed during the last hour before the onset of illumination, suggesting an additional role of BAM1 during nighttime guard cell starch degradation (Chapter 1, Figure 1 B). In the *bam3* mutant, predawn starch degradation occurred, although at lower rates at the end of the night compared to wild-type plants. Because the overall guard cell starch content between wild type and *bam3* mutant plants were different, the interpretation of these observations are difficult (Chapter1, Figure 1 B). One possibility is that BAM3 may participate in predawn starch breakdown. Alternatively, it could be that increased activity of BAM1 in the *bam3* mutant background during the night could explain this difference in starch content, but additional experimental evidence would be needed to support this idea.

Starch malate interconversion

In *Vicia faba* K^+ accumulation was estimated to occur within one or two hours after the initial membrane hyperpolarization (Schroeder et al., 1987), which fits with our observation that almost all guard cell starch is degraded within the first 30 minutes after illumination (Figure 2.1). This is in accordance with the generally accepted theory that starch breakdown yields carbon skeletons in the form of phosphoenolpyruvate (PEP) for the synthesis of malate, rather than contributing to sucrose synthesis (see Introduction section). Guard cells therefore seem to fix carbon dioxide (CO_2) primarily with PHOSPHOENOLPYRUVATE CARBOXYLASE (PEPC) instead of relying on photosynthetic carbon fixation by the Calvin cycle. Support for this hypothesis comes for example from early labelling experiments using $^{14}CO_2$, where radioactivity was observed primarily in organic acids but not in sugar phosphates (Schnabl, 1980).

Several recent reviews base their model of guard cell malate synthesis on the assumption that triose phosphates originating from starch breakdown are exported to the cytosol (Shimazaki et al., 2007; Lawson, 2009). Shimazaki and colleagues propose that guard cell starch is primarily broken down by α-GLUCAN PHOSPHORYLASE (PHS1) to yield Glucose-1-Phosphate (Glc1P), which is converted into triose phosphates within the chloroplast. However, we have collected evidence that PHS1 has only a minor role in guard cell starch breakdown (Figure 2.2) and that guard cell starch is mainly degraded by the concerted action of BAM1 and AMY3. This suggests maltose as the major starch degradation product, which is not known to be further metabolized in plastids, but is rather exported to the cytosol via the MALTOSE TRANSPORTER 1 (MEX1) transporter (Niittyla et al., 2004). Cytosolic maltose is supposedly processed by DISPROPORTIONATING ENZYME 2 (DPE2), which yields one glucose molecule, while the second glucose unit is transferred to cytosolic heteroglycan (Lu and Sharkey, 2004; Fettke et al., 2006). This second glucosyl unit is presumably released via PHS2 in the form of Glc1P (Lu et al., 2006). Both sugars can be further metabolised through glycolysis to yield 4 molecules of PEP, with a net gain of one molecule of ATP and four molecules of NADH. PEP is subsequently converted into oxaloacetate by the action of PEPC and finally into malate through NAD-dependent MALATE DEHYDROGENASE (MDH) (Outlaw and Kennedy, 1978; Gotow et al., 1985; Scheibe et al., 1990; Asai et al., 2000). Here, NADH generated during glycolysis is used for the reduction of oxaloacetate by cytosolic NAD-MDH, which shows higher activity compared to plastidial NADP-dependent MDH in guard cells (Gotow et al., 1985). In total this yields a final net conversion of one maltose molecule into four molecules of malate and one molecule of ATP. Strikingly, this proposed pathway does not rely on the production of ATP and reducing equivalents in the light reaction of guard cell chloroplasts usually assumed to be required for malate production (Shimazaki et al., 2007; Lawson, 2009), but it would explain how predawn malate synthesis could occur. Even the export of glucose produced by DPE1 and its conversion into malate would be self-sustained, without the requirement of plastidial ATP and NADH production.

Malate formation was reported to be required not only for counter balancing the charge introduced by the influx of K^+, but also to stabilize the cytosolic pH during the time of high H^+-ATPase activity (Robinson and Preiss, 1985). It was shown that the activation of PEPC is achieved through protein phosphorylation, which greatly reduces the allosteric inhibitory effect of malate on PEPC activity (Meinhard and Schnabl, 2001; Outlaw et al., 2002). The signalling events leading to the

phosphorylation dependent activation of PEPC can be induced by either light or by the treatment with fusicoccin and is therefore a response to the H^+-ATPase activity. Activation of the plasma membrane proton pumps causes an initial alkalinisation of the cytosol, which is proposed to be the link between H^+-ATPase and the activation of the PEPC phosphorylating kinase (Outlaw et al., 2002). Strikingly, this resembles the activation mechanism we observed for starch degradation. BAM1, AMY3 and other enzymes important for guard cell degradation could be activated via a similar, presumably pH dependent mechanism. Hereby, the link between changes in cytosolic pH and the activation of starch degradation in the chloroplast is not clear, but might depend on protein phosphorylation of BAM1 (see Chapter 3). Alternatively, the change in metabolic fluxes upon the activation of stomatal opening could trigger starch degradation indirectly through a metabolic signal such as an increase in the ADP/ATP ratio as a result of H^+-ATPase activity or the depletion of metabolic intermediates such as PEP and oxaloacetate (OAA) as a result of malate synthesis and elevated cellular respiration.

Similarly to the notion that malate production helps to stabilize the cytosolic pH during the high activity of the H^+-ATPase, the symport of Cl^- as well as sucrose with H^+ over the plasma membrane would help to reduce the effect of H^+-ATPase activity on cytosolic pH. This could explain why malate synthesis is not induced if guard cells can take up high amounts of Cl^- or sucrose from the apoplast (Outlaw et al., 2002).

The improved resolution of our PS-PI staining method using confocal laser scanning microscopy enables us to estimate the amount of starch that is broken down during the initial hour of illumination in order to calculate the theoretical amount of malate that can be produced in guard cells. As shown in Chapter 1 (Supplemental Data 1), we calculated a theoretical maximum of malate synthesis from starch breakdown of 470 mM per guard cell. Guard cells were reported to accumulate between 100 and 200 mM of malate on a full cell volume basis (Martinoia and Rentsch, 1994). We therefore propose that approximately half of the starch breakdown observed is sufficient for rapid guard cell malate synthesis during the initial opening phase, which is in agreement with the previous report on *Vicia faba* stating that starch breakdown is quantitatively sufficient for the synthesis of the required anions for stomatal opening (Outlaw and Manchester, 1979). The remaining carbon skeletons would be available for cellular respiration for the production of the ATP required by the H^+-ATPase and potentially for the synthesis of sucrose as an additional osmolyte. Sucrose can be synthesised via the conversion of Glc1P and UTP into UDP-Glucose through UDP-GLUCOSE PYROPHOSPHORYLASE (UGPase) and the subsequent

reaction catalysed by sucrose phosphate synthase (SPS) forming sucrose from UDP-Glucose and Fru6P to yield Sucrose-6-phosphate and UDP. Subsequently, sucrose-6-phosphate becomes dephosphorylated by sucrose phosphate phosphatases. Alternatively, sucrose can also be directly synthesised from UDP-Glucose and Fru by sucrose synthases (SUSs). Both SPS and SUS isoforms are known to be present in guard cells (Hite et al., 1993). Sucrose formed by this pathway could be involved in the process of stomatal opening, although as discussed above, it is usually assumed to accumulate only in the afternoon, when starch is synthesised rather than broken down. Nevertheless, it was questioned already in the 1980s if the accumulation of potassium with its counterions would be sufficient for the osmotic changes in guard cells (MacRobbie and Lettau, 1980). It is therefore possible that sugars, such as sucrose and hexoses derived from starch breakdown can also accumulate in guard cells. Antunes and colleagues recently reported a lower stomatal conductance in transgenic potato plants with reduced transcripts of SUCROSE SYNTHASE 3 (SUS3) (Antunes et al., 2012). In their report they suggest that sucrose breakdown by the reversible reaction catalysed through SUS3, is a prerequisite for the synthesis of malate and ATP for stomatal opening, although the use of a *35S* construct makes it difficult to draw a clear conclusion regarding the role of SUS3 in guard cells and the observed reduction in stomatal aperture might be due to overall changes in plant metabolism. Furthermore, in this study the role of guard cell starch breakdown was neglected. In a follow up report from the same group, no alterations in starch content in epidermal peel fragments from greenhouse grown tobacco plants upon stomatal opening were reported (Daloso et al., 2015). It should be mentioned that the use of an enzymatic assay used in this report to quantify starch in epidermal peels is most likely not sensitive enough to detect changes in guard cell starch content. In accordance with this, Daloso and colleagues reported starch in epidermal peels of approximately 2.5 ng/g dry weight (Daloso et al., 2015), while Streb and colleagues reported a detection limit for their enzymatic starch quantification method of about 2 µg/g fresh weight (Streb et al., 2009). Even taking into account the differences between the quantification based on dry and fresh weight, the estimations made by Daloso et al. is well below the detection limit, making it impossible to draw conclusions about the temporal changes in starch content. Therefore, the role of sucrose and hexose metabolism in guard cells still remains largely unknown, further obscured by the use of inadequate experimental methods.

The fate of malate during stomatal closure

The fate of malate during stomatal closure was already a matter of debate during the 1970s and 1980s (Robinson and Preiss, 1985). It is clear that during stomatal closure high amounts of vacuolar malate need to be removed from the cell. Three possibilities seem reasonable. Firstly, the export of malate into the apoplast, secondly the utilization of malate during gluconeogenesis and lastly the use of malate to fuel the mitochondrial tricarboxylic acid (TCA) cycle.

Early observations indicated that malate is exported during stomatal closure to the apoplast (Keller et al., 1989), followed by the recent elucidation of a malate exporter (Meyer et al., 2010). Malate accumulation in the apoplast will contribute to the depolarization of the plasma membrane and to the subsequent opening of K^+_{out} channels, which suggests an important role for malate export (Hedrich et al., 1994, 2001). But to which extent malate is exported is not clear and malate extrusion might be more important as a signalling mechanism than for the reduction of cellular osmolytes (Hedrich et al., 1994).

It seems likely that not all malate is exported during stomatal closure and that a certain amount is rather metabolised within the guard cells. *Vicia faba* guard cell protoplasts (GCP) incubated with uniformly ^{14}C-labelled malate suggested a possible role of gluconeogenic malate metabolism in guard cells, with radioactive label appearing in starch (Schnabl, 1980). In contrast, when GCP were incubated with specifically labelled [4-^{14}C]malate, almost no label appeared in starch due to the decarboxylation step during gluconeogenesis and the low capacity of guard cells to fix the released $^{14}CO_2$ into sugar phosphates.

Penfield and colleagues showed recently that in *Arabidopsis thaliana* the pathway of malate conversion into PEP during light-to-dark transition was important (Penfield et al., 2012). The mutant of PHOSPHOENOLPYRUVATE CARBOXYKINASE 1 (PCK1), which catalyses the decarboxylation of oxaloacetate to form PEP as an early step of gluconeogenesis, was more drought sensitive than wild-type plants and stomata of *pck1* mutant were more open and did not close completely after the transition from light to darkness. Alternatively, malate can also be converted into pyruvate via malic enzyme, which seems to be highly abundant in guard cells (Outlaw et al., 1981; Wheeler et al., 2005). Hexose phosphates resynthesized from malate during gluconeogenesis could be imported into the chloroplast via sugar phosphate transporter and contribute significantly to the synthesis of starch during stomatal closure, with starch synthesis apparently proceeding into the dark phase (Chapter 1, Figure 1 B).

On the other hand, pyruvate synthesised from malate can be used to fuel the TCA cycle in mitochondria and it has been argued that the complete oxidation of malate, rather than gluconeogenesis, is important during stomatal closure and that the ATP produced by cellular respiration can be used to resynthesize starch (Robinson and Preiss, 1985).

In conclusion, both the metabolic pathways of sugars and of organic acids in guard cells are not well understood and the elucidation of their contribution to guard cell regulation will require substantial future research efforts. Especially the precise determination of changes in metabolites during stomatal opening and closure in wild-type Arabidopsis plants needs to be compared to mutants of the diverse set of metabolic pathways mentioned above. This will allow us to draw a much more detailed regulatory network compared to our current understanding and will considerably improve quantitative models of guard cell movements (Hills et al., 2012).

Mutants and multiple mutant combinations of starch degrading enzymes

We continued our investigations of the enzymatic pathway responsible for guard cell starch degradation by creating multiple mutant combinations through crosses of available single and double mutants. Multiple mutants were isolated through genotyping of the F2 generation. Here, we also added a mutant devoid of PHS1, which has no obvious *sex* phenotype in the leaves under normal growth conditions, similar to *bam1* and *amy3*. The mutant alleles as well as the genotyping primers are described in Chapter 1, with the exception of the *phs1* (GABI_257A06) mutant line (Malinova et al., 2014), which was genotyped using the following oligonucleotide combination: phs1_fw TCCACCGTTTCTTACCATCTG and phs1_rev GAACCGAAAGC CAAAGTAACC.

As reported in Chapter 1, the *lda* as well as the *amy3* single mutants show only a weak guard cell starch excess phenotype after 1 h of illumination. Furthermore, the introduction of the *lda* mutant in the *isa3* mutant background strongly increased the *sex* phenotype of the *isa3* mutant, showing a functional redundancy between these two debranching enzymes, with *ISA3* encoding for the major enzymatic activity. In contrast, the *amy3lda* double mutant did not show an elevated guard cell starch excess phenotype compared to the single mutants (Figure 2.2 A), again illustrating that ISA3 is responsible for the majority of the debranching activity in these cells. Nevertheless, a minor role of LDA in guard cells is confirmed by the observation that

the limited starch degradation observed in the *amy3bam1* double mutant after 3 h of illumination was absent in the *amy3bam1lda* triple mutant (Figure 2.2 A).

As mentioned above, it is often assumed that guard cell starch is broken down to yield Glc1P, which is subsequently converted into triose phosphates in the plastids (Shimazaki et al., 2007; Lawson, 2009). Although we clearly established BAM1 and AMY3 as the major starch degrading enzymes, we could not rule out the involvement of PHS1. Guard cell starch seems to be degraded normally in the *phs1* single mutant, but similar to the effect of *lda* in the *amy3bam1lda* triple mutant, the *amy3bam1phs1* mutant combination did not show a statistical significant difference between the time points, hinting towards a minor role of PHS1 in guard cell starch degradation (Figure 2.2 A). Furthermore, the *amy3bam1phs1lda* quadruple mutant did not show any additional increase in starch content in guard cells (Figure 2.2 A). It should be mentioned that because guard cell starch degradation in the *amy3bam1* double mutant was almost completely inhibited, the relative contribution of other enzymes such as PHS1 and LDA deducted from the triple and quadruple mutants might be difficult to estimate. It will be therefore more informative to continue this investigation with multiple mutant combinations that do not include *bam1*, such as *amy3phs1*, *phs1lda*, *amy3ldaphs1*, *amy3ldaisa3* and *amy3isa3*. Furthermore, the guard cell starch content in double mutants including *bam1lda*, *bam1phs1* and *bam1phs1lda*, which are now available in our laboratory, can be analysed in the future.

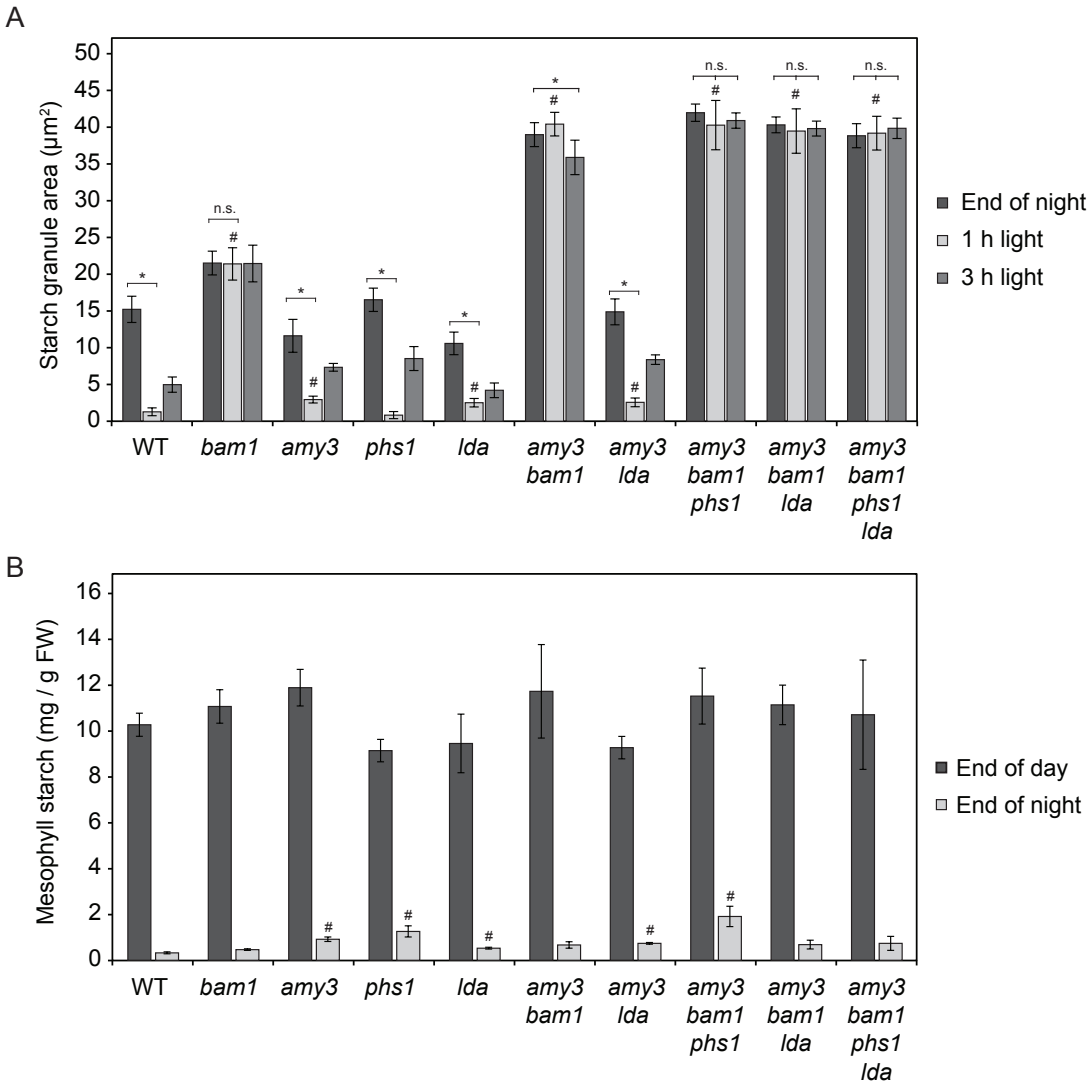

Figure 2.2: Guard cell and mesophyll starch of multiple mutant combinations.
(A) Guard cell starch content was quantified from confocal images of PS-PI stained epidermal peels of wild type plants, single mutants and multiple mutant combinations grown under standard growth conditions according to Chapter 1. Values represent averages of 3 independent experiments ± SE with a total of $n > 110$ analysed guard cells. Data for wild type control, *bam1*, *amy3, lda* and *amy3bam1* was included for comparison and is taken from Chapter 1, Figure 2 B. (B) Mesophyll starch content of wild type plants and single and multiple mutants was quantified enzymatically according to Chapter 1. Values are averages of at least 6 biological replicates ± SE. Data for wild type control, *bam1*, *amy3, lda* and *amy3bam1* was included for comparison and is taken from Chapter 1 Figure SI1. Statistical significance between mutants and the corresponding time points of the WT are indicated by a # (unpaired Student's *t* test, # denotes $P < 0.05$). Additional statistical tests are indicated by an asterisk (unpaired Student's *t* test, * denotes $p < 0.01$; n.s. = not significant).

Interestingly, the *amy3bam1phs1lda* quadruple mutant did not exhibit altered mesophyll starch content at the end of the night or at the end of the day (Figure 2.2 B), indicating that mesophyll starch degradation depends mainly on BAM3 and ISA3. While we observed a slight increase in guard cell starch content in the *amy3*, *phs1* and *lda* single mutants at the end of the night, the most pronounced effect was found

in the *amy3bam1phs1* triple mutant (Figure 2.2 B). Although at this point we cannot rule out that this effect is due to a relatively high variability in the starch data between the limited numbers of biological replicates in this experiment, it could hint towards a minor role of PHS1 in both guard cells and mesophyll cells.

Further investigation of the *phs1* mutant phenotype

The phosphorolytic cleavage of glucosyl residues from linear polyglucan chains by PHS1 can potentially release Glc1P, which could be exported by a hypothesized Glc1P transporter (Fettke et al., 2011). Alternatively, due to the reversibility of the catalysed reaction, PHS1 could also play a role in starch synthesis, utilizing Glc1P for the elongation of glucan chains. This latter function was described for the PHS1 homologues in heterotrophic storage tissue of rice, wheat and potato (Satoh et al., 2008; Tickle et al., 2009; Fettke et al., 2010). In contrast to this role in storage organs, the function of Arabidopsis PHS1 remains elusive, with the *phs1* mutant reported to lack obvious differences in mesophyll starch degradation, starch accumulation or granule structure compared to wild-type plants (Zeeman et al., 2004). Nevertheless, in a recent publication investigating the complex phenotypes associated with double knock-out mutants of *dpe2phs1* and *mex1phs1*, Malinova and colleagues argued that PHS1 does contribute to leaf starch metabolism in the dark (Malinova et al., 2014). We observed a slight elevation in mesophyll starch of our *phs1* mutant plants at the end of the night (Figure 2.2 B). This is in contrast to the report by Zeeman and colleagues who did not find differences in starch content (Zeeman et al., 2004). One possible explanation could be the use of different mutant alleles in different Arabidopsis ecotypes. In our experiments, as well as in the *mex1phs1* double mutant investigated by Malinova, a GABI line (GABI_257A06) in the Col-0 background was used, while the report by Zeeman and colleagues was based on two mutant alleles in the Wassilewskija ecotype (Zeeman et al., 2004; Malinova et al., 2014). Nevertheless, a more detailed investigation of *phs1* leaf starch content will be necessary to determine of this mutant has a weak *sex* phenotype or not.

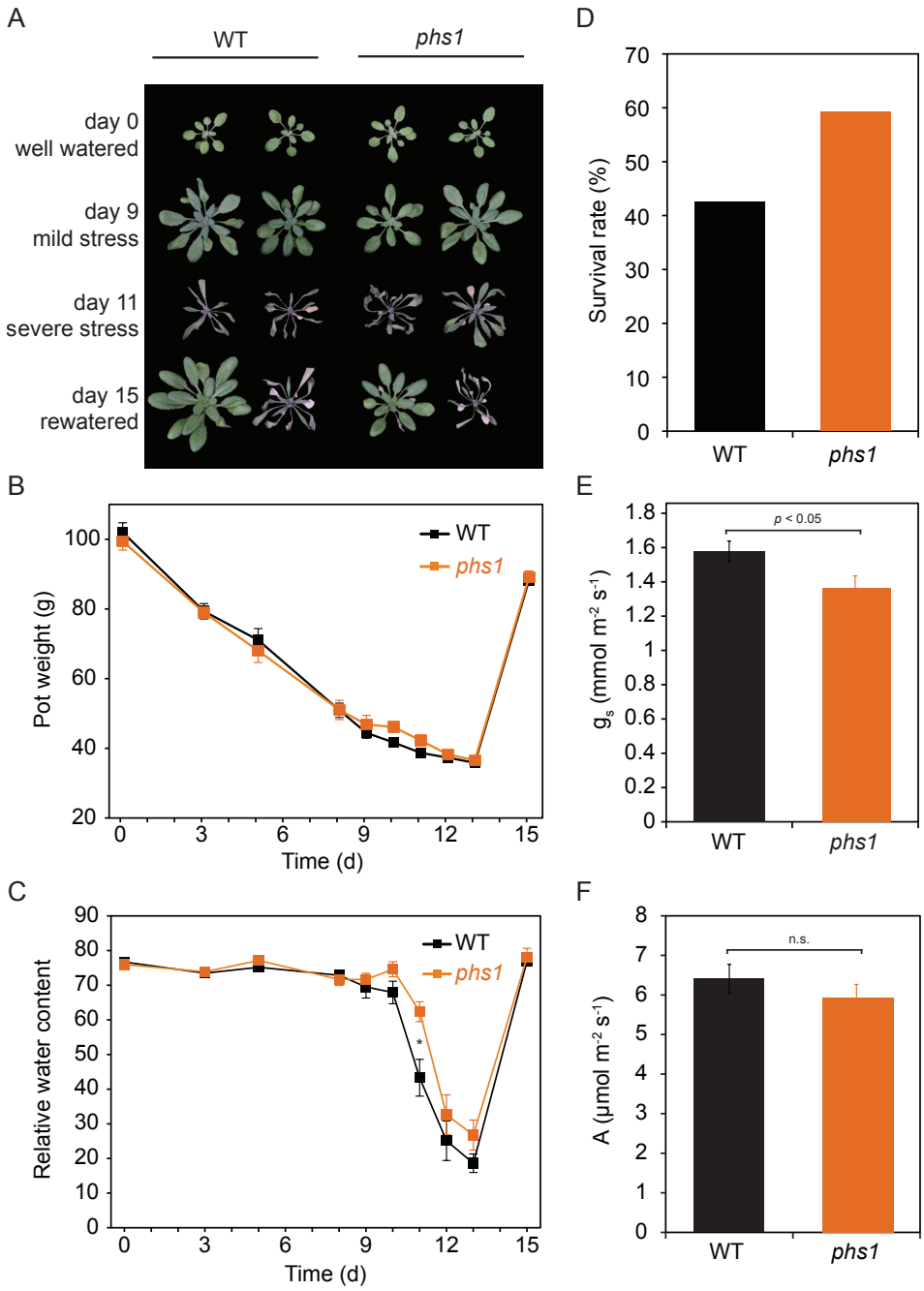

Figure 2.3: The *phs1* mutants show a drought avoidance phenotype.
The drought stress experiment was conducted as described in Chapter 5. (A) Photographs of representative plants throughout the drought stress experiment. (B) Water lost from the soil indicated as the reduction in the pot weight. Values are from the same 6 replicates as used in (C) and present averages ± SE. (C) Relative water content was calculated from 6 biological replicates and is presented as average ± SE. * denotes statistical significant differences between WT and *phs1* (unpaired Student's *t* test, $P < 0.05$). (D) Survival rate was calculated after rewatering at day 15 (n > 25). (E) Transpiration rate (g_s) and (F) assimilation rate (A) were measured over the 12 h day in well watered WT and *phs1* full rosettes (n = 8) using LICOR LI-7000 infrared gas analyser as described in (Kölling et al., 2015). Values presented in (E) and (F) are averages over the 12 h day from eight biological replicates ± SE. Statistical significant differences as indicated (unpaired Student's *t* test; n.s. = not significant).

As described above, we found evidence that PHS1 could also play a minor role in guard cell starch degradation. It was previously reported that no differences in stomatal conductance was observed between mutant and wild type when rosettes were separated from their roots (Zeeman et al., 2004). In contrast to this rapid dehydration stress, we decided to investigate a possible role of PHS1 during progressive drought stress. Well watered, 3 week-old plants at day 0 of the drought stress experiment showed a relative water content of roughly 78%, which did not decrease until the first signs of wilting appeared at day 9 (Figure 2.3 A and C). At this time point, the weight of the pots had fallen under the initial 60 g of soil (see Chapter 5 for experimental details), indicating a low soil water content, which continued to decrease to the values of completely dried soil (slightly below 40 g) at around day 13 (Figure 2.3 B). While we did not observe statistically significant differences in water content between wild type and *phs1* mutants under the later time points, the mutant plants could retain the initial relative water content over a longer period, resulting in significant difference at day 11 (Figure 2.3 A and C). This delayed onset of severe drought stress led to a higher survival rate of *phs1* mutants after the plants were re-watered at day 13 (Figure 2.3 A and D). Taken together, this suggests that the *phs1* mutant shows an altered carbon metabolism, which causes a drought avoidance phenotype compared to wild type plants. We further speculated that this phenotype could be related to reduced stomatal conductance, leading to lower rates of transpiration. Indeed, the transpiration rate in well-watered *phs1* mutant plants was significantly lower over the 12 h light cycle compared to the wild type, while carbon assimilation rates were not altered (Figure 2.3 E and F).

In a recent publication Prasch and colleagues showed a drought resistant phenotype for the *bam1* mutant compared to wild-type plants (Prasch et al., 2015). This is in contrast to our observations, where we could not find a clear difference between the relative water content of the *bam1* mutant and wild-type plants (Data not shown). This indicates that the determination of soil water content through the direct measurement of soil field capacity (Prasch and Sonnewald, 2013) used in this recent report allowed a more homogenous application of drought stress conditions compared to our experimental set-up. Therefore, it is necessary to perform a more in depth investigation of the *phs1* mutant phenotype under water limiting conditions.

In summary, we propose a role for PHS1 in guard cell regulation, despite the lack of a clear starch excess phenotype in guard cells of the single mutant (Figure 2.2 A). The slight increase in drought resistance of the *phs1* mutant observed in our experiments comes without an obvious negative effect on carbon assimilation rates,

something that usually is difficult to achieve, but highly desired for crop breeding (Lawson et al., 2014). Together with the results presented in Chapter 1, this further indicates the potential for improving drought stress resistance in plants with altered guard cell carbon metabolism, although improved methods for the application of drought stress will be needed in the future to unequivocally establish resistant phenotypes of mutants related to guard cell carbon metabolism.

3 – Abscisic acid-induced starch degradation confers osmotic stress tolerance in Arabidopsis

Matthias Thalmann, Diana Pazmino, David Seung, Arianna Nigro, Tiago Meier, Daniel Horrer, Katharina Kölling, Hartwig W. Pfeifhofer, Samuel C. Zeeman, Diana Santelia

Submitted to PLOS Genetics

Synopsis: Here we show that during osmotic stress elevated levels of the phytohormone ABA induces the transcription of BAM1. Subsequent leaf starch degradation through BAM1 and AMY3 and carbon export from the shoot leads to the accumulation of osmolytes in the root. This mechanism allows plants to better cope with osmotic stress through improved water uptake and improved root growth under adverse environmental conditions.

Experimental contributions: In this study I performed the analysis of publicly available transcriptomic data obtained under a variety of stresses and hormone treatments, which are incorporated in Figure S4, as well as preliminary analysis of *BAM1* and *AMY3* promoter motifs. I furthermore performed osmotic stress experiments on agar plates and native gel analysis of BAM activity in the early phase of this project, which were subsequently extended by M.T.

Abscisic Acid-Induced Starch Degradation Confers Osmotic Stress Tolerance in Arabidopsis

Matthias Thalmann[a], Diana Pazmino[a], David Seung[b], Arianna Nigro[a], Tiago Meier[a], Daniel Horrer[a], Katharina Kölling[b], Hartwig W. Pfeifhofer[c], Samuel C. Zeeman[b] and Diana Santelia[a,*]

[a]Institute of Plant and Microbial Biology, University of Zürich, Zollikerstrasse 107, 8008 Zürich, Switzerland

[b]Institute for Agricultural Sciences, ETH Zürich, Universitätstrasse 2, 8092 Zürich, Switzerland

[c]Institut für Pflanzenwissenschaften, Karl-Franzens-Universität Graz, Schuberstrasse 51, 8010 Graz, Austria

[*] dsantelia@botinst.uzh.ch

Running title: Starch degradation during osmotic stress

Abstract

Plants cope with the osmotic imbalance caused by high salinity and drought through the cellular accumulation of osmolytes, such as nonstructural carbohydrates and charged metabolites, including proline. Starch is the major carbohydrate reserve in plants. In response to osmotic stress, starch in leaf cell chloroplasts is degraded in the light. In Arabidopsis, osmotic stress-induced starch degradation is mediated by β-amylase1 (BAM1) and contributes to the osmolytes accumulating in leaves during stress. Here, we show that BAM1 acts synergistically with another starch-degrading enzyme, α-amylase3 (AMY3). The *amy3 bam1* double mutants have normal starch metabolism under control growth conditions, but fail to mobilize starch during osmotic stress, suggesting the presence of a previously uncharacterized stress-induced starch degradation pathway. Molecular-genetic evidence demonstrated that this pathway is under the direct control of the abscisic acid-dependent AREB/ABF-SnRK2 kinase signaling pathway, through the transcriptional activation of *BAM1* and *AMY3* genes. Furthermore, analysis of carbon partitioning by ^{14}C labeling, combined with sugar and proline measurements, revealed that inhibition of stress-induced starch degradation in *amy3 bam1* dramatically affects carbon export to the root, impairing osmotic adjustment, water uptake and root growth. Our discovery uncovers a critical function for starch in plant stress tolerance and opens a new perspective for breeding stress-tolerant crops.

Introduction

The increase in atmospheric CO_2 and average global temperature associated with climate change has caused alterations in precipitation patterns and more frequent extreme weather conditions - such as heat waves, drought episodes, cold snaps, and flooding [1]. These extreme climate events are typically short in duration, but generate sub-optimal growing conditions, which threaten agricultural productivity worldwide [2]. High salinity and drought limit the performance of cultivated plants more than any other environmental stresses, causing more than 50 % of the annual agricultural yield losses [3–5]. There is a growing need to understand plant responses to these stresses to identify key components for breeding stress-tolerant crops.

A common consequence of plant exposure to high salinity and drought is osmotic stress, leading to reduced water potential, cellular dehydration and loss of turgor. This cellular dehydration affects virtually every aspect of plant physiology and cellular metabolism. Membranes lose their integrity and selectivity, and cellular compartmentalization is disrupted. Proteins become denatured, aggregated and inactivated. Excess levels of reactive oxygen species (ROS) are produced leading to oxidative damage [3,6]. As a consequence, inhibition of photosynthesis, metabolic dysfunction, and damage of cellular structures contribute to growth reduction, reduced fertility, premature senescence and finally death.

The responses of plants to water stress differ significantly depending upon the intensity and the duration of the stress, between species, and on the stage of development. However, in most cases, plants tend to cope with water deficit through the cellular accumulation of compatible solutes, such as nonstructural carbohydrates (sucrose, hexoses, and sugar alcohols), complex sugars (trehalose and fructans), and charged metabolites (glycine betaine and proline)[7,8]. These non-toxic molecules decrease the osmotic potential of the cell, promoting water retention in the plant without interfering with normal metabolism.

This process of osmotic adjustment enables the maintenance of cell turgor for plant growth and survival under drought conditions. Compatible solutes can also help stabilize proteins and cell structures, particularly when the stress becomes severe or persists for longer periods [9]. They can also act as free radical scavengers, protecting against oxidation by removing excess ROS, re-establishing the cellular redox balance [6,10].

Increased soluble sugars in response to water deficit occurs in parallel with a decrease in stomatal aperture and photosynthetic activity, and sugar levels are maximal when the stomata are nearly closed [11–15]. This indicates that a big fraction of the soluble sugars accumulating during water deficit stress results from the degradation of previously stored carbohydrate compounds, most likely starch - the predominant storage carbohydrate [13]. Starch is composed of glucose polymers packed to form inert granules inside plastids. In the leaf cell chloroplasts, transitory starch is synthesized during the day and hydrolyzed at night

to support cell metabolism and continuous growth [16]. In response to water deficit, a decrease in starch content in photosynthetic organs coincides with a significant increase in soluble sugars [12,15,17]. This indicates an increased flux into soluble sugar pools at times when starch accumulation would normally occur [13]. The mobilization of transitory starch under these conditions may help plants to endure short periods of water stress, sustaining central carbon metabolism to produce energy and osmoprotectants. Despite the potential importance of starch degradation upon water deficit and the fact that it appears to be a well-conserved process amongst different species, the underpinning biochemical mechanisms remain mostly unknown.

Starch degradation at night begins with the phosphorylation of the glucan chains by glucan, water dikinase and phosphoglucan, water dikinase [18]. The chains are then simultaneously degraded by a set of glucan hydrolyzing enzymes (including β-amylase [BAM], α-amylase [AMY], and debranching enzymes [DBE]) and dephosphorylated by phosphoglucan phosphatases [19,20]. These enzymes work in synergy to completely degrade starch [21,22]. Maltose released by BAM represents the predominant product of starch degradation in leaves under normal growth conditions [22]. BAM3 is the major isoform required for starch degradation at night and Arabidopsis *bam3* mutants have elevated amounts of starch and reduced levels of maltose at night, compared to wild type [22,23]. BAM1 is the closest homolog of BAM3 [22], but diurnal starch turnover is not affected in *bam1* mutants, indicating that BAM1 is not normally required for starch degradation at night [22]. Recently, it was shown that osmotic stress enhanced total β-amylase activity and reduced transitory starch accumulation during the day in leaves of wild-type Arabidopsis but not of *bam1* mutants [24]. Thus, it appears BAM1 is important for stress-induced starch degradation during water deficit. However, it is unclear if other enzymes (e.g. DBEs or AMY) also play a role during stress, or how the process is controlled.

Here, we subjected hydroponically-grown Arabidopsis plants to osmotic stress showing that BAM1 acts synergistically with the chloroplastic α-amylase 3 (AMY3) to activate starch degradation. The *amy3 bam1* double mutant, which has normal starch metabolism under control conditions, failed to mobilize starch during osmotic stress. We also provide evidence that *BAM1* and *AMY3* expression is under the direct control of abscisic acid (ABA). Collectively our data reveal the presence of a previously uncharacterized stress- induced starch degradation pathway and uncover the mechanism by which it contributes to osmotic stress tolerance.

Results

Maltose accumulates during the day in plants subject to severe osmotic stress

To study the effects of water deficit on starch metabolism in *Arabidopsis thaliana,* three-week-old plants grown in hydroponic culture in a 12-h-light/12-h-dark cycle were subject to 300 mM mannitol treatment for 4 h, starting after 3 h of light. Plants visibly wilted (Fig. 1A) but, when returned to the control solution without mannitol for 24 h, they recovered fully (Fig. 1A). Leaf starch metabolism was severely affected in osmotically-stressed plants. After 2 h and 4 h of stress, wild-type Col-0 plants accumulated 32 % and 51 % less starch, respectively, compared with control plants (Fig. 1B). The reduced accumulation of starch was accompanied by a significant accumulation of maltose to levels comparable to, or higher than those normally observed at night (Fig. 1C)[22]. Given that maltose is the major starch degradation product [25], the reduction in starch accumulation in osmotically-stressed plants appeared, at least in part, to result from starch turnover (i.e. simultaneous synthesis and degradation). To exclude that the observed starch degradation was induced by a mannitol-specific signal [26], we repeated the same experiment by imposing osmotic stress with 300 mM sorbitol, which also resulted in starch turnover (S1 Fig.). Mobilization of the starch reserve is therefore a general response to high osmotic stress. Both sorbitol and mannitol had a drastic, concentration-dependent, inhibitory effect on shoot and root growth in plants grown on agar plates (S2 Fig.)[27].

BAM1 degrades starch in *bam3* in response to osmotic stress

It was recently reported that BAM1 in Arabidopsis catalyzes leaf starch degradation during osmotic stress [24]. Consistently, *BAM1* gene expression was induced 8-fold in Col-0 leaves after 2 h and 4 h mannitol treatment, compared with expression levels in the absence of stress (Fig. 1D). This expression pattern was similar to *RD29A* - a well-known osmotic stress-responsive gene (Fig. 1D)[28]. In response to mannitol treatment, *bam1* mutants showed reduced starch turnover and reduced maltose accumulation relative to the wild type (Fig. 1B and 1C). As expected, patterns of starch and maltose turnover in *bam1* were indistinguishable from wild type under control conditions (Fig. 1B and 1C; S3 Fig.). These results confirm that BAM1 is critical for leaf starch metabolism specifically upon osmotic stress.

Interestingly, there was still some starch turnover in *bam1* mutants after 4 h of stress (Fig. 1B). This may be attributed to the activity of other hydrolases, since the degradation of the glucans comprising starch is known to require the combined actions of several enzymes and isoenzymes [29]. One obvious candidate is BAM3, because of its high homology to BAM1 [22]. However, the transcripts of *BAM3* in Col-0 leaves were not induced by mannitol (Fig. 1D), a result supported by publicly accessible transcriptome data (S4 Fig.). Despite *bam3* having elevated starch levels with respect to the wild type, both under control and stress

conditions (Fig. 1B; S3 Fig.), the starch accumulation in *bam3* plants subject to osmotic stress for 4 h was 28 % lower compared to that of *bam3* plants kept in control solution (Fig. 1B). Maltose levels increased as the degree of starch accumulation decreased in response to osmotic stress (Fig. 1C). Thus, in *bam3,* starch turnover is activated in response to osmotic stress, similarly to wild type. *BAM1* expression was stress-induced in *bam3* mutants to the same extent as in wild type (14-fold in this experiment; S5 Fig.), suggesting that BAM1 is activated in *bam3,* promoting starch mobilization during the osmotic stress response. These results also show that while BAM3 is required for normal starch degradation at night, it is not induced by osmotic stress and that BAM1 and other starch hydrolytic enzymes can degrade starch without it. Interestingly, BAM3 has been shown to be induced and required for maltose accumulation during cold stress (S4 Fig.) [23].

Fig. 1. BAM1 and AMY3 synergistically degrade starch in leaves upon osmotic stress. (A) Three-week-old hydroponically-grown Arabidopsis plants were transferred to a nutrient solution optionally supplemented with 300 mM mannitol for 4 h. After the stress treatment, roots were rinsed with water and returned to a control solution for 24 h. Representative wild-type plants (Col-0) show the reduction in turgor in response to mannitol stress (denoted by asterisks) from which the plants recovered after 24 h in control nutrient solution. Bar = 1 cm. **(B, C)** Leaf starch **(B)** and maltose **(C)** content in osmotically-stressed leaves compared with controls. Values are means ± SE (n = 8). FW, fresh weight. **(D)** Leaf transcript abundance for *BAM1, BAM3* and *AMY3* in osmotically-stressed and control leaves, determined by qPCR. Plants grown as above were harvested at the indicated time points. The *ACTIN2* (ACT2) gene was used as reference gene. *RD29A* was used as a positive stress-induced control. Values were normalized against gene expression at T0 (set as 1) and represent means ± SE (n = 3). Statistical significances determined by unpaired two-tailed Student's *t* tests: * denotes $p < 0.05$ for the indicated comparison; # denotes $p < 0.05$ mutants versus wild type at the indicated time points; n.s. = not significant for the indicated comparison.

Starch turnover during osmotic stress is blocked in *amy3 bam1* mutant plants

We investigated which enzymes besides BAM1 are responsible for starch degradation in the light during osmotic stress. We recently showed that the chloroplastic α-amylase 3 (AMY3) degrades starch synergistically with BAM1 *in vitro* [30]. Like *bam1,* the *amy3* mutant has a wild-type phenotype under standard growth conditions (S3 Fig.)[31]. However, upon stress, *amy3* mutants showed a reduction in starch turnover and reduced maltose accumulation relative to the wild type, showing that AMY3 is also required for starch degradation under osmotic stress (Fig. 1B and 1C). The defects in *amy3* were not as severe as those in *bam1*. qPCR analysis of *AMY3* expression under osmotic stress showed that there was a small, but statistically significant and reproducible induction after 4 h of mannitol treatment (Fig. 1D). This induction was in addition to the previously-described increase in AMY3 transcript that

occurs during that day (apparent in our control plants; Fig. 1D; S10 Fig.)[32]. To further investigate the role of AMY3 in osmotic stress responses and its functional relationship with BAM1, we generated the double mutant, using *amy3-2* (SAIL_613_D12)[31] and *bam1* (SALK_039895)[22] as parents. Protein gel blots probed with anti-BAM1 or anti-AMY3 antibodies confirmed that both proteins were missing in the double mutant (S6 Fig.). No differences in leaf starch content were observed in *amy3 bam1* compared with wild type at the end of the day or night, indicating that normal diurnal starch turnover was not affected (S3 Fig.). Remarkably, however, under osmotic stress, starch turnover was abolished in *amy3 bam1* (Fig. 1B and 1C), with starch accumulating to the same extent as in unstressed plants. These results suggest that BAM1 and AMY3 are both induced during osmotic stress and work together to mediate efficient starch catabolism.

amy3 bam1 double mutants are impaired in osmotic stress-induced compatible solute accumulation

Starch mobilization under osmotic stress is considered to sustain plant central metabolism for the production of osmoprotectants and energy [33]. We therefore tested whether the inhibition of starch turnover under osmotic stress in *amy3 bam1* affected the accumulation of compatible solutes such as soluble sugars (glucose, Glc; fructose, Fru; sucrose, Suc) and proline (Pro) in the shoot and/or in the root of stressed plants. Upon mannitol treatment, wild-type plants accumulated much higher levels of all three sugars after 4 h, both in leaves and roots, than control plants (Fig. 2A-F; S1 Table; S2 Table). These increased sugars could result from starch turnover, from the diversion of photoassimilated carbon from other products, and from a cessation of sugar consumption for growth. The *amy3 bam1* double mutants responded differently to the osmotic stress than the wild type. After 2 h of stress, no increase in sugar content was observed in *amy3 bam1* leaves (Fig. 2A, 2C and 2E). Only after 4 h of stress were sugars higher in *amy3 bam1* plants than in the untreated plants, and the levels similar to those of wild type (Fig. 2A, 2C and 2E). The situation differed in the roots. Compared to controls, osmotically-stressed *amy3 bam1* plants accumulated more of all three sugars after 2 h of stress, similarly to wild type. Interestingly, however, after 4 h of stress, the amount of sugars decreased compared to 2 h and was lower than in wild-type roots (Fig. 2B, 2D and 2F). Similar analyses for *bam1* and *amy3* single mutants (S1 Table; S2 Table) revealed that they behaved like the wild type, both under control and stress conditions.

We also determined the content of free proline. Under normal growth conditions, Pro levels in shoot and root of wild-type plants were low, as expected, and there were no differences between wild type and *amy3 bam1* double mutants (Fig. 2G and 2H). Osmotic stress induced exceptionally high levels of Pro in the shoot of wild type, especially after 4 h of stress (Fig. 2G). In amy3 *bam1* leaves Pro levels were similar to wild type (Fig. 2G). In roots, Pro levels

in both genotypes were also significantly higher after 4 h of stress compared to control conditions. However, *amy3 bam1* roots accumulated less Pro compared to wild-type roots (Fig. 2H). These results show that sugar and proline metabolism is impaired during osmotic stress when both BAM1 and AMY3 are missing (i.e. when starch turnover in response to osmotic stress is completely inhibited), supporting the idea that starch is important for the biosynthesis osmoprotectants. The results also show that defective starch degradation in *amy3 bam1* during osmotic stress affects the root more than the shoot.

Fig. 2. Quantification of soluble sugars and proline in leaves and roots of osmotic stressed plants. Sucrose, glucose, fructose and proline content in shoot **(A, C, E** and **G)** and roots **(B, D, F** and **H)** of Col-0 and *amy3 bam1* plants in response to osmotic stress treatment. Hydroponically-grown plants were optionally supplemented with 300 mM mannitol for 4 h. Value are means ± SE (n = 5). FW, fresh weight. Statistical significances determined by unpaired two-tailed Student's *t* tests: * denotes $p < 0.05$ for the indicated comparison; n.s. = not significant for the indicated comparison.

amy3 bam1 double mutants show altered carbon partitioning during osmotic stress

Our analyses could not distinguish between compatible solutes deriving from photosynthetic carbon assimilation (i.e. *de novo* synthesis) or from hydrolysis of previously stored starch, nor could we determine the fate of the carbon skeletons deriving from osmotic stress-induced starch degradation. We therefore used $^{14}CO_2$ labeling to analyze carbon partitioning into different cellular compound classes and to measure carbon export from leaves to the roots in plants subject to osmotic stress. We supplied $^{14}CO_2$ to hydroponically grown plants (with or without mannitol) for 1 h, either at the beginning of the stress (after 3 h of light) or in the middle of the stress treatment (after 5 h of light). In each case, the $^{14}CO_2$ pulse was followed by 1 h chase in air (Fig. 3A), after which the rosettes and the roots were harvested separately. The different tissues were fractionated between water soluble (neutral, acidic and basic), ethanol soluble and insoluble (starch and cell wall) compounds and the amount of ^{14}C in each determined. Under control conditions, carbon partitioning varied only slightly between the two time points, in line with the observation that most changes in carbon partitioning occur in the first 2 h of light [34]. No significant differences were observed for carbon partitioning between unstressed wild-type and *amy3 bam1* plants (S3 Table; S4 Table).

Next, we compared the partitioning of photoassimilated ^{14}C in the control plants with plants subject to osmotic stress, which revealed a remarkable change in the amount of carbon exported to the root. After 2 h of stress, the export of carbon from the leaves to the roots in wild type increased more than 3-fold to 25.8 % of the total ^{14}C incorporated by the plant (Fig. 3B; S3 Table). Sub-fractionation of root soluble compounds revealed that most of the imported carbon was in neutral compounds (i.e. sugars). No significant changes were found in

the basic and acidic fractions (Fig. 3C; S3 Table). Carbon partitioning in osmotic-stressed *amy3 bam1* roots after 2h of stress was comparable to wild type (Fig. 3B and 3C; S3 Table). After 4 h of stress, wild type maintained a high rate of export of assimilated carbon to the root compared to control (+9.5 %, corresponding to 16.5 % of the total ^{14}C incorporated), although the overall transported carbon was lower than after 2 h of stress (Fig. 3B; S4 Table). Strikingly, *amy3 bam1* showed no increase in carbon flow to the root in response to osmotic stress at this time (Fig. 3B; S4 Table), compared with the unstressed control. Consistently, label found in neutral sugars was higher in wild-type roots compared with that in *amy3 bam1* (Fig. 3C).

Carbon partitioning within the leaf was also severely affected during osmotic stress. In wild type, carbon allocation into neutral sugars increased, both after 2 h and 4 h of stress (+2.9% and +9.9%, respectively; Fig. 3D; S3 table; S4 table), whereas partitioning into basic and acidic compounds decreased (-1.9 % and –3.9 % after 2 h, and –1.04 % and –3.5 % after 4 h, respectively; Fig. 3D; S3 table; S4 table). Conversely, carbon allocation into starch and cell wall decreased significantly (-10.7 % and –0.75 % after 2 h, and -7.9 % and -3.7 % after 4 h, respectively; Fig. 3E; S3 table; S4 table). A similar labeling pattern was observed in *amy3 bam1* leaves at the beginning of the stress (2h of stress). This included a decreased carbon partitioning into starch (Fig. 3D and 3E; S3 table), probably representing a reduction in starch synthesis. After prolonged mannitol treatment (4 h of stress), the labeling of starch and cell wall in *amy3 bam1* leaves was the same as in unstressed control plants (Fig. 3E). However, the amount of carbon incorporated into leaf soluble sugars was still elevated relative to the unstressed control plants, as with the wild type (Fig. 3D).

Thus, osmotic stress leads to 1) carbon accumulating in sugars, both in leaves and roots 2) increased carbon export to the root and 3) a reduction in carbon partitioning towards starch and cell wall. The most obvious consequence of defective starch turnover upon osmotic stress is a dramatic reduction in carbon allocation to the root in the latter part of the stress treatment.

Fig. 3. Carbon partitioning in Col-0 and *amy3 bam1* plants during osmotic stress. (A) Scheme of labeling set up. Whole Col-0 and *amy3 bam1* plants were labelled with $^{14}CO_2$ for 1 h, just after transfer to a mannitol containing nutrient solution or at the middle of the stress treatment. Following a 1-h chase period, the shoot and root were harvested separately and the ^{14}C in the different tissue's fractions determined by scintillation counting. **(B)** Carbon export to the root of osmotically-stressed and control plants. Relative changes in ^{14}C imported into

the root upon osmotic stress are given as percentages of that imported under control conditions (set as 0). Values are means ± SE (n = 4). **(C)** Incorporation of ^{14}C into the different water-soluble fractions (see Materials and Methods for extraction/fractionation protocols) of Col-0 and *amy3 bam1* roots. Relative changes in the amount of ^{14}C incorporated into the different fractions upon osmotic stress are given as percentages of that in corresponding fractions under control conditions (set as 0). Values are

means ± SE (n = 4). **(D)** Incorporation of ^{14}C into the different water-soluble fractions of Col-0 and *amy3 bam1* shoots in plants subject to osmotic stress compared with controls. Relative changes are expressed as described above for C. **(E)** Incorporation of ^{14}C into starch and cell wall compounds (see Materials and Methods for extraction/reactionation protocols) of Col-0 and *amy3 bam1* shoots in plants subject to osmotic stress compared with control. Relative changes are expressed as described above for C. Statistical significances determined by unpaired two-tailed Student's *t* tests: * denotes $p < 0.05$ for the indicated comparison; # denotes $p < 0.05$ mutant versus wild type at the indicated time points; n.s. = not significant.

The *amy3 bam1* double mutant is sensitive to osmotic stress

To assess the contribution of starch turnover to osmotic stress tolerance, we further investigated the responses of *amy3 bam1*. Under control conditions, *amy3 bam1* was indistinguishable from the wild type and, like wild type it wilted severely upon mannitol treatment. However, less water was absorbed and transpired by *amy3 bam1* under stress than by the wild type (only 63 % and 79 % as much after 2 h and 3 h of mannitol treatment, respectively; Fig. 4A; S1 Data). This was unlikely to be dependent on differences in stomatal function. Although stomatal aperture in the wild type was slightly greater than in *amy3 bam1* at the start of the treatment, there was no difference in water loss in control conditions and both lines closed their stomata at similar rates in response to the osmotic stress (S7 Fig.). Furthermore, measurements of leaf sap osmolality revealed an increased of 44 % after 4 h of stress in *amy3 bam1,* compared with a 29 % increase in the wild type (Fig. 4B). Together, these data point towards a reduced water absorption by *amy3 bam1* than by wild type.

Negative effects of a higher leaf osmolality in *amy3 bam1* may become visible only when the stress persists for longer than 4 h. As liquid medium containing mannitol is susceptible to fungal contamination, we assessed long-term osmotic stress responses using seedlings grown on agar plates in a 12-h-light/12-h-dark cycle. Six days after germination, seedlings with the same root lengths were transferred for additional 9 days to MS plates optionally supplemented with 300 mM mannitol. Primary root growth in Col-0 was reduced on 300 mM mannitol compared with control plants. However, *amy3 bam1* plants showed a higher degree of inhibition (Fig. 4C and 4D; S1 Data). Fresh weight measurements after the 9-day treatment showed that *amy3 bam1* and wild-type root growth was inhibited by 48 % and 61 %, respectively, relative to the controls (Fig. 4E; S1 Data). Interestingly, shoot growth inhibition was similar for both genotypes (about 63-66 % of control; Fig. 4E: S1 Data), resulting in substantial differences in root to shoot ratios. In response to osmotic stress, Col-0 plants increased their root to shoot ratio by 75 % relative to controls, whereas in *amy3 bam1* the ratios remained unaltered (Fig. 4F). Collectively, our results indicate that *amy3 bam1* is hypersensitive to osmotic stress, suggesting that leaf starch degradation upon stress plays a

crucial role in plant water homeostasis through provision of compatible solutes and substrates to drive root growth.

Fig. 4. Effects of osmotic stress on *amy3 bam1* double mutants. (A) Water absorption by Col-0 and *amy3 bam1* plants subject to mannitol stress compared with controls. The volume of water absorbed by plants in a nutrient solution supplemented with 300 mM mannitol is shown as a percentage of water absorbed by plants in a solution without mannitol (control, set as 100%). Values were corrected for water loss due to the evaporation from the liquid surface. Values are means ± SE (n = 6). **(B)** Osmolality of Col-0 and *amy3 bam1* leaf sap. Values are means ± SE (n = 6). **(C)** Morphology of the Col-0 and *amy3 bam1* plants under control (top panel) and osmotic stress conditions (bottom panel). Plants were grown in control media for 6 days, transferred to media optionally supplemented with 300 mM mannitol and photographed 2 days later. Scale bar = 0.5 cm. **(D)** Time course of the wild-type and *amy3 bam1* primary root growth after seedling transfer, as described in C. Root lengths were analyzed using the ImageJ plugin NeuronJ. Values represent proportion of growth in the presence of mannitol compared with growth without mannitol (set as 100%). Values are means ± SE of 70 replicate samples. Error bars are smaller than the symbols. **(E)** Shoot and root fresh weights (FW) measured 9 days after seedling transfer as described in C. Values represent the FW of osmotically-stressed plants compared with control plants (set as 100%). Values are means ± SE (n = 15). **(F)** Root to shoot ratio of Col-0 and *amy3 bam1* plants in response to 300 mM mannitol stress. Values are derived from the data shown in E. Statistical significances determined by unpaired two-tailed Student's *t* tests: * denotes $p < 0.05$ for the indicated comparison; n.s. = not significant for the indicated comparison.

Application of exogenous ABA induces *BAM1* and *AMY3* expression and results in increased BAM1 protein enzyme activity and starch degradation

Upon osmotic stress, cellular ABA levels increase drastically, activating the expression of many stress-inducible genes and triggering adaptive responses [35–41]. Our hydroponically-grown Col-0 plants maintained low ABA levels under normal growth conditions (S8 Fig.). Upon mannitol treatment, ABA increased dramatically (S8 Fig.) and expression of the ABA/osmotic stress-responsive gene *RD29A* was markedly induced (Fig. 1D). Exogenous ABA application also up-regulated *RD29A,* mimicking the osmotic stress response (Fig. 5A). Similarly, exogenous ABA induced *BAM1* and *AMY3* expression, but had no effect on *BAM3* (Fig. 5A), mirroring the behavior of these genes under osmotic stress treatment (Fig. 1D).

The BAM1 protein and activity increased in ABA-treated plants relative to untreated plants (Fig. 5B and 5C; S9 Fig.), indicating that transcriptional activation resulted in rapid *de novo* protein synthesis. In contrast, there was no detectable change in AMY3 protein level in response to ABA (S10A Fig.). However, *AMY3* transcripts and spectra matching AMY3-derived peptides are frequently detected in many tissues types, especially leaves (S10B Fig.) [42], indicating that the protein is already relatively abundant.

To investigate whether exogenous ABA affects starch degradation, wild-type plants were sprayed with 100 μM ABA. After 4 h, ABA-treated plants accumulated less starch than controls, and maltose levels were exceptionally high (Fig. 5D and 5E). Remarkably, ABA-sprayed *amy3 bam1* mutants accumulated similar amounts of starch to untreated plants, and maltose levels were slightly decreased (Fig. 5D and 5E). Thus, exogenous ABA triggers BAM1/AMY3-dependent starch degradation in the leaves.

Fig. 5. Effects of exogenous ABA on leaf starch metabolism. (A) Relative expression levels of *BAM1, BAM3* and *AMY3* in Col-0 leaves 4 h after treatment with 100 μM ABA, determined by qPCR. The *ACT2* gene served as a reference gene. *RD29A* served as a positive control for the ABA treatment. Values representing means ± SE (n = 3) were normalized against gene expression in control conditions (set as 1). **(B)** Immunodetection of BAM1 protein in Col-0 leaves after ABA treatment. Total protein was extracted from rosettes of hydroponically-grown plants at the indicated time points. Equal protein amounts were separated by SDS-PAGE. The Rubisco large subunit (RbcL) - the dominant band visualized by Coomassie-staining – confirmed uniform loading. BAM1 was detected using polyclonal antibodies raised against recombinant BAM1. Extracts of the *bam1* mutant served as a negative control. Replicate blots yielded the same result. C = mock treated control. **(C)** ABA-mediated changes in BAM1 activity. Leaf crude extracts from hydroponically-grown Col-0 and *bam1* plants harvested 4 h after ABA treatment were separated by native PAGE in gels containing 0.1% amylopectin. After electrophoresis and incubation for 2 h (see Materials and Methods), gels were stained in Lugol solution. BAM1 activity was detected in wild-type but not *amy3 bam1* plants. **(D, E)** Leaf starch **(D)** and maltose **(E)** content in Col-0 and *amy3 bam1* plants 4 h after ABA treatment, compared with controls. Values are means ± SE (n = 6). FW, fresh weight. Statistical significances determined by unpaired two-tailed Student's *t* tests: * denotes $p < 0.05$ for the indicated comparison; # denotes $p < 0.05$ mutant versus wild type at the indicated time points; n.s. = not significant for the indicated comparison.

The AREB/ABF-SnRK2 pathway regulates ABA-dependent *BAM1* and *AMY3* gene expression

To understand the molecular link between ABA and starch degradation during osmotic stress, we searched the promoter regions of *BAM1* and *AMY3* genes for known ABA- dependent *cis-regulatory* elements. Interestingly, both *BAM1* and *AMY3* promoters contain "ABA-responsive element" (ABRE) motifs, while none were present in the *BAM3* promoter (http://bioinformatics.psb.ugent.be/webtools/plantcare/html; S2 Data). The ABRE *cis*-regulatory elements are bound by a group of bZIP transcription factors (TFs), the ABRE-binding protein/ABRE-binding factors (AREB/ABFs). These TFs have pivotal functions in ABA-dependent osmotic stress-responsive gene expression [43]. In the presence of ABA, the AREB/ABF TFs are activated through phosphorylation by SNF1-related kinase 2s (SnRK2s)

[44,45], enabling them to bind the ABRE motifs in the promoters of the target genes, thereby activating their expression [46,47].

The transcriptional activation of *BAM1* and *AMY3* in response to exogenous ABA application was abolished or greatly reduced in mutants lacking three SnRK2 kinases, *snrk2.2 snrk2.3 snrk2.6,* or lacking three AREB/ABF TFs, *areb1 areb2 abf3* (Fig. 6A), known positive regulators of ABA signaling in the leaves [43,44,48–50]. Under control conditions, *BAM1* and *AMY3* transcript levels were similar to the wild type in the *snrk2.2 snrk2.3 snrk2.6* and *areb1 areb2 abf3* triple mutants (S11 Fig.). *BAM3* transcript levels remained unaltered in response to ABA treatment in both mutants, similarly to wild type (Fig. 6A), consistent with the idea that BAM3 induction is not part of the osmotic stress responses. In the *areb1 areb2 abf3* triple mutant, BAM1 protein levels did not change in response to exogenous application of ABA (Fig. 6B and 6C), and starch turnover upon mannitol treatment was significantly reduced compared to wild type (Fig. 6D and 6E). Collectively, these findings suggest that ABA-dependent SnRK2 signaling mediates *BAM1* and *AMY3* activation in response to osmotic stress through AREB1 AREB2 and ABF3 TFs.

Fig. 6. AREB1, AREB2 and ABF3 transcription factors regulate *BAM1* and *AMY3* expression in response to osmotic stress. (A) Relative expression levels of *BAM1, BAM3* and *AMY3* in Col-0 and *areb1 areb2 abf3* triple mutant leaves 4 h after treatment with 100 µM ABA, determined by qPCR. The *ACT2* gene served as a reference gene. *RD29A* served as a positive control for the ABA treatment. Values representing means ± SE (n = 3) were normalized against gene expression in control conditions (set as 1). **(B)** Immunodetection of BAM1 protein in Col-0, *areb1 areb2 abf3* and *amy3 bam1* leaves after ABA treatment. Total protein was extracted from rosettes of hydroponically-grown plants at the indicated time points. Equal amounts of protein were separated by SDS-PAGE and the Rubisco large subunit (RbcL) used for confirmation. BAM1 was detected using polyclonal antibody raised against recombinant BAM1. Replicate blots yielded the same result. C = control. **(C)** BAM1 protein quantification. Densitometry analysis (ImageJ) was used to quantify band intensities such as in B. Values are means ± SE of three biological samples, each analyzed with three technical replicates, and expressed relative to the mean band intensity at time 0 (T0, set as 1). **(D, E)** Starch **(D)** and maltose **(E)** content in Col-0 and *amy3 bam1* leaves in ABA-treated and control plants. Values are means ± SE (n = 6). FW, fresh weight. Statistical significances determined by unpaired two-tailed Student's *t* tests: * denotes $p < 0.05$ for the indicated comparison; # denotes $p < 0.05$ mutant versus wild type at the indicated time points; n.s. = not significant for the indicated comparison.

The ABA-deficient mutant *nced3* mimics the *amy3 bam1* phenotype under osmotic stress

During dehydration stress, an essential step in *de novo* ABA biosynthesis is the cleavage of epoxycarotenoids to produce xanthoxin (the first C15 intermediate) by the 9-cis epoxycarotenoid dioxygenase NCED3 [51]. Consequently, *nced3-null* mutant does not

accumulate ABA in response to dehydration [35,51]. Therefore we used *nced3* to further investigate the role of ABA in stress-responsive starch metabolism. Under osmotic stress, *nced3* showed a striking phenotype, mimicking the behavior of *amy3 bam1:* starch degradation was abolished and maltose levels remained unchanged compared with control plants. Wild type activated starch degradation as expected (Fig. 7A and 7B). Under control conditions, however, *nced3* already displayed a mild *starch-excess* (sex) phenotype and slightly lower sugars levels (Fig. 7A and 7B; S12 Fig.). This is not surprising, as a link between ABA and sugar signaling pathways was previously shown by many groups [52]. However, it raised the question as to whether the defective starch degradation in *nced3* under osmotic stress was simply a secondary effect of ABA-sugar cross-talk rather than a direct consequence of the lack of stress-induced *de novo* ABA biosynthesis. To discriminate between these possibilities, we investigated the phenotype of another ABA-related mutant lacking the abscisic aldehyde oxidase 3 AAO3, responsible for the final step in ABA biosynthesis [53]. Given that Arabidopsis contains four *AAO* genes, with partially redundant functions [54], *aao3* mutants accumulate reduced but still detectable levels of ABA in response to dehydration stress [55]. Under control conditions, *aao3* mutant displayed similar alterations in starch and sugar metabolism as *nced3* (Fig. 7A and 7B; S12 Fig.). However, in response to osmotic stress, *aao3* activated starch degradation similarly to wild type (Fig. 7A and 7B). Together, these results show that *de novo* ABA biosynthesis in response to osmotic stress is required for starch degradation. Consistently, exogenous application of ABA alone or in combination with mannitol restored starch degradation in the *nced3* mutant almost to wild-type levels (S13 Fig.). Furthermore, transcripts levels of *BAM1* and *AMY3,* as well as *RD29A,* were substantially lower in the *nced3* mutant than in the wild type, whereas that of *BAM3* remained unaltered (Fig. 7C). These data further support the idea that ABA accumulation in response to osmotic stress activates starch degradation in the light via BAM1 and AMY3 (Fig. 8).

Fig. 7. Starch degradation during osmotic stress is blocked in the ABA-deficient mutant *nced3*. (A, B) Leaf starch **(A)** and maltose **(B)** content in Col-0, *nced3* and *aao3* plants treated with 300 mM mannitol compared with controls. Values are means ± SE (n = 6). FW, fresh weight. **(C)** Relative expression levels of *BAM1, BAM3* and *AMY3* in leaves of Col-0 and *nced3* plants treated with 300 mM mannitol for 4 h, determined by qPCR. The *ACT2* gene served as a reference gene. *RD29A* served as a positive control for the osmotic stress treatment. Values representing means ± SE (n = 3) were normalized against gene expression in control conditions (set as 1). Statistical significances determined by unpaired two-tailed Student's *t* tests: * denotes $p < 0.05$ for the indicated comparison; n.s. = not significant for the indicated comparison.

Fig. 8. Proposed model of starch degradation mechanism and regulation during osmotic stress. In

response to stress ABA triggers *BAM1* and *AMY3* transcription through the ABA-dependent AREB/ABF-SnRK2 signaling pathway. This leads to rapid *de novo* BAM1 protein synthesis and increased amylolytic activity. A fraction of the maltose released from starch by the synergistic action of BAM1 and AMY3 is exported to the cytosol and metabolized into sucrose and free hexoses. Sucrose is then exported to the root to support osmotic adjustment, water uptake and root growth. The remaining sugars, including some maltose and the additional sugars originating from carbon assimilation, are retained in the leaves for osmotic adjustment, energy supply and for the protection of the photosynthetic apparatus from oxidative stress.

Discussion

Starch degradation is a general plant response to short-term, high osmotic stress

This study provides compelling evidence that the reduction in starch accumulation in Arabidopsis plants exposed to high osmotic stress in the light is a result of induced starch degradation, leading to starch turnover and the production of significant amounts of maltose - the major starch catabolite (Fig. 1C). In mutants lacking the two starch hydrolases, AMY3 and BAM1, this metabolic stress response is abolished and starch accumulation is the same as in control conditions (Fig. 1B and 1C). Thus, starch synthesis *per se* seems to be unaffected by the short-term, high osmotic stress applied here.

Rearrangements of starch metabolism have previously been observed in Arabidopsis and other plant species subjected to short periods of oxidative stress, cold, or heat [23,24,33,56–59]. In addition to the induction of degradation, inhibition of synthesis may also occur in some situations. This might be caused by changes in phosphorylated intermediates, especially 3-phosphoglycerate (3PGA), reduction of which would inactivate ADP-glucose pyrophosphorylase, the regulated enzyme of starch biosynthesis [60]. A decline in 3PGA under stress could result from impaired photosynthesis (S5 Table)[23,58], or from the activation of the sucrose synthesis in response to stress through sucrose synthase phosphate (SPS) [59], which would compete for assimilates.

In contrast, when plants are exposed to a mild osmotic stress for extended periods of time, photosynthesis is maintained and starch and soluble sugars accumulate in leaves, suggesting carbon abundance [56,61–65]. Thus, upon acclimation, metabolic homeostasis is restored, with only subtle differences at the level of major pathway enzymes [61,62,66].

Differential regulation and isoform sub-functionalization define a distinct pathway of starch degradation during osmotic stress

The two close homologs, BAM1 and BAM3, are differentially regulated in response to abiotic stresses (Fig. 1D; S4 Fig.) [33,63,67]. *BAM3* gene expression is induced by cold stress, whereas *BAM1* expression is induced by heat and by osmotic stress. The most obvious

interpretation of this differential transcriptional regulation is that starch degradation can be induced by different signals. Mutants studies substantiate the hypothesis that *BAM1* induction is critically important in the osmotic stress response. As first reported by Valerio et al (2011), we also found that *bam1* mutants had reduced starch degradation in response to mannitol treatment (Fig. 1B and 1C). In contrast, *bam3* mutants, though compromised in normal night-time starch degradation, could activate *BAM1* expression and starch degradation under osmotic stress conditions (Fig. 1B and 1C; S5 Fig.), showing that BAM3 is not part of the osmotic stressed-induced starch degradation pathway.

We showed that, in addition to BAM1, AMY3 contributes to starch breakdown in response to osmotic stress. It is conspicuous that the loss of both enzymes does not affect starch metabolism under normal conditions (S3 Fig.), yet completely blocks starch degradation upon osmotic stress (Fig. 1B and 1C). These contrasting phenotypes reveal the degree of sub-functionalization amongst the enzymes of starch degradation, with some required for the mobilization of starch to respond to stress, with others required for normal night-time starch degradation.

Previous work suggests that it may not just the gene expression patterns, but also the characteristics of encoded BAM1 and AMY3 enzymes themselves that distinguish them from other starch degrading enzymes and make them suitable for starch degradation during daytime stress conditions. For example, both enzymes are redox regulated, whereby they can be activated through reduction via the light-driven ferredoxin-thioredoxin system. Furthermore, both enzymes are preferentially active at a slightly alkaline pH [30,63,68,69]. Thus, the reducing environment and the alkaline pH of the stroma, generated by the photosynthetic electron transport chain in the light [70,71], would favor BAM1 and AMY3 activity. Conversely, there is no evidence for redox regulation of BAM3 and the enzyme has optimum activity at less alkaline pH [63,69]. These findings strongly support the presence of a unique, stress-induced, redox-regulated starch degradation pathway that can operate in the light.

It should be noted that there are likely to be factors required for starch degradation in osmotic stress conditions other than BAM1 and AMY3. For example, the enzymes mediating the phosphorylation and dephosphorylation of starch – a process that precedes its degradation by amylases - may be required for osmotic stress-induced degradation as well as for normal night-time degradation [56,72,73]. Similarly, starch debranching enzymes (isoamylase and limit dextrinase) and disproportionating enzymes may be required under both conditions. Some of these enzymes are also reportedly redox regulated [69,73,74]. Conversely, it may also be the case that BAM1 and AMY3 are important for starch degradation at other times besides just osmotic stress. Indeed, it has been shown that when other enzymes are missing, both BAM1 and AMY3 are active in night-time starch degradation under normal growth

conditions [19,21,22].

A critical role for starch degradation in osmotic stress tolerance

Our use of both hydroponic and agar plate systems enabled us to investigate the effects of osmotic stress on both leaves and roots and define the role of stress-induced starch degradation on the metabolism of the plant as a whole. As expected, wild type responded to osmotic stress by accumulating high levels of sugars and proline in the leaves (Fig. 2A, 2C, 2E and 2G: S1 Table), presumably for osmotic adjustment and energy supply to maintain cell survival and metabolic activity [8,10]. Our data suggest that most of these osmolytes derive from photosynthetic carbon assimilation and only partly from starch hydrolysis. Firstly, *amy3 bam1* plants were only mildly impaired in leaf sugar accumulation during stress and showed no differences from wild type in leaf proline accumulation (Fig. 2A, 2C, 2E and 2G; S1 Table). Moreover, our ^{14}C labeling experiments showed that carbon partitioning into the leaf soluble neutral fraction during stress was similar in wild type and *amy3 bam1* plants (Fig. 3D). Consistent with this, we showed that osmotic stress caused a transient decrease in the PSII operating efficiency (ΦPSII), which was similar in the two genotypes (S5 Table). Sugars may also accumulate in leaves because of decreased demand, as a consequence of shoot growth limitation [61].

Major differences between the wild type and *amy3 bam1* were apparent in the amount of carbon channeled to the root under osmotic stress. This was markedly reduced in the mutant compared to the wild type, especially after 4 h of mannitol treatment (Fig. 3B). Consequently, *amy3 bam1* had reduced levels of sugars and proline in the roots (Fig. 2B, 2D, 2F and 2H). Therefore, we propose that starch degradation in the shoot is required to increase carbon exported to the roots during a prolonged stress. If carbon supply becomes limiting, due to the exhaustion of reserves or, in this case, due to impaired starch mobilization, the available sugars may be retained in the leaves at the expense of the roots to protect photosynthetic tissues from oxidative damage (Fig. 8)[10].

Reduced carbon export to the root in response to stress impaired the short-term osmotic adjustment in *amy3 bam1,* reducing the ability of the root to absorb water from the medium (Fig. 4A). There was also a dramatic impact on root growth during long-term exposure to high osmotic stress. While wild-type plants responded to osmotic stress by increasing their root to shoot ratio, the ratio in *amy3 bam1* remained unchanged compared to non-stress conditions (Fig. 4F). Remodeling root growth and architecture is an important survival strategy, allowing plants to expand the root (at the expenses of shoot growth) to increase nutrient and water uptake capacity [75–77]. Our results are consistent with these observations and reveal a novel function of starch degradation in root remodeling in response to osmotic stress (Fig. 8).

ABA is the primary signal for starch degradation in leaves in response to osmotic stress

One of the pivotal events in dehydration stress responses is the rapid, transient accumulation of ABA, which facilitates stomatal closure and expression of ABA responsive genes that protect plants from further water loss and damage. Several transcriptomic analyses have reported ABA-dependent induction of a multitude of drought-stress related genes, as well as some involved in primary carbohydrate metabolism [35,37,38,40,41,78]. Here, we showed that *BAM1* and *AMY3* are direct targets of the ABA/osmotic-dependent AREB/ABF-SnRK2 pathway and that ABA is required for osmotic stress-induced starch degradation in the leaves (Fig. 8). Application of exogenous ABA induced *BAM1* and *AMY3* expression in Col-0, but not in mutants lacking key components of the leaf ABA/osmotic-dependent signaling pathway (Fig. 6A)[46,50]. Consistently, application of exogenous ABA stimulated starch degradation in Col-0, but not in the double mutant *amy3 bam1* (Fig. 5D and 5E). Thus, activation of BAM1 and AMY3 in response to ABA (Fig. 5B, 5C, S11 Fig.) induces starch degradation.

Both *BAM1* and *AMY3* promoters contain ABRE motifs (S2 Data), which are absent in the *BAM3* promoter, consistent with the observation that *BAM3* is not ABA induced. Pairs of BAM1 and BAM3 orthologs are found in the genome of several species, suggesting that BAM isoform sub-functionalization is a general feature of plants [63][22]. Interestingly, bioinformatics analyses of the promoters of *BAM1* and *BAM3* orthologs from 30 different plant species using the MEME software (http://meme.nbcr.net; S2 Data)[79] revealed an enrichment of ABRE elements in the proximity of the ATG codon in all examined *BAM1-like* gene promoters, with the exception of that of the grasses. Furthermore, ABREs were absent in all examined *BAM3-like* gene promoters (S14 Fig.). This suggests that the regulation of starch degradation by ABA during stress through the AREB/ABF-SnRK2 pathway is a conserved mechanism across many plant species.

Lastly, osmotic stress-induced starch degradation was abolished in the *nced3* mutant, but not in a mutant lacking AAO3 (Fig. 7A and 7B). Given the major difference between these two ABA biosynthetic mutants is their capacity to accumulate ABA in response to stress [35,51,55], our data suggest that the lack of stress-induced starch degradation in *nced3* was specifically caused by the complete absence of ABA accumulation. This is supported by the fact that the stress-induced transcriptional induction of *BAM1* and *AMY3* was substantially impaired in *nced3,* but not in *aao3* (Fig. 7C). These observations are in line with previous transcriptomic and metabolic data and lead to the conclusion that ABA induces starch degradation in the light in response to osmotic stress.

Materials and Methods

Plant materials and growth conditions

The following *Arabidopsis thaliana* T-DNA insertion mutants were used in this study: *bam1* (Salk_039895), *bam3* (CS92461)[22], *amy3-2* (Sail_613 D12) [31], *snrk2.2 snrk2.3 snrk2.6* [50], *aao3-4* (Salk_072361)[54] and *nced3* (GABI_129B08) [80]. The *amy3 bam1* double mutant was obtained by crossing *bam1* and *amy3-2* single mutants. Homozygous double mutants were identified by PCR-based screening and DNA sequencing, using gene-specific primers alone and in combination with a T-DNA left border-specific primer (see S7 Table for primer sequences). Arabidopsis ecotype Columbia-0 (Col-0) was used as the wild type in all experiments. Plants were grown in soil or in hydroponic culture as previously described [34] in a controlled environment chamber (KKD Hiross, CLITEC Boulaguiem, Root, Switzerland) in a 12-h-light/12-h-dark cycle with a constant temperature of 23 °C, 60 % relative humidity, and a uniform illumination of 120 µmol m^{-2} sec^{-1}. To induce osmotic stress, three-week-old hydroponically-grown plants were transferred to a nutrient solution supplemented with 300 mM mannitol or 300 mM sorbitol for 4 h, starting after 3 h of light. The rosettes and the roots were harvested separately at the indicated time points for further analyses. As a control, a subset of plants were kept in a nutrient solution without osmotic agents and harvested at the same time points. For long-term osmotic stress treatment, sterilized seeds were germinated on half-strength Murashige and Skoog (MS) vertical plates, containing 0.8 % (w/v) agar. Six days after germination, seedlings with the same root length were transferred for additional 9 days or 22 days to MS plates optionally supplemented with of mannitol or sorbitol. Primary roots were measured using the ImageJ plugin NeuronJ [81] to determine growth rates. For ABA treatment, three-week-old hydroponically-grown plants were sprayed with 100 µM ABA-KOH in 0.01 % (v/v) Tween-20, or a mock solution, starting after 3 h of light, and rosettes were harvested at different time points for further analyses.

Real time qPCR analysis of transcript levels

Total RNA was extracted from leaves using an RNeasy Plant Mini Kit (Qiagen) according to the manufacturers' instructions. Following DNase-I treatment, 1 µg of total RNA of each sample was used to produce cDNA using the M-MLV reverse transcriptase and oligo(dT) primers (Promega). Quantitative PCR was performed using the SYBR green master mix with the 7500 Fast Real-Time PCR System (Applied Biosystems). Reactions were run in triplicate with three different cDNA preparations, and the instrument's iQ5 Optical System Software was used to determine the threshold cycle (Ct). Gene-specific transcripts were normalized to *Actin2* gene (ACT2; At3g18780) and quantified by the ΔCt method (Ct of gene of interest – Ct of *ACT2* gene). Real-time SYBR green dissociation curves showed one species of amplicon for each primer combination listed in S7 Table.

Iodine staining

Four-week-old Arabidopsis rosettes were harvested at the end of day or end of night and incubated in 80% (v/v) ethanol for 12 h to remove the chlorophyll. The cleared plants were rinsed in water and stained in Lugol solution (Sigma-Aldrich) for 10 min.

Quantification of starch and leaf soluble sugars

Rosettes from plants grown in hydroponic culture or in soil were harvested into liquid N_2 and extracted in 0.7 M perchloric acid as previously described [82]. Starch in the insoluble fraction was determined by measuring the amount of glucose released by treatment with α-amylase and amyloglucosidase (both from Roche). Sugars (maltose, glucose, fructose and sucrose) in the soluble fraction were determined using HPAEC-PAD (Dionex ICS-5000; Thermo Scientific). Samples of the neutralized soluble fraction (200 µL) were applied to sequential 1.5 ml columns of cation exchanger Dowex 50 W and anion exchanger Dowex 1 (Sigma-Aldrich). Neutral compounds were eluted with 5 mL of water, lyophilized, redissolved in 200 µL of water, and separated on a CarboPac PA20 column on an ICS-3000 system (Dionex) as previously described [83]. Peaks were identified by co-elution with known malto-oligosaccharide standards and areas were determined using the instrument's Chromeleon software.

Quantification of root soluble sugars

Root sugar measurements were performed on three-week-old hydroponically-grown plants optionally supplemented with 300 mM mannitol for 2 or 4 h. At the indicated time points, roots from three plants were harvested and pooled, rinsed briefly with deionized water to remove residual mannitol, weighed, and snap frozen in liquid N_2. Roots were pulverized while still frozen using the Mix Mill MM-301 (Retsch) and extracted in 1 mL 80 % (v/v) ethanol (EtOH) for 15 min at 80 °C. The pellet was sequentially washed with 0.5 mL 50% (v/v) EtOH, 20 % (v/v) EtOH, and deionized water. The supernatants from each wash were pooled, dried under vacuum, and resuspended in 200 µL of water. Glucose, fructose and sucrose were quantified enzymatically by adapting an existing method [84]. Briefly, 15 µL of samples were added to 183 mL of 50 mM HEPES buffer, pH 7.5, containing 1 mM ATP, 1 mM NAD and 1 mM $MgCl_2$. To measure glucose, hexokinase (Roche) and glucose-6-phosphate dehydrogenase (Roche) were used to convert glucose to 6-phosphogluconate with concomitant reduction of NAD to NADH, which was monitored spectrophotometrically at 340 nm. Subsequently, phosphoglucoisomerase (PGI; Roche) was added determine the amount of fructose. Finally, invertase (Sigma-Aldrich) was added to cleave sucrose into fructose and glucose. The further increase in OD340 represented sucrose.

$^{14}CO_2$ pulse-chase labeling

Whole-plant labeling experiments of were performed with three-week-old hydroponically-grown plants optionally supplemented with 300 mM mannitol for 2 or 4 h. Plants were labeled as previously described [34] using a sealed Plexiglas chamber illuminated with 120 μmol m^{-2} sec^{-1}. $^{14}CO_2$ (300 μCi) was supplied for 60 min, either at the beginning of the stress (after 3 h of light) or in the middle of the stress treatment (after 5 h of light), after which the Plexiglas chamber was opened and the plants were kept in normal air for a chase period of 60 min (see S8 Fig. for a schematic representation of the labeling set up). After the chase, the rosettes and the roots were harvested separately, the different tissues was fractionated between water soluble (neutral, acidic and basic), ethanol soluble and insoluble (starch and cell wall) compounds and the ^{14}C determined as described previously [85].

Proline quantification

Free proline content of rosettes and roots of hydroponically grown plants under control conditions or subject to mannitol stress was measured by adaptation of an existing method [86]. In short, 200 μL of the soluble fraction from the sugar measurements were mixed with 800 μL of water, 1 mL of glacial acetic acid and 1 mL of ninhydrin reagent (2.5 % ninhydrin in a 6:3:1 mixture of glacial acetic acid:water:orthophosphoric acid). Samples were incubated for 1 h at 90°C, cooled to 25°C, combined with an equal volume of toluene, and mixed vigorously. Following phase partitioning, 1 mL of the upper organic phase was transferred into a quartz cuvette and the OD at 546 nm was measured spectrophotometrically. A calibration curve was prepared using different proline concentration as a standard.

Measurements of endogenous ABA levels

Endogenous ABA content was measured in leaves of hydroponically-grown plants with or without mannitol treatment for 4 h. Samples were extracted and measured as described in [87].

Stomatal aperture

For stomatal aperture measurement, epidermal peels isolated from the abaxial side of the middle part of leaf 6 were glued onto a coverslip using a non-toxic medical adhesive (Medical Adhesive B Liquid, VM 355-1, Ulrich Swiss). The adaxial epidermis and mesophyll layers were gently removed. The coverslips with the glued abaxial epidermis were rinsed with 10 mM MES-KOH, pH 6.15, and stomata were immediately imaged using an inverted microscope (Nikon Eclipse TS100) at 40 x magnification. Stomatal apertures were measured manually using the ImageJ software (v 1.42q, NIH USA, http://rsbweb.nih.gov/ij/). Around 20 pictures per leaf and per time point were taken and more than 50 stomatal apertures were

measured.

Absorbed and transpired water

Three-week-old hydroponically-grown plants were transferred into pre-weighed tubes containing 15 mL nutrient solution optionally supplemented with 300 mM mannitol for 4 h. The weight of the tubes with the plants was determined every hour. The water absorbed and subsequently transpired by the plants was measured by the difference between the weight of the tube containing the plants and the empty tubes. Changes in the weight of empty tubes were used to normalize for the loss of water due to the evaporation of the liquid surface.

Osmolality (π)

For osmolyte concentration measurements, leaves from three plants were pooled, subject to five cycles of freezing/thawing, and subsequently mechanically ground. After centrifugation for 10 min at 16,000 *g* at 4°C, 10 µL of the diluted supernatant (generally 1:3) was used to determine the osmolality using a Micro-Osmometer (Advance Instruments, inc).

Determination of F_v/F_m and ΦPSII

Chlorophyll fluorescence transients of Col-0 and *amy3 bam1* leaves in response to osmotic stress were measured using the FluorCam 800MF (Photo Systems Instruments). The fluorescence measurement protocol uses short (30 µs) measuring flashes to measure the initial minimal fluorescence (F_o) emitted from dark-adapted leaves, followed by a strong saturating flash for 0.8 sec measure the maximal fluorescence (F_m). After 15 min of dark adapatation, the leaf was exposed to actinic light for 4 min. Three strong flashes of saturating light probed the effective quantum yield (ΦPSII) during the actinic light exposure. The chlorophyll fluorescence transients were measured at the indicated time points in plants subject to 300 mM mannitol stress or kept in control nutrient solution. Image processing software integrated with the FluorCam was used to process the captured time-resolved ChlF images. The numeric value of each ChlF parameter was determined by integrating it over the measured leaf area, using the following formula: $F_v/F_m = (F_m - F_o)/F_m$; $\Phi PSII = F_m' - F'/F_m'$, where F_m' is the maximal fluorescence from light-adapted leaves and F' is the fluorescence emission from light-adapted leaves.

Measurement of chlorophyll *a/b* content

Freshly harvested rosettes were weighed, frozen in liquid N_2, pulverized while still frozen using the Mix Mill MM-301 (Retsch Haan, Germany), and then extracted by vigorous mixing in 10% (v/v) 0.2 M Tris-HCl, pH 8, in acetone. After centrifugation for 1 min at 16,000 *g,* chlorophyll (Chl) concentrations of the supernatants were determined spectrophotometrically

by measuring the OD in a glass cuvette at 649 nm (Chl *b)* and 665 nm (Chl *a)*. The chlorophyll content was calculated using the following formulas: Chl *a* [µg ml^{-1}] = 11.63 x OD_{665} – 2.39 x OD_{649}; Chl *b* [µg ml^{-1}] = 20.11 x OD_{649} – 5.18 x OD_{665}; Chla+b [µg ml^{-1}] = 6.45 x OD_{665}+17.72 x OD_{649}.

Native PAGE and activity staining

Entire rosettes of hydroponically-grown culture were harvested at the indicated time points and frozen in liquid N_2. Rosettes were ground using mix mill MM-301 (Retsch) and incubated for 30 min at 4°C in extraction buffer (50 mM Tris-HCl, pH 7.5, 1 mM $CaCl_2$, 1 mM $MgCl_2$, 5 mM DTT and 1x Complete EDTA Free Protease Inhibitor [Roche]; 300 µl per 100 mg fresh weight) for 30 min at 4°C. Insoluble material was removed by centrifugation at 15,000 *g* for 5 min. Protein content was quantified using the BCA Protein Assay kit (Thermo Scientific), and 5 µg of protein was loaded onto the PAGE gels. For native PAGE, resolving gels contained 7.5 % (w/v) acrylamide, 9 % (v/v) glycerol, 375 mM Tris-HCl, pH 8.8, and 0.1 % (w/v) amylopectin. The stacking gel contained 3.75 % (w/v) acrylamide, 63 mM Tris-HCl, pH 6.8, and 0.1 % (w/v) amylopectin. Protein extracts from leaves were mixed with PAGE loading buffer (final concentration 50 mM Tris-HCl, pH 6.8, 3 % (v/v) glycerol, 0.005 % (w/v) bromophenol blue) and loaded on the gel (5 µg protein). After 3 h electrophoresis at 4°C with a constant 120 V, gels were washed once in a reducing incubation buffer (100 mM HEPES-KOH, pH 7.5, 1 mM $CaCl_2$, 1 mM $MgCl_2$, 5 mM DTT) and then incubated for 2 h in the same buffer at 25 °C. Gels were stained for 16 h at 4 °C in Lugol's solution. Excess stain was removed by several washes in cold water.

Immunodetection of BAM1 and AMY3 protein and quantification

Rosettes of control and ABA-treated plants were harvested into microcentrifuge tubes containing three glass beads, and kept frozen at -80 °C prior to analysis. The tissue was ground into a fine powder using a Mix Mill. Protein extraction medium (40 mM Tris-HCl, pH 6.8, 5 mM $MgCl_2$, and Protease inhibitor cocktail [Roche]) was added to the powder at a ratio of 1 mL per 100 mg tissue. Insoluble material was spun down at 20,000 *g* for 5 min, and soluble proteins were collected in the supernatant. Protein (5 µg) was loaded onto SDS-PAGE gels and electrophoresis performed using standard protocols. For immunoblotting, proteins were transferred onto a PVDF membrane following SDS-PAGE. The BAM1 protein was detected using polyclonal rabbit antibodies raised against a recombinant His-tagged Arabidopsis BAM1 protein, which was expressed and purified from *E. coli.* AMY3 was detected using polyclonal antibodies raised against recombinant AMY3 protein [31]. Bands were visualized by chemiluminescence detection. Quantification of band intensities was conducted using the densitometry feature of ImageJ software.

Supporting information

S1 Data. Excel spreadsheet containing, in separate sheets, the underlying numerical data for Figs. 4A, 4D and 4E. (XLSX)

S2 Data. Promoter sequences used for the MEME analysis in S14 Fig. (DOCX)

S1 Fig. Starch and maltose levels in Col-0 plants upon mannitol or sorbitol treatment. Leaf starch **(A)** and maltose **(B)** content in Col-0 Arabidopsis plants treated with 300 mM mannitol or 300 mM sorbitol for 4 h compared with controls. Each value is the mean ± SE (n = 6). FW, fresh weight. Statistical significances determined by unpaired two-tailed Student's *t* tests: different letters denote $p < 0.05$.

S2 Fig. Effects of mannitol or sorbitol treatment on shoot and root growth in Col-0 plants. Col-0 seeds were germinated on half strength MS agar plates and after 6 days were transferred to MS plates optionally supplemented with different concentrations of mannitol or sorbitol (0, 50, 100, 200, 300 mM). Quantification of shoot **(A)** and root **(B)** growth after 21 days of treatment. FW, fresh weight. Statistical significances determined by unpaired two-tailed Student's *t* tests: different letters denote $p < 0.05$.

S3 Fig. Impact of simultaneous loss of BAM1 and AMY3 on starch metabolism in plants grown under control conditions. (A) Photographs of iodine-stained Col-0, *bam1, amy3, amy3 bam1* and *bam3* rosettes harvested at the end of the day (EoD) and at the end of the night (EoN) after 4 weeks of growth. Bar = 1 cm. **(B)** Starch content at the end of the day and at the end of the night in Col-0, *bam1, amy3, amy3 bam1* and *bam3* leaves. Values are means ± SE (n = 8). FW, fresh weight. Statistical significances determined by unpaired two-tailed Student's *t* tests: * denotes $p < 0.05$ for the indicated comparison.

S4 Fig. *BAM1* and *BAM3* are differentially regulated by abiotic stresses. Comparison of expression profiles of *BAM1* and *BAM3* in response to various abiotic stresses (drought, salt, cold and osmotic stress). Data were retrieved from the public eFP browser microarray dataset 'Abiotic Stress' (http://www.bar.utoronto.ca/efp/cgi-bin/efpWeb.cgi).

S5 Fig. Expression levels of *BAM1* in Col-0 and *bam3* mutant plants. Hydroponically-grown Col-0 and *bam3* plants were transferred to fresh nutrient solution (control) or nutrient solution containing 300 mM mannitol for 4 h. *BAM1* transcript abundance, determined by qPCR, was compared in osmotically-stressed and control leaves. The *ACT2* gene served as a

reference gene. Values representing means ± SE (n =3) were normalized against gene expression in control conditions (set as 1). Statistical significances determined by unpaired two-tailed Student's *t* tests: * denotes $p < 0.05$ for the indicated comparison.

S6 Fig. The *amy3 bam1* double mutant. Immunodetection of BAM1 and AMY3 protein in total protein extracts of four-week-old rosettes. Equal amounts of protein (5 ìg) were separated by SDS-PAGE. BAM1 and AMY3 were then detected by immunoblotting using antibodies raised against Arabidopsis BAM1 or AMY3, respectively. Each antiserum recognized a protein in the wild type that was missing in the *amy3 bam1* mutant. Replicate blots yielded the same result. The Rubisco large subunit (RbcL), visualized by Coomassie staining, confirmed equal protein loading.

S7 Fig. Stomatal closure in response to high osmotic stress in Col-0 and *amy3 bam1* plants. (A) Epidermal peels isolated from leaves of hydroponically-grown plants treated with mannitol for 4 h or kept in a control nutrient solution were used for stomatal aperture measurements. After peel preparation, stomata were immediately imaged with a light microscope. Aperture was determined manually using ImageJ software. Values represent the stomatal aperture of osmotically-stressed plants compared with the aperture of plants grown under control conditions (set as 100%). Values are means ± SE (n = 4 biological replicates with more than 50 individual stomata measured in total). **(B)** Numerical data used in **(A).** Statistical significances determined by unpaired two-tailed Student's *t* tests: * denotes $p < 0.05$ for the indicated comparison; n.s. = not significant for the indicated comparison.

S8 Fig. Accumulation of endogenous ABA in response to mannitol treatment. ABA levels in rosette of hydroponically-grown Col-0 and *amy3 bam1* plants subject to 300 mM mannitol stress for 4 h were determined at the indicated time points as described in Materials and Methods. Values are means ± SE (n = 4). FW, fresh weight.

S9 Fig. Quantification of BAM1 protein in leaves of Col-0 plants treated with ABA. Densitometry analysis (ImageJ) of three replicate blots was used to quantify band intensities. Values are expressed relative to the mean band intensity at time 0 (T0, set as 1). Each value is the mean ± SE of three biological samples. Each sample was blotted in three technical replicates. Statistical significances determined by unpaired two-tailed Student's *t* tests: different letters denote $p < 0.05$.

S10 Fig. AMY3 is a highly abundant protein in plant leaves. (A) Immunodetection of AMY3 protein in leaves of Col-0 and *bam1* plants treated with ABA. Total protein was

extracted from entire rosettes of hydroponically-grown plants at the indicated time points after treatment with 100 µM ABA. Equal amounts of protein (5 µg) were separated by SDS-PAGE. AMY3 was detected by immunoblotting using antibodies raised against the recombinant AMY3 protein. No differences in AMY3 protein abundance were observed between control (C) and ABA-treated plants. Replicate blots yielded the same result. The loading control for this blot is the same as the one presented in Fig. 5B, as the two experiments were performed in parallel. **(B)** Relative *AMY3* and *BAM1* transcript abundance was determined in hydroponically-grown Col-0 after 3 h, 5 h and 7 h of light, using qPCR. The *ACT2* gene served as a reference gene. Values are means ± SE (n = 3).

S11 Fig. Expression levels of *RD29A, BAM1, BAM3* and *AMY3* in *snrk2.2 snrk2.3 snrk2.6* and *areb1 areb2 abf3* mutants under control conditions. Leaf transcript abundance was determined in hydroponically-grown Col-0 and *snrk2.2 snrk2.3 snrk2.6* **(A)** or *areb1 areb2 abf3* **(B)** mutants after 3 h of light, using qPCR. The *ACT2* gene was used as reference gene. Expression values are given relative to the levels in Col-0 (set as 1). Values are means ± SE (n = 3). No statistically significant differences were observed, as determined by unpaired two-tailed Student's *t* tests.

S12 Fig. Soluble sugars content in Col-0, *nced3* and *aao3* plants grown in control conditions. Glucose **(A)** and sucrose **(B)** content in shoot of Col-0, *nced3* and *aao3* mutant plants after 3 h, 5 h and 7 h of light. Values are means ± SE (n = 4). FW, fresh weight.

S13 Fig. Starch levels in response to mannitol, ABA or a combination of mannitol and ABA treatment. Leaf starch in Col-0, *amy3 bam1* and *nced3* plants treated with 300 mM mannitol, 100 µM ABA or 300 mM mannitol + 100 µM ABA for 4 h, compared with controls. Values are means ± SE (n = 6). FW, fresh weight. Statistical significances determined by unpaired two-tailed Student's *t* tests: * denotes $p < 0.05$ for the indicated comparison.

S14 Fig. Unbiased bioinformatics analysis of *BAM1* ortholog genes promoter sequences. 1.5 Kb promoter regions of *BAM1-like* genes from 30 plant species were analyzed using the MEME suite (http://meme.nbcr.net). The conserved sequence logos of the ABA responsive elements (ABRE) and the Coupling Element 3 like (CE3-like) found by MEME are depicted in **(A)** and **(B),** respectively. **(C)** Distribution of ABRE and CE3-like *cis-regulatory* elements within the analyzed promoters. CE3-like elements were enriched in all promoters. ABRE elements were found enriched in the proximity of the ATG codon in all examined promoters, except those of the *BAM1* genes from grasses.

S1 Table. Soluble sugars content of shoots in response to osmotic stress. Glucose, fructose and sucrose content in the shoots of Col-0, *bam1* and *amy3* plants in response to osmotic stress treatment. Hydroponically-grown plants were optionally supplemented with 300 mM mannitol for 4 h. Sugars were measured at the indicated time points using high-performance anion-exchange chromatography with pulsed amperometric detection (HPAEC-PAD). Values are means ± SE (n = 6). FW, fresh weight. No statistically significant differences were observed between genotypes, as determined by unpaired two-tailed Student's *t* tests.

S2 Table. Soluble sugar content of roots in response to osmotic stress. Glucose, fructose and sucrose content in root of Col-0, *bam1* and *amy3* plants in response to osmotic stress treatment. Hydroponically-grown plants were optionally supplemented with 300 mM mannitol for 4 h. Sugars were measured enzymatically at the indicated time points. Value are means ± SE (n = 3). FW, fresh weight. No statistically significant differences were observed between genotypes, as determined by unpaired two-tailed Student's *t* tests.

S3 Table. Carbon partitioning into the major cellular compound classes in shoot and root of plants labelled at the beginning of the stress treatment. Whole Col-0, *bam1, amy3,* and *amy3 bam1* plants were labelled with $^{14}CO_2$ for 1 h, just after transfer to a mannitol containing nutrient solution. Following a 1-h chase period, the shoot and root were harvested separately and the amount of ^{14}C incorporated into the different compound classes in each organ was determined by liquid scintillation counting. The sum of the label in each organ is set to 100%. The relative amount of ^{14}C incorporated into the different compound classes (as a percentage of the total label in the corresponding organ) is shown. Values are means ± SE (n = 4).

S4 Table. Carbon partitioning into the major cellular compound classes in shoot and root of plants labelled in the middle of the stress treatment. Whole Col-0, *bam1, amy3,* and *amy3 bam1* plants were labelled with $^{14}CO_2$ for 1 h, in the middle of the stress treatment. Following a 1-h chase period, the shoot and root were harvested separately and the amount of ^{14}C incorporated into the different compound classes in each organ was determined by liquid scintillation counting. The sum of the label in each organ is set to 100%. The relative amount of ^{14}C incorporated into the different compound classes (as a percentage of the total label in the corresponding organ) is shown. Values are means ± SE (n = 4).

S5 Table. Chlorophyll *a* fluorescence parameters of Col-0 and *amy3 bam1* plants subject to osmotic stress. The chlorophyll fluorescence transients F_v/F_m and ΦPSII were measured at

the indicated time points in Col-0 and *amy3 bam1* plants subject to 300 mM mannitol stress or kept in control nutrient solution, using a FluorCam. The plants were dark adapted for about 15 min prior each measurement. Values are means ± SE of four independent determinations. Asterisks indicate statistically significant differences between control and osmotic-stressed plants for each genotype, as determined by unpaired two-tailed Student's *t* tests. No statistically significant differences were observed between genotypes. The maximum quantum efficiency of PSII photochemistry (F_v/F_m) was reduced in both genotypes at a similar level after 2 h (0.767±0.010 and 0.767±0.011 for *amy3 bam1* and wild-type plants, respectively).

A reduction was also observed in the PSII operating efficiency (FPSII), indicating a decrease in the relative quantum yield of linear electron transfer through the photosystems. This suggests that osmotic stress led to negative effects on PSII efficiency, but to a similar extent in the two genotypes.

S6 Table. Chlorophyll content of Col-0 and *bam1, amy3, amy3 bam1* plants in response to osmotic stress treatment. Chlorophyll *a* content (Chl *a),* chlorophyll *b* content (Chl *a),* total chlorophyll and chlorophyll *a/b* ratio (Chl *a/b)* of hydroponically-grown plants optionally supplemented with 300 mM mannitol were determined at the indicated time points. Values are means ± SE (n = 6). No statistically significant difference between genotypes or between control and mannitol-treated samples were detected, as determined by unpaired two-tailed Student's *t* tests. Total chlorophyll content was not affected by osmotic stress in either genotype, nor was the ratio of chlorophyll *a* to chlorophyll *b* (Chl *a/b).*

S7 Table. Sequences of primers used in this work.

Acknowledgments

We thank Michaela Stettler for technical help with the ^{14}C labelling experiments and the HPAEC-PAD analysis; Simon Krattinger for support with the water uptake experiments; Martina Zanella for support with the free proline measurements; Mario Coiro for support with the MEME analysis: Enrico Martinoia, Stefan Hörtensteiner and Luis Lopez Molina for helpful discussion; Jan-Kang Zhu for providing *snrk2.2 snrk2.3 snrk2.6* mutant; Kazuko Yamaguchi-Shinozaki for providing *areb1 areb2 abf3* mutant; Florian Bittner for providing *aao3-4* mutant. This work was supported by the Swiss National Science Foundation SNSF-Grant 31003A_147074 (to DSa), by the Forschungskredit_13-101 from the University of 39 Zürich (to MT), by a Heinz-Imhof Fellowship from the ETH Foundation (to DSe), by the SystemsX.ch RTD project "Plant growth in a changing environment" and the EU FP7 project TiMet, grant nr. 245143 (to SCZ).

Author contributions

DSa conceived the project. DSa and MT designed the experiments. DSa, MT, DP, DSE, DH, AN, TM, KK, HWP performed the experiments and analyzed the data. DSa, MT and SCZ wrote the paper.

References

1. IPCC. Summary for policy makers. In: Managing the risks of extreme events and disasters to advance climate change adaptation: "A special report of working groups I and II of the Intergovernmental Panel on Climate Change" (eds Field CB, Barros V, Stocker TF, Qin. Cambridge Univ Press Cambridge. 2012; 1–19.
2. Ciais P, Reichstein M, Viovy N, Granier a, Ogée J, Allard V, et al. Europe-wide reduction in primary productivity caused by the heat and drought in 2003. Nature. 2005;437: 529–33. doi:10.1038/nature03972
3. Cramer GR, Urano K, Delrot S, Pezzotti M, Shinozaki K. Effects of abiotic stress on plants: a systems biology perspective. BMC Plant Biol. BioMed Central Ltd; 2011;11: 163. doi:10.1186/1471-2229-11- 163
4. Long SP, Ort DR. More than taking the heat: Crops and global change. Curr Opin Plant Biol. Elsevier Ltd; 2010;13: 241–248. doi:10.1016/j.pbi.2010.04.008
5. Bartels D, Sunkar R. Drought and Salt Tolerance in Plants. CRC Crit Rev Plant Sci. 2005;24: 23–58. doi:10.1080/07352680590910410
6. Miller G, Suzuki N, Ciftci-Yilmaz S, Mittler R. Reactive oxygen species homeostasis and signalling during drought and salinity stresses. Plant, Cell Environ. 2010;33: 453–467. doi:10.1111/j.1365- 3040.2009.02041.x
7. Krasensky J, Jonak C. Drought, salt, and temperature stress-induced metabolic rearrangements and regulatory networks. J Exp Bot. 2012;63: 1593–1608. doi:10.1093/jxb/err460
8. Verslues. Proline Metabolism and Its Implications for Plant-Environment Interaction. Arab B. 2011; doi:10.1199/tab.0140
9. Hoekstra F a, Golovina E a, Buitink J. Mechanisms of plant desiccation tolerance. Trends Plant Sci. 2001;6: 431–438. doi:10.1016/S1360-1385(01)02052-0
10. Couée I, Sulmon C, Gouesbet G, El Amrani A. Involvement of soluble sugars in reactive oxygen species balance and responses to oxidative stress in plants. J Exp Bot. 2006;57: 449–459. doi:10.1093/jxb/erj027
11. Farrant JM, Moore JP. Programming desiccation-tolerance: From plants to seeds to resurrection plants. Curr Opin Plant Biol. Elsevier Ltd; 2011;14: 340–345. doi:10.1016/j.pbi.2011.03.018
12. Damour G, Vandame M, Urban L. Long-term drought modifies the fundamental relationships between light exposure, leaf nitrogen content and photosynthetic capacity in leaves of the lychee tree (Litchi chinensis). J Plant Physiol. 2008;165: 1370–1378. doi:10.1016/j.jplph.2007.10.014
13. Lee BR, Jin YL, Jung WJ, Avice JC, Morvan-Bertrand A, Ourry A, et al. Water-deficit accumulates sugars by starch degradation - Not by de novo synthesis - In white clover leaves (Trifolium repens). Physiol Plant. 2008;134: 403–411. doi:10.1111/j.1399-3054.2008.01156.x
14. Pelleschi S, Rocher JP, Prioul JL. Effect of water restriction on carbohydrate metabolism and

photosynthesis in mature maize leaves. Plant Cell Environ. 1997;20: 493–503. doi:10.1046/j.1365- 3040.1997.d01-89.x

15. Pinheiro C, António C, Ortuño MF, Dobrev PI, Hartung W, Thomas-Oates J, et al. Initial water deficit effects on Lupinus albus photosynthetic performance, carbon metabolism, and hormonal balance: Metabolic reorganization prior to early stress responses. J Exp Bot. 2011;62: 4965–4974. doi:10.1093/jxb/err194

16. Zeeman SC, Kossmann J, Smith AM. Starch: its metabolism, evolution, and biotechnological modification in plants. Annu Rev Plant Biol. 2010;61: 209–234. doi:10.1146/annurev-arplant-042809- 112301

17. Yang J, Zhang J, Wang Z, Zhu Q. Activities of starch hydrolytic enzymes and sucrose-phosphate synthase in the stems of rice subjected to water stress during grain filling. J Exp Bot. 2001;52: 2169–79. Available: http://www.ncbi.nlm.nih.gov/pubmed/11604456

18. Ritte G, Heydenreich M, Mahlow S, Haebel S, Kötting O, Steup M. Phosphorylation of C6- and C3- positions of glucosyl residues in starch is catalysed by distinct dikinases. FEBS Lett. 2006;580: 4872– 4876. doi:10.1016/j.febslet.2006.07.085

19. Kötting O, Santelia D, Edner C, Eicke S, Marthaler T, Gentry MS, et al. STARCH-EXCESS4 is a laforin-like Phosphoglucan phosphatase required for starch degradation in Arabidopsis thaliana. Plant Cell. 2009;21: 334–46. doi:10.1105/tpc.108.064360

20. Santelia D, Kotting O, Seung D, Schubert M, Thalmann M, Bischof S, et al. The Phosphoglucan Phosphatase Like Sex Four2 Dephosphorylates Starch at the C3-Position in Arabidopsis. Plant Cell. 2011;23: 4096–4111. doi:10.1105/tpc.111.092155

21. Streb S, Eicke S, Zeeman SC. The simultaneous abolition of three starch hydrolases blocks transient starch breakdown in Arabidopsis. J Biol Chem. 2012;287: 41745–56. doi:10.1074/jbc.M112.395244

22. Fulton DC, Stettler M, Mettler T, Vaughan CK, Li J, Francisco P, et al. Beta-AMYLASE4, a noncatalytic protein required for starch breakdown, acts upstream of three active beta-amylases in Arabidopsis chloroplasts. Plant Cell. 2008;20: 1040–58. doi:10.1105/tpc.107.056507

23. Kaplan F, Guy CL. RNA interference of Arabidopsis beta-amylase8 prevents maltose accumulation upon cold shock and increases sensitivity of PSII photochemical efficiency to freezing stress. Plant J. 2005;44: 730–43. doi:10.1111/j.1365-313X.2005.02565.x

24. Valerio C, Costa A, Marri L, Issakidis-Bourguet E, Pupillo P, Trost P, et al. Thioredoxin-regulated beta- amylase (BAM1) triggers diurnal starch degradation in guard cells, and in mesophyll cells under osmotic stress. J Exp Bot. 2011;62: 545–555. doi:10.1093/jxb/erq288

25. Niittylä T, Messerli G, Trevisan M, Chen J, Smith AM, Zeeman SC. A previously unknown maltose transporter essential for starch degradation in leaves. Science (80-). 2004;303: 87–89.

26. Trontin C, Kiani S, Corwin JA, Hématy K, Yansouni J, Kliebenstein DJ, et al. A pair of receptor-like kinases is responsible for natural variation in shoot growth response to mannitol treatment in Arabidopsis thaliana. Plant J. 2014;78: 121–33. doi:10.1111/tpj.12454

27. Claeys H, Van Landeghem S, Dubois M, Maleux K, Inzé D. What Is Stress? Dose-Response Effects in Commonly Used in Vitro Stress Assays. Plant Physiol. 2014;165: 519–527. doi:10.1104/pp.113.234641

28. Yamaguchi-Shinozaki K, Shinozaki K. A novel cis-acting element in an Arabidopsis gene is involved in responsiveness to drought, low-temperature, or high-salt stress. Plant Cell. 1994;6: 251–264. doi:10.1105/tpc.6.2.251

29. Streb S, Zeeman SC. Starch metabolism in Arabidopsis. Arabidopsis Book. 2012;10: e0160.

doi:10.1199/tab.0160

30. Seung D, Thalmann M, Sparla F, Abou Hachem M, Lee SK, Issakidis-Bourguet E, et al. Arabidopsis thaliana AMY3 is a unique redox-regulated chloroplastic α-amylase. J Biol Chem. 2013;288: 33620– 33633. doi:10.1074/jbc.M113.514794

31. Yu T-S, Zeeman SC, Thorneycroft D, Fulton DC, Dunstan H, Lue W-L, et al. a-Amylase is not required for breakdown of transitory starch in Arabidopsis leaves. J Biol Chem. 2005;280: 9773–9. doi:10.1074/jbc.M413638200

32. Smith SM, Fulton DC, Chia T, Thorneycroft D, Chapple A, Dunstan H, et al. Diurnal changes in the transcriptome encoding enzymes of starch metabolism provide evidence for both transcriptional and posttranscriptional regulation of starch metabolism in Arabidopsis leaves. Plant Physiol. 2004;136: 2687–2699. doi:10.1104/pp.104.044347

33. Kaplan F, Guy CL. beta-Amylase induction and the protective role of maltose during temperature shock. Plant Physiol. American Society of Plant Biologists; 2004;135: 1674–84. doi:10.1104/pp.104.040808

34. Kölling K, Thalmann M, Müller A, Jenny C, Zeeman SC. Carbon partitioning in Arabidopsis thaliana is a dynamic process controlled by the plants metabolic status and its circadian clock. Plant Cell Environ. 2015;38: 1975–1979. doi:10.1111/pce.12512

35. Urano K, Maruyama K, Ogata Y, Morishita Y, Takeda M, Sakurai N, et al. Characterization of the ABA-regulated global responses to dehydration in Arabidopsis by metabolomics. Plant J. 2009;57: 1065–1078. doi:10.1111/j.1365-313X.2008.03748.x

36. Yamaguchi-Shinozaki K, Shinozaki K. Transcriptional regulatory networks in cellular responses and tolerance to dehydration and cold stresses. Annu Rev Plant Biol. 2006;57: 781–803. doi:10.1146/annurev.arplant.57.032905.105444

37. Choudhury a., Lahiri a. Comparative analysis of abscisic acid-regulated transcriptomes in Arabidopsis. Plant Biol. 2011;13: 28–35. doi:10.1111/j.1438-8677.2010.00340.x

38. Böhmer M, Schroeder JI. Quantitative transcriptomic analysis of abscisic acid-induced and reactive oxygen species-dependent expression changes and proteomic profiling in Arabidopsis suspension cells. Plant J. 2011;67: 105–118. doi:10.1111/j.1365-313X.2011.04579.x

39. Zeller G, Henz SR, Widmer CK, Sachsenberg T, Rätsch G, Weigel D, et al. Stress-induced changes in the Arabidopsis thaliana transcriptome analyzed using whole-genome tiling arrays. Plant J. 2009;58: 1068–1082. doi:10.1111/j.1365-313X.2009.03835.x

40. Matsui A, Ishida J, Morosawa T, Mochizuki Y, Kaminuma E, Endo T a., et al. Arabidopsis transcriptome analysis under drought, cold, high-salinity and ABA treatment conditions using a tiling array. Plant Cell Physiol. 2008;49: 1135–1149. doi:10.1093/pcp/pcn101

41. Kempa S, Krasensky J, Dal Santo S, Kopka J, Jonak C. A central role of abscisic acid in stress-regulated carbohydrate metabolism. PLoS One. 2008;3. doi:10.1371/journal.pone.0003935

42. Baerenfaller K, Hirsch-Hoffmann M, Svozil J, Hull R, Russenberger D, Bischof S, et al. pep2pro: a new tool for comprehensive proteome data analysis to reveal information about organ-specific proteomes in Arabidopsis thaliana. Integr Biol (Camb). 2011;3: 225–237. doi:10.1039/c0ib00078g

43. Yoshida T, Fujita Y, Sayama H, Kidokoro S, Maruyama K, Mizoi J, et al. AREB1, AREB2, and ABF3 are master transcription factors that cooperatively regulate ABRE-dependent ABA signaling involved in drought stress tolerance and require ABA for full activation. Plant J. 2010;61: 672–85. doi:10.1111/j.1365-313X.2009.04092.x

44. Fujita Y, Nakashima K, Yoshida T, Katagiri T, Kidokoro S, Kanamori N, et al. Three SnRK2

protein kinases are the main positive regulators of abscisic acid signaling in response to water stress in arabidopsis. Plant Cell Physiol. 2009;50: 2123–2132. doi:10.1093/pcp/pcp147

45. Furihata T, Maruyama K, Fujita Y, Umezawa T, Yoshida R, Shinozaki K. Abscisic acid-dependent multisite phosphorylation regulates the activity of a transcription activator AREB1. PNAS. 2006;103: 1988–1993.

46. Yoshida T, Mogami J, Yamaguchi-Shinozaki K. ABA-dependent and ABA-independent signaling in response to osmotic stress in plants. Curr Opin Plant Biol. Elsevier Ltd; 2014;21C: 133–139. doi:10.1016/j.pbi.2014.07.009

47. Fujita Y, Yoshida T, Yamaguchi-Shinozaki K. Pivotal role of the AREB/ABF-SnRK2 pathway in ABRE-mediated transcription in response to osmotic stress in plants. Physiol Plant. 2013;147: 15–27. doi:10.1111/j.1399-3054.2012.01635.x

48. Nakashima K, Fujita Y, Kanamori N, Katagiri T, Umezawa T, Kidokoro S, et al. Three Arabidopsis SnRK2 Protein Kinases, SRK2D/SnRK2.2, SRK2E/SnRK2.6/OST1 and SRK2I/SnRK2.3, Involved in ABA Signaling are Essential for the Control of Seed Development and Dormancy. Plant Cell Physiol. 2009;50: 1345–1363. doi:10.1093/pcp/pcp083

49. Umezawa T, Sugiyama N, Mizoguchi M, Hayashi S, Myouga F, Yamaguchi-Shinozaki K, et al. Type 2C protein phosphatases directly regulate abscisic acid-activated protein kinases in Arabidopsis. Proc Natl Acad Sci U S A. 2009;106: 17588–17593. doi:10.1073/pnas.0907095106

50. Fujii H, Zhu J-K. Arabidopsis mutant deficient in 3 abscisic acid-activated protein kinases reveals critical roles in growth, reproduction, and stress. Proc Natl Acad Sci U S A. 2009;106: 8380–8385. doi:10.1073/pnas.0903144106

51. Iuchi S, Kobayashi M, Taji T, Naramoto M, Seki M, Kato T. Regulation of drought tolerance by gene manipulation of 9- cis -epoxycarotenoid dioxygenase , a key enzyme in abscisic acid biosynthesis in Arabidopsis. Plant J. 2001;27: 325–333.

52. Hey SJ, Byrne E, Halford NG. The interface between metabolic and stress signalling. Ann Bot. 2010;105: 197–203. doi:10.1093/aob/mcp285

53. Seo M, Koshiba T. Complex regulation of ABA biosynthesis in plants. Trends Plant Sci. 2002;7: 41–48. doi:10.1016/S1360-1385(01)02187-2

54. Seo M, Aoki H, Koiwai H, Kamiya Y, Nambara E, Koshiba T. Comparative studies on the Arabidopsis aldehyde oxidase (AAO) gene family revealed a major role of AAO3 in ABA biosynthesis in seeds. Plant Cell Physiol. 2004;45: 1694–703. doi:10.1093/pcp/pch198

55. Seo M, Peeters a J, Koiwai H, Oritani T, Marion-Poll a, Zeevaart J a, et al. The Arabidopsis aldehyde oxidase 3 (AAO3) gene product catalyzes the final step in abscisic acid biosynthesis in leaves. Proc Natl Acad Sci U S A. 2000;97: 12908–12913. doi:10.1073/pnas.220426197

56. Yano R, Nakamura M, Yoneyama T, Nishida I. Starch-Related a -Glucan / Water Dikinase Is Involved in the Cold-Induced Development of Freezing Tolerance in Arabidopsis 1. 2005;138: 837–846. doi:10.1104/pp.104.056374.dehydration-responsive

57. Sitnicka D, Orzechowski S. Cold-induced starch degradation in potato leaves — intercultivar differences in the gene expression and activity of key enzymes. Biol Plant. 2014;58: 659–666. doi:10.1007/s10535- 014-0453-2

58. Scarpeci TE, Valle EM. Rearrangement of carbon metabolism in Arabidopsis thaliana subjected to oxidative stress condition: An emergency survival strategy. Plant Growth Regul. 2008;54: 133–142. doi:10.1007/s10725-007-9236-5

59. Geigenberger P, Reimholz R, Geiger M, Merlo L, Canale V, Stitt M. Regulation of sucrose

and starch metabolism in potato tubers in response to short-term water deficit. Planta. 1997;201: 502–518. doi:10.1007/s004250050095

60. Heldt HW, Chon CJ, Maronde D. Role of orthophosphate and other factors in the regulation of starch formation in leaves and isolated chloroplasts. Plant Physiol. 1977;59: 1146–1155. doi:10.1104/pp.59.6.1146

61. Hummel I, Pantin F, Sulpice R, Piques M, Rolland G, Dauzat M, et al. Arabidopsis plants acclimate to water deficit at low cost through changes of carbon usage: an integrated perspective using growth, metabolite, enzyme, and gene expression analysis. Plant Physiol. 2010;154: 357–72. doi:10.1104/pp.110.157008

62. Harb A, Krishnan A, Ambavaram MMR, Pereira A. Molecular and physiological analysis of drought stress in Arabidopsis reveals early responses leading to acclimation in plant growth. Plant Physiol. 2010;154: 1254–71. doi:10.1104/pp.110.161752

63. Monroe JD, Storm a. R, Badley EM, Lehman MD, Platt SM, Saunders LK, et al. b-amylase1 and b- amylase3 are plastidic starch hydrolases in Arabidopsis that seem to be adapted for different thermal, pH, and stress conditions. Plant Physiol. 2014;166: 1748–1763. doi:10.1104/pp.114.246421

64. Skirycz A, De Bodt S, Obata T, De Clercq I, Claeys H, De Rycke R, et al. Developmental stage specificity and the role of mitochondrial metabolism in the response of Arabidopsis leaves to prolonged mild osmotic stress. Plant Physiol. 2010;152: 226–44. doi:10.1104/pp.109.148965

65. Hannah M a, Wiese D, Freund S, Fiehn O, Heyer AG, Hincha DK. Natural genetic variation of freezing tolerance in Arabidopsis. Plant Physiol. 2006;142: 98–112. doi:10.1104/pp.106.081141

66. Usadel B, Bläsing OE, Gibon Y, Poree F, Höhne M, Günter M, et al. Multilevel genomic analysis of the response of transcripts, enzyme activities and metabolites in Arabidopsis rosettes to a progressive decrease of temperature in the non-freezing range. Plant, Cell Environ. 2008;31: 518–547. doi:10.1111/j.1365-3040.2007.01763.x

67. Maruyama K, Takeda M, Kidokoro S, Yamada K, Sakuma Y, Urano K, et al. Metabolic pathways involved in cold acclimation identified by integrated analysis of metabolites and transcripts regulated by DREB1A and DREB2A. Plant Physiol. 2009;150: 1972–80. doi:10.1104/pp.109.135327

68. Sparla F, Costa A, Lo Schiavo F, Pupillo P, Trost P. Redox regulation of a novel plastid-targeted b- Amylase. Plant Physiol. 2006;141: 840–850. doi:10.1104/pp.106.079186.of

69. Santelia D, Trost P, Sparla F. New insights into redox control of starch degradation. Curr Opin Plant Biol. Elsevier Ltd; 2015;25: 1–9. doi:10.1016/j.pbi.2015.04.003

70. Heldt HW, Werdan K, Milovancev M, Geller G. Alkalization of the chloroplast stroma caused by light- dependent proton flux into the thylakoid space. Biochim Biophys Acta - Bioenerg. 1973;314: 224–241. doi:10.1016/0005-2728(73)90137-0

71. Buchanan BB, Balmer Y. Redox regulation: a broadening horizon. Annu Rev Plant Biol. 2005;56: 187– 220. doi:10.1146/annurev.arplant.56.032604.144246

72. Silver DM, Kötting O, Moorhead GBG. Phosphoglucan phosphatase function sheds light on starch degradation. Trends Plant Sci. 2014;19: 471–8. doi:10.1016/j.tplants.2014.01.008

73. Kötting O, Kossmann J, Zeeman SC, Lloyd JR. Regulation of starch metabolism: the age of enlightenment? Curr Opin Plant Biol. Elsevier Ltd; 2010;13: 321–9. doi:10.1016/j.pbi.2010.01.003

74. Glaring M a, Skryhan K, Kötting O, Zeeman SC, Blennow A. Comprehensive survey of redox

sensitive starch metabolising enzymes in Arabidopsis thaliana. Plant Physiol Biochem. 2012;58: 89–97. doi:10.1016/j.plaphy.2012.06.017

75. Wu Y, Cosgrove DJ. Adaptation of roots to low water potentials by changes in cell wall extensibility and cell wall proteins. J Exp Bot. 2000;51: 1543–1553. doi:10.1093/jexbot/51.350.1543

76. Rogers ED, Benfey PN. Regulation of plant root system architecture: implications for crop advancement. Curr Opin Biotechnol. Elsevier Ltd; 2015;32: 93–98. doi:10.1016/j.copbio.2014.11.015

77. Roycewicz P, Malamy JE. Dissecting the effects of nitrate, sucrose and osmotic potential on Arabidopsis root and shoot system growth in laboratory assays. Philos Trans R Soc B Biol Sci. 2012;367: 1489– 1500. doi:10.1098/rstb.2011.0230

78. Fujita Y, Fujita M, Shinozaki K, Yamaguchi-Shinozaki K. ABA-mediated transcriptional regulation in response to osmotic stress in plants. J Plant Res. 2011;124: 509–525. doi:10.1007/s10265-011-0412-3

79. Bailey TL, Boden M, Buske FA, Frith M, Grant CE, Clementi L, et al. MEME SUITE: tools for motif discovery and searching. Nucleic Acids Res. 2009;37: W202–2088. doi:10.1093/nar/gkp335

80. Wan X-R, Li L. Regulation of ABA level and water-stress tolerance of Arabidopsis by ectopic expression of a peanut 9-cis-epoxycarotenoid dioxygenase gene. Biochem Biophys Res Commun. 2006;347: 1030–8. doi:10.1016/j.bbrc.2006.07.026

81. Meijering E, Jacob M, Sarria J-CF, Steiner P, Hirling H, Unser M. Design and validation of a tool for neurite tracing and analysis in fluorescence microscopy images. Cytometry A. 2004;58: 167–176. doi:10.1002/cyto.a.20022

82. Hostettler C, Kölling K, Santelia D, Streb S, Kötting O, Zeeman SC. Analysis of starch metabolism in chloroplasts. Methods Mol Biol. 2011;775: 387–410. doi:10.1007/978-1-61779-237-3_21

83. Egli B, Kölling K, Köhler C, Zeeman SC, Streb S. Loss of cytosolic phosphoglucomutase compromises gametophyte development in Arabidopsis. Plant Physiol. 2010;154: 1659–1671. doi:10.1104/pp.110.165027

84. Viola R, Davies H V. A microplate reader assay for rapid enzymatic quantification of sugars in potato tubers. Potato Res. 1992;35: 55–58. doi:10.1007/BF02357723

85. Kölling K, Müller A, Flütsch P, Zeeman SC. A device for single leaf labelling with CO2 isotopes to study carbon allocation and partitioning in Arabidopsis thaliana. Plant Methods. 2013;9: 45. doi:10.1186/1746-4811-9-45

86. Bates LS, Waldren RP, Teare ID. Rapid determination of free proline for water-stress studies. Plant Soil. 1973;39: 205–207. doi:10.1007/BF00018060

87. Großkinsky DK, Albacete A, Jammer A, Krbez P, van der Graaff E, Pfeifhofer H, et al. A rapid phytohormone and phytoalexin screening method for physiological phenotyping. Mol Plant. Elsevier; 2014;7: 1053–6. doi:10.1093/mp/ssu015

Figure 1

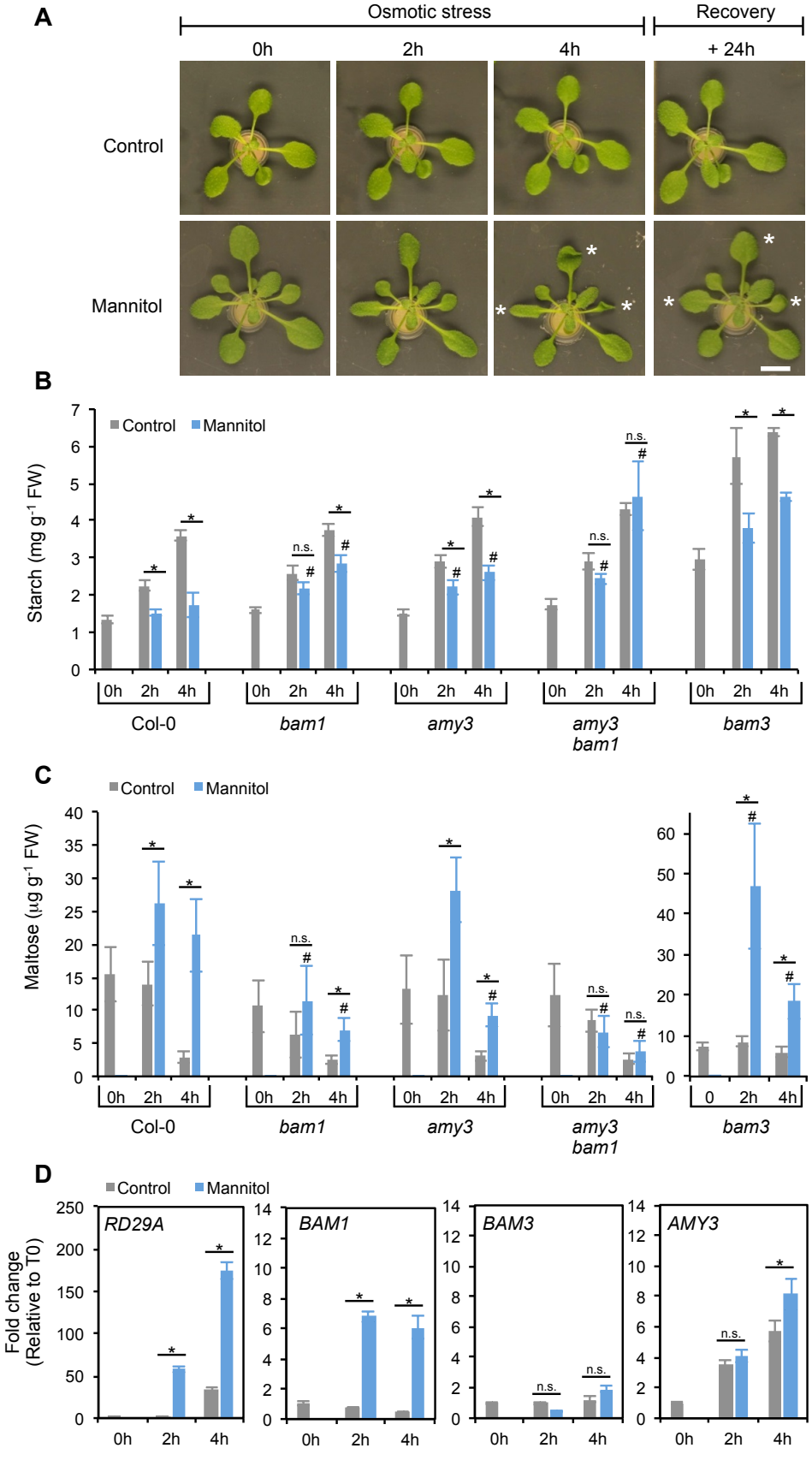
A
Osmotic stress
Recovery
0h
2h
4h
+ 24h
Control
Mannitol
B
Control
Mannitol
Starch (mg g-1 FW)
0h 2h 4h
Col-0
bam1
amy3
amy3 bam1
bam3
C
Maltose (µg g-1 FW)
D
Fold change (Relative to T0)
RD29A
BAM1
BAM3
AMY3
n.s.

Figure 2

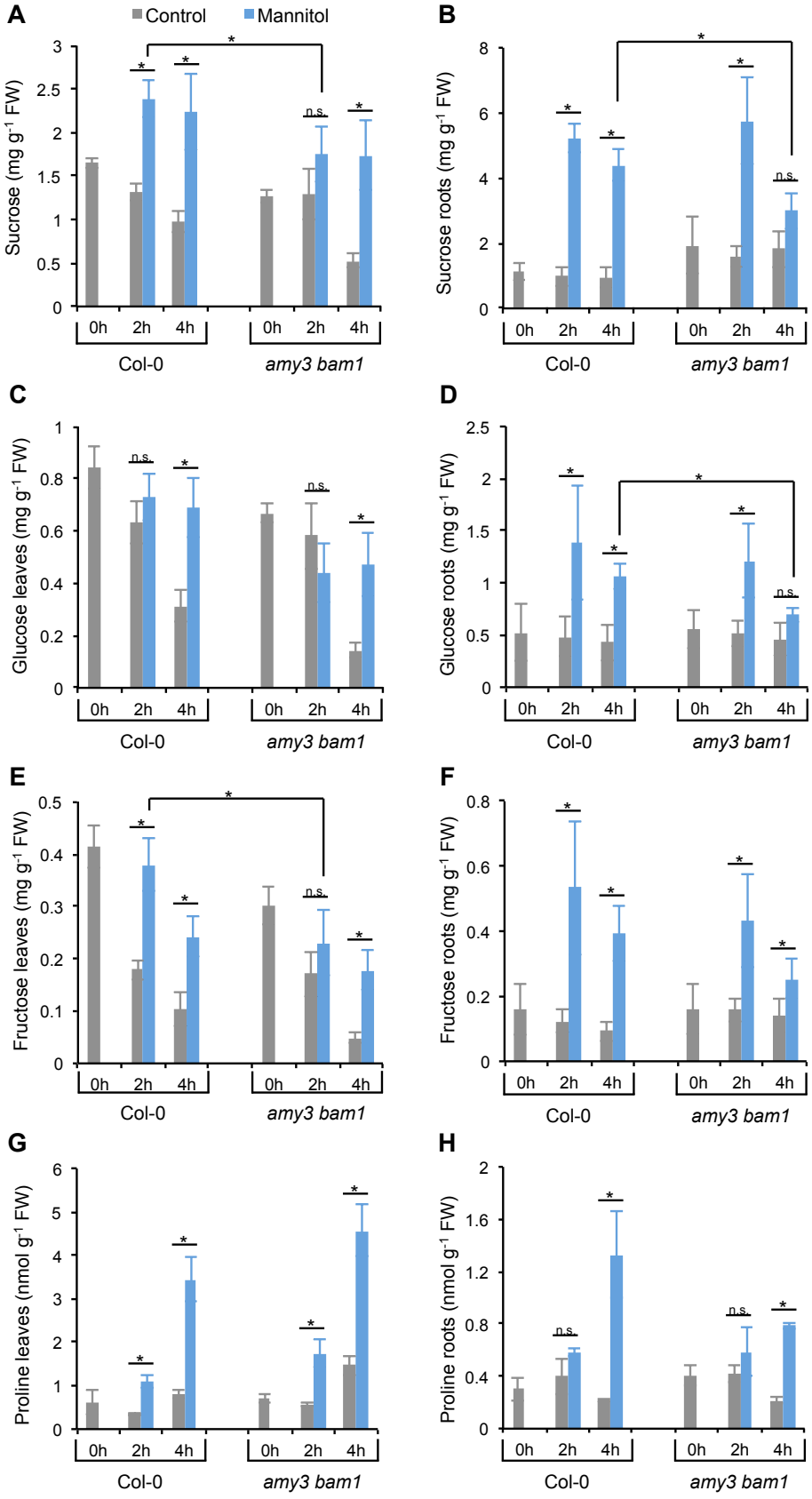
A
Control
Mannitol
Sucrose (mg g-1 FW)
B
Sucrose roots (mg g-1 FW)
C
Glucose leaves (mg g-1 FW)
D
Glucose roots (mg g-1 FW)
E
Fructose leaves (mg g-1 FW)
F
Fructose roots (mg g-1 FW)
G
Proline leaves (nmol g-1 FW)
H
Proline roots (nmol g-1 FW)
0h
2h
4h
Col-0
amy3 bam1
n.s.
*

Figure 3

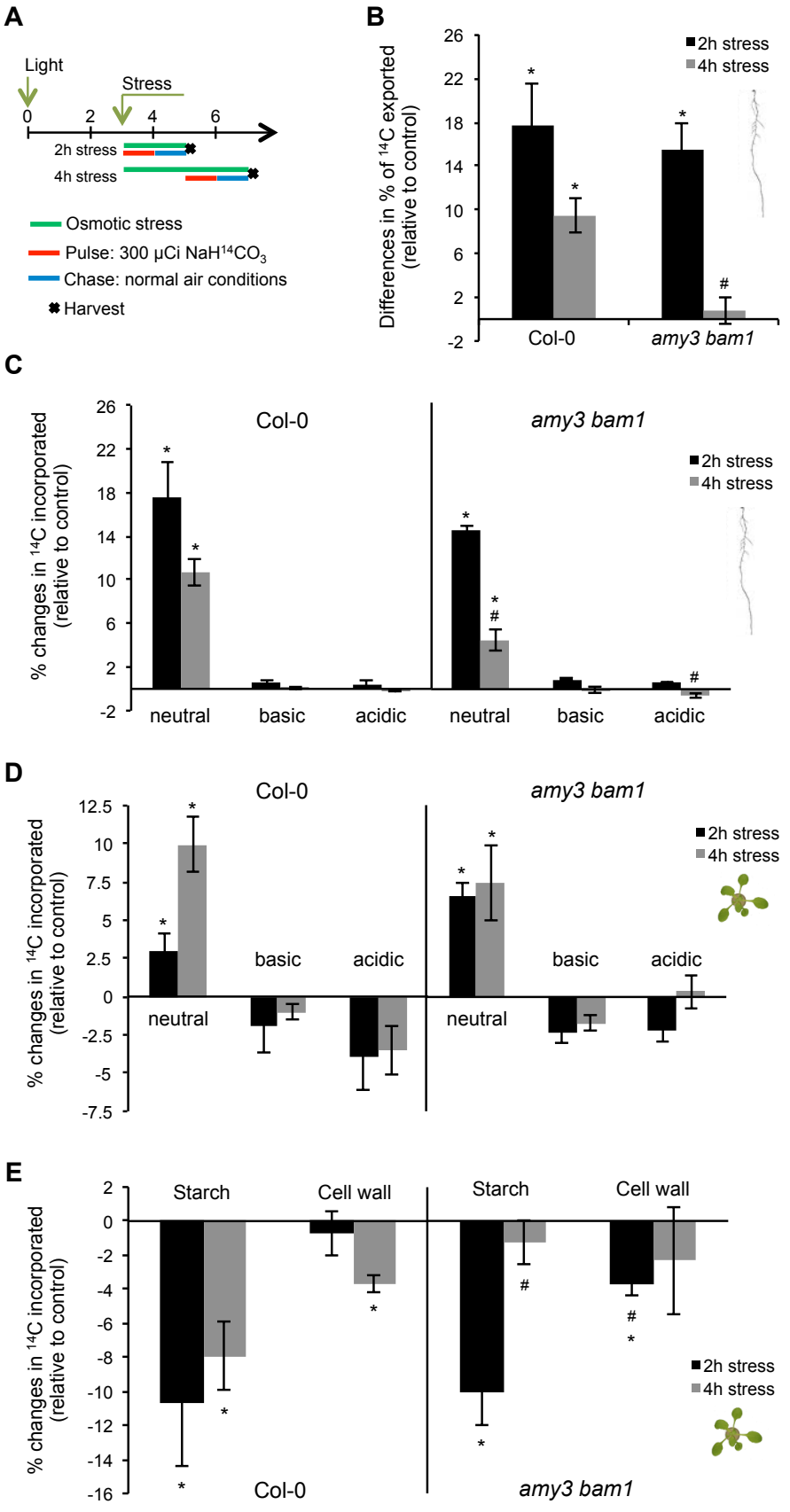
A
Light
Stress
0
2
4
6
2h stress
4h stress
Osmotic stress
Pulse: 300 µCi NaH14CO3
Chase: normal air conditions
Harvest
B
Differences in % of 14C exported (relative to control)
2h stress
4h stress
Col-0
amy3 bam1
C
% changes in 14C incorporated (relative to control)
Col-0
amy3 bam1
neutral
basic
acidic
D
% changes in 14C incorporated (relative to control)
Col-0
amy3 bam1
neutral
basic
acidic
E
% changes in 14C incorporated (relative to control)
Starch
Cell wall
Col-0
amy3 bam1

Figure 4

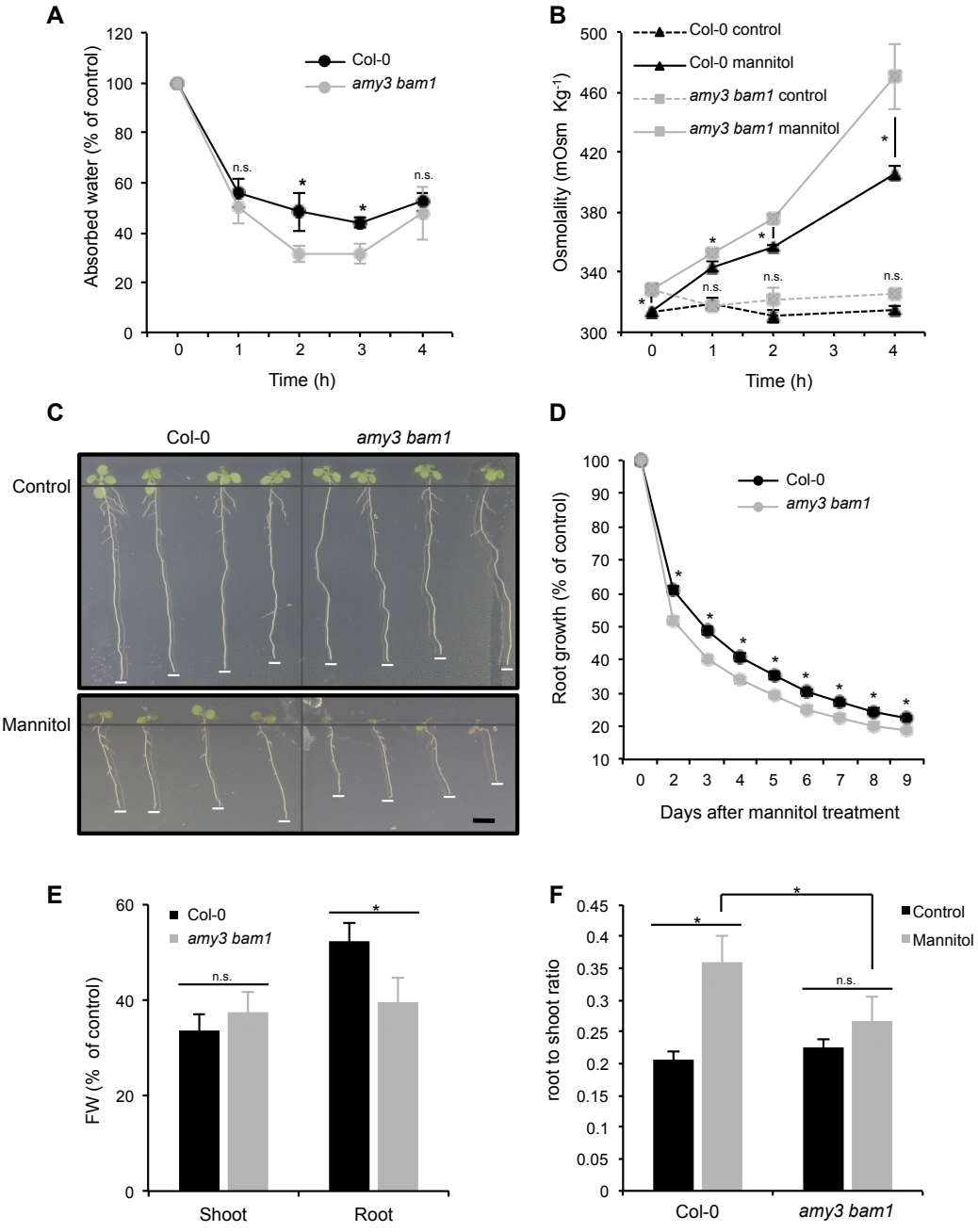
A
Absorbed water (% of control)
Col-0
amy3 bam1
n.s.
Time (h)
B
Osmolality (mOsm Kg-1)
Col-0 control
Col-0 mannitol
amy3 bam1 control
amy3 bam1 mannitol
Time (h)
C
Col-0
amy3 bam1
Control
Mannitol
D
Root growth (% of control)
Days after mannitol treatment
E
FW (% of control)
Shoot
Root
F
root to shoot ratio
Control
Mannitol

Figure 5

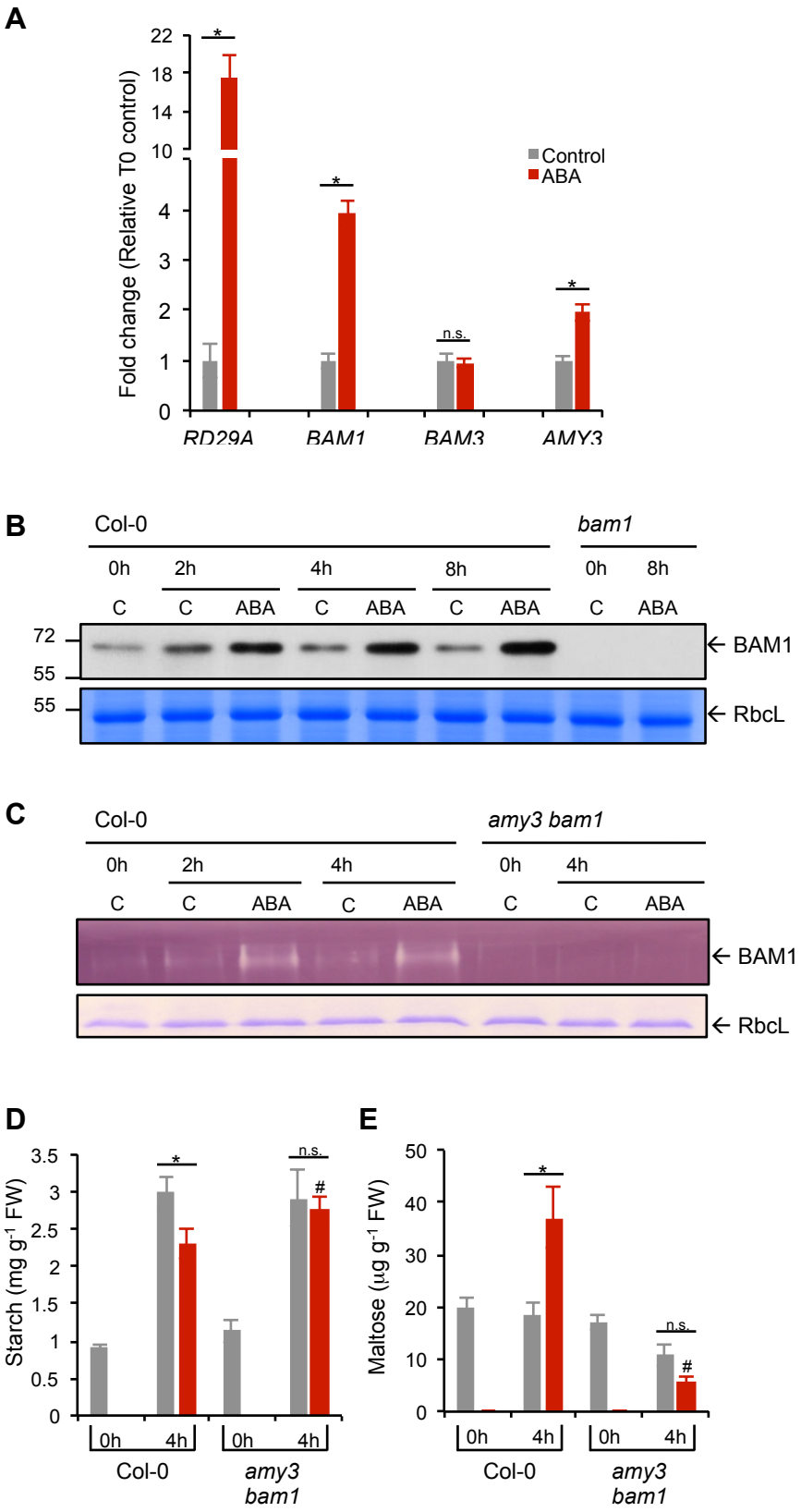
A
Fold change (Relative T0 control)
Control
ABA
RD29A
BAM1
BAM3
AMY3
n.s.
B
Col-0
bam1
0h
2h
4h
8h
C
ABA
72
55
BAM1
RbcL
C
Col-0
amy3 bam1
D
Starch (mg g-1 FW)
E
Maltose (µg g-1 FW)
Col-0
amy3 bam1

Figure 6

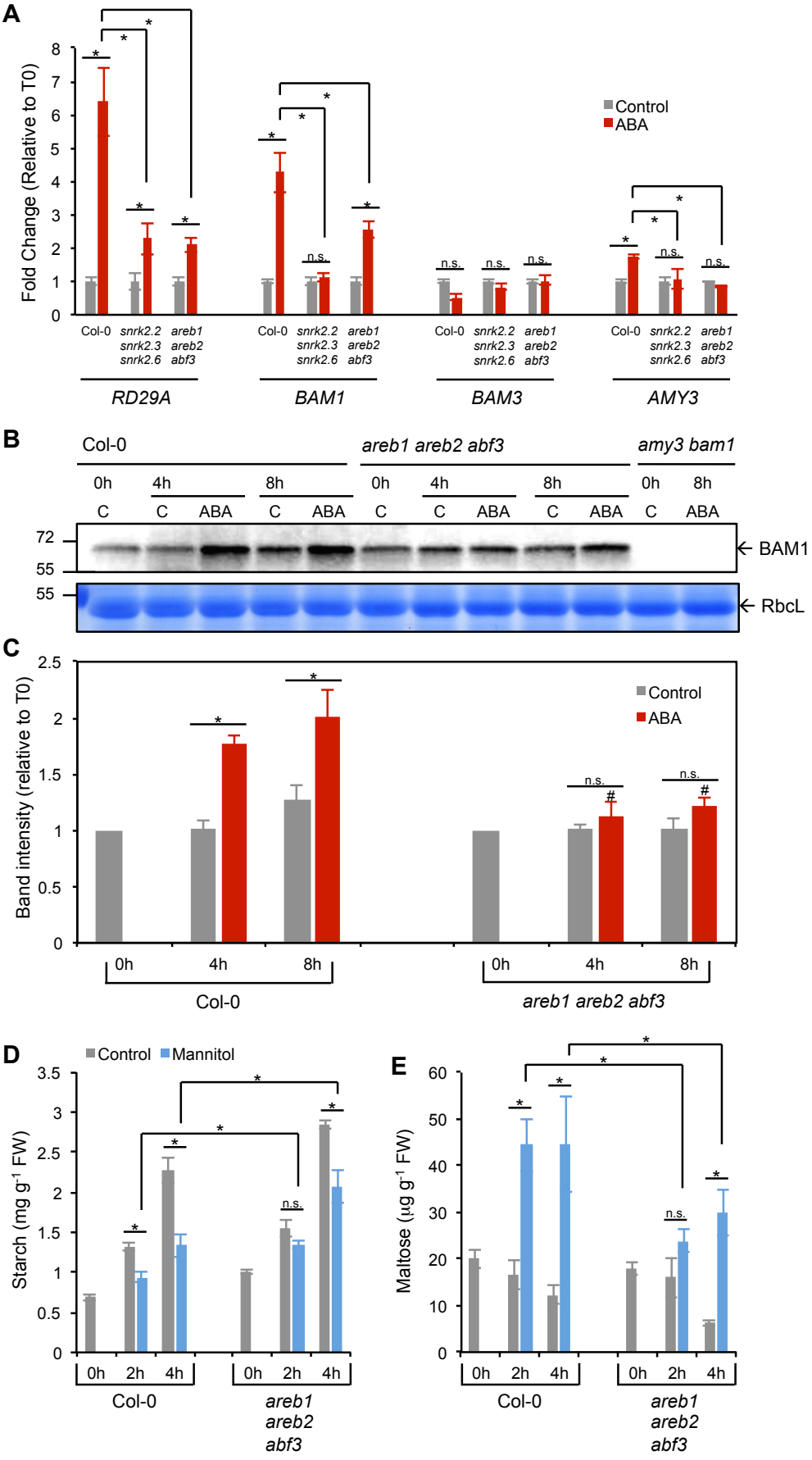
A
Fold Change (Relative to T0)
Control
ABA
Col-0
snrk2.2 snrk2.3 snrk2.6
areb1 areb2 abf3
RD29A
BAM1
BAM3
AMY3
B
Col-0
areb1 areb2 abf3
amy3 bam1
0h
4h
8h
C
ABA
72
55
BAM1
RbcL
C
Band intensity (relative to T0)
Control
ABA
n.s.
#
D
Control
Mannitol
Starch (mg g-1 FW)
0h
2h
4h
E
Maltose (µg g-1 FW)

Figure 7

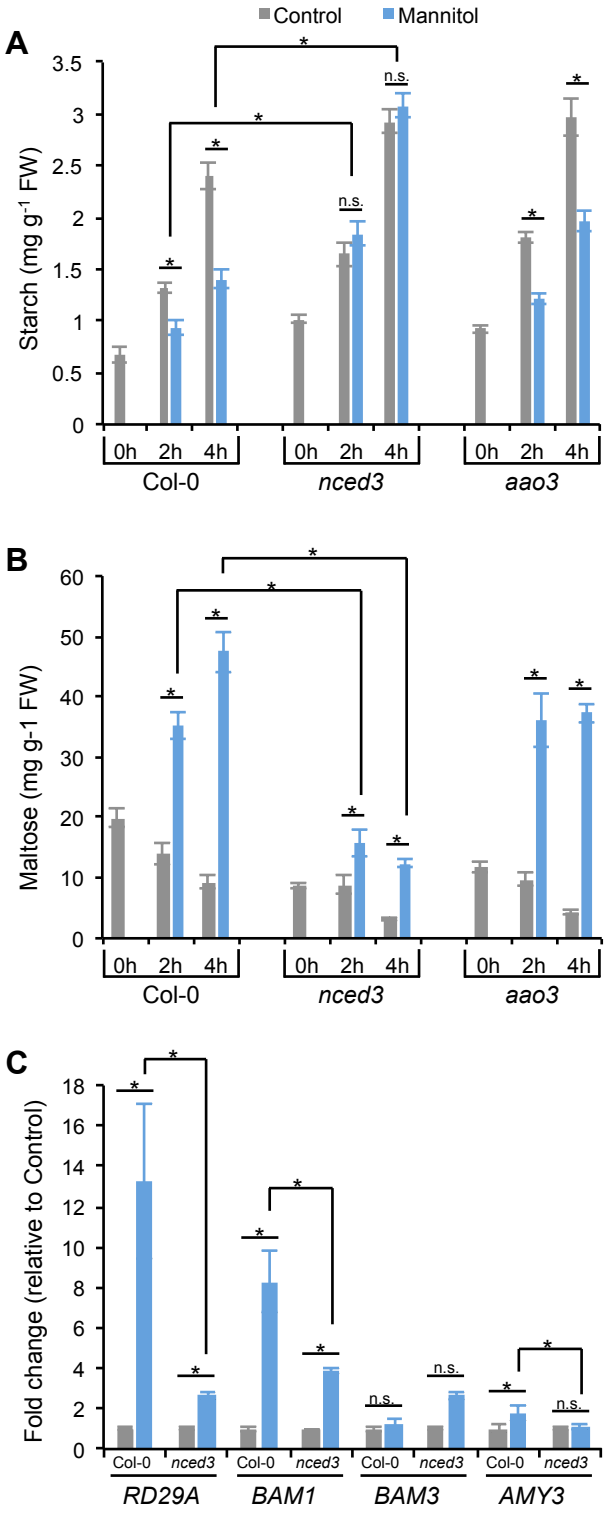
A
Control
Mannitol
Starch (mg g-1 FW)
3.5
3
2.5
2
1.5
1
0.5
0
0h 2h 4h
Col-0
nced3
aao3
n.s.
B
Maltose (mg g-1 FW)
60
50
40
30
20
10
0
C
Fold change (relative to Control)
18
16
14
12
10
8
6
4
2
0
Col-0
nced3
RD29A
BAM1
BAM3
AMY3

Figure 8

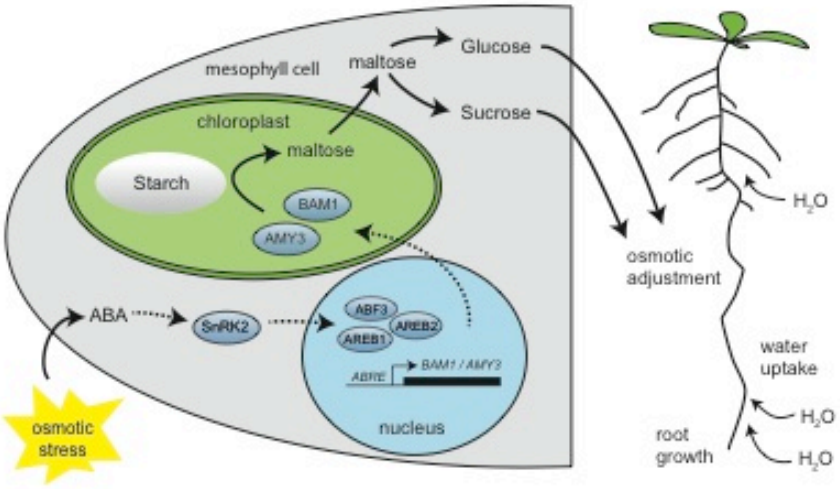
mesophyll cell
maltose
Glucose
Sucrose
chloroplast
maltose
Starch
BAM1
AMY3
ABA
SnRK2
ABF3
AREB2
AREB1
ABRE
BAM1 / AMY3
nucleus
osmotic stress
osmotic adjustment
water uptake
root growth
H2O
H2O
H2O

S1 Data

related to Figure 4A

Water absorption ability of Col-0 and *amy3 bam1* in response to high osmotic stress

	Col-0		*amy3 bam1*	
	Control	**Mannitol**	**Control**	**Mannitol**
	mg H_2O loss mg^{-1} FW · h^{-1}		mg H_2O loss mg^{-1} FW · h^{-1}	
1h	0.076±0.007	0.043±0.005	0.067±0.009	0.034±0.005
2h	0.080±0.005	0.038±0.006	0.078±0.01	0.024±0.003
3h	0.060±0.003	0.024±0.001	0.066±0.006	0.020±0.003
4h	0.071±0.007	0.037±0.003	0.063±0.004	0.029±0.007

related to Figure 4D

Quantification of primary root inhibition in Col-0 and *amy3 bam1* in response to high osmotic stress

	Col-0		*amy3 bam1*	
	Control	**Mannitol**	**Control**	**Mannitol**
	(cm of primary root)		(cm of primary root)	
Day 0	0.98±0.025	0.91±0.023	0.92±0.025	0.76±0.029
Day 2	1.82±0.029	1.11±0.02	1.78±0.033	0.92±0.030
Day 3	2.41±0.036	1.17±0.029	2.40±0.038	0.97±0.030
Day 4	2.97±0.046	1.21±0.035	2.96±0.042	1.00±0.032
Day 5	3.54±0.050	1.250±040	3.56±0.044	1.05±0.037
Day 6	4.17±0.059	1.260±045	4.24±0.051	1.06±0.038
Day 7	4.69±0.065	1.27±0.048	4.81±0.055	1.08±0.041
Day 8	5.27±0.076	1.29±0.052	5.45±0.064	1.10±0.046
Day 9	5.83±0.085	1.30±0.052	6.12±0.067	1.13±0.046

related to Figure 4E

Quantification of root and shoot vegetative growth in Col-0 and *amy3 bam1* in response to high osmotic stress

	Col-0		*amy3 bam1*	
	Control	**Mannitol**	**Control**	**Mannitol**
	(mg)		(mg)	
Shoot	5.67±0.25	1.92±0.18	4.49±0.26	1.69±0.19
Root	1.18±0.10	0.62±0.04	1.03±0.26	0.40±0.05

S1 Fig.

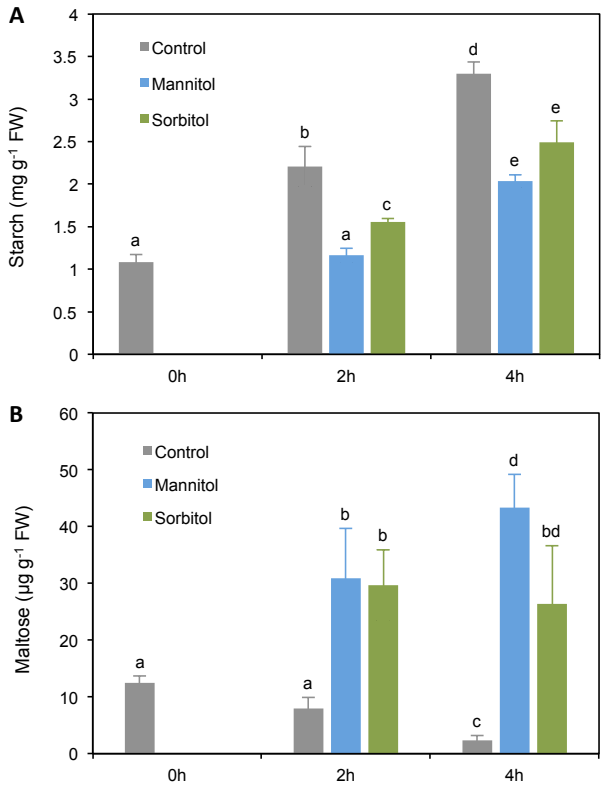
A
Starch (mg g-1 FW)
Control
Mannitol
Sorbitol
0h
2h
4h
B
Maltose (µg g-1 FW)
Control
Mannitol
Sorbitol
0h
2h
4h

S2 Fig.

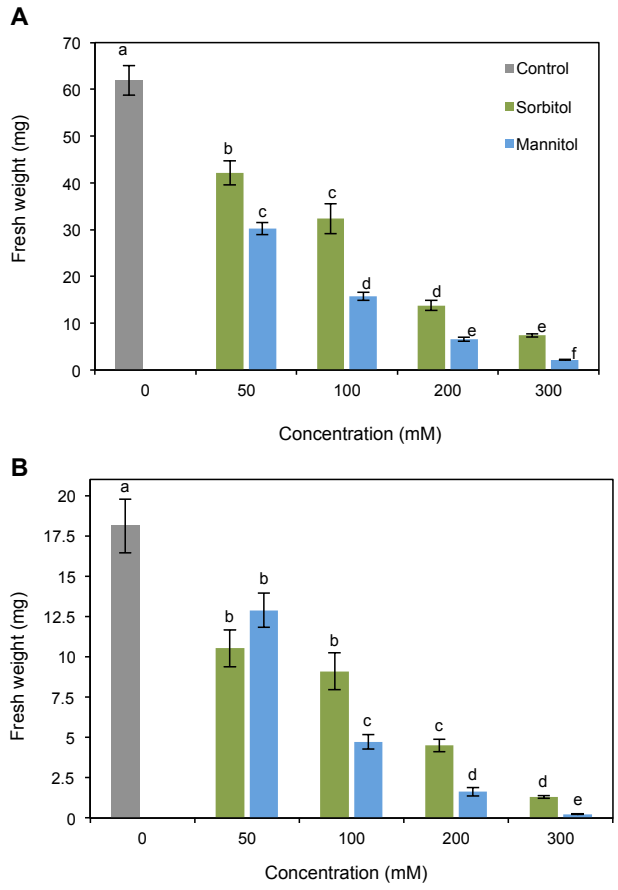
A
Fresh weight (mg)
Control
Sorbitol
Mannitol
Concentration (mM)
B
Fresh weight (mg)
Concentration (mM)

S3 Fig.

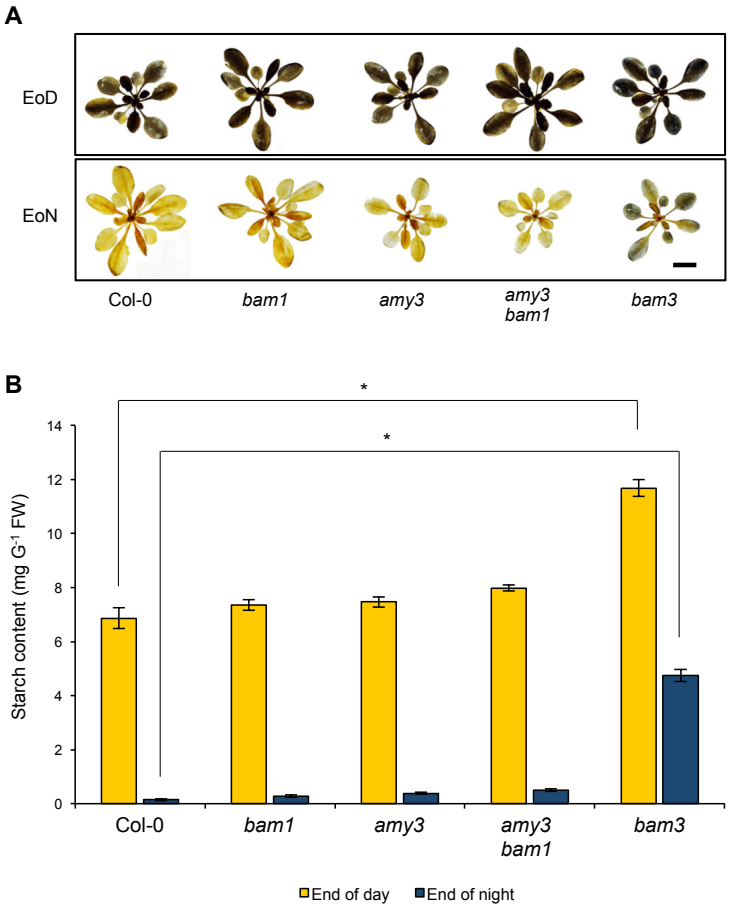
A
EoD
EoN
Col-0
bam1
amy3
amy3 bam1
bam3
B
Starch content (mg G-1 FW)
14
12
10
8
6
4
2
0
*
*
Col-0
bam1
amy3
amy3 bam1
bam3
End of day
End of night

S4 Fig.

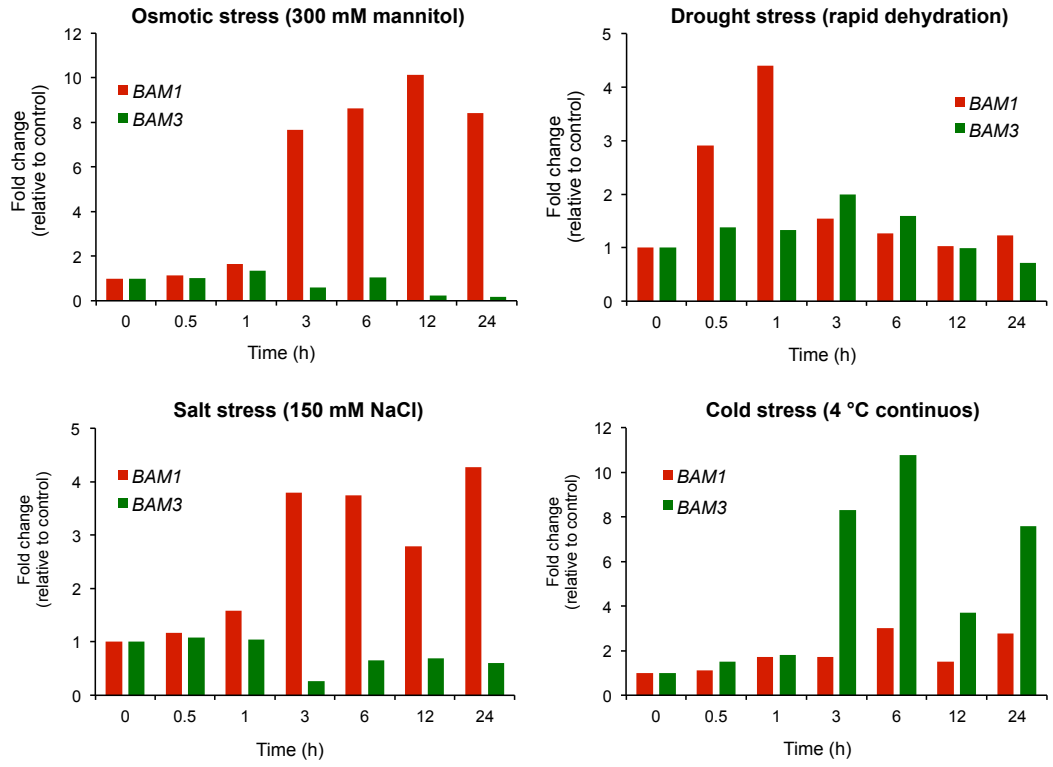
Osmotic stress (300 mM mannitol)
Drought stress (rapid dehydration)
Salt stress (150 mM NaCl)
Cold stress (4 °C continuos)
Fold change (relative to control)
BAM1
BAM3
0
0.5
1
3
6
12
24
Time (h)

S5 Fig.

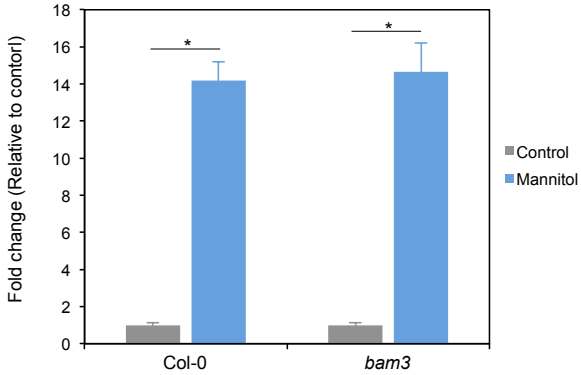

S6 Fig.

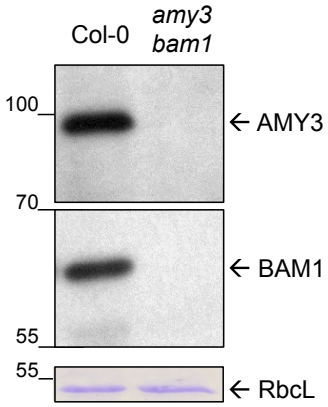

S7 Fig.

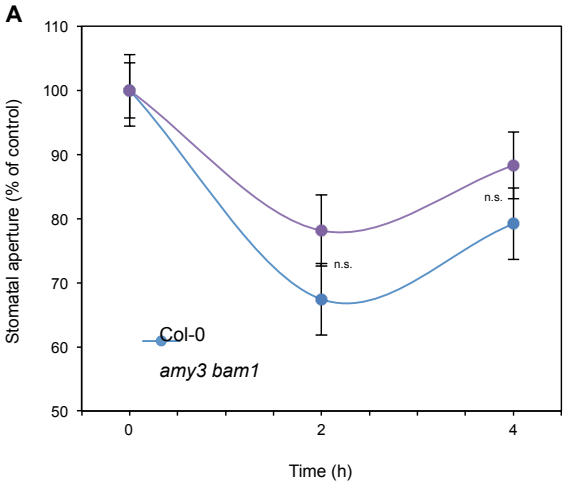

B

		Stomatal aperture (μm)
Col-0	0h	2.01±0.07
	2h	1.52±0.06
	4h	1.78±0.09
amy3 bam1	0h	1.64±0.05
	2h	1.28±0.07
	4h	1.41±0.06

S8 Fig.

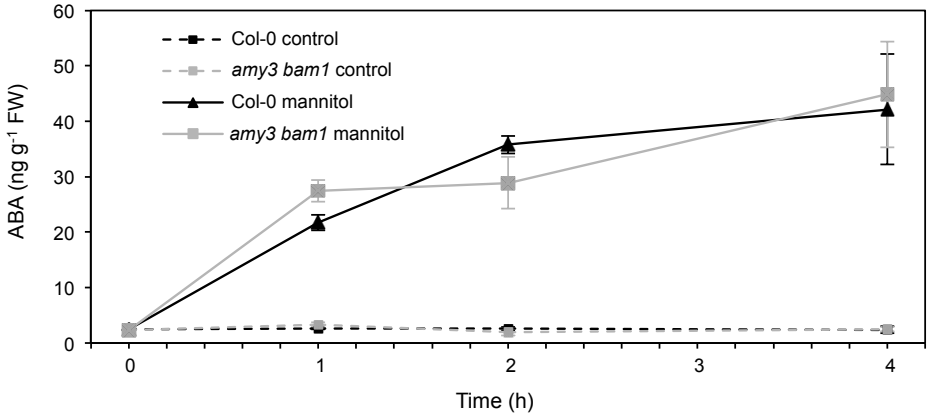

S9 Fig.

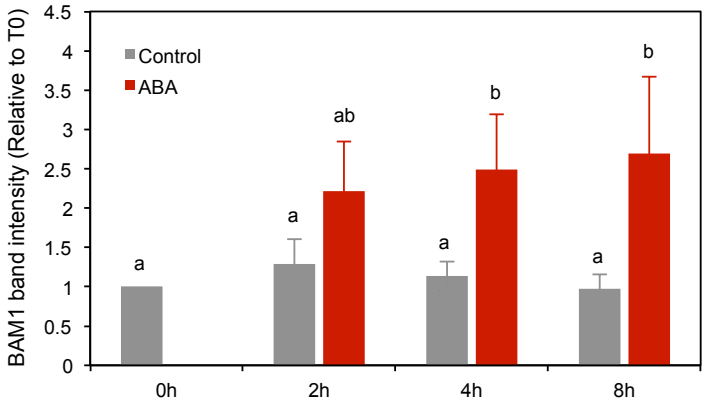

S10 Fig.

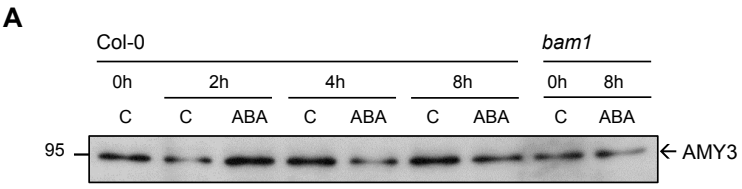

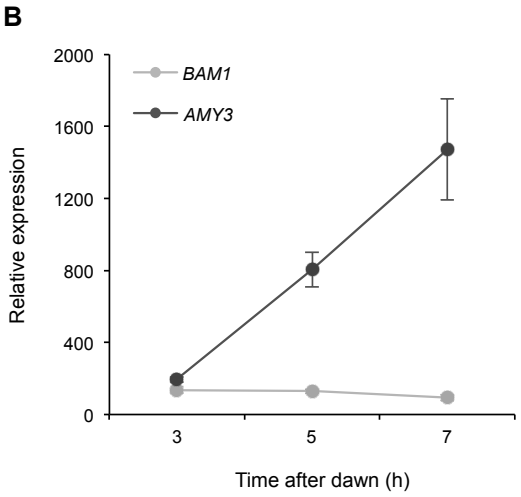

S11 Fig.

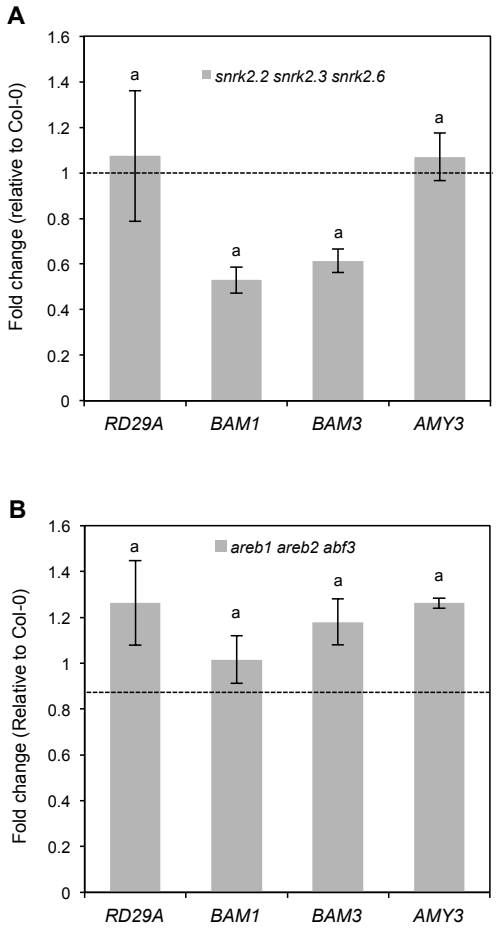
A
snrk2.2 snrk2.3 snrk2.6
Fold change (relative to Col-0)
1.6
1.4
1.2
1
0.8
0.6
0.4
0.2
0
a
a
a
a
RD29A
BAM1
BAM3
AMY3
B
areb1 areb2 abf3
Fold change (Relative to Col-0)
1.6
1.4
1.2
1
0.8
0.6
0.4
0.2
0
a
a
a
a
RD29A
BAM1
BAM3
AMY3

S12 Fig.

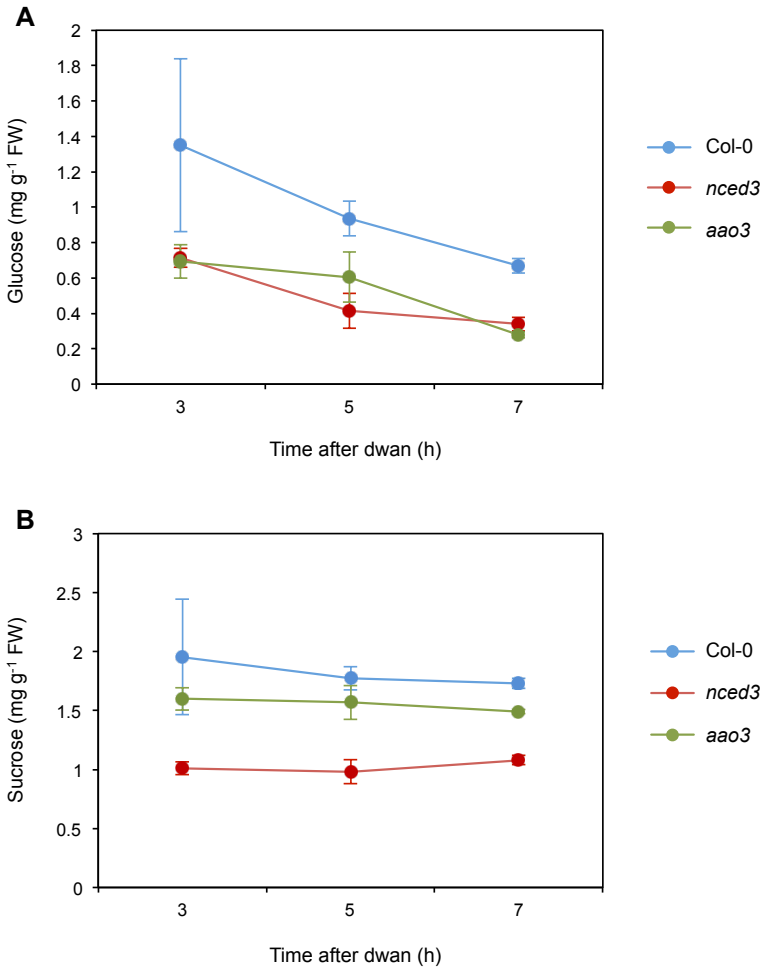

S13 Fig.

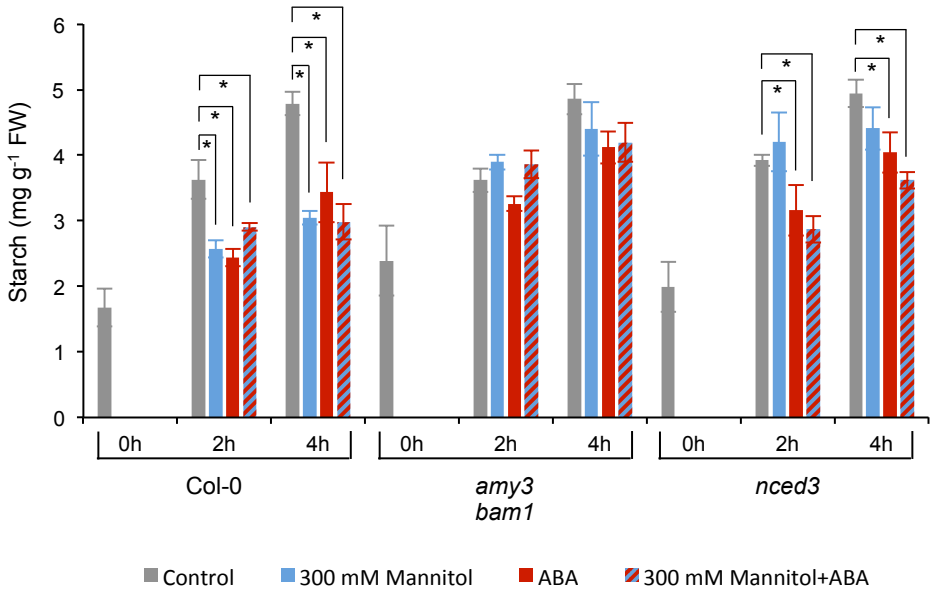

S14 Fig.

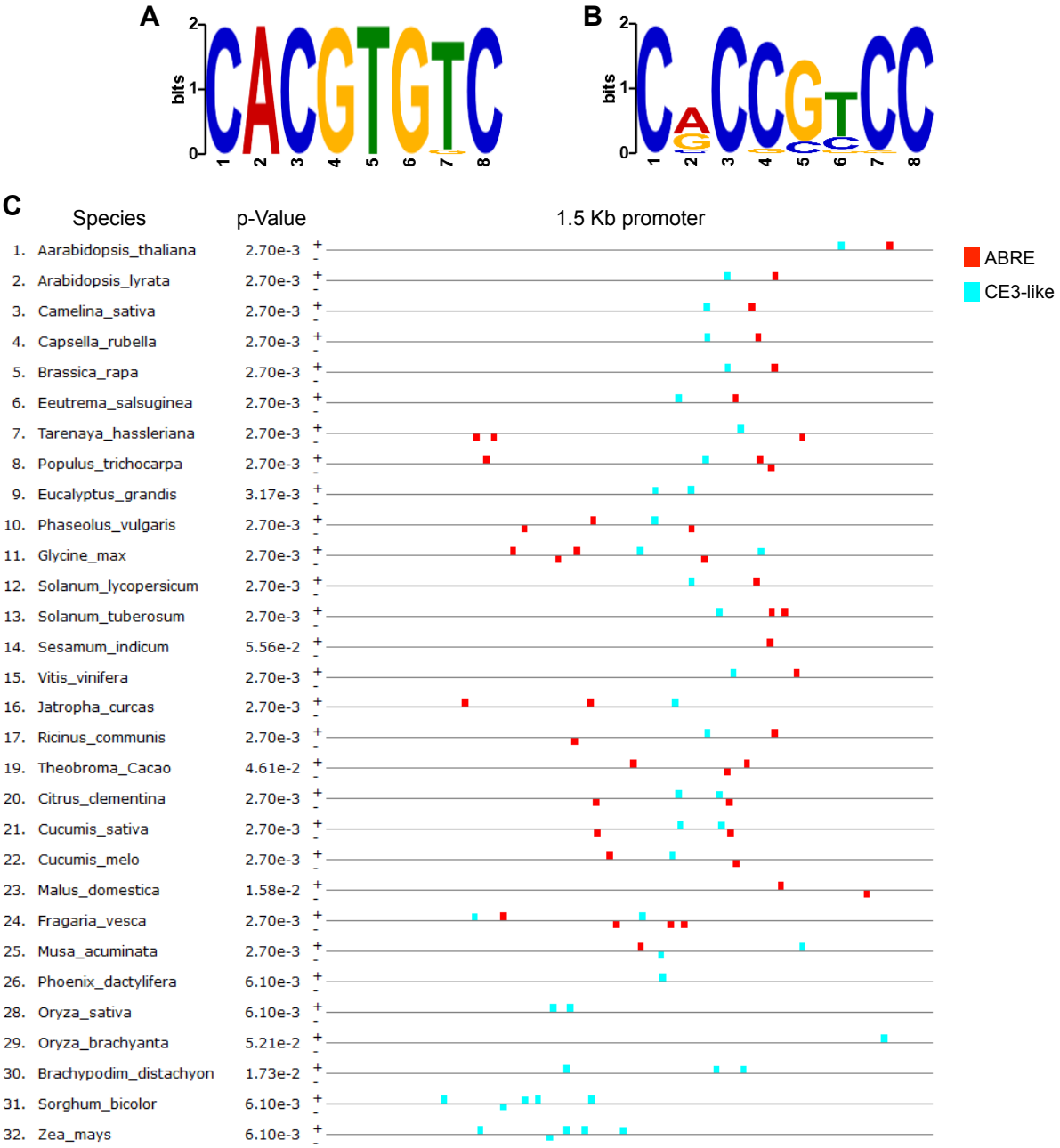
A
B
bits
C
Species
p-Value
1.5 Kb promoter
ABRE
CE3-like
1. Aarabidopsis_thaliana 2.70e-3
2. Arabidopsis_lyrata 2.70e-3
3. Camelina_sativa 2.70e-3
4. Capsella_rubella 2.70e-3
5. Brassica_rapa 2.70e-3
6. Eeutrema_salsuginea 2.70e-3
7. Tarenaya_hassleriana 2.70e-3
8. Populus_trichocarpa 2.70e-3
9. Eucalyptus_grandis 3.17e-3
10. Phaseolus_vulgaris 2.70e-3
11. Glycine_max 2.70e-3
12. Solanum_lycopersicum 2.70e-3
13. Solanum_tuberosum 2.70e-3
14. Sesamum_indicum 5.56e-2
15. Vitis_vinifera 2.70e-3
16. Jatropha_curcas 2.70e-3
17. Ricinus_communis 2.70e-3
19. Theobroma_Cacao 4.61e-2
20. Citrus_clementina 2.70e-3
21. Cucumis_sativa 2.70e-3
22. Cucumis_melo 2.70e-3
23. Malus_domestica 1.58e-2
24. Fragaria_vesca 2.70e-3
25. Musa_acuminata 2.70e-3
26. Phoenix_dactylifera 6.10e-3
28. Oryza_sativa 6.10e-3
29. Oryza_brachyanta 5.21e-2
30. Brachypodim_distachyon 1.73e-2
31. Sorghum_bicolor 6.10e-3
32. Zea_mays 6.10e-3

S1 Table

		Glucose [mg g^{-1} FW]		Fructose [mg g^{-1} FW]		Sucrose [mg g^{-1} FW]	
		Control	Mannitol	Control	Mannitol	Control	Mannitol
Col-0	0 h	0.84±0.08		0.41±0.04		1.65±0.06	
	2 h	0.63±0.08	0.73±0.09	0.18±0.02	0.38±0.05	1.32±0.10	2.39±0.21
	4 h	0.31±0.06	0.69±0.11	0.10±0.03	0.24±0.04	0.97±0.12	2.24±0.44
bam1	0 h	0.74±0.07		0.34±0.04		1.39±0.12	
	2 h	0.47±0.04	0.73±0.05	0.14±0.02	0.42±0.02	1.06±0.04	3.04±0.16
	4 h	0.22±0.05	0.61±0.14	0.06±0.01	0.23±0.06	0.74±0.10	2.16±0.48
amy3	0 h	0.71±0.08		0.35±0.04		1.47±0.09	
	2 h	0.50±0.10	0.54±0.07	0.13±0.03	0.31±0.04	1.15±0.19	2.21±0.18
	4 h	0.21±0.04	0.52±0.10	0.08±0.01	0.26±0.06	0.79±0.10	2.17±0.50

S2 Table

		Glucose [mg g^{-1} FW]		Fructose [mg g^{-1} FW]		Sucrose [mg g^{-1} FW]	
		Control	Mannitol	Control	Mannitol	Control	Mannitol
Col-0	0 h	0.52±0.27		0.16±0.08		1.12±0.27	
	2 h	0.48±0.19	1.38±0.54	0.12±0.03	0.53±0.21	0.98±0.29	5.24±0.44
	4 h	0.43±0.17	1.06±0.12	0.09±0.03	0.39±0.08	0.94±0.30	4.40±0.49
bam1	0 h	0.51±0.29		0.15±0.05		1.19±0.31	
	2 h	0.62±0.22	0.89±0.59	0.14±0.02	0.34±0.16	1.56±0.85	4.94±0.89
	4 h	0.35±0.10	0.92±0.29	0.09±0.01	0.34±0.07	1.07±0.24	3.66±0.30
amy3	0 h	0.59±0.38		0.16±0.05		1.47±0.42	
	2 h	0.63±0.29	1.18±0.42	0.14±0.05	0.46±0.14	2.05±1.55	5.89±0.55
	4 h	0.27±0.12	0.95±0.34	0.07±0.03	0.32±0.12	1.62±1.13	4.88±1.10

S3 Table

	% of ^{14}C recovered in each fraction related to the total amount per tissue (2 h stress)							
	Col-0		***bam1***		***amy3***		***amy3 bam1***	
	Control	**Mannitol**	**Control**	**Mannitol**	**Control**	**Mannitol**	**Control**	**Mannitol**
Root	8.21±0.65	25.88±3.86	7.40±0.71	21.07±2.29	7.93±0.82	24.27±0.87	7.76±0.63	23.20±0.28
Water soluble	5.00±0.40	23.62±3.71	4.61±0.29	18.92±2.03	5.04±0.57	21.42±0.90	4.25±0.31	20.48±0.30
Acidic	0.33±0.02	0.71±0.33	0.94±0.06	1.36±0.14	1.04±0.15	1.54±0.07	0.89±0.06	1.51±0.04
Basic	1.68±0.13	2.30±0.22	1.39±0.11	1.94±0.20	1.47±0.21	2.12±0.08	1.37±0.11	2.24±0.08
Neutral	2.96±0.28	20.50±3.28	2.17±0.14	15.58±1.75	2.47±0.24	17.62±0.78	1.96±0.16	16.64±0.29
Nucleotide	0.035±0.002	0.097±0.032	0.110±0.009	0.031±0.003	0.058±0.015	0.139±0.004	0.027±0.002	0.083±0.03
Water insoluble	3.21±0.33	2.26±0.34	2.79±0.22	2.16±0.30	2.90±0.30	2.84±0.56	3.51±0.32	2.73±0.26
Starch	-0.11±0.11	0.02±0.04	-0.05±0.04	0.02±0.01	0.02±0.03	0.02±0.03	-0.06±0.04	0.04±0.07
Protein	0.870.12	0.410.19	1.52±0.39	0.32±0.08	1.11±0.19	0.57±0.15	1.06±0.34	1.01±0.47
Remaining	2.45±0.37	1.83±0.39	1.32±0.45	1.81±0.31	1.77±0.36	2.26±0.58	2.51±0.47	1.67±0.54
Shoot	91.79±3.69	74.12±4.13	92.60±2.75	78.93±3.44	92.07±5.51	75.73±1.53	92.24±1.65	76.80±1.28
Ethanol soluble	10.57±0.75	8.83±0.73	10.47±0.15	9.49±0.34	11.00±1.21	8.23±0.23	10.34±0.37	8.31±0.06
Water soluble	29.80±3.08	26.74±2.61	25.28±1.99	27.47±2.20	35.97±2.76	34.03±0.71	29.71±1.04	31.62±0.82
Acidic	8.43±0.77	6.47±1.58	6.94±0.34	5.94±0.43	9.15±0.94	6.69±0.35	8.41±0.39	6.01±0.45
Basic	13.72±1.62	9.72±1.35	11.53±0.81	10.44±1.09	17.05±1.44	12.05±0.47	13.19±0.40	10.96±0.57
Neutral	6.78±0.69	9.76±0.92	6.10±0.36	10.25±0.97	8.66±0.48	14.38±1.00	7.19±0.45	13.82±0.71
Nucleotide	0.87±0.08	0.79±0.11	0.71±0.03	0.83±0.09	1.11±0.05	0.91±0.04	0.92±0.06	0.82±0.03
Water insoluble	51.42±1.89	38.55±3.12	56.85±1.89	41.97±2.62	45.09±4.61	33.47±1.34	52.19±1.23	36.87±0.98
Starch	32.41±1.00	21.70±3.54	40.81±3.24	25.63±2.39	27.05±1.54	18.01±1.02	31.99±1.69	22.01±1.01
Protein	7.15±0.28	5.74±0.51	7.84±0.18	6.67±0.18	8.48±0.68	5.55±0.50	8.09±0.26	6.40±0.13
Remaining	11.86±1.11	11.10±0.67	8.19±2.27	9.67±1.04	14.56±3.52	9.91±0.95	12.11±0.62	8.46±0.38

S4 Table

	% of ^{14}C recovered in each fraction related to the total amount per tissue (4 h stress)							
	Col-0		***bam1***		***amy3***		***amy3 bam1***	
	Control	**Mannitol**	**Control**	**Mannitol**	**Control**	**Mannitol**	**Control**	**Mannitol**
Root	7.01±0.25	16.52±1.56	7.01±0.40	17.21±1.21	6.26±1.18	15.39±2.24	8.65±1.88	9.44±1.37
Water soluble	4.31±0.23	14.86±1.41	4.25±0.22	15.41±1.13	3.82±0.75	13.48±1.93	4.21±0.67	8.09±1.25
Acidic	1.21±0.05	1.00±0.10	1.24±0.02	1.19±0.06	1.21±0.23	1.15±0.16	1.43±0.21	0.88±0.15
Basic	0.94±0.12	1.01±0.14	0.99±0.06	1.31±0.06	0.92±0.15	1.14±0.15	1.10±0.20	1.03±0.19
Neutral	2.13±0.14	12.83±1.24	2.01±0.15	12.90±1.09	1.67±0.36	11.18±1.62	1.65±0.26	6.17±0.94
Nucleotide	0.015±0.002	0.014±0.001	0.014±0.001	0.014±0.002	0.015±0.004	0.017±0.003	0.027±0.006	0.013±0.002
Water insoluble	2.71±0.09	1.66±0.17	2.76±0.18	1.79±0.09	2.44±0.43	1.91±0.33	3.58±0.47	1.34±0.17
Starch	0.06±0.06	0.09±0.04	0.03±0.08	0.05±0.02	-0.02±0.06	0.03±0.02	0.00±0.01	0.03±0.02
Protein	0.60±0.05	0.30±0.07	0.90±0.16	0.28±0.04	0.81±0.23	0.21±0.02	0.61±0.09	0.36±0.05
Remaining	2.05±0.12	1.27±0.18	1.84±0.26	1.47±0.10	1.65±0.49	1.67±0.33	2.96±0.48	0.95±0.18
Shoot	92.99±2.80	83.48±2.01	92.99±1.31	82.79±2.36	93.74±4.53	84.61±2.88	91.35±2.65	90.56±2.86
Ethanol soluble	8.29±0.30	6.77±0.03	8.90±0.49	6.76±0.23	9.20±0.23	6.83±0.34	8.11±0.68	6.57±0.29
Water soluble	29.27±2.15	34.36±1.72	23.85±0.85	28.57±2.05	22.35±3.28	34.16±1.25	32.34±1.06	38.11±1.93
Acidic	14.85±1.46	11.33±0.63	12.12±0.39	9.39±1.13	10.96±1.53	13.01±0.27	14.74±0.50	15.07±0.96
Basic	6.29±0.45	5.24±0.24	5.82±0.48	5.27±0.47	5.50±0.85	6.39±0.15	8.54±0.45	6.86±0.31
Neutral	7.18±0.45	17.10±1.75	5.17±0.24	13.35±0.55	5.18±0.82	14.05±1.08	8.02±1.19	15.42±2.15
Nucleotide	0.95±0.06	0.69±0.03	0.74±0.08	0.55±0.06	0.70±0.13	0.72±0.05	1.04±0.02	0.76±0.04
Water insoluble	55.42±1.76	42.35±1.03	60.24±0.86	47.47±1.15	62.19±3.11	43.61±2.57	50.91±2.33	45.89±2.09
Starch	38.83±1.75	30.90±0.96	43.69±1.41	33.65±1.28	44.58±2.94	30.75±1.97	36.17±1.82	34.93±1.84
Protein	7.36±0.12	5.91±0.11	8.13±0.35	5.77±0.16	8.06±0.35	5.51±0.15	6.78±0.65	5.32±0.14
Remaining	9.24±0.41	5.54±0.25	8.42±1.21	8.05±1.73	9.54±0.41	7.35±2.06	7.96±1.47	5.64±2.77

S5 Table

		F_v/F_m		ΦPSII	
		Control	Mannitol	Control	Mannitol
Col-0	0 h	0.817±0.003		0.658±0.003	
	2 h	0.815±0.002	0.767±0.011*	0.647±0.002	0.602±0.010*
	4 h	0.817±0.002	0.802±0.002	0.648±0.002	0.635±0.004
	24 h	0.807±0.003	0.811±0.003	0.640±0.001	0.649±0.004
amy3 bam1	0 h	0.818±0.003		0.655±0.003	
	2 h	0.811±0.003	0.767±0.010*	0.644±0.003	0.602±0.011*
	4 h	0.813±0.003	0.802±0.004	0.648±0.005	0.637±0.005
	24 h	0.810±0.006	0.813±0.002	0.635±0.005	0.651±0.002

S6 Table

		Chl a [mg g^{-1} FW]		Chl b [mg g^{-1} FW]		Total Chl [mg g^{-1} FW]		Chla/Chl b ratio	
		Control	Mannitol	Control	Mannitol	Control	Mannitol	Control	Mannitol
Col-0	0 h	1.09±0.15		0.47±0.06		1.56±0.21		2.35±0.26	
	2 h	1.11±0.16	1.28±0.20	0.48±0.07	0.56±0.09	1.59±0.24	1.84±0.29	2.29±0.28	2.29±0.33
	4 h	1.11±0.16	1.32±0.22	0.49±0.07	0.58±0.10	1.60±0.24	1.91±0.33	2.27±0.28	2.26±0.35
bam1	0 h	1.10±0.13		0.48±0.06		1.59±0.19		2.30±0.26	
	2 h	1.18±0.17	1.37±0.20	0.52±0.08	0.60±0.09	1.69±0.24	1.97±0.29	2.28±0.28	2.28±0.31
	4 h	1.13±0.14	1.37±0.21	0.50±0.06	0.61±0.11	1.63±0.20	1.98±0.30	2.28±0.24	2.24±0.32
amy3	0 h	1.08±0.17		0.47±0.07		1.55±0.24		2.31±0.30	
	2 h	1.13±0.17	1.40±0.24	0.49±0.08	0.62±0.11	1.62±0.25	2.02±0.35	2.29±0.30	2.26±0.37
	4 h	1.21±0.17	1.29±0.20	0.53±0.07	0.58±0.10	1.74±0.24	1.87±0.30	2.28±0.28	2.23±0.33
amy3 bam1	0 h	1.12±0.10		0.48±0.05		1.60±0.15		2.32±0.18	
	2 h	1.16±0.18	1.32±0.15	0.51±0.08	0.58±0.06	1.66±0.26	1.91±0.21	2.28±0.30	2.26±0.23
	4 h	1.18±0.16	1.32±0.20	0.53±0.08	0.59±0.09	1.71±0.24	1.92±0.29	2.23±0.27	2.23±0.31

S7 Table

Primer	Sequence
Primers used for genotyping T-DNA insertion lines	
***bam1* (Salk_039895)**	
BAM1 Salk_fw	CCATTGTGGAAATCCAAGTG
BAM1 Salk_rev	ACGAGTACTTATCATAGCACTG
Salk LBb1.3	ATTTTGCCGATTTCGGAAC
***amy3* (Sail_613 D12)**	
AMY3 Sail_fw	GGTTCCTCTTGTAGACGATGTTCC
AMY3 Sail_rev	CCGACCTTGTGAAATTTCTTCACTG
Sail LBb	GCCTTTTCAGAAATGGATAAATAGCCTTGCTTCC
***nced3* (GABI_129B08)**	
NCED3 GABI_fw	GTCAGCCACGAGAAGCTACAC
NCED3 GABI_rev	ACAGAGGCTCTCCTCCGTAAC
GABI LBb	ATATTGACCATCATACTCATTGC
Primers used for qPCR	
***BAM1* (AT3G23920)**	
BAM1 RT_fw	CCATTGTGGAAATCCAAGTG
BAM1 RT_rev	ACGAGTACTTATCATAGCACTG
***AMY3* (AT1G69830)**	
AMY3 RT_fw	TGCTTACATCCTAACTCATCC
AMY3 RT_rev	CTCTTGTCTATATTCACCTCACTC
***BAM3* (AT4G17090)**	
BAM3 RT_fw	TGATTCTGTGCCTGTCCT
BAM3 RT_rev	GAATTTCCGCAATAACTCCTC
***RD29A* (AT5G52310)**	
RD29A RT_fw	CCCACCAAAGAAGAAACTGGA
RD29A RT_rev	TTCAAATTGTCCTGGCTTCTG
***Actin2* (AT3G18780)**	
Actin RT_fw	TGGAATCCACGAGACAACCTA
Actin RT_rev	TTCTGTGAACGATTCCTGGAC

4 – Evidence for the phosphorylation of BAM1 by the GSK3-like kinase AtK4 and its role in guard cell starch degradation

Daniel Horrer, Julia Krasensky, Diana Pazmino, Claudia Jonak, Diana Santelia

Unpublished results

Synopsis: BAM1 was recently reported to be phosphorylated at several serine residues. Here we show that a GSK3-like kinase is able to phosphorylate BAM1 specifically at Ser^{59}. This modification does not seem to influence the enzymatic activity of recombinant BAM1 protein *in vitro*. In order to elucidate the role of BAM1 phosphorylation we started to establish phosphoproteomic techniques.

Experimental contributions: J.K. performed the *in vitro* phosphorylation assay shown in Figure 4.3 A in the laboratory of C.J. and D.P. performed the qPCR analysis shown in Figure 4.4 A. I want to thank Peter Gehrig from the Functional Genomics Centre Zürich for his help with data analysis.

Introduction

We could recently show that β-amylase1 (BAM1) plays an important role during early morning starch degradation in guard cells (Chapter 1). Furthermore, BAM1 is also important for mesophyll cell starch degradation in response to osmotic stress, where it degrades starch in the light (Chapter 3). In contrast, BAM3 is thought to be the major β-amylase for transitory starch degradation in mesophyll cells during the night (Kaplan and Guy, 2005; Fulton et al., 2008). These observations suggest a functional specialization of the two enzymes. Firstly, *BAM1* is known to be expressed preferentially in guard cells and root cap cells under normal growth conditions (Valerio et al., 2011; Chapter1), while its expression can be induced under osmotic stress in an ABA-dependent manner in mesophyll cells (Valerio et al., 2011) (Chapter 3). In contrast, *BAM3* transcription is reduced in guard cells compared to mesophyll cells (Chapter 1). The basis for the expression pattern of *BAM1* in response to osmotic stress seem to be related to the presence of ABRE elements in its promoter region, while the guard cell specific expression under normal growth conditions might be linked to DOF elements (Chapter 3 and Outlook).

An important difference between BAM1 and BAM3 proteins is based on the redox sensitivity of BAM1. The BAM1 protein forms an intramolecular disulphide bridge between Cys^{73} and Cys^{511}, which inhibits its enzymatic activity (Sparla et al., 2006; Valerio et al., 2011). Under reducing conditions, which are usually assumed to occur in illuminated chloroplasts when electrons are transferred from the photosynthetic electron transport chain to thioredoxins, which in turn reduce cysteine residues in target proteins (Kumar et al., 2004; Lemaire et al., 2007; Montrichard et al., 2009), BAM1 becomes activated through the reduction of its disulphide bridge. This is in accordance with the roles of BAM1 in starch degradation during the light. Interestingly, more enzymes related to both starch synthesis and degradation are known to be redox sensitive or were shown to be redox regulated (Glaring et al., 2012; Kötting et al., 2010; Santelia et al., 2015). Besides redox control of protein activity, which is known to be involved in the regulation of many plastidial processes (Lemaire et al., 2007), posttranslational protein phosphorylation also plays an important role in the regulation of plastidial enzymes and metabolism (Baginsky and Gruissem, 2009). For example, the acclimation of photosynthesis to changing light conditions, a process called state transition, depends on the phosphorylation of photosystem II (PSII) and the light harvesting complex II (LHCII) subunits (Staehelin and Arntzen, 1983). It comes with no surprise that the evidence for a role of protein phosphorylation in the regulation of starch metabolism is increasing (Baginsky and

Gruissem, 2009; Kötting et al., 2005). Several enzymes of the starch biosynthetic pathway in Arabidopsis such as PGI, PGM, APL1, APS1 and SS3 as well as enzymes of the starch degradation pathway such as GWD1, AMY3, BAM1, BAM3 and LDA were found to be phosphorylated in phosphoproteomic studies (Heazlewood et al., 2008; Kötting et al., 2010). The significance of protein phosphorylation in starch metabolism and the kinases responsible for the posttranslational modification of these enzymes are not known.

While the chloroplast genome does not encode any protein kinase, around 1050 of these kinases are predicted to be encoded by the nuclear genome of *Arabidopsis thaliana* (Bayer et al., 2012). Despite this high number, only few were experimentally confirmed to be localized to the plastids (Bayer et al., 2012). Well studied plastidial kinases of Arabidopsis are STN7 and STN8, the kinases responsible for the phosphorylation of PSII and LHCII during state transition (Depège et al., 2003; Bonardi et al., 2005). Amongst others, kinases described in plastids belong to the family of casein kinase II (CKII) (Salinas et al., 2006) which seems to be involved in different cellular processes such as controlling RNA stability through the phosphorylation of RNA binding proteins (Lisitsky and Schuster, 1995).
Interestingly, a member of the GLYCOGEN SYNTHASE KINASE 3 / SHAGGY-like (GSK3) Ser/Thr kinase family of *Medicago sativa*, MsK4, was reported to be associated with the starch granule in alfalfa root cap amyloplasts (Kempa et al., 2007). GSK3/SHAGGY Ser/Thr kinases are found in all eukaryotes and play important roles in a variety of cellular processes. The mammalian GSK3 protein kinase as well as the Drosophila orthologue SHAGGY are involved in the regulation of diverse processes such as glycogen metabolism, organ development and oncogenesis (Siegfried et al., 1992; Oreña et al., 2000; Webster et al., 2000). The overexpression of *MsK4* in Arabidopsis leads to enhanced salt-stress tolerance and to alterations in overall metabolite levels including elevated maltose content (Kempa et al., 2007). GSK3-like kinases are known to phosphorylate target proteins at serine residues forming the consensus sequence (S/T)P-XX-(S/T)P (de la Fuente van Bentem et al., 2008), which can be found in the N-terminal region of the mature BAM1 protein. It is therefore possible that one or several Arabidopsis GSK3 kinases could be involved in the regulation of BAM1-dependent starch breakdown in response to osmotic stress. Richard and colleagues suggested from their study on the GSK3-like family of *Physcomitrella patens* that the responsiveness of this kinase family to desiccation and osmotic stress represents an evolutionarily ancestral

function (Richard et al., 2005), which would fit with our observation regarding the role of BAM1 during osmotic stress (Chapter 3).

In their recent study, Bayer and colleagues could not observe a clear plastidial localization of the closest Arabidopsis homologue of MsK4, the protein kinase AtK1 (Bayer et al., 2012). Arabidopsis contains ten genes encoding for GSKs, with highly conserved kinase domains, but more diverse C- and N-terminal regions, which fall into four distinct classes (Jonak and Hirt, 2002; Charrier et al., 2002). The best studied plant GSK3-like kinase is BRASSINOSTEROID-INSENSITIVE 2 (BIN2), an important negative regulator of Arabidopsis brassinosteroid signalling (Li et al., 2002). The exact subcellular localization of the GSK3 protein family is largely unknown, while the spatial differentiation of gene expression in different organs of Arabidopsis was described (Charrier et al., 2002). Intriguingly, one member of the Arabidopsis GSK3 gene family, *AtK4* (also referred to as *AtSK13*), was reported to be amongst the genes showing the highest preference for expression in guard cells (Bates et al., 2012). Furthermore, *AtK4* expression seems to be induced in the leaves of osmotically stressed plants (Charrier et al., 2002). Therefore, the expression pattern of *AtK4* makes it a prime candidate for the putative phosphorylation of BAM1 in guard cells under normal growth conditions as well as in mesophyll cells under stress conditions.

Material and Methods

Genotypes and plant growth conditions

Mutant plants lacking the GSK3-like kinase AtK4 as well as the two transgenic lines overexpressing *AtK4* under the *35S* promoter (OE1 and OE27) were isolated in the laboratory of Claudia Jonak at the Gregor Mendel Institute, Vienna, Austria. All plants, including wild type of the Columbia-0 (Col-0) ecotype and *bam1* (SALK_039895) mutants were grown on soil in a controlled climate chamber (KKD Hiross, CLITEC Boulaguiem, Root, Switzerland) at 22°C, 60% relative humidity under a 12 h light / 12 h dark photoperiod with 120 µmol m^{-2} s^{-1} illumination from a mixture of white (Osram Biolux) and purple light (Osram Fluora). Experiments were performed with approximately 3.5 week-old, non-flowering plants.

Multiple sequence alignment

Several protein sequences of BAM1-related enzymes of different plant species were extracted from the Uniprot database (uniprot.org). The multiple sequence alignment was created with the Clustal Omega program version 1.2.0 (ebi.ac.uk/tools/msa/clustalo).

Site-directed mutagenesis for the creation of phosphomutant and phosphomimic versions of BAM1

The pET21dsa/BAM1-cTP plasmid for the bacterial expression of 6x His tagged recombinant BAM1 protein without the N-terminal chloroplast targeting peptide (-cTP, lacking the 41 most N-terminal amino acids) was provided by David Seung, ETH Zürich.

This plasmid was used as the template for the site directed mutagenesis reactions to create phosphomutant and phosphomimic versions of BAM1 (Table 4.1) using the QuickChange Site-Directed Mutagenesis Kit (Agilent Technologies, Santa Clara, USA), with the exception of pDH30 and pDH31, for which the constructs pDH23 (S55D) and pDH24 (S59D) served as templates. Half reactions (20 µl total volume) were set up consisting of 25 ng of the template plasmid in 1x reaction buffer supplemented with 1.25 U PfuTurbo DNA Polymerase, 0.55 µl of the oligonucleotides (according to Table 4.1) and 0.5 µl of the provided dNTP stock. A total of 12 PCR cycles using the following parameters were run for each mutagenesis reaction:

30 sec	95°C
1 min	55°C
15 min	68°C

The template DNA was subsequently digested through the addition of 10 U DpnI restriction enzyme and incubation at 37°C for 4 h. 5 µl of the reaction mix were used for a standard heat shock transformation of *E. coli* DH5α cells, which were finally plated on ampicillin containing LB agar plates.

After confirmation by sequencing, constructs were transformed into the BL21codon+ *E. coli* cells by a standard heat shock protocol and glycerol stocks were prepared from single colonies. In addition to the ampicillin resistance introduced by the pET21dsa constructs, these cells contain a helper plasmid with a chloramphenicol selection marker in order to express tRNA genes for codon optimization during expression of eukaryotic genes in *E. coli*.

Table 4.1: Phosphomutant and phosphomimic versions of BAM1 constructed using the indicated oligonucleotide with its reverse complement in the site directed mutagenesis reaction. The depicted oligonucleotides were designed with the PrimerDesignProgram provided by Agilent (http://www.genomics.agilent.com/primerDesignProgram.jsp)**.**

Construct	Mutant	Oligonucleotide
pDH20	S55A	cacggaacagatccagcaccgccgatgagtc
pDH21	S59A	gatccatcaccgccgatggctccaattttaggtgcgac
pDH22	S55A S59A	gatccagcaccgccgatggctccaattttaggtgcgac
pDH23	S55D	ctacaaggctcacggaacagatccagatccgccgatgagtc
pDH24	S59D	gatccatcaccgccgatggatccaattttaggtgcgac
pDH25	S55D S59D	ctacaaggctcacggaacagatccagatccgccgatggatccaattttaggtgcg
pDH30	S55D S59A	gatccagatccgccgatggctccaattttaggtgcgac
pDH31	S55A S59D	cacggaacagatccagcaccgccgatggatc

Purification of recombinant BAM1 proteins from *E. coli*

50 ml of LB medium supplemented with 35 µg/ml chloramphenicol and 100 µg/ml ampicillin were inoculated with BL21codon+ cells containing the constructs listed in Table 4.1. These pre-cultures were grown over night at 37°C with shaking at 200 rpm.

500 ml of pre-warmed LB medium supplemented with 35 µg/ml chloramphenicol and 100 µg/ml ampicillin was inoculated with the pre-culture so that the initial OD_{600}

reached 0.3 - 0.4. After incubation at 30°C, shaking at 200 rpm for approximately 1 h, OD_{600} was between 0.5 and 0.8. Protein expression was induced by the addition of Isopropyl-β-D-thiogalactopyranosid (IPTG, 1 mM final concentration) and cultures were grown over night at 20°C, shaking at 200 rpm.

Cultures were centrifuged 10 min at 4°C, 3000 g and pellets were subsequently resuspended gently in 30 ml basic buffer (50 mM Tris-HCl pH 7.5, 300 mM NaCl, 40 mM imidazole) supplemented with 0.1% (w/v) lysozyme, 1x protease inhibitor (Roche, Basel, Switzerland) and 2 mM dithiothreitol (DTT) ('lysis buffer'). Cell lysis continued for 1 h at 4°C with light rotation. In order to ensure complete lysis of cells, samples were sonicated on ice three times with 2 sec cycles at 60% maximal intensity for 30 sec using an UW 2200 Sonopuls sonicator (Bandelin, Berlin, Germany). This crude extract was centrifuged for 20 min at 4°C, 10000 g, after which the supernatant was filtered through 0.45 µm Millex-HP syringe filters (Merck Millipore, Billerica, USA). The clear solution containing the isolated proteins was then incubated with equilibrated 2 ml Ni-NTA resin (Roche, Basel, Switzerland) for 1 h at 4°C with light rotation. After this incubation step, recombinant BAM1 protein is bound to the Ni-NTA resin via its C-terminal His-tag. The resin was spun down at 200 g for 1 min and resuspended in 5 ml lysis buffer. This solution was carefully loaded on 10 ml polypropylene columns (Thermo Fisher Scientific, Waltham, USA). Resin was subsequently washed 5 times with 5 ml basic buffer supplemented with 2 mM DTT, 0.5% (w/v) Triton X-100, followed by 5 wash steps using 5 ml basic buffer supplemented with 2 mM DTT. Finally, protein fractions of 1 ml each were eluted using elution buffers of increasing imidazole concentrations. The first three fractions were eluted using 1 ml of 50 mM Tris HCl pH 7.5, 50 mM NaCl and 100 mM imidazole solution, followed by three fractions where the imidazole concentration was raised to 250 mM and finally three fractions using 500 mM imidazole. All fractions were loaded on 10% sodium dodecyl sulphate (SDS) polyacrylamide gel electrophoresis (PAGE) gels and protein bands were visualized with Coommassie staining. The recombinant BAM1 proteins typically eluted in fractions 2 to 6 with high purity. These fractions were pooled and concentrated to approximately 0.5 ml in an Amicon Ultra-4 centrifugation filter (10k molecular weight cut off, Merck Millipore, Billerica, USA), followed by buffer exchange using Illustra NAP-5 columns Sephadex G-25 (Chalfont St Giles, UK) equilibrated using 5 times 2 ml storage buffer (50 mM Tris/HCl pH 7.5, 10% (w/v) glycerol and 2 mM DTT). Proteins were eluted from NAP-5 columns using twice 0.5 ml storage buffer. Proteins were stored as 50 µl aliquots at -80°C.

The concentration of isolated recombinant BAM1 protein was determined using the Biorad protein assay (Biorad, Hercules, USA) according to manufacturers instructions. Final purity of protein preparation was confirmed by loading 1 µg of protein onto a 10% SDS-PAGE gel, run with the Biorad Mini-Protean Gel system (Biorad, Hercules, USA) and subsequently stained using a standard Coomassie staining protocol: Gels were incubated with Coomassie solution (40% (v/v) methanol, 10% (v/v) glacial acetic acid, 0.1% (w/v) Coomassie R250) over night, followed by washing in water and destaining using destaining solution (20% (v/v) methanol, 10% (v/v) glacial acetic acid) until bands were clearly distinguishably from background.

Analysis of BAM1 enzyme activity on native gels

The activity of the recombinant BAM1 proteins were visualized on native gels containing amylopectin stained with Lugol solution. For this, a 10% polyacrylamide gel electrophoresis (PAGE) gel without SDS but supplemented with 0.1% potato amylopectin (Sigma-Aldrich, St. Louis, USA) were cast using the Biorad Mini-Protean Gel system (Biorad, Hercules, USA). In order to ensure its solubility, amylopectin was boiled for 5 min at 95°C in water and slowly cooled down to room temperature prior to the addition to the master mix. Recombinant protein dilutions between 0.01 and 0.1 µg were mixed with native PAGE loading buffer (50% glycerol, 0.05% (w/v) bromphenol blue) and run in ice-cold native PAGE running buffer (30.3 g Tris, 144 g glycin in H_2O in a final volume of 1 l) at 4°C for 2 to 3 h. For the digestion of the amylopectin by the BAM1 proteins, the PAGE gels were subsequently washed for 15 min in incubation buffer (100 mM Tris-HCl pH6.8, 5 mM DTT, 1 mM $MgCl_2$, 1 mM $CaCl_2$) and finally incubated in fresh incubation buffer at 4°C over night. To visualize the degradation of amylopectin, the gels were stained for 8 h at 4°C in Lugol solution (Iodine/Potassium iodide solution, Sigma-Aldrich, St. Louis, USA). After destaining in cold water resulted in a good contrast between the bands and the background, pictures were taken with a Canon EOS 60D camera.

Enzymatic activity assays

An easy way to investigate the activity of β-amylases is through the betamyl method using the artificial substrate *p*-nitrophenyl maltotrioside (PNPG3) (Megazyme, Wicklow, Ireland). β-Amylases present in the reaction mix are able to cleave PNPG3, although at a low rate, releasing maltose and *p*-nitrophenyl glucoside (PNPG), which is subsequently cleaved by α-Glucosidase present in the substrate mixture into

glucose and *p*-nitrophenol (PNP). PNP can be quantified spectrophotometrically. This enzymatic activity assay was performed according to manufacturers instructions. Each reaction mix contained 60 µl of betamyl reagent in 100 mM Tricine pH 7.9 supplemented with 5 mM DTT. The addition of 1 µg of recombinant BAM1 protein started the reaction, which was incubated at 37°C until the indicated time points, when the reaction was stopped by the addition of 900 µl 1% (w/v) Trizma base (Sigma-Aldrich, St. Louis, USA). While the reactions cooled down to room temperature, the yellow colour of PNP, with absorption at 400 nm, developed. From the spectrophotometrically determined absorption values the amount of released PNP and therefore β-amylase activity of the recombinant proteins was calculated.

As an alternative to the above-described assay using the artificial PNPG3 substrate, we quantified the amount of reducing ends released from amylopectin. This assay is based on the binding of two molecules of 3-Methyl-2-benzothiazolinone hydrazone (MBTH) to aldehyde groups of sugars, which results in the development of a specific colour with a maximal absorption at 620 nm. The assay was performed according to the protocol developed by Anthon & Barrett (Anthon and Barrett, 2002). Per reaction 0.025 µg of recombinant protein was equilibrated in a total of 70 µl master mix solution (100 mM Tricine pH 7.9, 5 mM DTT and 30 µg/ml BSA final concentration) for 15 min at room temperature. The addition of 30 µl of 5 mg/ml potato amylopectin, which was solubilized through the incubation at 95°C for approximately 10 min, started the reaction. At the indicated time points the reaction in the samples was stopped through the addition of 100 µl 0.5 M NaOH. Maltose released during this reaction was quantified through the reducing end assay. For this, a 3 mg/ml MBTH solution was diluted 1:1 with 1 µg/µl DTT in order to obtain a working solution. 50 µl of each sample was subsequently mixed with 50 µl 0.5 M NaOH and 50 µl of the MBTH working solution followed by the immediate incubation at 80°C for precisely 15 min. Finally, the MBTH reaction was stopped and the colour formation occurred through the addition of 100 µl of an acidic iron solution (0.5% (w/v) $FeNH_4(SO_4)_2$, 0.5% (w/v) sulfamic acid, 4% (v/v) 37% HCl). The blue colour is quantified through its absorption at 620 nm.

***In vitro* phosphorylation assay**

The ability of the ATK4 kinase to phosphorylate BAM1 *in vitro* was investigated through incubation of the two recombinant proteins in the presence of [γ-^{32}P]ATP. This experiment was performed in the laboratory of Claudia Jonak at the Gregor

Mendel Institute, Vienna, Austria, using previously purified recombinant ATK4 and ATK4 loss-of-function (ATK4 LOF) proteins.
2 µg of the different recombinant BAM1 versions were mixed with 1 µl of recombinant ATK4 or with 5 µl of the ATK4 loss of function (LOF) protein, purified from *E. coli* through their GSH tag, in 1x kinase buffer (20 mM Tricine pH 7.9, 15 mM $MgCl_2$ final concentration), supplemented with 10 mM [γ-^{32}P]ATP and 30 ng/µl BSA. The reaction was incubated for 30 min at room temperature, after which the proteins were loaded on a SDS-PAGE gel. Phosphopeptides were made visible with autoradiography films.
The same reaction was used in a cold phosphorylation experiment with non-radioactive ATP in order to investigate a possible change in BAM1 enzyme activity after the phosphorylation by ATK4. After the 30 min incubation period, a fraction of the cold phosphorylation reaction mix corresponding to a final amount of 0.025 µg BAM1 was used in a reduced end assay with amylopectin as a substrate as described above.

Phosphatase treatment of isolated plant proteins

Full plant proteins were isolated from 3-week-old plants of the Col-0 wild type and the *bam1* mutant using 3 rosettes each. Plant material was frozen in liquid nitrogen and ground with mortar and pestle. Protein extraction was done with approximately 200 mg leaf tissue by the addition of 200 µl extraction buffer (100 mM Tricine pH 7.9, 10% ethylene glycol, 5 mM DTT, 1x protease inhibitor (Roche, Basel, Switzerland)) and centrifugation at 13000 g, 4°C for 15 min. A dephosphorylation reaction was set up by mixing 75 µg of total protein (as determined by the Biorad protein assay (Biorad, Hercules, USA)) with 400 U Lambda Protein Phosphatase (New England Biolabs, Ipswich, USA), 1x PMP reaction buffer and 1 mM $MnCl_2$ in a total volume of 50 µl. Control reaction were set up in the same way but lacked the phosphatase enzyme. Incubation of the reaction mix proceeded for 30 min at 30°C. Afterwards, 45 µl of this reaction mix (containing 38 µg of crude plant protein) was used in the betamyl activity assay as described above. The reaction was incubated at 37°C for 1 h.

Large scale preparation of epidermal peels

In order to obtain a sufficient amount of tissue for the isolation of RNA from epidermal peel fragments, at least 100 mature leaves per replicate and genotype

were removed from rosettes of 12 to 18 4-week-old plants in the morning at 4°C under green light illumination. After the middle veins were removed manually, leaves were blended in 100 ml cold H_2O for 1.5 minutes in a Sorvall Omni Mixer (Thermo Fisher Scientific, Waltham, USA). The fragments were collected in a 200 µm mesh (Sefar, Thal, Switzerland) and rinsed extensively with H_2O. Peels were carefully transferred into Erlenmeyer flasks containing 50 ml enzymatic solution prepared from 22.5 ml H_2O and 27.5 ml basic solution (5 mM MES-TRIS pH 5.5, 0.5 mM $CaCl_2$, 0.5 mM $MgCl_2$, 10 µM KH_2PO_4, 0.55 M sorbitol) containing 0.7% (w/v) cellulysin cellulase from *Trichoderma viride* (Calbiochem, Merck Millipore, Billerica, USA), 0.1% (w/v) PVP-40, 0.25% (w/v) BSA fraction V and 0.5 mM ascorbic acid (Pandey et al., 2002). Incubation of the peel fragments for 1 h in the dark in this solution causes the degradation of the cell wall of contaminating mesophyll cells and epidermal cells, while guard cells stay protected because of their significantly thicker cell wall. The low osmolality of the digestion solution causes the swelling and ultimately bursting of the released epidermal and mesophyll cell protoplasts. The addition of 30 ml of basic solution to each flask after this initial incubation step raises the osmolality in order to protect guard cells from bursting. The viability of guard cells was checked under a Nikon Eclipse TC100 microscope (Nikon, Tokio, Japan) by fluorescin diacetate (FDA) staining of an aliquot. The non-fluorescent FDA is taken up by viable cells and cleaved by cellular esterases, releasing a fluorescent product. Fragments are subsequently collected in a new 200 µm mesh and rinsed with distilled H_2O. Tissue was transferred into reaction tubes, frozen in liquid nitrogen and stored at -80°C until needed for protein or RNA extraction.

qPCR analysis of gene expression using full leaves and epidermal peels

RNA was isolated with the RNeasy Plant Mini Kit (Qiagen, Venlo, Netherlands) according to manufacturers instructions from approximately 100 mg of epidermal peel fragments or from 100 mg of full leaf tissue, which was frozen in liquid nitrogen and grinded using a mortar and pestle. Eluted RNA was checked for integrity on agarose gels after quantification using a NanoDrop ND-1000 spectrophotometer (Thermo Fisher Scientific, Waltham, USA). cDNA was synthesized with 1 µg of RNA using the M-MLV reverse transcriptase with oligo(dT) primer (Promega, Fitchburg, USA) according to manufacturers guidelines. Finally, quantitative PCR (qPCR) was performed with the SYBR green master mix using the 7500 Fast Real Time PCR System (Applied Biosystems, Waltham, USA). Results of the triplicate qPCR reactions were analysed with the iQ5 Optical Systems Software (Applied

Biosystems), with specific amplification being confirmed by a single peak in the melting curves. The obtained cycle threshold value (Ct value) of the gene specific amplification reactions were normalized to the Ct values of *ACTIN2* (ACT2, At3g18780). Fold change was calculated as the ratio of transcript abundance in epidermal peel fragments to transcript abundance in the full leaf samples. All primer combinations are listed in Table 4.2.

Table 4.2: Oligonucleotides used in this part of the thesis

Oligo ID	sequence
atk4_fw	GGAGCAGCCAGTTTTCAGCC
atk4_rev	CGTGAAACAAACAAGTGGTCTGTAAC
bam1_fw	ACTTGGCGCTGATACACTCC
bam1_rev	GGCTGTTCGTGATCCCTCAT
act2_fw	TGGAATCCACGAGACAACCTA
act2_rev	TTCTGTGAACGATTCCTGGAC

Visualisation of leaf starch content

Leaf starch was visualised using Lugol solution (Iodine/Potassium iodide solution, Sigma-Aldrich, St. Louis, USA). Leaves were harvested at the end of the day (EoD) or at the end of the night (EoN), destained with 80% (v/v) hot ethanol to remove the chlorophyll and stained floating in Lugol solution. Excess staining solution was removed with H_2O and plant pictures were taken with a Canon EOS 60D camera.
In order to quantify guard cell starch content from full leaves, small fragments of the abaxial epidermis were manually dissected using a fine forceps and immediately fixed in 50% (v/v) methanol, 10% (v/v) acetic acid fixative solution, incubating at least 12 h at 4°C. Tissue was destained in 80°C hot 80% (v/v) ethanol for 5 min, followed by incubation in fixative solution for 1 h at room temperature. After carefully washing of the epidermal fragments in distilled H_2O, tissue was oxidised using 1% (w/v) periodic acid for 20 to 40 min at room temperature. This step oxidises the hydroxyl groups of the glucose subunits of starch into ketone and aldehyde groups, enabling the covalent linkage of propidium iodide (Truernit et al., 2008). After the acid was removed, peels were washed in water, followed by a 30 min incubation period at room temperature in Schiff reagent (100 mM sodium metabisulphite, 0.15 N HCl) supplemented with propidium iodide (0.1 mg/ml final concentration) in each well of a standard 12-well plate. Excess staining solution was removed by washing with water

for at least 20 min, after which the pink peels were carefully transferred into a drop of chloral hydrate solution (prepared by dissolving 40 g of chloral hydrate in 10 ml glycerol and 20 ml H_2O) onto microscopy slides. Slides were kept over night in the dark. Finally, tissue was covered with Hoyer's solution (30 g gum arabic, 200 g chloral hydrate, 20 g glycerol dissolved with 50 ml H_2O) and covered with a cover slip. Mountant was allowed to settle for at least 3 days after which images were acquired by confocal laser scanning microscopy using a Leica TCS SP5 microscope (Leica Microsystem, Wetzlar, Germany). To acquire images an excitation wavelength of 488 nm from the argon laser source was used and the emission spectrum was detected by HyD3 detectors between 610 to 640 nm. Starch granule areas were determined using ImageJ version 1.45s (NIH USA, http://rsbweb.nih.gov/ij/).

Full plant protein isolation for mass spectrometry

3-week-old plants grown in soil at 22°C, 60% relative humidity and a 12h light / 12 h dark cycle were sprayed with an abscisic acid solution (100 µM ABA pH8, 0.01% Tween20) three hours into the light phase in order to induce the expression of *BAM1* in mesophyll cells (see Chapter 3). Four individual rosettes were collected per replicate 4 hours after this treatment and frozen in liquid nitrogen. Proteins from approximately 200 mg of ground leaf powder were isolated using two volumes of a SDS extraction buffer (4% sodium dodecyl sulphate, 0.1 M dithiothreitol in 100 mM Tris HCl pH 8.2). The samples were incubated at 95°C for 5 min at 800 rpm, followed by sonication for 15 min with an amplitude of 65% and a cycle of 0.5. This ensured the complete extraction of the proteins including integral membrane proteins, their denaturation, the reduction of disulphide bridges and the shearing of any nucleotides. After centrifugation at 16.000 g for 10 min the protein concentration was quantified using the Qubit protein assay kit (Thermo Fisher Scientific, Waltham, USA).

FASP protein digestion

Protein digestion was performed using the filter-aided sample preparation (FASP) method (Wiśniewski et al., 2009), which eliminates contaminants such as cell compounds and the SDS from the extraction buffer, while ensuring a relatively high peptide recovery rate. 300 µg of the total protein samples were mixed with UA buffer (8 M urea in 100 mM Tris HCl pH8.2) for a final volume of 920 µl, of which 230 µl were loaded on the Microcon-30kDa centrifugal units containing the Ultracel-30 membrane (Merck Millipore, Billerica, USA) in each centrifugation round. All

centrifugation steps were performed at 14.000 g at room temperature for 20 min. After loading of the columns, the membrane was washed with UA buffer once, after which the proteins were incubated with 100 µl IAA solution (0.05 M iodoacetamide in UA buffer) in order to carboxyamidomethylate reactive thiol groups of the proteins. After a short incubation for 1 min, excessive IAA solution was removed by centrifugation and the columns were washed three times with UA buffer, twice with a 0.5 M NaCl solution and three times with TEAB (0.05 M triethylammonium bicarbonate). A Trypsin/Lys-C mix (Promega, Fitchburg, USA) was diluted in TEAB in a 1:30 trypsin to protein ratio for a final volume of 120 µl per sample and added to the matrix-bound proteins. Protein digestion was performed over night at room temperature in a wet cell.

Digested peptides were eluted by centrifugation at 14.000 g for 15 min, followed by a second elution step using 80 µl of TEAB. Qubit protein quantification confirmed the expected recovery rate of approximately 50%. 5 µg aliquots were taken for the mass spectrometry analysis of non-enriched samples, while the remaining peptides were used for the enrichment procedure.

Ti-IMAC phosphopeptide enrichment

Ti^{4+} immobilized metal affinity chromatography (Ti-IMAC) was performed using the MagReSyn magnetic microspheres (ReSyn Bioscienc,es, Edenvale, South Africa). For each sample of 200 µg desalted peptides 1 mg of the magnetic spheres were washed and equilibration in loading buffer (1 M glycolic acid in 80% acetonitrile, 5% trifluoroacetic acid) according to manufacturers instructions. Peptides were concentrated to 10 µl using a speed-vac and mixed with 100 µl of the loading buffer prior to the enrichment procedure. Binding of the phosphate groups of phosphopeptides to the Ti^{4+} ions was performed at room temperature with light shaking for 20 min. Unbound peptides were subsequently removed by pipette aspiration with the help of a magnetic separator. The magnetic spheres were washed with wash buffer (80% acetonitrile, 1% trifluoroacetic acid) followed by the elution of phosphopeptides in 1% ammonia solution according to manufacturers instructions. For the acidification of the resulting 240 µl eluate 60 µl 10% formic acid was added to each sample.

ZipTip desalting

For the desalting of the samples, peptides were partially dried in a speed-vac and 7.5 µg of enriched phosphopeptides were subsequently resuspended in 10 µl 3%

acetonitrile, 0.1% trifluoroacetic acid. Desalting was performed using C_{18} ZipTips (Merck Millipore, Billerica, USA) according to manufacturers instructions. After the elution of the peptides in 60% acetonitrile, 0.1% trifluoroacetic acid, the acetonitrile was removed in a speed-vac and the samples were resuspended in LC-MS solvent (3% acetonitrile, 0.1% formic acid) for a final volume of 12 µl.

LC-MS/MS data acquisition and analysis

4 µl of each of the enriched phosphopeptides and non-phosphopeptide enriched samples were loaded by the autosampler into the EASY-nLC (Thermo Fisher Scientific, Waltham, USA) for nano-scale liquid chromatography coupled with mass spectroscopy using an Orbitrap Fusion Tribrid mass spectrometer (Thermo Fisher Scientific, Waltham, USA) with a set scan range of 350 to 1550 m/z.
The mass spectrometry raw data was analysed using the MASCOT MS/MS ion search engine (Matrix Science, Boston, USA). Annotation of peptide sequences was done using the TAIR10 database allowing up to 2 missed cleavages with a peptide mass tolerance of ± 10 ppm and a fragment mass tolerance of ± 0.7 Da. Carbamidomethylated cysteine residues were set as a fixed modification and the following frequently occurring variable modifications were considered by the search algorithm: oxidation of methionine residues, phosphorylation of serine, threonine and tyrosine residues, the acetylation of the protein N-terminus and the deamidation of asparagine and glutamine residues as well as the N-terminal modification of glutamine to pyro-glutamate. Only peptides annotated with an expect value of less than 0.05 were considered to be correctly identified.

Results

In a first step we searched current publicly available phosphoproteomic data for the presence of phosphorylation sites in the BAM1 protein in order to get a complete picture of the possible modification sites. We collected the described phosphopeptide sequences from the PhosPhAt 4.0 database at www.phosphate.uni-hohenheim.de (Heazlewood et al., 2008). All found BAM1 related phosphopeptides are shown in Table 4.3.

Table 4.3: Summary of BAM1 phosphopeptides from publicly available phosphoproteomic studies taken from the PhosPhAt 4.0 database. The original studies, treatments (if any), tissue types as well as used genotypes are indicated. Modified amino acids are shown in brackets. Database last accessed October 2015).

Publication	Modified Peptide	Treatment	Tissue	Genotype
Sugiyama et al. 2008	AHGTDP(pS)PP(oxM)(pS)PILGATR		cell culture	Col-0
	AHGTDP(pS)PPM(pS)PILGATR		cell culture	Col-0
	SGEMTDSSLLSI(pS)PPSAR		cell culture	Col-0
Reiland et al. 2009	AHGTDP(pS)PP(oxM)(pS)PILGATR	end of night	rosette	Col-0
	AHG(t)DP(s)PP(oxM)(s)PILGA(t)R	end of night	rosette	Col-0
	AHG(t)DP(s)PP(oxM)(s)PILGA(t)R	end of day	rosette	Col-0
	AHG(t)DP(s)PP(oxM)(s)PILGA(t)R	end of night	rosette	Col-0
	AHGTDP(pS)PP(oxM)(pS)PILGATR	end of night	rosette	Col-0
	(s)GE(oxM)(t)D(s)(s)LL(s)I(s)PP(s)AR	end of night	rosette	Col-0
	(s)GE(oxM)(t)D(s)(s)LL(s)I(s)PP(s)AR	end of day	rosette	Col-0
	(s)GE(oxM)(t)D(s)(s)LL(s)I(s)PP(s)AR	end of day	rosette	Col-0
	SGE(oxM)TDSSLLSI(pS)PPSAR		seedlings	Col-0
	SGE(oxM)TDSSLLSI(pS)PPSAR	end of night	rosette	Col-0
	(s)GE(oxM)(t)D(s)(s)LL(s)I(s)PP(s)AR	end of day	rosette	Col-0
	(s)GE(oxM)(t)D(s)(s)LL(s)I(s)PP(s)AR	end of night	rosette	Col-0
	(s)GE(oxM)(t)D(s)(s)LL(s)I(s)PP(s)AR	end of night	rosette	Col-0
	(s)GE(oxM)(t)D(s)(s)LL(s)I(s)PP(s)AR	end of day	rosette	Col-0
	(s)GE(oxM)(t)D(s)(s)LL(s)I(s)PP(s)AR	end of night	rosette	Col-0
	(s)GE(oxM)(t)D(s)(s)LL(s)I(s)PP(s)AR	end of day	rosette	Col-0
	(s)GE(oxM)(t)D(s)(s)LL(s)I(s)PP(s)AR	end of night	rosette	Col-0
Nakagami et al. 2010	AHGTDP(pS)PP(oxM)SPILGA(pT)R		cell culture	Col-0
	AHGTDP(pS)PPM(pS)PILGATR		cell culture	Col-0
	AHGTDP(pS)PP(oxM)(pS)PILGATR		cell culture	Col-0
	SGEMTDSSLLSI(pS)PPSAR		cell culture	Col-0
	SGEMTDSSLL(pS)ISPPSAR		cell culture	Col-0
Wang et al. 2013b	AHGTDP(pS)PPMSPILGATR	nitrate starvation	seedlings	Col-0
	AHGTDP(pS)PP(oxM)(pS)PILGATR	nitrate starvation	seedlings	Col-0
	AHGTDP(pS)PPM(pS)PILGATR	nitrate starvation	seedlings	Col-0
Zhang et al. 2013	AHGTDP(pS)PPM(pS)PILGATR	auxin	roots	Col-0

Publication	Modified Peptide	Treatment	Tissue	Genotype
	AHG(pT)DPSPPM(pS)PILGATR	auxin	roots	Col-0
	AHGTDP(pS)PP(oxM)(pS)PILGATR	auxin	roots	Col-0
	SGE(oxM)TDSSLLSI(pS)PPSAR	auxin	roots	Col-0
	SGEMTDSSLLSI(pS)PPSAR	auxin	roots	Col-0
Umezawa et al. 2013	AHGTDP(pS)PP(oxM)(pS)PILGATR	abscisic acid	leaf	srk2dei
	AHGTDP(pS)PPM(pS)PILGATR	abscisic acid	leaf	srk2dei
	AHGTDP(pS)PPMSPILGATR	abscisic acid	leaf	srk2dei
	AHGTDP(pS)PP(oxM)(pS)PILGATR	abscisic acid	leaf	srk2dei
	AHGTDP(pS)PPM(pS)PILGATR	abscisic acid	leaf	srk2dei
	AHGTDP(pS)PPMSPILGA(pT)R	abscisic acid	leaf	srk2dei
	AHGTDP(pS)PPMSPILGATR	abscisic acid	leaf	srk2dei
	AHGTDP(pS)PP(oxM)(pS)PILGATR	abscisic acid	leaf	srk2dei
	AHGTDP(pS)PPM(pS)PILGATR	abscisic acid	leaf	srk2dei
	SGE(oxM)TDSSLLSI(pS)PPSAR	abscisic acid	leaf	srk2dei
	SGEMTDSSLL(pS)ISPPSAR	abscisic acid	leaf	srk2dei
	SGEMTDSSLLSI(pS)PPSAR	abscisic acid	leaf	srk2dei
	SGE(oxM)TDSSLLSI(pS)PPSAR	abscisic acid	leaf	srk2dei
	SGEMTDSSLL(pS)ISPPSAR	abscisic acid	leaf	srk2dei
	SGEMTDSSLLSI(pS)PPSAR	abscisic acid	leaf	srk2dei
Xue et al. 2013	AHGTDP(pS)PPMSPILGATR	mannitol	seedlings	Col-0
	AHGTDPSPPM(pS)PILGATR	mannitol	seedlings	Col-0
	SGE(oxM)TDSSLLSI(pS)PPSAR	Abscisic acid	seedlings	Col-0
	SGEMTDSSLLSI(pS)PPSAR	Abscisic acid	seedlings	Col-0
Wang et al. 2013a	AHGTDP(pS)PP(oxM)(pS)PILGATR	abscisic acid	seedlings	snrk2.2/2.3/2.6
	AHGTDP(pS)PP(oxM)(pS)PILGATR	abscisic acid	seedlings	Col-0
	AHGTDP(pS)PPM(pS)PILGATR	abscisic acid	seedlings	Col-0
	AHGTDP(pS)PPMSPILGATR	abscisic acid	seedlings	Col-0
	AHGTDPSPPM(pS)PILGATR	abscisic acid	seedlings	Col-0
	AHGTDP(pS)PPM(pS)PILGATR	abscisic acid	seedlings	snrk2.2/2.3/2.6
	SGE(oxM)TDSSLLSI(pS)PPSAR	abscisic acid	seedlings	snrk2.2/2.3/2.6
	SGE(oxM)TDSSLLSI(pS)PPSAR	abscisic acid	seedlings	Col-0
	SGEMTDSSLLSI(pS)PPSAR	abscisic acid	seedlings	Col-0
	SGEMTDSSLLSI(pS)PPSAR	abscisic acid	seedlings	snrk2.2/2.3/2.6
Yang et al. 2013	AHGTDP(pS)PPM(pS)PILGATR	ethylene	rosettes	ctr1-1; rcn1-1
Rayapuram et al. 2014	AHGTDP(pS)PPM(pS)PILGATR	flg22	seedlings	Col-0
	AHGTDP(pS)PPM(pS)PILGATR	flg22	seedlings	Col-0
	AHGTDP(pS)PPM(pS)PILGATR	flg22	seedlings	Col-0
	AHGTDP(pS)PPM(pS)PILGATR	flg22	seedlings	Col-0
	AHGTDP(pS)PPM(pS)PILGATR	flg22	seedlings	Col-0
Roitinger et al. 2015	AHGTDP(pS)PP(oxM)(pS)PILGATR	irradiation	rosette	
	AHGTDPSPP(oxM)(pS)PILGATR	irradiation	rosette	
	AHGTDP(pS)PP(oxM)SPILGATR	irradiation	rosette	
	AHG(pT)DPSPP(oxM)(pS)PILGATR	irradiation	rosette	
	SGE(oxM)TDSSLLSI(pS)PPSAR	irradiation	rosette	

(continued from last page)

As shown in Table 4.3, BAM1 phosphopeptides were reported in several large-scale phosphoproteomic studies on different Arabidopsis tissue types. While two studies were conducted on Arabidopsis cell culture (Sugiyama et al., 2008; Nakagami et al., 2010), several studies used either seedlings (Wang et al., 2013b; Xue et al., 2013; Wang et al., 2013a; Rayapuram et al., 2014) or mature plants (Reiland et al., 2009; Umezawa et al., 2013; Yang et al., 2013; Roitinger et al., 2015) and one study was conducted on root samples (Zhang et al., 2013). Despite the differences in the tissue samples as well as in the applied treatments and the used genotypes, most studies found phosphopeptides of BAM1. Three particular serine (Ser) residues were reported to be phosphorylated: Ser^{31}, Ser^{55} and Ser^{59} (Table 4.3). Figure 4.1 shows the protein sequence of *Arabidopsis thaliana* BAM1 protein with these putative phosphorylation sites indicated (Figure 4.1 A). Ser^{31} lies within the predicted chloroplast targeting peptide (cTP), which is thought to be cleaved after Lys^{41} during the import of the BAM1 preprotein into the plastid, giving rise to the mature protein (Sparla et al., 2006). The other two phosphorylated serines are part of the N-terminus of the mature BAM1 protein, whose sequence is different compared to the N-terminal part of BAM3 and which contains one of the cysteins (Cys^{73}) that participates in the formation of the disulphide bridge (Sparla et al., 2006). We therefore speculated that the N-terminal part of the BAM1 protein may be responsible for the different roles of BAM1 compared to BAM3, and that the phosphorylation of Ser^{55} and Ser^{59} residues may participate in the regulation of the mature BAM1 protein. This is further corroborated by the observation that both Ser^{55} and Ser^{59} amino acids are conserved and can be found in diverse plant species including Brassicaceae, Populus and Solanaceae species (Figure 4.1 B; M. Thalmann unpublished results), while most other amino acids in the BAM1 N-terminus of these species are more variable.

A

MALNLSHQLGVLAGTPIKSGEMTDSSLLSI**S**PPSARMMTPKAMNRNYK**AHGTDP*S*PPM*S*PILGATR**ADL
SVACKAFAVENGIGTIEEQRTYREGGIGGKKEGGGGVPVFVMMPLDSVTMGNTVNRRKAMKASLQALKS
AGVEGIMIDVWWGLVEKESPGTYNWGGYNELLELAKKLGLKVQAVMSFHQCGGNVGDSVTIPLPQWVVE
EVDKDPDLAYTDQWGRRNHEYISLGADTLPVLKGRTPVQCYADFMRAFRDNFKHLLGETIVEIQVGMGP
AGELRYPSYPEQEGTWKFPGIGAFQCYDKYSLSSLKAAAETYGKPEWGSTGPTDAGHYNNWPEDTQFFK
KEGGGWNSEYGDFFLSWYSQMLLDHGERILSSAKSIFENMGVKISVKIAGIHWHYGTRSHAPELTAGYY
NTRFRDGYLPIAQMLARHNAIFNFTCIEMRDHEQPQDALCAPEKLVNQVALATLAAEVPLAGENALPRY
DDYAHEQILKASALNLDQNNEGEPREMCAFTYLRMNPELFQADNWGKFVAFVKKMGEGRDSHRCREEVE
REAEHFVHVTQPLVQEAAVALTH

B

Fig. 3.1: Summary of bioinformatic analysis of AtBAM1 and related β-amylase enzymes. (A) The 575 amino acid long sequence of AtBAM1 is shown. The predicted chloroplast transit peptide (cTP) is underlined and the three putative phospho-Ser residues are indicated in red. Furthermore, the Ser^{55} and Ser^{59} containing peptide derived from the protein after trypsin digestion is indicated in bold. (B) Multiple sequence alignment of the BAM1 N-terminus using Clustal Omega version 1.2.0. The green box indicates Cys^{73}, which forms the disulphide bridge together with Cys^{511} (not shown), the blue box indicates the conserved (S/T)P-XX-(S/T)P motif including the putative phosphorylation sites Ser^{55} and Ser^{59} and the red box indicates the SXSXP motif found in the BAM1-like proteins of other Brassicaceae plant species.

In order to get a first insight into the possible roles of BAM1 phosphorylation, we generated constructs for the expression of phosphomimic and phosphomutant versions of BAM1 in *E. coli*. These recombinant proteins incorporate altered amino acids at position 55 and/or at position 59, with phosphomutant proteins containing an alanine, while phosphomimic versions contained an aspartate residue instead of the serine of the wild type protein (Figure 4.2 A). All recombinant proteins lacked the cTP region to ensure proper folding in bacteria (Sparla et al., 2006), were isolated with a

high degree of purity (Figure 4.2 A) and were active enzymes as indicated by the degradation of amylopectin in native gel zymograms (Figure 4.2 B).

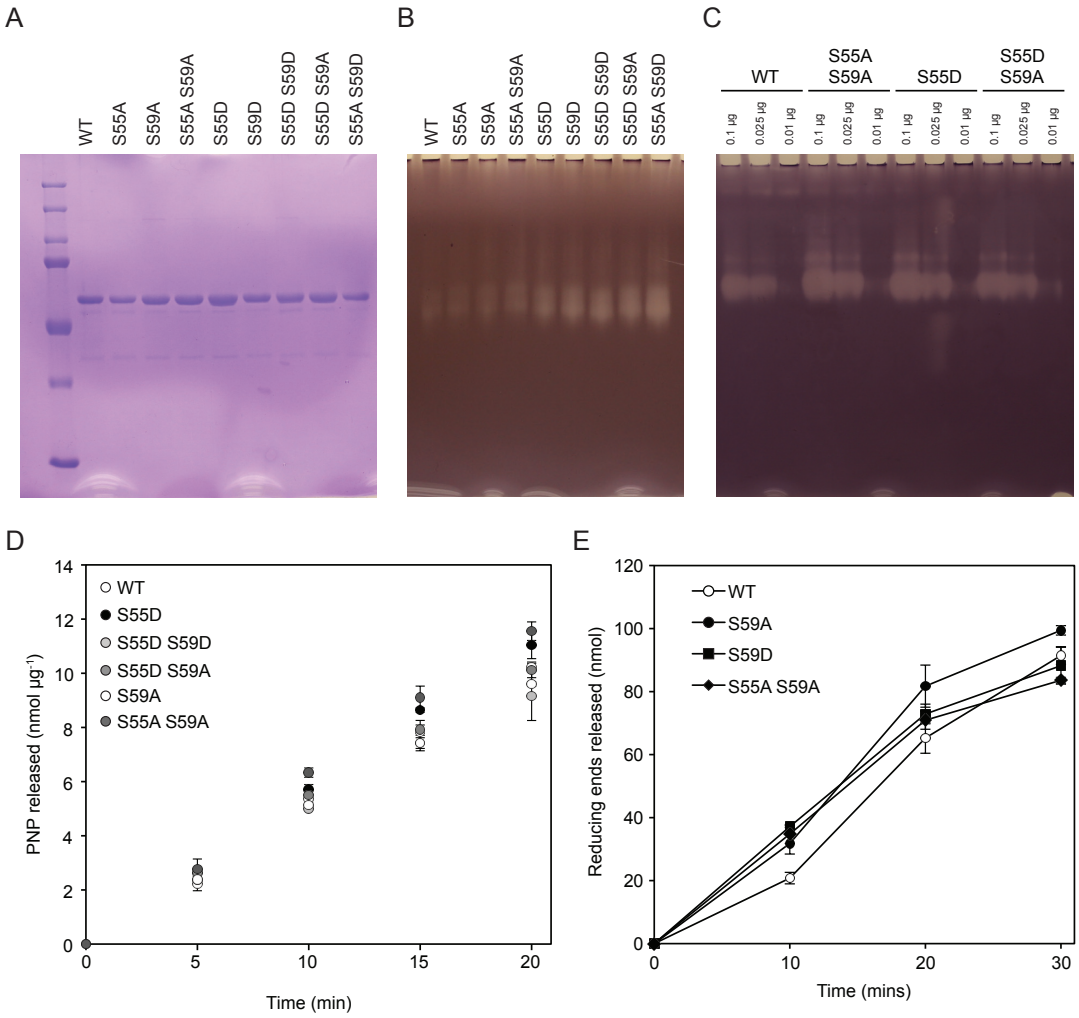

Figure 4.2: BAM1 mutant enzyme activity assays. (A) Recombinant proteins of BAM1-cTP wild type (WT), phosphomutants (S55A, S59A, S55A S59A) as well as phosphomimics (S55D, S59D, S55D S59D) and combinations of those (S55D S59A, S55A S59D) were isolated with high efficiency and purity from *E. coli*. (B) Recombinant BAM1 proteins are catalytically active as indicated by the degradation of amylopectin in a 10% polyacrylamide native gel stained with Lugol solution. The gel contained 0.1% potato amylopectin and 0.025 µg of recombinant protein was loaded per well. (C) Different dilutions of WT, S55A S59A, S55D and S55D S59A recombinant protein loaded on a 10% polyacrylamide native gel containing 0.1% potato amylopectin. The gel was stained with Lugol solution following the incubation period (for details see the Material and Methods section). (D) β-Amylase activity assay using the artificial PNPG3 substrate for the BAM1 proteins. 1 µg of recombinant protein was used per reaction and values represent three technical replicates ± SE. (E) Quantification of the reducing ends released from amylopectin by the action of different versions of 0.025 µg recombinant enzymes on 150 µg potato amylopectin. Values represent three technical replicates ± SE.

From the native PAGE experiment shown in Figure 4.2 B, it seemed that the introduction of a negative charged amino acid at either position 55 or 59 enhanced

the activity of BAM1 against the amylopectin in the gel (Figure 4.2 B). However, these observations were not consistently observed in subsequent zymogram experiments. In the gel shown in Figure 4.2, it seems that all mutants have a slightly higher activity compared to the wild type protein, no matter if they contain a phosphomimic or only phosphomutant amino acid substitution (Figure 4.2 C). Therefore, we employed a more quantitative experimental assay to investigate if the recombinant BAM1 proteins differ in their specific activity against the artificial substrate PNPG3 (Figure 4.2 D). In contrast to the initial zymogram analysis, we could not observe any differences in the ability of selected recombinant BAM1 proteins in releasing maltose from PNPG3 in this assay. Because this could have been due to the limited enzymatic activity of BAM1 against short glucosyl chains, with almost no activity against maltotriose *in vivo*, we also compared the ability of amylopectin degradation between the different protein versions. Again, no obvious differences could be observed in the release of maltose between WT BAM1 and phosphomutant and phosphomimic versions of this β-amylase (Figure 4.2 E). In summary, it seems that the mutation of serine either to an alanine or to an aspartate, which introduces a negative charge mimicking the phosphorylation of the native serine residue, does not influence enzymatic activity *in vitro*.

In a phosphoproteomics study, which is not included in the PhosPhAt database, phosphopeptides from Arabidopsis Col-0 plants were investigated for the occurrence of conserved phosphorylation motifs (de la Fuente van Bentem et al., 2008). Amongst other proteins, BAM1 was suggested to contain a GSK3/Shaggy-like kinase phosphorylation motif of the (S/T)P-XX-(S/T)P form, with the two phosphorylation sites corresponding to Ser^{55} and Ser^{59}. We therefore conducted an *in vitro* phosphorylation assay using the recombinant AtK4 protein as the GSK3 kinase, whose expression pattern closely matches the one from *BAM1* (see above). Furthermore, AtK4 is thought to localize to the chloroplast, while other members of this family are not (C. Jonak, personal communication). As reported previously, AtK4, like other GSK3 kinases shows a strong autophosphorylation activity, confirming the integrity of the assay (Figure 4.3 A). Besides this strong band on the radiography film, a weaker band corresponding to phosphorylated WT BAM1 and the phosphomutant S55A can be observed, while no phosphorylation band is evident for the S59A or the S55A S59A mutant proteins. This shows the *in vitro* specificity of AtK4 for phosphorylation of Ser^{59} of BAM1 (Figure 4.3 A).

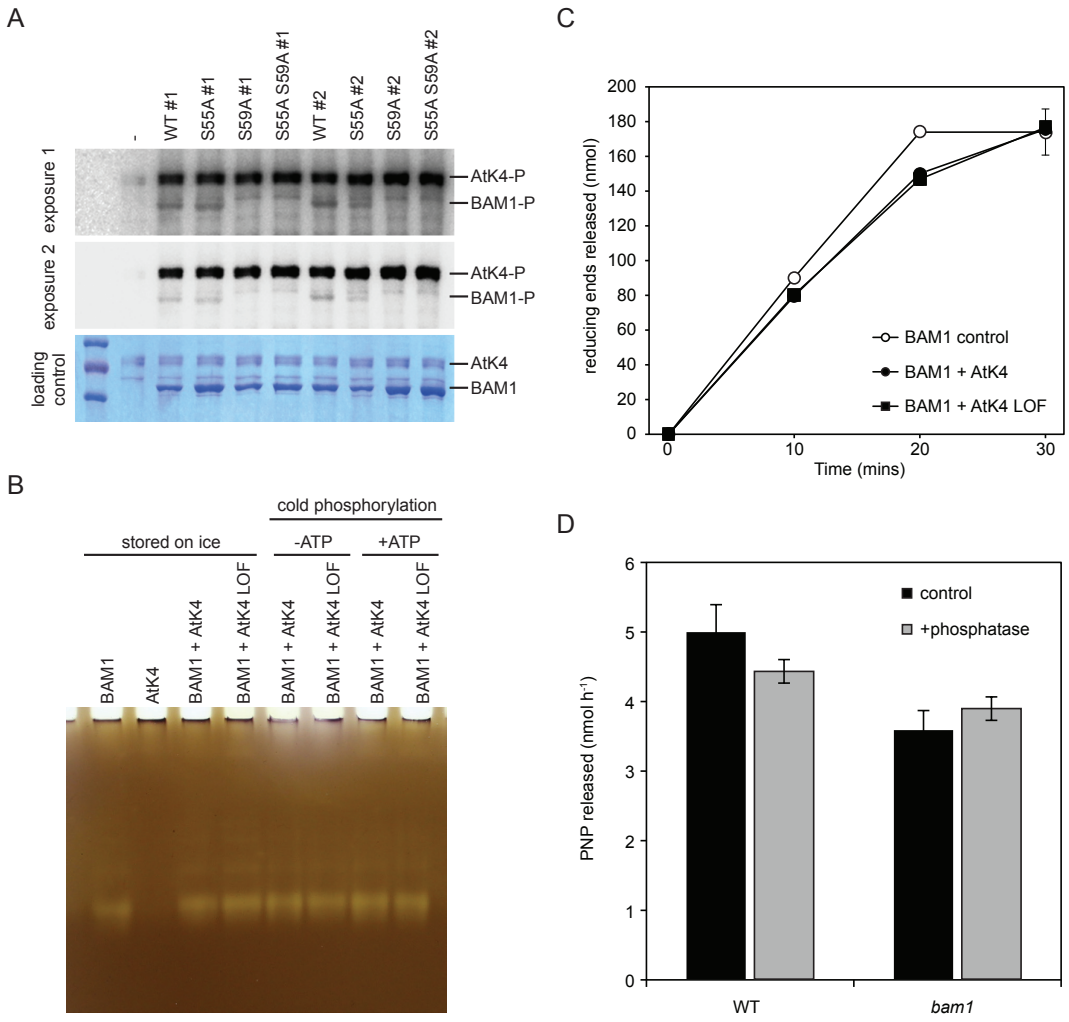

Figure 4.3: Recombinant BAM1 can be phosphorylated by the AtK4 kinase *in vitro*, but the enzymatic activity is not altered. (A) Visualization of *in vitro* phosphorylation events by autoradiography (upper two panels) and protein loading control by Coomassie staining (lower panel) indicate phosphorylation of BAM1 at Ser[59] by the AtK4 kinase. Proteins from two independent isolations are shown. (B) Zymogram analysis of recombinant BAM1 protein preincubated with or without AtK4 or a loss of function version of this kinase (AtK4-LOF). Proteins were either kept on ice or cold-phosphorylated by the incubation in the presence of ATP. As a control, cold phosphorylation was also performed in the absence of ATP. 0.025 µg of recombinant BAM1 protein was loaded per lane. (C) Reducing end assay following cold phosphorylation reaction of BAM1 using either AtK4 or the loss of function AtK4-LOF protein. BAM1-cTP protein stored on ice is shown as a control. Assay was performed using amylopectin as a substrate for a total of 0.025 µg recombinant BAM1 protein. Values shown are averages of three technical replicates ± SE. (D) Crude protein extract from rosettes of Col-0 wild-type (WT) and *bam1* mutant plants was incubated with or without lambda protein phosphatase prior to the betamyl activity assay using PNPG3 as a substrate. Bars show averages of two technical replicates ± SE.

Next, we used the recombinant proteins to phosphorylate BAM1 *in vitro* in a cold phosphorylation experiment (replacing the radioactive labelled ATP with unlabelled ATP in the kinase reaction mixture) and used the BAM1 proteins in subsequent

activity assays (Figure 4.3 B and C). Similar to the results obtained in Figure 4.2, we did not observe clear differences in the in gel activity of recombinant BAM1 against amylopectin with or without the prior phosphorylation through AtK4 (Figure 4.3 B). Furthermore, wild type BAM1 protein pre-phosphorylated by AtK4 or incubated with the loss of function version AtK4 LOF did not show differences in their activities against PNPG3 (Figure 4.3 C).

In a preliminary experiment, we incubated isolated full plant proteins from WT and *bam1* mutants with lambda protein phosphatase, in order to investigate a potential influence of the dephosphorylation of BAM1 *in vivo* (Figure 4.3 D). As reported previously, *bam1* plant extracts show a reduced β-amylase activity compared to wild-type plant extracts, although the overall activity is still relatively high due to other BAMs such as BAM3 and the cytosolic BAM5 (Monroe et al., 2014). We could observe a small reduction of the activity against PNPG3 in the WT but not in the *bam1* extracts pretreated with the phosphatase, suggesting a possible influence of protein dephosphorylation on β-amylase activity *in vivo*. The reduction in β-amylase activity was rather small and further experiments will be needed to determine if phosphatase treatment can indeed influence BAM activity significantly in plant extracts. Nevertheless, this experimental approach might provide valuable insights into the regulation of the BAM protein family.

Next, we wanted to investigate a possible role of AtK4 in the regulation of guard cell starch degradation. In agreement with previously published microarray data (Bates et al., 2012), we showed that *AtK4* expression is much higher in guard cells compared to full leaves, which is similar to the expression of *BAM1* (Figure 4.4 A). Mutant *atk4* plants grown in our standard growth conditions did not show an obvious growth phenotype (Figure 4.4 B) and starch degradation in full leaves seems to proceed normally (Figure 4.4 C). In contrast, the *atk4* mutant showed strongly elevated starch levels in guard cells illuminated for 1 h compared with wild-type controls (Figure 4.4 D), similar to the starch excess phenotype observed in plants lacking BAM1 (Chapter 1). This shows that the AtK4 kinase may play an important role in the regulation of guard cell starch metabolism under normal growth conditions. Overall, guard cell starch degradation occurred between the end of the night and 1 h of illumination in the two AtK4 overexpression lines OE 1 and OE 27 (Figure 4.4 D).

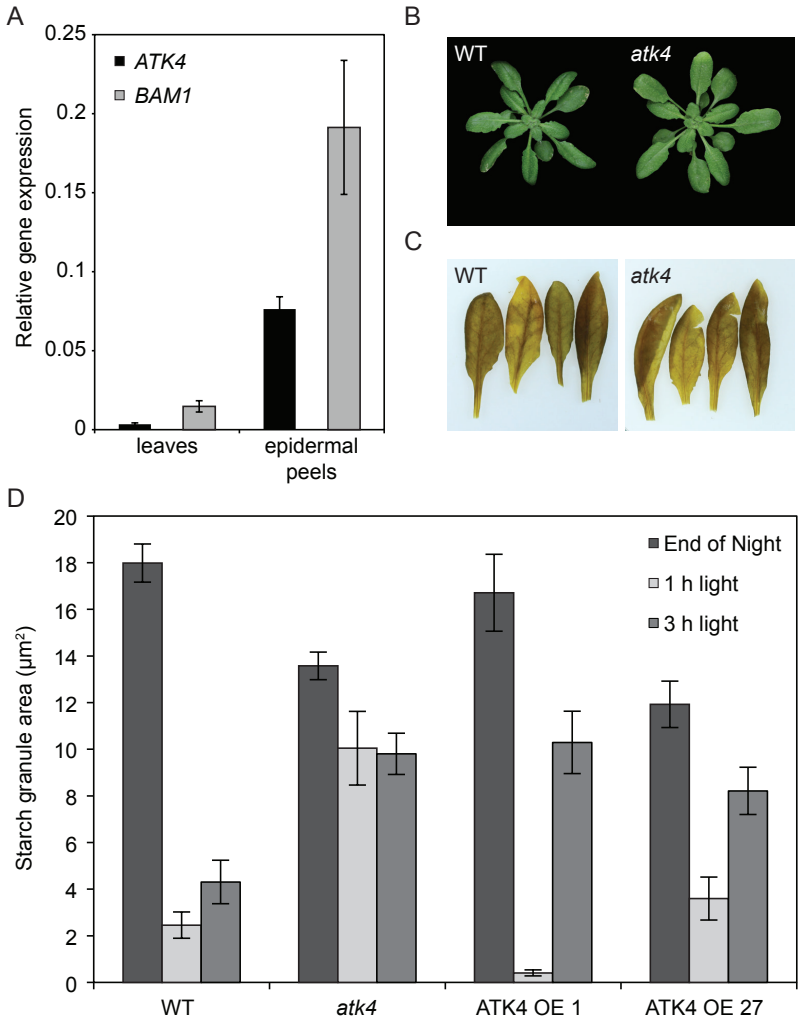

Figure 4.4: ATK4 and BAM1 show a similar expression pattern and guard cell starch degradation is inhibited in the *atk4* mutant. (A) Relative gene expression of *BAM1* and *AtK4* in wild-type leaves and epidermal peels relative to the expression of *ActII*. Oligonucleotides used for qPCR analysis are shown in Table 4.2. Bars represent averages of three technical replicates ± SE. (B) Photographs of 4 week-old Col-0 wild type (WT) and *atk4* mutant plants grown in soil under standard 12 h light / 12 h night growth conditions. (C) Leaves of 4 week-old Col-0 wild type (WT) and *atk4* mutant plants were collected at the end of the night and stained with Lugol solution. (D) Starch granule area per guard cell was determined following confocal microscopy imaging from PS-PI stained epidermal peels collected at the indicated time points. Values represent averages from at least 35 guard cells ± SE from a single experiment.

Because the results obtained so far show only the *in vitro* phosphorylation of BAM1 by AtK4, we started to investigate the phosphorylation pattern of BAM1 *in vivo* using a mass spectrometry based phosphoproteomic approach. Fragment ion spectra were obtained through nano-scale liquid chromatography coupled with MS/MS analysis (LC-MS/MS) at the Functional Genomics Centre Zürich (FGCZ) (see Material and Methods for details). Peptides were mapped to the Arabidopsis proteome based on the TAIR10 genome using the MASCOT search engine (Matrix Science, Boston,

USA). Prior to harvest, plants were treated with ABA, which was shown to induce the transcription of *BAM1* in mesophyll cells (Material and Methods; Chapter 3). In peptide samples without a phosphoenrichment proceedure only few fragment ion spectra assigned to BAM1 could be identified, leading to overall low sequence coverage (approximately 10%), with no phosphopeptides assigned to BAM1 (data not shown). This might be due to the low BAM1 protein abundance even under ABA treatment compared to other cellular proteins. Therefore, we enriched phosphopeptides using a Ti-IMAC approach following the trypsin digestion of the sample proteins. BAM1-derived peptides, identified with high certainty (expect value < 0.05) following the enrichment of phosphopeptides are shown in Table 4.5 and the results are summarized in Table 4.4.

Table 4.4: Overview of the number of detected phosphorylation sites in the two identified sequences of Arabidopsis BAM1. All identified peptides with an expect value < 0.05 (see Table 4.5) were considered for wild type and *atk4* samples. The last row indicates in how many peptides the phospho modification was found for the indicated Ser residue.

peptide sequence	genotype	total number of peptides considered	phosphorylation site	phosphosites detected
SGEMTDSSLLSISPPSAR	wild type	6	S29	
			S31	6 out of 6
			S34	
	atk4	6	S29	1 out of 6
			S31	4 out of 6
			S34	1 out of 6
AHGTDPSPPMSPILGATR	wild type	8	T52	1 out of 8
			S55	7 out of 8
			S59	8 out of 8
	atk4	7	T52	1 out of 7
			S55	6 out of 7
			S59	7 out of 7

Two phosphorylated peptides (corresponding to a sequence coverage of 6%) were observed in all the phospho-enriched samples: AHGTDPSPPMSPILGATR, which includes the putative GSK3 phosphorylation motif and SGEMTDSSLLSISPPSAR, which is part of the N-terminal cTP region (Figure 4.1 and Table 4.5). In the N-terminal region of wild type and *atk4* plants, 10 out of 12 phospho-modifications occurred at Ser^{31}. In two other cases, serine residues two amino acids downstream or upstream of Ser^{31} were predicted to be phosphorylated. If this is due to a miss annotation, which can occur due to the close proximity of the Ser residues, is not

clear at the moment, but we propose that Ser^{31} is most likely the phosphorylation site in the cTP.

For the second peptide, which includes the (S/T)P-XX-(S/T)P motif, we found 15 fragmentation ion spectra that fit the expected m/z values with high certainty (Table 4.5). In all 15 peptides, Ser^{59} was phosphorylated, while Ser^{55} was predicted to be phosphorylated in 13 peptides, with two additional phosphorylation sites assigned to Thr^{52} (Table 4.4). The assignment of the latter two phosphorylation sites might be a false annotation, indicated by the low prediction probabilities obtained from these two fragment ion spectra (49.56% and 78.73% respectively) (Table 4.5).

Taken together, our results confirm the previously observed phosphorylation sites found in large-scale phosphoproteomic studies (Table 4.3), with no additional phospho-modifications identified. Furthermore, no unphosphorylated peptides were identified with an expect value < 0.05, indicating an effective enrichment proceedure.

We did not observe any differences between wild type samples and proteins extracted from the *atk4* mutant (Table 4.4 and Table 4.5). Furthermore, phosphopeptides with the phosphorylation of Ser^{59} were clearly observed in *atk4* mutant BAM1 proteins, suggesting that AtK4 may not be the only responsible kinase for the phosphorylation of this amino acid residue in BAM1 and that other members of this kinase family are able to partially complement the loss of AtK4 in the mutant plants. It should be mentioned that our experimental procedure yields only a qualitative, not a quantitative, description of the phosphorylation patter in BAM1. It is therefore possible that the frequency of Ser^{59} phosphorylation is indeed reduced in the *atk4* mutant plants. The establishment of quantitative phosphoprotemic techniques can help to solve this question (see Conclusion and Outlook).

Table 4.5: Identified BAM1 phosphopeptides detected with high certainty (expect value < 0.05) in wild type and *atk4* plants. For each peptide the most probable phosphorylation sites are indicated in red. If alternative phosphorylation sites were predicted with a probability score higher than 5% they are indicated in the prediction probability column in brackets. The peptide containing the putative GSK3 phosphorylation is AHGTDPSPPMSPILGATR with Ser^{55} at position 7 and Ser^{59} at position 11 in this peptide. The phosphopeptide of the cTP (SGEMTDSSLLSISPPSAR) contains the Ser^{31} at position 13. °M denotes an oxidized methionine residue.

Wild type	peptide sequence	prediction probability	expect value	expected m/z	delta
Replicate 1	SGEMTDSSLLSISPPSAR	S31 95.13%	1.7E-04	957.9297	0.0007
	SGE°MTDSSLLSISPPSAR	S31 92.17%	2.2E-09	965.9282	0.0028
	SGE°MTDSSLLSISPPSAR	S31 45.42% (S29 29.73%)	1.7E-02	965.9289	0.0042
	AHGTDPSPPMSPILGATR	S55, S59 59.71% (T52, S11 39.09%)	1.2E-03	982.9199	-0.0012
	AHGTDPSPPMSPILGATR	S55, S59 80.91% (T52, S11 16.18%)	2.2E-03	982.9213	0.0017
	AHGTDPSPP°MSPILGATR	T52, S55 49.56% (S55, S59 46.35%)	2.9E-04	990.9189	0.002
Replicate 2	SGE°MTDSSLLSISPPSAR	S31 77.79% (S34 6.59%)	7.1E-07	965.9278	0.002
	AHGTDPSPPMSPILGATR	S55, S59 67.55% (T52, S59 31.09%)	1.6E-02	982.9185	-0.004
	AHGTDPSPPMSPILGATR	S55, S59 85.04% (T52, S59 9.79%)	9.0E-05	982.9203	-0.0003
	AHGTDPSPP°MSPILGATR	S55, S59 60.24% (T52, S59 36.81%)	3.7E-03	660.9478	0.0001
	AHGTDPSPP°MSPILGATR	S55, S59 91.31%	7.1E-05	990.9181	0.0003
Replicate 3	SGE°MTDSSLLSISPPSAR	S31 76.39% (S34 20.28%)	1.1E-04	965.9269	0.0001
	SGE°MTDSSLLSISPPSAR	S31 79.06% (S34 11.48%)	3.4E-03	965.9312	0.0087
	AHGTDPSPP°MSPILGATR	S55, S59 91.54%	5.4E-05	990.9187	0.0015
atk4	peptide sequence	prediction probability	expect value	expected m/z	delta
Replicate 1	AHGTDPSPPMSPILGATR	S55, S59 59.72% (T52, S59 38.29%)	3.2E-04	982.9194	-0.0021
	AHGTDPSPP°MSPILGATR	S55, S59 99.74%	3.4E-07	990.9196	0.0034
	SGE°MTDSSLLSISPPSAR	S31 86.72% (S29 6.79%)	1.3E-03	965.9226	-0.0084
	SGE°MTDSSLLSISPPSAR	S34 88.59% (S31 11.2%)	1.7E-06	965.9281	0.0026
	SGEMTDSSLLSISPPSAR	S31 99.32%	5.7E-08	957.9326	0.0064
	AHGTDPSPPMSPILGATR	T52, S59 78.73 (S55, S59 18.33%)	3.2E-03	982.9216	0.0022
Replicate 2	SGEMTDSSLLSISPPSAR	S31 99.06%	2.1E-07	957.9304	0.0021
	SGE°MTDSSLLSISPPSAR	S31 98.48%	1.6E-06	965.9274	0.0012
	AHGTDPSPPMSPILGATR	S55, S59 75.68% (T52, S59 23.93%)	4.8E-04	982.9222	0.0034
	AHGTDPSPP°MSPILGATR	S55, S59 81.72% (T52, S59 15.08%)	2.0E-05	990.9179	-0.0002
	AHGTDPSPP°MSPILGATR	S55, S59 66.42% (T52, S59 23.9%)	1.1E-02	660.9498	0.0063
Replicate 3	SGE°MTDSSLLSISPPSAR	S29 30.97% (S31 29.11%) (T23 26.36%)	3.5E-05	965.9285	0.0034
	AHGTDPSPP°MSPILGATR	S55, S59 99.08%	9.7E-06	990.9176	-0.0007

Discussion

Carbon metabolism is known to respond to changes in environmental conditions such as osmotic stress (see Chapter 3) and drought conditions (Damour et al., 2008; González-Cruz and Pastenes, 2012). BAM1, together with AMY3, degrades starch during the day under osmotic stress. This enables Arabidopsis plants to better cope with the adverse environmental condition through reallocation of carbon compounds. (Chapter 3). The elucidation of the molecular mechanism underlying these changes in carbon partitioning will increase our understanding of plant stress physiology, leading to the identification of novel targets for plant breeding. One aspect of the regulation was shown to be ABA-dependent activation of *BAM1* transcription in mesophyll cells (Chapter 3). Furthermore, BAM1 is also important during the rapid stomatal opening through the degradation of guard cell starch under normal growth conditions (Chapter 1), suggesting a complex regulatory network.

Besides transcriptional regulation, posttranslational modifications are increasingly described for enzymes involved in starch synthesis and degradation (Kötting et al., 2010; Santelia et al., 2015). Here, we showed that a kinase of the GSK3-like family phosphorylates BAM1 *in vitro* at Ser^{59}, a modification that is also found *in vivo* using mass spectrometry based phosphoproteomic approaches (Figure 4.3 and Table 4.4). Besides BAM1, other enzymes related to starch synthesis and degradation are known to be phosphorylated (Kötting et al., 2010), but what triggers this posttranslational modification and its consequences are not known. Using phosphomimic versions of the recombinant BAM1 protein expressed in *E. coli*, we did not observe a significant change in enzymatic activity through the introduction of a negative charge at either Ser^{55} or Ser^{59} (Figure 4.2). Besides a direct influence on enzyme activity, protein phosphorylation is known to be able to alter subcellular localization, protein stability and protein complex formation (Cohen, 2000).

Tetlow and colleagues reported the *in vitro* phosphorylation of starch branching enzymes in wheat amyloplasts, which is proposed to change its enzymatic activity as well as protein complex formation of different isoforms of BEs and SSs (Tetlow et al., 2004, 2008). Furthermore, a PHS1 homologue from maize was shown to form a protein complex with starch synthases and branching enzymes in the seed amyloplast (Hennen-Bierwagen et al., 2008; Liu et al., 2009), while the PHS1 homologue from wheat forms a complex with BEs (Tetlow et al., 2004). In both cases the role of this protein complex formation is not clear and even less information is available concerning possible protein complexes in Arabidopsis.

The signalling pathway leading to BAM1 phosphorylation in either mesophyll or guard cells is not known. In both cell types many proteins are phosphorylated in response to ABA, including important regulators of stomatal behaviour such as the ion channels SLAC1 and KAT1, as well as ABA-RESPONSIVE ELEMENT BINDING 1 (AREB1) transcription factors in mesophyll cell (Fujita et al., 2009). However, the phosphorylation of BAM1 at Ser^{55} or at Ser^{59} was not amongst the ABA responsive posttranslational modifications observed in a recent report (Wang et al., 2013a). BAM1 phosphorylation was also not reported to depend on the presence of the ABA-responsive SnRK kinases, suggesting that transcriptional regulation of *BAM1* upon stress treatment is dependent on ABA (see Chapter 3), while posttranslational phosphorylation is not. It is possible that the phosphorylation of BAM1 is a positive regulatory mechanism in stomatal opening involved in the rapid degradation of guard cell starch (Chapter 1) and that this posttranslational modification does not influence stress induced starch degradation in mesophyll cells. Indeed, we found evidence that AtK4 participates in the regulation of guard cell starch degradation (Figure 4.4), but an additional involvement in mesophyll carbon metabolism under stress cannot be ruled out at the moment.

AtK4 and related Arabidopsis GSK3-like kinases such as ASK11 and ASK12, which form sub-clade I (Jonak and Hirt, 2002) might work together to activate a variety of targets during the adaptation process to environmental stress conditions. ASK11 (also referred to as ASKα) was recently shown to activate a cytosolic isoform of GLUCOSE-6-PHOSPHATE DEHYDROGENASE (G6PD) in response to salt and oxidative stress (Dal Santo et al., 2012). G6PD catalyses a key step in the oxidative pentose phosphate pathway, which helps to generate NADPH for the detoxification of reactive oxygen species. Although ASK11 is considered to phosphorylate a cytosolic target (Dal Santo et al., 2012), an influence on the plastidial response to stress conditions by this or other GSK3-like kinases cannot be ruled out.

The redundancy in GSK3-like kinase function in plants might also be an explanation for the observed phosphorylation of Ser^{59} in the *atk4* mutant plants. One limitation of our analysis using mass spectrometry is the qualitative nature of the results, which makes it impossible to rule out if the extend of Ser^{59} phosphorylation is reduced in the *atk4* mutant. The remaining phosphorylation events could be well due to the redundant action of other GSK3-like kinases. Therefore, the establishment of quantitative phosphoproteomic approaches for the investigation of BAM1 phosphorylation will be crucial as a next step in the elucidation of BAM1 regulation (see Conclusion and Outlook).

Another question that needs to be addressed in the future is the exact role of the different phosphorylation sites. GSK3-like kinases were reported to require a stable substrate-kinase interaction, which is achieved in animal cells through the specific interaction of the kinase with a phosphopeptide of the substrate protein, therefore requiring the initial modification of an amino acid usually situated at the +4 position from the GSK3 target residue (ter Haar et al., 2001; Dajani et al., 2001). This introduces the so-called priming phosphate, which can be specifically bound by GSK3-like proteins. Based on this, we would expect the priming phosphorylation of Ser^{59} by a distinct kinase followed by the AtK4-mediated phosphorylation of Ser^{55}, which is clearly not the case in our *in vitro* experiment (Figure 4.3 A). It was recently shown that BIN2 activity does not require a priming phosphorylation of its substrate, the transcription factor BRASSINAZOLE-RESISTANT 1 (BZR1), but rather establishes a relatively strong protein-protein interaction through a specific 12 amino acid long peptide (Peng et al., 2010). The requirement of priming phosphate sites in plants is therefore less strict and the interaction of BAM1 with AtK4 might rely on different factors. It might be illuminating to investigate this protein-protein interaction using different BAM1 mutant versions, including S55A and S55D BAM1, in yeast two hybrid and co-immunoprecipitation experiments.

In previous phosphoproteomic studies, as well as in our own analysis, a phosphopeptide derived from the BAM1 cTP was found, with the phosphorylation predicted to occur at Ser^{31} (Table 4.3 and Table 4.4). Several studies indicate that cTP sequences can be phosphorylated by a small family of cytosolic Ser/Thr kinases in order to assist the binding of 14-3-3 proteins (May and Soll, 2000; Martin et al., 2006). Together with the Hsp70, the 14-3-3 proteins and the target preprotein build a complex that interacts with the primary import receptor Toc34 at the outer chloroplast membrane. This mechanism promotes the preferential uptake of these complexed preproteins into the chloroplast (May and Soll, 2000; Schleiff et al., 2002). Interestingly, Ser^{31} of the BAM1 cTP and the surrounding amino acid sequence ($S^{29}I^{30}S^{31}P^{32}P^{33}$) resembles a putative 14-3-3 protein binding site of the SXSXP consensus sequence, with the phosphorylation of the C-terminal Ser^{31} required for 14-3-3 binding (Yaffe et al., 1997). Therefore, Ser^{31} phosphorylation through a cytosolic kinase might induce binding of 14-3-3 proteins to the cTP sequence, facilitating the preferential import of the BAM1 preproteins into the plastids. It is tempting to speculate that this mechanism is involved in the response to stress conditions, when the transcription of *BAM1* is induced through ABA-signalling in mesophyll cells (see Chapter 3). If the Ser^{31} phosphorylation is also involved in the

regulation of BAM1 activity in guard cells should be addressed in the future using guard cell enriched samples (see Conclusion and Outlook). These working hypotheses would add another layer to the regulation of BAM1-mediated starch degradation in the light, but further research is required to clearly establish a role of cTP phosphorylation in BAM1.

In order to address this questions, the use of quantitative phosphoproteomics (Picotti and Aebersold, 2012) will be a valuable tool to elucidate the role of protein phosphorylation in the regulation of starch metabolism enzymes.

5 – Starch synthesis in Arabidopsis guard cells

Daniel Horrer, Sabrina Flütsch, Diana Pazmino, Arianna Nigro, Diana Santelia

Synopsis

Starch synthesis was so far mostly studied in mesophyll cells. Here we provide first insights into the early steps of guard cell starch synthesis, namely the generation of the glucosyl donor ADP-Glc. Furthermore, we provide evidence for a role of sugar import into the chloroplast and argue against a primary role of guard cell photosynthetic carbon fixation for the provision of sugars.

Experimental contributions: Sabrina Flütsch performed the experiments shown in Figure 5.2 E and helped with the analysis of experiments shown in Figure 5.3 E and 4.3 F. Diana Pazmino performed the qPCR analysis shown in Figure 5.3 D. Arianna Nigro isolated the homozygous *gpt1* mutant line.
Figure 5.2 E was previously published as part of the Master Thesis submitted by Sabrina Flütsch at the University of Zürich, 2015.

Introduction

Despite a long history of research and the importance of plant water use efficiency for agriculture, the molecular pathways of guard cell carbon metabolism are largely unknown (Vavasseur and Raghavendra, 2005; Lawson, 2009). We could recently establish the genetic and molecular basis of guard cell starch degradation in *Arabidopsis thaliana* (Chapter 1). This process is thought to be important for providing the carbon skeletons for malate and possibly sucrose and hexose synthesis to increase the osmotic potential in these cells. In contrast to the diurnal rhythm of mesophyll starch accumulation and breakdown, Arabidopsis guard cells show rapid starch degradation early in the morning, which is crucial for proper stomatal function and plant biomass accumulation (Chapter 1). After this initial phase of starch degradation, granules reappear after an additional 2 h of illumination and starch synthesis continues in an almost linear fashion well into the dark phase (Chapter 1).

Starch is formed by the oligosaccharides amylopectin and amylose and can be found in storage organs like potato tubers and cereal grains or as transitory starch in many different plant cell types including root cap cells. Both oligosaccharides consist of linear chains of α-1,4-linked glucose molecules, which can contain α-1,6-linked branch points (Streb and Zeeman, 2012). The activated glucosyl donor ADP-Glucose (ADP-Glc), the substrate for the synthesis of the linear chains, is generally assumed to be formed through the subsequent action of PHOSPHOGLUCOSE ISOMERASE (PGI), which converts Fructose-6-phosphate (Fru6P) into Glucose-6-phosphate (Glc6P), followed by the PHOSPHOGLUCOSEMUTASE (PGM) catalysed conversion of Glc6P into Glucose-1-phosphate (Glc1P) and the final reaction catalysed by ADP-GLUCOSE PYROPHOSPHORYLASE (AGPase) (Figure 5.1 A). AGPase uses Glc1P and ATP to synthesize ADP-Glc and inorganic pyrophosphate (PP_i). This reaction is made irreversible through the rapid hydrolysis of PP_i into orthophosphate. ADP-Glc is subsequently used by STARCH SYNTHASEs (SSs) for the synthesis of the linear oligosaccharides, while both branching enzymes (BEs) and debranching enzymes (DBEs) are necessary for the correct introduction of branch points, which are crucial for the formation of the semi-crystalline layers of the starch granule (Streb and Zeeman, 2012).

Mesophyll cell starch synthesis is mainly regulated at the level of the heterotetrameric AGPase enzyme. The Arabidopsis genome codes for two genes of the AGPase small subunit (*APS1* and *APS2*) and four genes of the AGPase large

subunit (*APL1-4*) (Lin et al., 1988a, 1988b; Crevillén et al., 2003; Ventriglia et al., 2008). The main catalytic subunit of AGPase is the ubiquitously expressed APS1, while APS2 was shown to be inactive due to several mutations in its catalytic site (Crevillén et al., 2003). Although APL1 and APL2, but not APL3 and APL4, were recently shown to be able to catalyse the synthesis of ADP-Glc in the presence of a catalytically inactive form of APS1, the large subunits are thought to be primarily involved in the regulation of AGPase activity rather than participating in catalysis (Crevillén et al., 2003; Ventriglia et al., 2008). Different isoforms of the large subunit were shown to influence kinetic and allosteric regulatory properties of the active AGPase enzyme. Enzymatic activity is elevated by high concentrations of the Calvin cycle intermediate 3-phosphoglycerate (3-PGA) and inhibited by high cellular concentrations of inorganic phosphate, linking the synthesis of starch to the activity of carbon assimilation (Crevillén et al., 2003). The heterotetramers consisting of two subunits of APS1 and two subunits of APL1 show a high sensitivity to the 3-PGA/P_i ratio and high affinity to Glc1P, while APL3 and APL4 containing heterotetramers show a much lower response to the allosteric regulators (Crevillén et al., 2003). Furthermore, the activity of AGPase can be increased through the reductive opening of a disulphide bridge between the two N-terminal parts of the small subunits (Fu et al., 1998; Tiessen et al., 2002; Hendriks et al., 2003). This redox control of AGPase activity, presumably through the action of thioredoxins, links starch synthesis to the activity of photosystem I (PSI).

It is possible that different catalytic properties in source and sink tissue are dependent on differences in the composition of the regulatory AGPase subunits. *APL1* is mainly expressed in photosynthetically active source tissues, while *APL2* is generally expressed at very low levels. In contrast, *APL3* and the highly similar *APL4*, sharing 88% identity at the protein level (Crevillén et al., 2003), are primarily expressed in sink tissues such as roots, flowers and fruits (Crevillen et al., 2005; Tsai et al., 2009). Furthermore, the expression of the *APL3* and *APL4* genes can be induced through sugar signalling, which presumably changes the large subunit composition of the AGPase and therefore reduces its sensitivity towards allosteric effectors (Crevillen et al., 2005).

During the day, Arabidopsis mesophyll cells partition approximately 40 - 50% of the assimilated carbon into starch as energy reserves for the night (Zeeman and Ap Rees, 1999). Carbon assimilation is a result of the Calvin cycle, which utilizes ATP and reducing equivalents in the form of NADPH produced through the light reaction of photosynthesis to drive a series of reactions. The key enzymatic step is catalysed by RIBULOSE-1,5-BISPHOSPHATE CARBOXYLASE/OXYGENASE (RubisCO),

which consists of a barrel shaped homotetramer of the catalytic large subunit and two tetrameric caps formed by the small chain subunits (Andersson, 2008). In contrast to mesophyll cells, the source of sugars for starch synthesis in guard cells is not known, especially because the capacity of guard cells to photosynthetically fix CO_2 is still debated (Lawson, 2009). Initially, the capacity of carbon assimilation in these cells was questioned in general (Outlaw et al., 1982). Later, studies using chlorophyll content as a basis for quantification contradicted these earlier studies. Zemel & Gepstein confirmed the presence of Rubisco in guard cell chloroplasts by *in situ* cytoimmunofluorescence approach using intact epidermal peels of *Vicia faba* (Zemel and Gepstein, 1985). While Gotow and colleagues argued for carbon fixation in the plastids of guard cells for generating osmolytes (Gotow et al., 1988), other research groups suggested a very low contribution of the Calvin cycle to osmolyte accumulation (Shimazaki et al., 1989; Reckmann et al., 1990). Therefore, we hypothesized that guard cell starch synthesis requires sugars derived from mesophyll cells, which are imported from the apoplast (Figure 5.1 B). Alternatively, osmolytes excreted from the vacuole during stomatal closure could be used as substrates for starch synthesis (Figure 5.1 B), explaining the continued starch synthesis during the first hours of the dark phase, although import of sugars derived from mesophyll starch breakdown could also explain this observation. Substrates for starch synthesis as well as for the oxidative pentose phosphate pathway (OPPP) and biosynthetic pathways like the shikimic acid synthesis can be imported from the cytosol into the chloroplasts. The inner envelope membrane of the plastid forms the permeability barrier for carbon compounds. The plastidic phosphate translocator (pPT) protein family exchanges inorganic phosphate with phosphorylated C_3-, C_5- or C_6-compounds across this membrane (Facchinelli and Weber, 2011). The Arabidopsis pPT gene family consists of 6 nuclear coded genes for functional antiporters, which facilitate the 1:1 exchange of phosphate and phosphorylated carbon compounds under physiological conditions (Flügge, 1992; Kammerer et al., 1998).

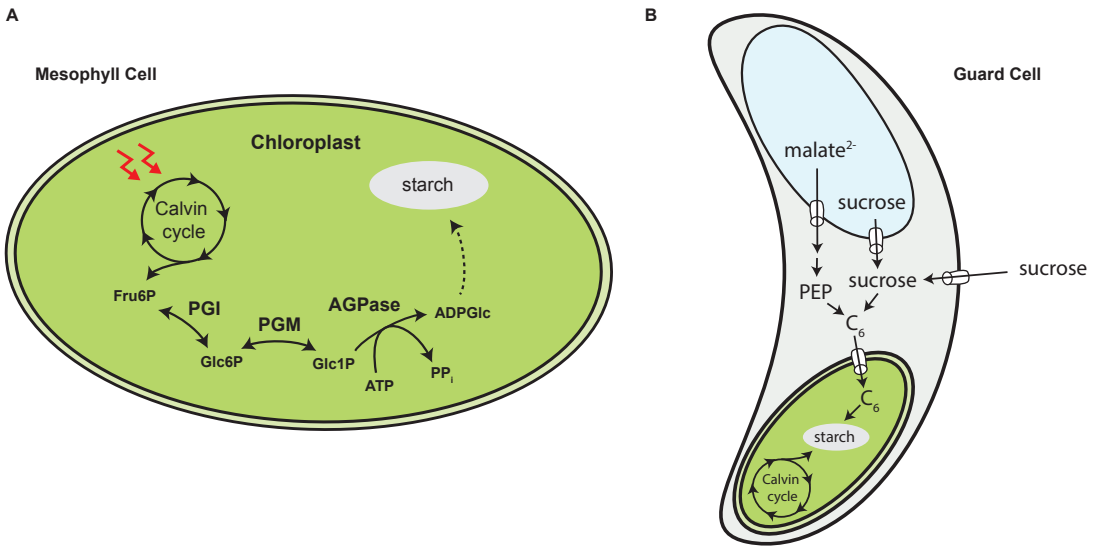

Figure 5.1: Pathway of starch synthesis. (A) In mesophyll cells starch is synthesised from sugars derived from the Calvin cycle. Alternatively, sugars are exported to the cytosol (not shown). (B) Possible sources for sugars used in guard cell photosynthesis. For details please refer to the text.

Two genes of the pPT family code for Glucose-6-phosphate / phosphate antiporters (GPT1 and GPT2), which facilitate the import of Glc6P, but not Glc1P or Fru6P into plastids of non-green tissues (Kammerer et al., 1998; Knappe et al., 2003). The Glc6P can be used for the synthesis of starch, while the antiport activity with inorganic phosphate ensures the phosphate equilibrium. *GPT1* was shown to be preferentially expressed in heterotrophic tissues like roots and reproductive organs, while the expression of *GPT2* seems to be generally low with the exception of senescing leaves and sepals (Niewiadomski et al., 2005). Furthermore, *GPT1* expression was found to be 10-fold higher in guard cell protoplasts compared to mesophyll protoplasts (Niewiadomski et al., 2005) and guard cells were shown to contain Glc6P import activity at the plastidial envelope membrane (Overlach et al., 1993). While the role of GPTs in many heterotrophic tissues is well established, their suggested role in guard cell plastids still lacks experimental support.

In this project, we intended to investigate the origin of the sugars used as substrates for the synthesis of guard cell starch and to elucidate the functional role of the different APL isoforms in *Arabidopsis thaliana* guard cells.

Material and Methods

Plant material

Seeds of the *gpt1* mutant allele (SALK_021762) in the Col-0 background were ordered from the Nottingham Arabidopsis Stock Centre (NASC) and genotyped using oligonucleotides according to Table 5.1. The *apl3-1* (FLAG_458A07) mutant line was provided by Alison Smith (John Innes Centre, Norwich, UK) and the *apl4-3* (SALK_108632) line was provided by Samuel Zeeman (ETH, Zürich, Switzerland). The other single mutants used in this study were described previously: *apl1* (*adg2*) (Lin et al., 1988b), *pgm1-1* (Caspar et al., 1985) and *pgi1-1* (Yu et al., 2000).

The *apl3-1apl4-3* double mutant was created by initially back-crossing of the *apl3-1* mutant four times into the Col-0 wild type in order to reduce the Was background. Crosses using either the Col-0 WT or the *apl3-1* mutant as the pollen donor always yielded heterozygous plants in the expected ratio. In each generation heterozygous *apl3* mutant plants were selected by genotyping using primers according to Table 5.1. Heterozygous *apl3* mutants of the fourth generation were crossed with homozygous *apl4* plants, followed by the selection of $apl3^{+/-}apl4^{+/-}$ plants in the F1 generation and finally double homozygous *apl3-1apl4-3* mutants.

The *gpt1pgi1-1* double mutant was created by crossing the corresponding single mutants and the subsequent screening of the F2 population for homozygous double mutants. In the initial screening population only $gpt1^{-/-}pgi1\text{-}1^{+/-}$ plants were found, which were kept for seed production and the final selection of double homozygous plants in the F3 generation. Genotyping of the *gpt1* allele was performed by PCR using the oligonucleotides described in Table 5.1.

Genotyping of the *pgi1-1* point mutation was done by sequencing the PCR product obtained using the pgi_fw and pgi_rev oligonucleotides (Table 5.1). 1 µl of purified genomic DNA was used in a standard GoTaq G2 (Promega, Fitchburg, USA) PCR reaction with the pgi_fw and pgi_rev oligonucleotides (Table 5.1) according to manufacturers description, followed by column purification using the Wizard SV Gel and PCR Clean-Up System (Promega, Fitchburg, USA). 2 µl of the purified PCR reaction (around 100 ng) was used in the sequencing reaction with the pgi_rev oligonucleotide (Table 5.1). Sequencing chromatograms were visually analysed for the single C to T substitution at base 834 (Yu et al., 2000). In the case of heterozygous plants a double peak corresponding to both C and T bases could be clearly observed at this position.

For all genotyping PCR reactions genomic DNA was isolated from plants using the CTAB buffer method. Around 20 mg of plant material was homogenized in 200 µl 2x CTAB buffer (2% CTAB, 1% Polyvinylpyrolidon, 100 mM Tris-HCl pH8, 20 mM EDTA, 1.4 M NaCl). After a 30 min incubation period at 65°C, the homogenate was mixed with 200 µl of a 24:1 chloroform:isoamylalcohol solution and centrifuged at 12.000 g for 5 min. The upper aqueous phase was transferred in a fresh tube and the DNA was precipitated adding 200 µl isopropanol. The pellet obtained after centrifugation for 15 min at 12.000 g was washed once with 100 µl 70% ethanol followed by centrifugation at 12.000 g for 5 min. The pellet was resuspended in 100 µl distilled H_2O.

Table 5.1: Oligonucleotides used in this study

Oligo ID	line	Atg code	sequence
Primers used for genotyping			
gpt1_fw	SALK_021762	At5g54800	TTGACATACTCACCGTTGCAG
gpt1_rev	SALK_021762	At5g54800	TCTCTCCCAGTATATACGCGC
pgi1-1_fw	TSY254	At4g24620	AGGAACTCTAAGCTCGCACC
pgi1-1_rev	TSY254	At4g24620	ACAAACAAAATTGAGTGGGAGT
apl3_fw	FLAG_458A07	At4g39210	GGAGGTTTCACATTCTCTCCC
apl3_rev	FLAG_458A07	At4g39210	TCCTATAGCATCCACCCACAG
apl4_fw	SALK_108632	At2g14640	CGAATTAGGACCTCAAGGGTC
apl4_rev	SALK_108632	At2g14640	GTGATCTCTTATGGCTGCAGG
LBb1.3			ATTTTGCCGATTTCGGAAC
FLAG			CTACAAATTGCCTTTTCTTATCGAC
Primers used for qPCR analysis			
apl3_fw		At4g39210	TGGCATAAACTTTGGAGATGG
apl3_rev		At4g39210	CTTAGCATCCTCAAACACCC
apl4_fw		At2g14640	GCTGAGAAATGTCGGATGG
apl4_rev		At2g14640	ACATCAATGTATCCTGAAGCTC

Growth conditions and drought stress experiment

Plants were grown in controlled climate chambers as described in Chapter 4. For the investigation of plant water loss and survival under water limiting conditions, seeds were germinated after three days of stratification in standard growth conditions. One-week-old seedlings were transplanted into single pots containing 60 g of sieved soil, previously watered for exactly 25 min. Seedlings were initially covered with transparent lids, which were removed after six days. After another six days, plants

were watered by soaking the pots for 5 min in water. 25 days after germination pots weighted again approximately 60 g, indicating a relatively low soil water content. At this time point the measurements for determining the relative plant water content were started (day 0). When the weight of the pots reached 40 g at day six (corresponding approximately to the dry weight of the initial 60 g of soil), plants showed severe signs of wilting. The remaining plants were soaked for 30 minutes in water and the rate of survival was determined two days later (day 8).

Full rosettes were collected at each time point and the fresh weight (FW) was determined, after which the rosettes were floated on distilled water for 24 h in order to gain the full turgor weight (TW). Finally, rosettes were dried completely at 60°C, after which the dry weight (DW) was measured. The relative leaf water content (RWC) was determined as described previously (Smart and Bingham, 1974) using the following equation:

RWC = 100 x (FW – DW) / (TW - DW).

Guard cell starch quantification from full leaves and blended peels

Guard cell starch content from full leaves was quantified using the mPS-PI staining method described in Chapter 4.

In a second experimental system, epidermal peel fragments were isolated by blending the middle part of mature leaves number 5 and 6 of at least 4 Arabidopsis rosettes for 30 sec in 100 ml distilled H2O using a Sorvall Omni Mixer (Thermo Fisher Scientific, Waltham, USA). During the isolation plants and epidermal fragments were kept in the dark in order to avoid the induction of stomatal opening. Fragments of the epidermis were collected in a 200 µm mesh (Sefar, Thal, Switzerland), washed with water and transferred into 12-well plates containing 1 ml of basic opening buffer (5 mM MES/BIS-TRIS propane pH 6.5, 50 mM KCl, 0.1 mM CaCl2). Epidermal fragments were adapted to the buffer conditions for 1 h in the dark at 22°C in a temperature controlled climate chamber (Fytoscope FS130, Photon System Instruments, Drasov, Czech Republic). After this initial incubation period a fraction of peels was collected in 1.5 ml reaction tubes containing 1 ml fixative solution (time point 0) and the remaining peels were illuminated with 300 µmol m-2 s-1 of red light from light emitting diodes (LEDs) and peels were collected at the indicated time points in fixative solution. Staining was performed in the 1.5 ml reaction tubes following the protocol described in Chapter 4 with the exception that the destaining step was not necessary. In order to remove solutions from the tubes, epidermal fragments were pelleted by centrifugation at 12.000 g for 30 sec. During

image acquisition epidermal fragments from the abaxial side of the leaves could be clearly distinguished from adaxial epidermal fragments based on the jigsaw like shape of their epidermal cells.

Plant protein isolation and SDS-PAGE analysis

Proteins were isolated from 3 to 4 mature rosettes ground in liquid nitrogen using a mortar and pestle. Alternatively, proteins were isolated from epidermal peel fragments, prepared as described above (Chapter 4). In both cases approximately 150 – 200 mg of plant tissue was mixed with 200 µl 2x extraction buffer (200 mM MOPS buffer pH 6.8, 2 mM EDTA, 10 mM DTT, 20% ethylene glycol, 1x protease inhibitor (Roche, Basel, Switzerland)), vortexed and centrifuged for 10 min at 4°C, 13.000 g. The supernatant was transferred into a fresh tube and centrifuged again at 13.000 g, 4°C for 10 min. The supernatant was again transferred into a fresh tube and used for protein quantification with the Bradford assay using the Biorad Protein assay kit (Biorad, Hercules, USA). 10% SDS-PAGE gels were cast und run using the Biorad Mini-Protean Gel system (Biorad, Hercules, USA). 10 µg of the plant proteins were loaded per well.
Protein gels were stained with Coomassie staining solution (40% (v/v) methanol, 10% (v/v) glacial acetic acid, 0.1% (w/v) Coomassie R250) over night. After washing the gels in H2O, destaining was performed with destaining solution (20% (v/v) methanol, 10% (v/v) glacial acetic acid) until a good contrast between bands and background was achieved.

qPCR analysis

qPCR analysis of gene expression was performed as described above (Chapter 4) using the oligonucleotides listed in Table 5.1.

Qualitative and quantitative mesophyll starch quantification

For the qualitative visualization of the starch content in full leaves, rosettes were harvested at the end of the night (EoN) or at the end of the 12 h light phase (EoD). Plant material was immediately transferred into 80% (v/v) ethanol for destaining until all chlorophyll was removed. Destained leaves were then immersed in the Lugol solution (Iodine/Potassium iodide solution, Sigma-Aldrich, St. Louis, USA) for one to

two hours. Excess Lugol solution was washed away with distilled H2O and plants were imaged with a Canon EOS 60D camera.

Full rosette starch quantification followed a previously published protocol based on the enzymatic conversion of starch-derived glucose coupled to NADH production, which can be quantified using a spectrophotometer (Smith and Zeeman, 2006). Full rosettes of 3 to 4-week-old plants were harvested at the indicated time points, immediately frozen in liquid nitrogen and stored at -80°C. Plant material was homogenized in 0.7 M cold perchloric acid (1 ml per 150 mg tissue) using precision glass tubes (B.Braun AG, Melsungen, Germany). Of the homogenate, 1 ml was transferred in new 2 ml reaction tubes on ice containing 2 glass beads (4 mm in diameter), followed by centrifugation at 4°C, 10.000 g for 5 min. After the supernatant was removed, the insoluble pellet was washed with 500 µl ice cold H2O using the mixer mill MM300 (Retsch, Haan, Germany) to ensure complete resuspension of the samples. Subsequently, the samples were centrifuged at 4°C, 10.000 g for 3 min. The supernatant was discarded and the washing step was repeated at least twice with 1 ml 80% ice-cold ethanol. Excess ethanol was dried for one to two hours at room temperature, after which the pellet was resuspended in H2O, using 600 µl for end of night samples and 800 µl for end of day samples.
Two 200 µl aliquots of each starch sample were transferred into screw cap tubes and boiled in a water bath at 95°C for 15 min, followed by the enzymatic hydrolysis of the solubilized starch into glucose molecules. For this 10 µl of a 9:1 mixture of amyloglucosidase and α-Amylase (Roche, Basel, Switzerland), in a total volume of 200 µl of 0.22 M Na-Acetate buffer pH 4.8, was added to one of the aliquots, while for a control reaction only Na-Acetate buffer without enzymes was added to the second aliquot of each starch sample. The hydrolysis reaction was incubated at 37°C for 2 h.
After a brief centrifugation at 10.000 g, between 2 and 45 µl of the supernatant was used for the glucose assay in a 96-well microplate (see Table 5.2 for guidelines). For this 50 µl of a master mix containing 25 mM HEPES-KOH pH 7.5, 1 mM MgCl2, 1 mM ATP, 1 mM NAD and 1.4 U Hexokinase (Roche, Basel, Switzerland) was mixed with the samples and H2O was added up to 198 µl in each well. Samples were prepared in three technical replicates. After the initial read of the absorbance at 340 nm using the Synergy H1 plate reader (BioTek Instruments, Winooski, USA), 2 µl of a 1:4 diluted Glucose-6-P-Dehydrogenase (from *Leuconostoc mesenteroides*, Roche, Basel, Switzerland) was added in order to convert the Glc-6-P provided by the Hexokinase into 6-P-Glucono-δ-lacton. For each oxidized Glc-6-P one NADH is

generated, which increases the absorbance of the reaction mix at 340 nm. The reaction was followed through the continuous measurement of the absorbance at 340 nm for 40 min to ensure a complete conversion.

For the calculation of the starch content, the initial reads were subtracted from the final read values. To correct for sugar contamination of the starch samples, the read values of the non-hydrolysed control reactions were subsequently subtracted and an average of the replicates for each sample was calculated. From this the amount of starch per g of fresh weight of each sample was calculated using a glucose standard curve.

Table 5.2: Guideline on sample volume for glucose assay

no starch excess (*sex*) phenotype e.g. wild type, *bam1* mutant	End of Day 5 µl End of Night 45 µl
mild to medium sex phenotype e.g. *bam3* mutant	End of Day 3 µl End of Night 4 µl
strong sex phenotype e.g. *bam1bam3* mutant	End of Day 2 µl End of Night 2 µl

Results

The capacity of guard cells to photosynthetically fix CO_2 is widely debated in the literature (Lawson, 2009) and the source of Glc1P for the synthesis of ADP-Glc during guard cell starch synthesis is not known. In order to gain first insights into the nature of guard cell carbon metabolism, we investigated publicly available transcriptomic data from intact guard cells (Bates et al., 2012). Because the RNA in this study was extracted from manually dissected, freeze-dried guard cells, instead of isolating it from GCPs after the time consuming and harsh protoplasting procedure used in previously studies (Leonhardt et al., 2004; Yang et al., 2008; Pandey et al., 2010), this data can be considered a better representation of the actual transcriptome of guard cells. Interestingly, the gene expression of all selected Calvin cycle enzymes were found to be strongly reduced in intact guard cells (Table 5.3), suggesting a low capacity of Arabidopsis guard cells to generate sugars via the Calvin cycle. On the other hand, the transcriptomic data of the large Rubisco subunit did not show a significant reduction (Table 5.3). We therefore isolated proteins from full leaves and from epidermal peels containing only guard cells as viable cells and analysed the protein band pattern on a Coomassie stained SDS-PAGE (Figure 5.2 A). The strong band of the full leaf protein extracts running at around 50 kDa is commonly observed on polyacrylamide gels loaded with crude Arabidopsis protein extracts and represents the large subunit of Rubisco (RBCL, AtCg00490). Intriguingly, the protein pattern of the epidermal peel samples lacked a visible 50 kDa RBCL band. This indicates that, although no significant differences were found on the level of gene expression, the amount of RBCL is strongly reduced in guard cells compared to mesophyll cells on a total protein basis (Table 5.3, Figure 5.2 A), at least under our experimental conditions. Therefore it seems unlikely that a significant amount of sugars for starch synthesis originates from the guard cell Calvin cycle.

Table 5.3: Published guard cell transcriptomic data for genes involved in starch biosynthesis. Data from Bates *et al.* 2012. RNA from manually dissected guard cells was hybridized to an Affymetrix ATH1 chip.

Abbreviation	Name	Atg code	leaf	guard cell	log2 fold difference
RBCL	Ribulose bisphosphate carboxylase large chain	AtCg00490	10.1	8.2	n.s.
RBCS1A	Ribulose bisphosphate carboxylase small chain 1A	At1g67090	13.7	12.5	-1.1
RBCS1B	Ribulose bisphosphate carboxylase small chain 1B	At5g38430	---	---	---
RBCS2B	Ribulose bisphosphate carboxylase small chain 2B	At5g38420	---	---	---
RBCS3B	Ribulose bisphosphate carboxylase small chain 3B	At5G38410	---	---	---
RCA	Ribulose bisphosphate carboxylase activase	At2g39730	13.4	11.4	-2
RMT	Rubisco methyl transferase	At1g14030	---	---	---
PGK1	3-Phosphoglycerate Kinase 1	At3g12780	7.8	5.7	-2.1
PGK2	3-Phosphoglycerate Kinase 2	At1g56190	10	7.7	-2.3
GAPA1	Glyceraldehyde-3-phosphate Dehydrogenase subunit A1	At3g26650	13.1	11.4	-1.7
GAPA2	Glyceraldehyde-3-phosphate Dehydrogenase subunit A2	At1g12900	11.9	10.2	-1.7
GAPB	Glyceraldehyde-3-phosphate Dehydrogenase subunit B	At1g42970	11.9	10.2	-1.7
TPI	Plastidic Triosephosphate Isomerase	At2g21170	10.8	9.7	n.s.
FBA1	Sedoheptulose/fructose-bisphosphate aldolase 1	At2g21330	11.3	6.4	-4.9
FBA2	Sedoheptulose/fructose-bisphosphate aldolase 2	At4g38970	12.8	9.9	-2.9
cFBP1	chloroplastic Fructose-1,6-bisphosphate phosphatase 1	At3g54050	11	7.2	-3.9
SBPase	Sedoheptulose-1,7-bisphosphate phosphatase	At3g55800	11.3	8.5	-2.8
TKL1	Transketolase 1	At3g60750	11.8	9.5	-2.3
RPE	Ribulose-5-phosphate Epimerase	At5g61410	12.2	9.8	-2.4
RPI	Ribulose-5-phosphate Isomerase	At3g04790	10.6	8.5	-2.2
PRK	Phosphoribulokinase	At1g32060	12	8.8	-3.3
GPT1	Glucose-6-phosphate / phosphate translocator 1	At5g54800	7.2	8.7	1.5
GPT2	Glucose-6-phosphate / phosphate translocator 2	At1g61800	---	---	---
PGI	Phosphoglucose isomerase	At4g24620	8.9	8.4	n.s.
PGM	Phosphoglucomutase	At5g51820	7.8	5.7	-2.1
APS1 (ADG1)	ADP-glucose pyrophosphorylase small subunit 1	At5g48300	10.1	9.2	n.s.
APS2	ADP-glucose pyrophosphorylase small subunit 2	At1g05610	4.1	4.6	n.s.
APL1 (ADG2)	ADP-glucose pyrophosphorylase large subunit 1	At5g19220	9.4	5	-4.4
APL2	ADP-glucose pyrophosphorylase large subunit 2	At1g27680	6.1	6.9	n.s.
APL3	ADP-glucose pyrophosphorylase large subunit 3	At4g39210	5.6	7	n.s.
APL4	ADP-glucose pyrophosphorylase large subunit 4	At2g21590	4	7.9	3.9
GBSS	Granule-bound starch synthase 1	At1g32900	---	---	---
SS1	Soluble starch synthase 1	At5g24300	8.5	8.3	n.s.
SS2	Soluble starch synthase 2	At3g01180	7.1	6.6	n.s.
SS3	Soluble starch synthase 3	At1g11720	6.9	6.4	n.s.
SS4	Soluble starch synthase 4	At4g18240	7.6	7.1	n.s.
BE1	Starch branching enzyme 1	At3g20440	---	---	---
BE2	Starch branching enzyme 2	At5g03650	9.1	8.4	n.s.
BE3	Starch branching enzyme 3	At2g36390	8	8.1	n.s.
ISA1	Isoamylase 1	At2g39930	7.7	5.9	-1.8
ISA2, DBE1	Isoamylase 2	At1g03310	6.8	5.3	n.s.

The first step usually attributed to the pathway of mesophyll starch synthesis is the conversion of Fru6P into Glc6P by the plastidial isoform of PGI. The EMS mutant *pgi1-1* shows a strongly reduced growth rate caused by the insufficient synthesis of transitory starch during the day and therefore a premature depletion of energy reserves during the night (Yu et al., 2000; Figure 5.2 B and C). Most of the photosynthetically fixed carbon is exported from mesophyll chloroplasts and either metabolized further or exported in the form of sucrose. A certain fraction can be re-imported into the plastids in the form of Glc6P (Kammerer et al., 1998), which explains the remaining starch synthesis capacity of *pgi1-1* leaf cells (Figure 5.2 C). Glc6P is primarily imported into plastids by GPT1, with this transporter showing a slight increase in guard cell transcript abundance compared to mesophyll cells (Table 5.3). Generally, the GPT1 mediated import of sugars into chloroplasts is important for optimal growth as indicated by the reduced growth of the *gpt1* mutant, although the effect was much less pronounced compared to the *pgi1-1* phenotype and did not alter transitory leaf starch accumulation in any major way (Figure 5.2 B and C).

In order to investigate the relative contribution of Glc6P import by GPT1 and PGI mediated conversion of Fru6P into Glc6P in guard cell starch synthesis, we investigated the guard cell starch content in intact leaves of the corresponding mutants over the 12 h light phase (Figure 5.2 D). Guard cells of the wild type quickly degraded their starch at the onset of light, followed by resynthesis during the remainder of the day. Interestingly, starch content in guard cells of the *gpt1* mutant showed a similar pattern to that of wild type, although with overall reduced starch contents throughout the day and an apparent lag phase of starch synthesis evident at around 3 h of illumination. This lag phase was also observed in *pgi1-1* plants, while the starch content in the afternoon rose to wild type levels (Figure 5.2 D). These results suggest an involvement of both PGI and GPT1 in supplying Glc6P for starch synthesis in guard cells, therefore suggesting that both sugar import and carbon fixation in the guard cell chloroplast are important for starch synthesis.

In a second experiment we illuminated epidermal peels with 300 µmol m^{-2} s^{-1} red light, which would not induce starch degradation, but could possibly drive guard cell photosynthesis (Figure 5.2 E). Starch synthesized in these peels floating on a buffer containing 5 mM MES-bistrispropane pH 6.5, 50 mM KCl, 0.1 mM $CaCl_2$, would presumably originate from guard cell photosynthesis, because the import of apoplastic sugars is not possible. As expected, we did not observe guard cell starch degradation, which is induced by blue, but not red light (Chapter 1, Figure 5.2 E).

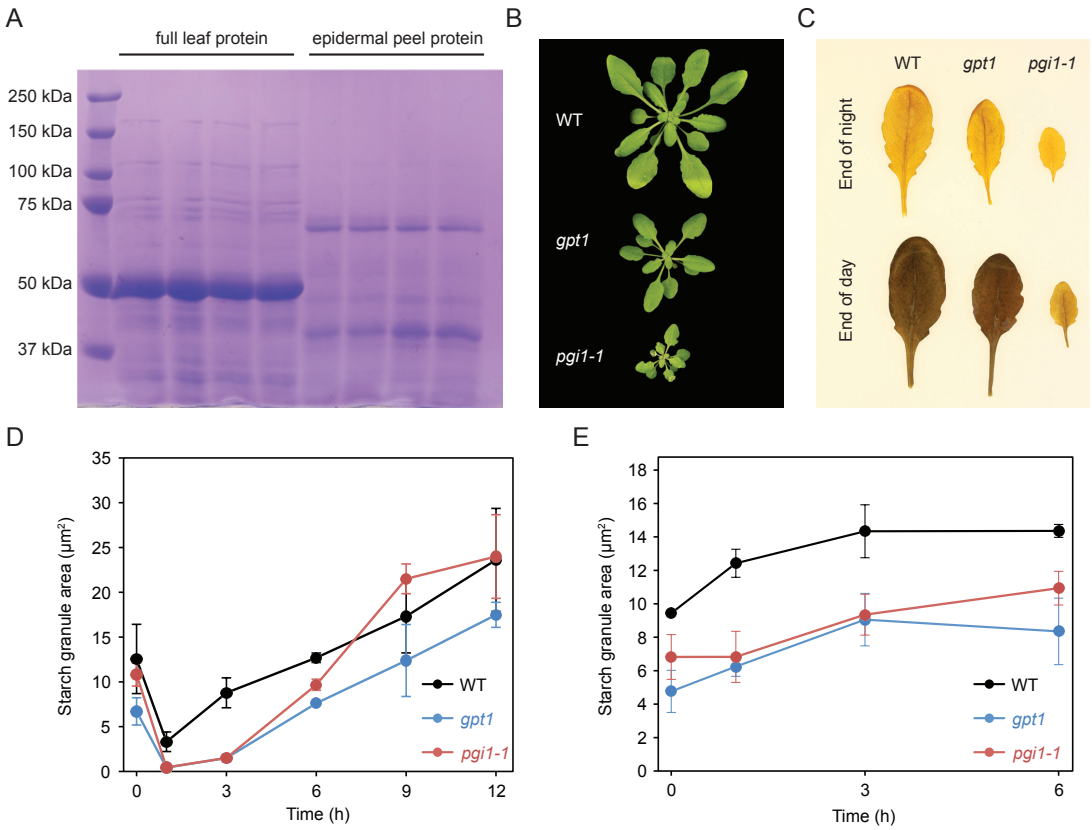

Figure 5.2: Guard cell starch content in *gpt1* and *pgi* mutants. (A) Coomassie stained 10% SDS-PAGE loaded with 10 µg protein per lane shows differences in the abundance of the large subunit of Rubisco between protein samples from full leaves and epidermal peels. (B) Pictures of 3.5 weeks old Col-0 WT, *gpt1* and *pgi1-1* mutant plants grown under a mixture of white and purple light at 120 µmol m^{-2} sec^{-1} in 12 h light, 12 h dark cycles. (C) Lugol staining of leaf number 6 collected from 3.5-week-old Col-0 WT, *gpt1* and *pgi1-1* plants at the end of the night or at the end of the day. (D) Guard cell starch content of Col-0 WT, *gpt1* and *pgi1-1* intact leaves over the 12 h light phase under illumination with 120 µmol m^{-2} s^{-1} white light. Values shown are averages of two independent experiments ±SE (n > 70 guard cells). (E) Guard cell starch content in epidermal peels prepared from Col-0 WT, *gpt1* and *pgi1-1* plants incubated with 300 µmol m^{-2} s^{-1} of red light. Values represent the averages of three independent experiments ±SE with at least 110 analysed guard cells. Data in Figure 5.2 E was published previously (Sabrina Flütsch, Master Thesis at the University of Zürich, 2015).

In contrast, starch synthesis proceeded in isolated wild type guard cells, showing an increase in starch content of approximately 50% within the 6 h of the experiment. Similarly to intact leaves, the overall starch levels were reduced in *gpt1* mutant guard cells compared to wild type, yet they did show a 75% increase in starch content throughout the experiment. These results suggest a small but significant contribution of guard cell photosynthesis. Surprisingly, we also observed starch synthesis in *pgi1-1* mutants with the guard cell starch values increasing approximately 60% between 0 h and 6 h, indicating a contribution of guard cell photosynthesis for providing sugar substrates used in starch synthesis.

In mesophyll cells, the AGPase heterotetramer consists mainly of the two small APS1 subunits together with two regulatory APL1 proteins, conferring high sensitivity to the allosteric regulators and to its substrate (Crevillén et al., 2003). Although starch synthesis in guard cells is known to occur over most of the light phase (Chapter 1), we do not know much about the responsible enzymes. Most importantly, the composition of the heterotetrameric AGPase in guard cells, thought to be the key regulatory step in starch synthesis, is not known. It is tempting to speculate that in guard cells, similar to heterotrophic cells containing starch granules like root tip cells, the AGPase is composed of the APS1 and the APL3 and / or APL4 subunits (Ventriglia et al., 2008). The primary role of APL1 in regulating mesophyll starch synthesis is indicated by the stunted growth phenotype of *apl1* mutants and their reduced starch content in full leaves at the end of the light phase (Figure 5.3 A and B). In contrast, the *apl3* mutant in the Wasiljevskaja (Was) wild-type background and the *apl4* mutant in the Col-0 background did not show obvious alterations in either growth or starch accumulation (Figure 5.3 A and B). These results were confirmed by quantitative analysis of the starch content of full rosettes, where *apl1* mutant plants show a clear reduction in starch content per g fresh weight at the end of the day (Figure 5.3 C), while *apl3* mutants surprisingly showed a significantly higher starch content when compared to the Was wild type plants (unpaired Student's *t* test, $P < 0.01$) (Figure 5.3 C).

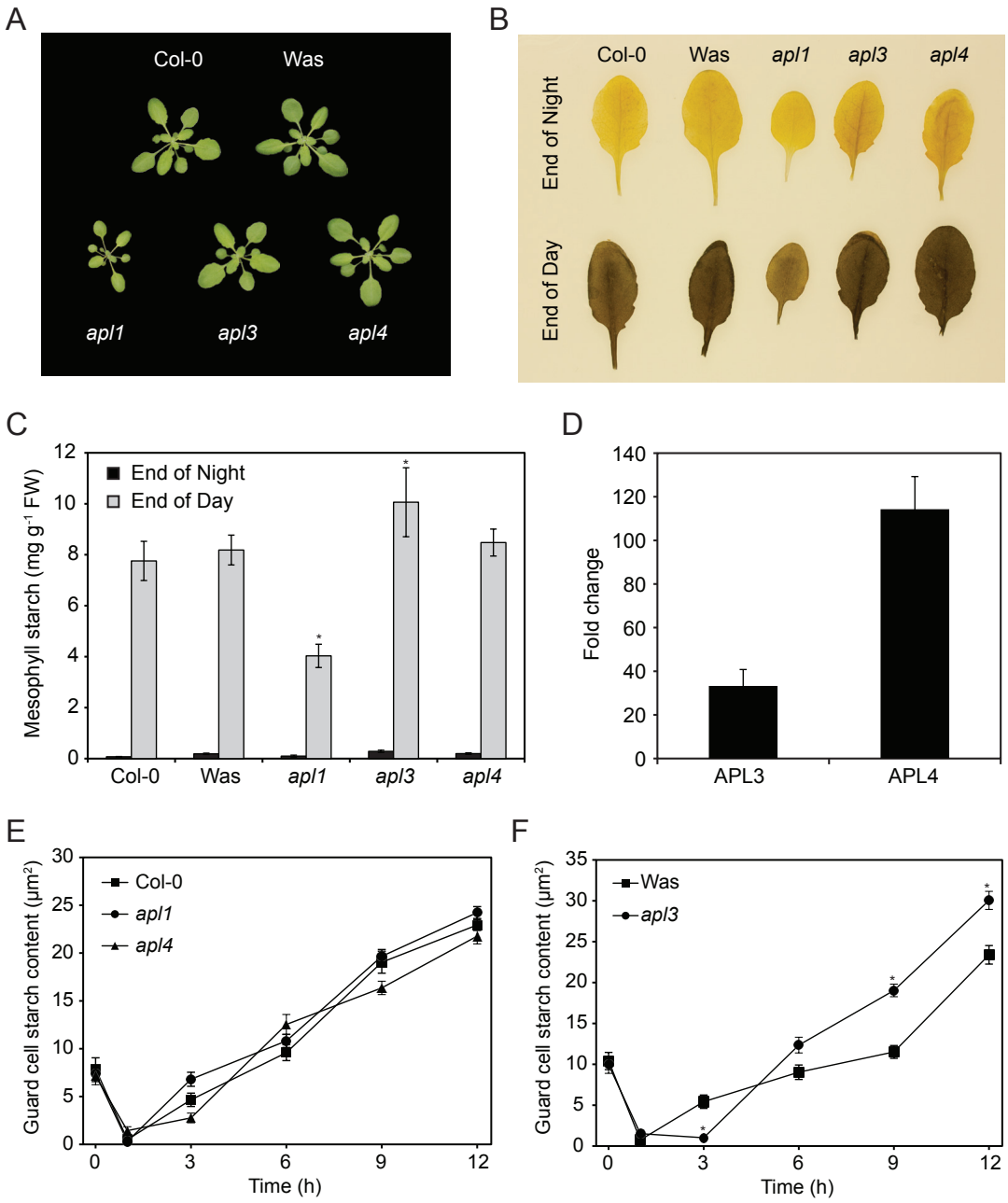

Figure 5.3: Loss of APL3, but not APL4 causes changes in guard cell starch accumulation. (A) 3-week-old Arabidopsis wild type plants of the ecotypes Col-0 and Was and mutant *apl1*, *apl3* and *apl4* plants. (B) Lugol stained single leaves of Col-0, Was, *apl1*, *apl3* and *apl4* plants harvested at the end of the night and at the end of the day. (C) Mesophyll starch content in the two wild type ecotypes and the three *apl1*, *apl3* and *apl4* single mutants harvested at the end of the day and at the end of the night. Bars represent averages from 8 individual plants ±SE. Asterisks indicate significant differences compared to the corresponding wild type (unpaired Student's *t* test, $P < 0.01$). (D) qPCR analysis of *APL3* and *APL4* expression in epidermal peels compared to full leaves ±SE. (E) and (F) Quantification of guard cell starch content from mPS-PI stained epidermal peels. For each time point the starch content of 40 guard cells taken from four individual plants was determined. (E) Guard cell starch content of the *apl1* and *apl4* mutants in comparison to the Col-0 wild type background. (F) Starch content in guard cells of the *apl3* single mutant compared to the corresponding wild type Was. An asterisk denotes statistical significant differences between wild type and mutant plants (unpaired Student's *t* test, $P < 0.01$).

Transcriptome data published by Bates and colleagues indicate a low expression level of *APL1*, while *APL4* expression was significantly higher in guard cells compared to mesophyll cells (Table 5.3). In contrast, no significant changes in the expression levels were observed for *APL2*, *APL3* or the small subunit *APS1*. This suggests a different subunit composition of the AGPase enzyme in Arabidopsis guard cells. In order to investigate if APL3 and the closely related APL4 protein, which share 88% sequence identity (Crevillén et al., 2003), are the major regulatory subunit in these cells, we investigated the gene expression in epidermal peels by qPCR analysis and confirmed the strong preferential expression of *APL4* (Figure 5.3 D). In contrast to the previous report, we also observed a strong upregulation of *APL3*, although less pronounced than the cell type specific expression of *APL4* (Table 5.3, Figure 5.3 D).

In a next step we quantified the starch content in guard cells of the *apl1*, *apl3* and *apl4* mutants. Single *apl1* and *apl4* mutant plants showed no strong difference in guard cell starch content when compared to the Col-0 controls (Figure 5.3 E). Both mutants degrade guard cell starch within the first hour of the day, followed by starch synthesis throughout the remaining day in a near linear fashion. Similar overall starch content and rates of degradation and synthesis were observed in the Was wild type guard cells (Figure 5.3 F). In contrast, the observed pattern of starch accumulation was different in the *apl3* single mutant. While starch content at the end of the night was similar to the wild type and was also degraded within the first hour, starch re-synthesis started only after three hours of light and became visible in the middle of the day. Surprisingly, the overall increase in starch content in *apl3* guard cells after this initial lag phase was higher than in all other investigated genotypes, leading to an approximately 30% higher starch content at the end of the day (Figure 5.3 F). It seems possible that the APL3 regulatory subunit is necessary for early starch synthesis by the AGPase enzyme complex. Its loss could lead to an AGPase conformation with a higher proportion of other APL isoforms, such as the close homologue APL4. This in turn might lead to an increased starch synthesis throughout the rest of the day, ultimately leading to a guard cell starch excess phenotype. In order to investigate a possible functional redundancy of APL3 and APL4 in guard cells, we created the *apl3apl4* double mutant in the Col-0 background (see Material and Methods).

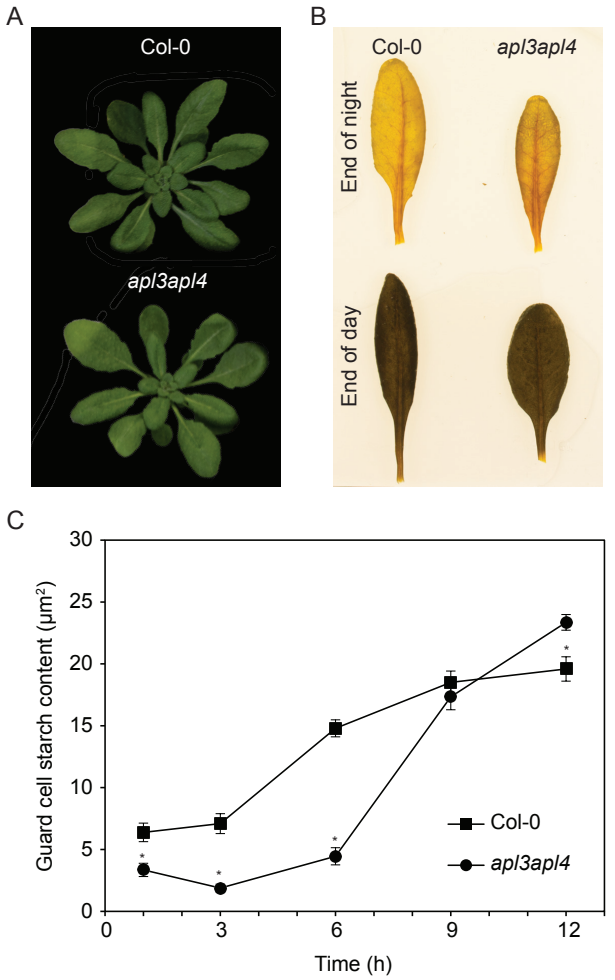

Figure 5.4: Analysis of the newly created *apl3apl4* double mutant. (A) 4-week-old Arabidopsis plants of the Col-0 wild type and the apl3apl4 double mutant. (B) Fully developed leaves of 4-week-old Col-0 and apl3apl4 plants were harvested at the end of the night and at the end of the 12 h light phase and stained with Lugol solution. (C) Guard cell starch content as determined from confocal microscopy pictures of PS-PI stained epidermal peels. Values are averages of at least 35 analysed guard cells from four individual plants. Asterisks indicate significant differences in starch content (unpaired Student's *t*-test, $P < 0.01$).

In contrast to the *apl1* single mutant, the *apl3apl4* double mutant does not depict an obvious growth defect (Figure 5.3 A and Figure 5.4 A). Furthermore, starch synthesis during the day does not seem to be affected in any major way (Figure 5.4 B), although quantitative determination of leaf starch content will be needed in order to investigate if the slightly higher mesophyll starch observed in the *apl3* single mutant (Figure 5.3 C) is also present in the double mutant.

In the initial investigation of the *apl3apl4* mutant, we found only low levels of guard cell starch during the first half of the day (Figure 5.4 C). While the lag phase in the *apl3* single mutant was observed only at the 3 h time point compared to wild-type guard cells, the additional loss of APL4 seems to prolonge the phase with reduced starch synthesis rates. Surprisingly, a strong increase in guard cell starch content

was observed between 6 h and 9 h of the 12 h light phase. Guard cell starch content at the end of the day reached an elevated level compared to the wild type, similar, although less pronounced than in the *apl3* single mutant (Figure 5.3 F and Figure 5.4 C). It is therefore clear that the right subunit composition of the AGPase is crucial for the regulation of starch synthesis in guard cells.

Finally, we wanted to investigate the physiological effects of reduced or completely blocked starch synthesis in guard cells. It was previously shown that the starchless *pgm* mutant stomata opened much slower in response to blue light compared to wild type and that this difference in the opening kinetics leads to a decrease in transpirational water loss (Lasceve et al., 1997). As suggested by this report, as well as in our gas exchange measurements on the *bam1* and *amy3bam1* mutants (Chapter 1), we reasoned that the reduced transpiration in the *pgm* mutant would lead to a drought tolerant phenotype. We therefore investigated the behaviour of *pgm* mutant under water limiting growth conditions as an extreme case of the absence of starch synthesis. Indeed, no starch granules were visible at the end of the day in *pgm* guard cells stained with the PS-PI method (Chapter 1, Figure 5.5 A).
The relative water content in full rosettes of *pgm* plants was significantly higher at almost all time points throughout the experiment (Figure 5.5 B), indicating that the reduced stomatal aperture could lead to a drought tolerance, with a delayed reduction in RWC compared to wild type plants. Under severe water limiting conditions (at day 6), no statistically significant differences could be observed between WT and *pgm* plants, but upon re-watering almost all of the *pgm* mutant plants recovered, while approximately one quarter of the wild type plants could not (Figure 5.5 B and C). In contrast, the pot weight measured over the course of the experiment indicates a similar rate of soil drying (Figure 5.5 D), suggesting that the observed drought resistant phenotype is due to the loss of the PGM protein and not to a difference in soil water evaporation.

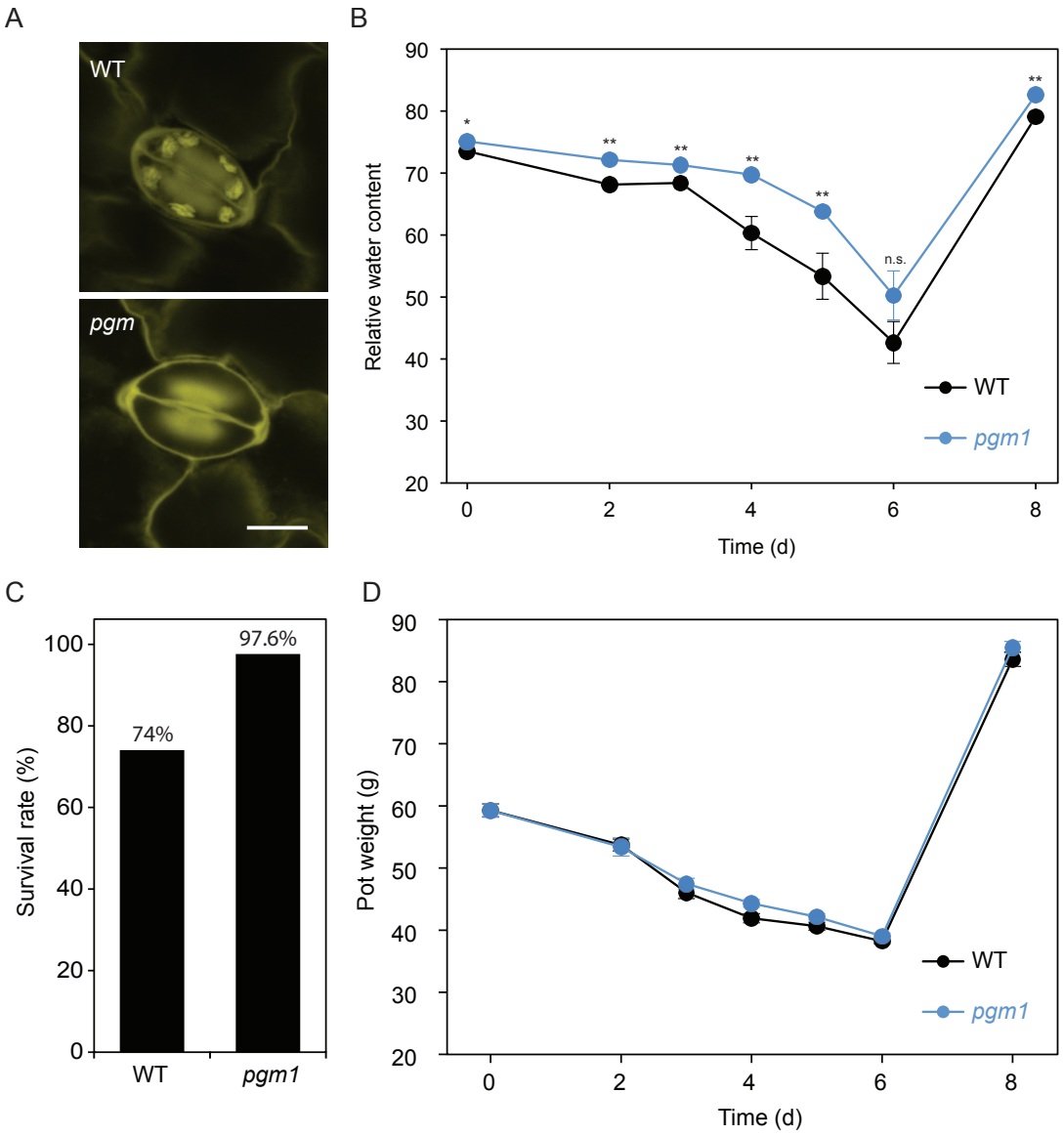

Figure 5.5: Investigation of the *pgm* mutant phenotype.
(A) Wild type and *pgm* mutant mPS-PI stained guard cells from epidermal peels collected at the end of the 12 h light phase. Scale bar = 10 µm. (B) Relative water content of WT and *pgm* mutant plants under water limiting conditions. For details of the experimental procedure see the Material and Methods section. Asterisks indicate statistically significant differences (n = 18, unpaired Student's *t* test, * denotes $P < 0.05$; ** denotes $P < 0.01$; n.s. = not significant). (C) Plant survival rates of at least 25 plants were calculated after rewatering at day 8 of the drought stress experiment shown in (B). (D) Pot weight as an indicator of soil water content was measured at each time point of the experiment shown in (B) (n = 18).

Discussion

The question wether guard cells can produce significant amounts of osmolytes through photosynthesis, or if they rely on starch breakdown and sugar import from the apoplast, is a long standing debate (Lawson, 2009). We showed that starch degradation is an important process during the early opening of Arabidopsis stomata, with the *amy3bam1* double mutant guard cells being almost completely inhibited in their responses to light (Chapter 1). Here we wanted to address the question wether the sugars used for the synthesis of starch in guard cells originate from apoplastic sugars or from guard cell photosynthesis. Several research groups argued over the last decades that guard cells, although containing all enzymes necessary for photosynthetic carbon assimilation (Zemel and Gepstein, 1985; Gotow et al., 1988), are not able to produce significant amounts of sugars through the Calvin cycle (Tarczynski et al., 1989; Shimazaki, 1989; Reckmann et al., 1990). In accordance with this, Bates and colleagues reported a strong reduction in Calvin cycle related gene transcripts (Table 5.3). Furthermore, we observed a strong reduction in the RBCL subunit in proteins isolated from epidermal peels compared to mesophyll cells (Figure 5.2 A). This suggests that sugar uptake from the apoplast serves as the major source of substrates for starch synthesis, besides its proposed role in the accumulation of guard cell osmolytes.

Sucrose content in the apoplast surrounding guard cells was shown to increase during the day, correlating with increases in cellular sucrose levels, therefore suggesting an uptake of sucrose by plasma membrane sucrose importer (Tallman and Zeiger, 1988; Poffenroth et al., 1992; Kang et al., 2007). Indeed, sucrose uptake into guard cell protoplasts of *Pisum sativum* and *Vicia faba* guard cells was previously reported (Lu et al., 1995; Ritte et al., 1999) and the sucrose / H^+ symporter SUC3 was suggested as the responsible transporter based on its expression in guard cells (Meyer et al., 2004). In the cytoplasm, sucrose can be cleaved by cytosolic INVERTASES (cytINV) (Sherson et al., 2003), releasing Fru and Glc. Alternatively, sucrose can be cleaved by the reversible reaction catalysed by SUCROSE SYNTHASEs (SUSs), which are highly active in guard cells (Hite et al., 1993) and UDP-GLUCOSE PYROPHOSPHORYLASE (UGPase), releasing Fru and Glc1P. Furthermore, apoplastic sucrose is thought to be processed by cell wall INVERTASES (cwINV) (Sherson et al., 2003), releasing Fru and Glc in the apoplast, of which at least the latter could be imported into the cytoplasm of guard cells through the monosaccharide / H^+ symporter SUGAR TRANSPORT PROTEIN 1

(STP1) and related proteins such as STP4, which are highly expressed in these cells (Stadler et al., 2003; Bates et al., 2012). Cytosolic Glc and Fru are subsequently phosphorylated by HEXOKINASE (HXK) and FRUCTOKINASE (FRK) (Granot, 2008). Finally, hexose phosphates can be imported into the guard cell plastids, where they serve as substrates for starch synthesis. In addition to sugar import from the apoplast, another source of substrates for starch synthesis could be provided by osmolytes exported from the vacuole at the end of the day. This, together with sugars derived from night-time starch degradation in mesophyll cells, could explain the observed extension of starch synthesis in guard cells into the night phase (see Chapter 1).

Interestingly, HXK is known to act as a sugar sensor, influencing the transcription levels of ABA related genes (Ramon et al., 2008). Besides its crucial role in generating hexose phosphates, HXK was recently implicated in the regulation of stomatal closure. Kelly and colleagues showed that the overexpression of *AtHXK1* from the guard cell specific *KST1* promoter (Müller-Röber et al., 1995) in tomato and Arabidopsis plants leads to a reduction in stomatal opening, indicating a role of HXK1-mediated sugar signalling in stomatal movements, most likely via the alterations of ABA synthesis or ABA sensitivity (Kelly et al., 2013). This would also explain the inhibitory effect of extracellular glucose and sucrose on stomatal opening (Lawson et al., 2014). HXK1 is therefore proposed to play a role in a feedback regulatory loop linking mesophyll photosynthesis to stomatal regulation via a sugar-dependent rise in ABA signalling (Kelly et al., 2013; Lawson et al., 2014). It is possible that early in the day cytoplasmic sucrose does not accumulate to levels sufficient to induce HXK1-dependent sugar signalling due to the import of sucrose into the vacuole and the import of sucrose breakdown products into plastids for starch synthesis. Only in the afternoon, when sucrose levels are already high in the vacuole and starch synthesis has progressed significantly, rising in cytosolic sugar levels induces stomatal closure via HXK1. Therefore, the questions concerning guard cell sugar metabolism are not limited to its contribution to osmolytes and to the substrate pool for starch synthesis, but also to a more general role in guard cell regulation, which is not well understood. Besides the suggested role of STP1 and SUC3, which are mainly based on their expression in guard cells (Stadler et al., 2003; Meyer et al., 2004), the exact molecular pathway of sugar import into the guard cell cytosol, the metabolic interconversions of sugars and the relative contributions to both osmolyte accumulation and starch synthesis are not well understood and will be an important future research area for understanding guard cell metabolism.

Similar to the sugar transport over the guard cell plasma membrane, the importer of carbohydrates into guard cell plastids are not well known, although many are characterized for the inner envelope of the mesophyll chloroplasts, which is generally considered to comprise the diffusion barrier (Facchinelli and Weber, 2011; Flügge et al., 2011).

In order to get first insights into the role of plastidial sugar import for guard cell starch synthesis, we investigated the starch content in guard cells of intact leaves of the *gpt1* mutant. We could observe a strong overall reduction in starch content, with a pronounced lag phase in starch synthesis in the first half of the day compared to wild type guard cells, where starch granules already reappeared after 3 h of illumination (Figure 5.2 D). Therefore, despite the proposed diverse set of plastidial carbohydrate transporters, the loss of the Glc6P import capacity of the single knockout mutant *gpt1* leads already to a remarkable loss of starch synthesis, clearly establishing GPT1 as a major importer of sugar substrates for guard cell starch synthesis. The continuous rise in starch content in this mutant during the afternoon could be explained by the import activities of other transporters, especially the closely related GPT2. Although usually not described as a major contributor to sugar import into plastids, Bates and colleagues recently reported a strong induction of *GPT2* expression in guard cells of leaf strips floated on a solution containing 150 mM sucrose (Bates et al., 2012). We therefore propose the involvement of GPT2 in the late afternoon import of Glc6P for starch synthesis, through a mechanism involving transcriptional activation of *GPT2* in response to high sucrose levels in guard cells during the second half of the day (Talbott and Zeiger, 1996). In order to test this hypothesis further, the *gpt2* as well as the *gpt1gpt2* double mutants should be included in future experiments. Alternatively, the starch accumulation observed in *gpt1* could be due to guard cell photosynthesis, although the transcript levels of Calvin cycle enzymes (Table 5.3), as well as RBCL protein concentrations (Figure 5.2 A), together with previous reports (Tarczynski et al., 1989; Shimazaki, 1989; Reckmann et al., 1990) suggest that guard cell carbon assimilation would be insufficient to explain the observed increase in guard cell starch content in intact leaves (Figure 5.2 D). It should be mentioned that the contribution of guard cell photosynthesis was always investigated in relation to the early morning osmolyte accumulation, but not for its role in providing substrates for guard cell starch synthesis, which progresses over a longer part of the day. Therefore, a certain part of sugars used for the synthesis of starch could still originate from the guard cell Calvin cycle. Indeed, in epidermal peels floating on a standard opening buffer without sugar supplement, starch synthesis still occurred in wild type and *gpt1* mutant guard cells (Figure 5.2 E). The rate of wild type and *gpt1*

guard cell starch accumulation was small and comparable, although *gpt1* contained less starch overall. Starch levels were reduced at the end of the day in guard cells of *gpt1*, which might cause lower starch content throughout the night and therefore lower starch levels at the beginning of the next light phase.

We propose that guard cell photosynthesis can contribute to a certain extent to starch synthesis in guard cell chloroplasts. The amount of starch after 6 h of red light illumination in the experiment using epidermal peels (Figure 5.2 E) was similar to the levels observed under white light around midday (Figure 5.2 D), but considering the initial starch breakdown in the plants under white light illumination, the starch synthesis rate in the intact leaves is much higher. Additionally, intact wild type leaves under sole red light illumination (300 µmol m^{-2} s^{-1}) increased their starch content between the end of the night and midday (6 h into the light) to approximately 19 $µm^2$, an increase to 316% of the initial value (Sabrina Flütsch, unpublished results). Therefore, the small increase of starch observed in epidermal peels represents only a small fraction of the overall starch synthesis occurring in guard cells of intact leaves, suggesting that sugar import from the apoplast contributes to most of the substrates required for starch synthesis, with the Calvin cycle playing a minor, but still significant role.

For a better understanding of guard cell photosynthetic carbon assimilation, we included the *pgi1-1* mutant in our analysis. It seems that after an initial lag phase, similar to that observed for the *gpt1* mutant, guard cell starch can be synthesized to wild type levels in intact leaves of *pgi1-1* guard cells during the second half of the day (Figure 5.2 D). This could be explained by a high supply of sugars originating from mesophyll photosynthesis, especially at later time points, which are subsequently imported into the plastids via GPT1 and other sugar transporters such as GPT2. This might compensate for the loss of the contribution of guard cell photosynthetic carbon assimilation in the *pgi1-1* mutant during the afternoon. The inclusion of the *gpt1pgi1-1* double mutant, which is under selection in our group at the moment (see Material and Methods), as well as multiple mutant combinations including *gpt2*, could help to further clarify the sources of sugars for starch synthesis. Due to the impaired growth phenotype of *pgi1-1* and other mutants such as *pgm*, guard cell specific gene silencing and overexpression will furthermore supplement the studies on T-DNA insertion mutants in the future.

At the moment, the slight increase in starch content in the *pgi1-1* mutant epidermal peels seems less intuitive. While the direct conversion of sugars originating from the Calvin cycle is mainly blocked in this mutant, no import of apoplastic sugars can occur in the epidermal peels. One way of reconciliating this data might be due to the

export of triose phosphates from the plastids, which accumulate due to the lack of carbon flux into starch synthesis and can be exported via triose phosphate/P_i translocators (Ritte and Raschke, 2003; Facchinelli and Weber, 2011). Subsequently, Glc6P generated through gluconeogenesis might be reimported into the plastid for starch synthesis, thereby circumventing the loss of PGI (Kunz et al., 2010). This pathway was shown to work in mesophyll cells when *GPT1* or *GPT2* were overexpressed in the *pgi* mutant background, complementing its reduced starch phenotype (Niewiadomski et al., 2005). Furthermore, guard cells of the *pgi1gpt2* double mutant still accumulate starch granules, which was attributed to Glc6P import via GPT1 (Kunz et al., 2010). However, we cannot exclude that the low remaining activity in the *pgi1-1* mutant line (Yu et al., 2000; Niewiadomski et al., 2005) is responsible for the observed starch accumulation in the epidermal peels.

Another possibility to circumvent the *pgi1-1* mutation was proposed through an alternative pathway of ADP-Glc synthesis through the action of cytosolic SUCROSE SYNTHASEs (SUS). It was suggested that SUS enzymes can catalyse the conversion of sucrose and ADP into ADP-Glc and Fru and that this ADP-Glc is taken up into the plastids via specific transporter for starch synthesis (Baroja-Fernandez et al., 2004; Muñoz et al., 2005). Bates and colleagues showed that *SUS3* transcripts are highly abundant in Arabidopsis guard cells and suggested the involvement of the SUS3 enzyme in starch synthesis (Bates et al., 2012). This pathway would resemble the situation in cereal endosperm, where the AGPase enzyme is located in the cytosol (Denyer et al., 1996) and ADP-Glc is transferred into the plastids for starch synthesis by specific transporters such as the maize Brittle1 (BT1) ADP-Glc / ADP exchanger (Kirchberger et al., 2007). In contrast, no such transport activity was shown for the Arabidopsis homologue BT1-LIKE TRANSPORTER (BT1L), which rather exchanges ATP, ADP and AMP between cytosol and the chloroplast (Kirchberger et al., 2008) and no route of cytosolic ADP-Glc import into the plastids is known (Neuhaus et al., 2005). In any case, this proposed pathway should also contribute to starch synthesis in the *pgm* mutant. Although we did not observe any starch granules in the PS-PI stained guard cells (Figure 5.5 A), very small granules were sometimes found in mesophyll cells of this mutant (Muñoz et al., 2006; Streb et al., 2009), but the overall contribution of SUS to starch synthesis via the production of ADP-Glc seems to be rather limited or completely negligible (Neuhaus et al., 2005; Streb et al., 2009) and the very low starch content in *pgm* mutants could simply be explained by leakage of Glc1P or ADPGlc into plastids (Streb et al., 2009). Taken together, the observed phenotypes in the single *gpt1* and *pgi1-1* mutants are already

remarkable and will set a starting point for the future elucidation of the involved transport mechanisms.

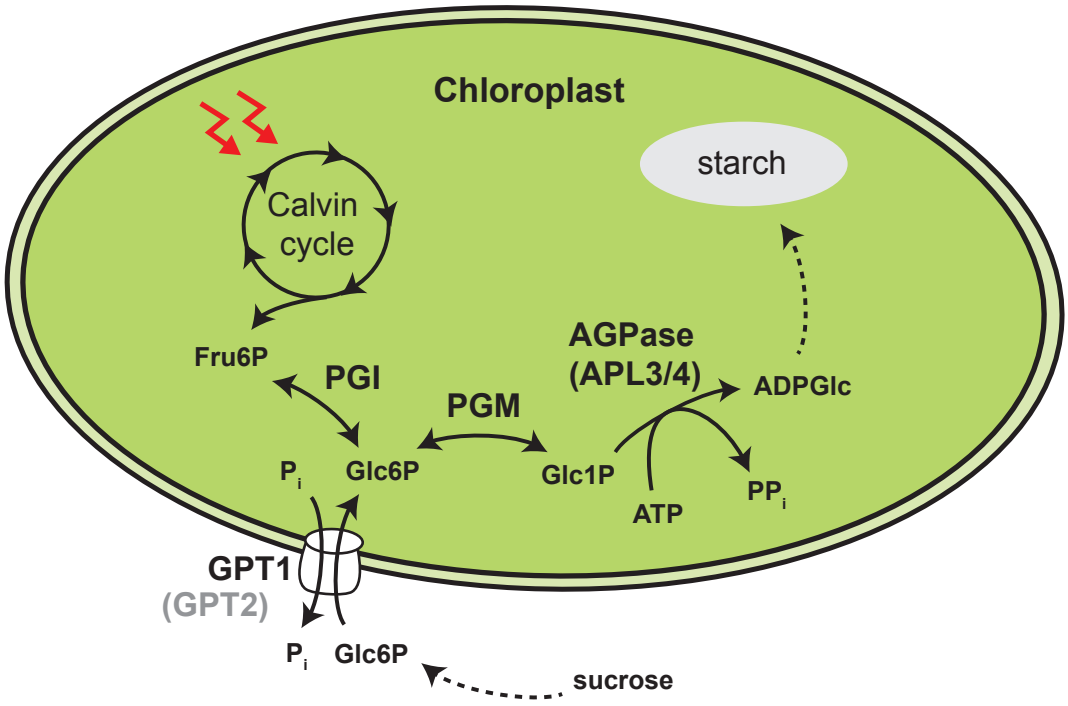

Figure 5.6: The proposed pathway of starch synthesis in guard cells

We previously showed that the Arabidopsis β-amylases acquired a tissue specific function, with BAM3 being the major starch-degrading enzyme in mesophyll cells, while BAM1 is responsible for a large part of guard cell starch degradation in the light (Chapter 1). Interestingly, *BAM1* was also shown to be expressed in root cap cells (Valerio et al., 2011). Similarly, *APL3* and *APL4* are thought to be the major large subunits of the AGPase enzyme in heterotrophic tissue such as root cap cells, while APL1 mainly contributes to starch synthesis in mesophyll cells during the day (Ventriglia et al., 2008). We therefore speculated that APL3 and APL4 would be the predominant large subunit isoforms in guard cell chloroplasts and constitute another example for the tissue specific set of enzymes responsible for the specialized carbon metabolism found in these cells. Both genes are preferentially expressed in guard cells (Figure 5.3 D) and while the mutants do not show a strong starch related phenotype in the whole rosette (Figure 5.3 B and C), guard cell starch content is altered in the *apl3* single mutant but not in *apl4* mutant guard cells (Figure 5.3 E and F). Interestingly, *apl3* mutants show an initial lack in starch synthesis during the first

three hours of illumination, which seems to be over-compensated in the evening, resulting in a starch excess phenotype at the end of the light phase (Figure 5.3 F). It is possible that this is due to an alteration in the enzyme kinetic properties of AGPase caused by an altered composition of the hererotetramer, such as the replacement of APL3 subunit with APL4.

Indeed, the additional loss of APL4 in the *apl3apl4* double mutant exacerbates the lag phase, which lasts until after the 6 h time point (Figure 5.4 C). Surprisingly, this severely reduced synthesis was compensated by a massive increase in starch content between the 6 h time point and the 9 h time point. It could be possible that the composition of the AGPase heterotetramer changes several times throughout the day, with different APL subunits showing a distinct temporal participation in ADP-Glc synthesis. It could also be the case that in the double mutant *APL1* or *APL2* gene expression is induced and that these two subunits are able to complement the phenotype of the *apl3apl4* mutant in the afternoon, but not in the early morning. In a next step we would need to investigate the transcript levels of the different *APL* genes throughout the day in epidermal peels of both the wild type and the different mutants. Future research will be needed to untangle the roles of the APL subunits in Arabidopsis guard cell starch synthesis. The newly created *apl3apl4* double mutant described here is a first step in this direction.

As described above, the different isoforms of the regulatory subunit confer distinct kinetic properties such as sensitivities to allosteric inhibitors to the AGPase enzyme. One particularly interesting regulatory property is the redox-activation of AGPase through sucrose-mediated trehalose-6-phosphate and glucose-induced hexokinase signalling (Tiessen et al., 2003; Kolbe et al., 2005). Therefore, high sugar levels would on the one hand increase the expression of *APL3* and *APL4* isoforms in guard cells as shown previously (Crevillén et al., 2003; Bates et al., 2012) and activate the AGPase enzyme via the reduction of the disulphide bridge. This would potentially link the HXK-dependent stomatal closure response mediated by ABA (Kelly et al., 2013) to the removal of osmolytes through the activation of starch synthesis. Therefore it would be interesting to further investigate guard cell starch synthesis in relationship to sugar and ABA concentrations, possibly including the previously described HXK overexpression lines in the analysis (Kelly et al., 2013).

With the exception of a lower expression of *ISA1*, Bates and colleagues did not find significant differences between guard cells and mesophyll cells in the gene expression of starch synthesis related enzymes downstream of AGPase (Table 5.3). ADP-Glc can be used by several SS enzymes, which possess different affinities for

the length of the glucan chains they elongate. Besides the soluble SS, GBSS is important for the synthesis of amylose and defines to a large part the physicochemical properties of starch granules. It is possible that changes in protein abundance of these SS, as well as differences in branching and debranching activities through alterations in BEs and DBEs can contribute to significant alterations in guard cell granules including, but not limiting to, the shape, chain length distribution as well as the necessity of glucan phosphorylation for the induction of starch breakdown. While this is already challenging using mesophyll starch granules, it will be even more difficult to investigate the composition of guard cell starch granules due to their smaller size and very low number in the epidermis. Therefore it will be challenging to quantify the effects of the loss of different SSs, BEs and DBEs on the properties of guard cell granules, but in order to refine the calculations presented in Chapter 1 and for the precise quantification of the contribution of starch degradation to the accumulation of osmolytes, a better understanding of the physical and chemical properties of guard cell granules will be necessary. One possibility to gain a much better estimation of guard cell starch breakdown would be through the use of focused ion beam scanning electron microscopy (FIB-SEM, see Conclusion and Outlook).

Besides the characterization of the guard cell granule morphology, the physiological effect of alterations in guard cell starch need to be further investigated in order to fully understand the potential of improving water use efficiency through alterations in guard cell starch metabolism. It was recently reported that *bam1* mutant plants show a drought tolerance phenotype (Prasch et al., 2015). Besides the drought stress experiment using a *phs1* mutant allele presented in Chapter 2, we wanted to continue to investigate the effect of impaired starch metabolism in guard cells under drought stress conditions. Here, we used the starchless *pgm* mutants, which retained higher amounts of water in the leaves over a longer period when challenged with increasingly severe drought stress compared to wild type plants leading to higher survival rates upon re-watering (Figure 5.5 B and C). This is in agreement with the findings of Lasceve and colleagues, who reported inhibited stomatal opening resulting in lower transpiration rates in *pgm* plants (Lasceve et al., 1997). Because the defect in starch accumulation strongly impairs plant growth, these mutants are considerably smaller than wild type plants, which might contribute to the drought tolerant phenotype we observed. Furthermore, it is well known that *pgm* plants accumulate high concentrations of sugars in the leaves during the day (Gibon et al., 2004), which might act as osmoprotectants and retain water through increasing the

cellular osmotic potential, which reduces water loss in addition to the reduction in stomatal conductance. We tried to overcome this limitation of our experimental system through the guard cell specific silencing of *PGM*. For this we transformed wild type plants with a MIGS construct targeting *PGM* transcripts under the guard cell specific promoter *pCYP86A2* (see BAM1 MIGS silencing lines described in Chapter 1). In contrast to the silencing lines in which *BAM1* transcripts were reduced leading to a similar phenotype compared to the *bam1* T-DNA insertion mutant (Chapter 1), we were unfortunately unable to obtain transgenic lines with significantly reduced guard cell starch contents at the end of the day. It is possible that the overall transcriptional activity of the *PGM* gene in guard cells is much higher compared to *BAM1*, causing an insufficient knockdown of *PGM* in the lines obtained. Alternative silencing methods could be used, although the same problem of insufficient knockdown might be encountered. In an alternative approach we will therefore overexpress *PGM* specifically in guard cells of the *pgm* mutant, which should lead to plants showing wild type behaviour in their stomatal movements, while mesophyll cells should be still starch free, enabling us to discriminate between the sugar accumulation and growth phenotype and the effect of loss of starch on stomatal physiology.

Conclusion and Outlook

Day-time starch degradation in both guard and mesophyll cells

Our current knowledge of starch metabolism comes to a large part from studies conducted on storage starch of cereal grains and from investigations of Arabidopsis transitory leaf starch breadown. In our recent work (Chapter 1 and Chapter 3), we could elucidate the molecular and genetic basis of transitory starch breakdown in the light. Functional specialization within the family of β-amylases seems to be the basis of this observation. While BAM3 is the major β-amylase in night-time transitory leaf starch degradation, BAM1 acquired novel functions. First, BAM1 is the key enzyme for the degradation of starch in guard cells upon illumination (Chapter 1). Under prolonged drought stress, guard cell starch breakdown was shown to be reduced, correlating with a reduction in the transcript levels of *BAM1* in these cells (Prasch et al., 2015). In contrast to this reduction in *BAM1* gene expression, this β-amylase is involved in day-time mesophyll starch breakdown under acute osmotic stress, where *BAM1* transcription is upregulated in an ABA-dependent way (Chapter 3). It seems that, at least on the transcriptional level, BAM1 regulation differes between cell types and between different growth conditions (standard, severe acute stress, prolonged water deficit). Transcriptional regulation of *BAM1* will be further considered below. In both cases of day-time starch degradation, BAM1 seems to work in concert with AMY3, which plays no or only a minor role in starch breakdown during the night. Together, BAM1 and AMY3 are able to induce rapid starch degradation, which is distinct from the slower night-time leaf starch breakdown.

Novel insights and questions about guard cell starch breakdown

In the work presented in this thesis we began the molecular characterization of the carbon metabolism in guard cells of the model plant *Arabidopsis thaliana*. Although carbon metabolism and especially starch degradation in the early morning was implicated in stomatal movements for a long time, the lack of precise methods for the quantification of guard cell starch content in the small cells of the Arabidopsis leaves made it difficult to elucidate the molecular and biochemical basis of this pathway. The recent observation showing a guard cell specific starch excess phenotype in *bam1*

mutant plants (Valerio et al., 2011), together with the establishment of a novel guard cell starch quantification method in our lab based on the pseudo-Schiff propidium iodide staining protocol (Truernit et al., 2008) set the starting point of the presented studies.

First, we established the molecular pathway of starch degradation in guard cells and, besides BAM1, we showed that AMY3, ISA3 and to a lesser extend LDA contribute to the rapid starch degradation, which occurs within the first hour of illumination (Chapter 1). Furthermore, we showed unequivocally that proper starch degradation is necessary for full stomatal opening, with severely reduced transpiration rates in the *amy3bam1* double mutant, which ultimately reduced biomass accumulation under higher light intensities. In the final part of this study we showed that the blue light-mediated pathway activating the plasma membrane proton pumps is required for guard cell starch degradation. Fusicoccin, a fungal plant toxin, induces proton extrusion across the plasma membrane through the activation of the proton pumps and stimulates starch degradation in guard cells. Interestingly, the effect of fusicoccin on stomatal opening was almost completely abolished in the *amy3bam1* double mutant, indicating again the importance of proper starch degradation in the process of stomatal opening. From this first study several new questions arose that will be discussed below.

Early morning guard cell starch degradation is almost absent if plants are kept in the dark (Chapter 2). In contrast, we could observe starch degradation during the second part of the night, although at lower rates compared to illuminated plants in the morning. This pre-dawn starch degradation might be under circadian control and contribute to pre-dawn stomatal opening. A first step in addressing this hypothesis is the comparison of wild type and *amy3bam1* pre-dawn guard cell starch levels as well as stomatal aperture and conductance. We would expect that the pre-dawn opening in the double mutant is severely impaired, similarly to what was described for the *pgm* mutant (Lasceve et al., 1997). Based on the observations of the *pgm* mutant phenotype, it was already suggested that predawn guard cell starch degradation is necessary for the observed increase in stomatal aperture at the end of the night and that starch breakdown is under circadian control (Lasceve et al., 1997; Caird et al., 2007), but no direct evidence was presented up until now. Dodd and colleagues showed that in plants with disrupted circadian rhythms, the rhythmicity of stomatal conductance under continuous light is altered (Dodd et al., 2004, 2005). It would be interesting to investigate if guard cell starch levels also change under continuous illumination with an approximately 24 h periodicity. Furthermore, guard cell starch levels in short-period mutants such as *timing of cab 1-1* (*toc1-1)* and the long-period

mutant *zeitlupe-1* (*ztl-1)* can be compared with wild type guard cells under normal 12 h light / 12 h dark photoperiods as well as under 10 h light / 10 h dark (approximately corresponding to the endogenous *toc1-1* clock periods) and 14 h light / 14 h dark photoperiods (approximately corresponding to the *ztl-1* clock periods).
In a next step the link between the circadian clock and the activation of BAM1 and AMY3 for pre-dawn starch degradation would need to be addressed. It can be imagined that posttranslational modifications, for example protein phosphorylation (see below) brought about by circadian clock controlled kinases, could induce the relatively low rates of pre-dawn starch degradation observed in our experiments (Chapter 1). In this cenario, illumination could subsequently elevate BAM1 and AMY3 activities for the rapid early morning starch degradation through redox-activation (see below). Circadian control of starch degrading enzymes in guard cells could furthermore be responsible for the inhibition of breakdown after the first hours of the light phase, enabling net starch synthesis to occur (Chapter 1 and Chapter 5).

Another important consideration for the detailed modelling of guard cell movements concerns the fate of guard cell starch breakdown products. As discussed in Chapter 1 and Chapter 2, we estimate that around half of the observed starch breakdown is sufficient to account for the accumulation of around 200 mM malate in the morning. The other half might be converted into sucrose and hexose phosphates for the accumulation of additional osmolytes in the vacuole. It seems furthermore reasonable that a significant proportion of sugars originating from starch are further metabolized in mitochondria, fuelling cellular respiration for ATP production, which might contribute significantly to the energy requirement of the plasma membrane proton pumps. It is often assumed that the energy for this process originates from photosynthetic electron transport, but it was also shown that blue light-induced stomatal opening in epidermal peels of *Vicia faba* and *Commelina communis* is sensitive to potassium cyanide (KCN), a well-known inhibitor of cellular respiration (Schwartz and Zeiger, 1984; Shimazaki et al., 2007). Therefore, the inhibition of stomatal opening in the *amy3bam1* double mutant could not only be due to the inhibition of malate production, but also a consequence of reduced mitochondrial respiration. This would affect the proton pump activity through the limitation of ATP production. Similar to other aspects of guard cell metabolism, the literature concerning the relative role of ATP provision from photosynthetic electron transport and / or cellular respiration in mitochondria to supply energy for proton pumping is fragmentary and will require thorough and novel approaches in the future.

In order to address these questions, we will need to compare the activity of the plasma membrane proton pump in the wild type with its activity in the *amy3bam1* double mutant using guard cell protoplasts of Arabidopsis for the measurement of proton extrusion activity via the acidification of the extracellular medium. These experiments can be conducted in collaboration with Nathalie Leonhardt at the CEA Cadarache, France. Furthermore, the recently created pHusion pH sensor, allowing ratiometric analysis of pH changes in the cytosol (pHusion) and in the apoplast (apo-pHusion) of Arabidopsis epidermal peels (Gjetting et al., 2012). Transforming this construct into our wild type and mutant plants (*bam1*, *amy3bam1* etc.) could help answer the question if the inhibition of starch breakdown negatively influences proton pump activity at the guard cell plasma membrane.

In addition, patch clamp experiments, which will be conducted in collaboration with Mike Blatt, University of Glasgow, investigating K^+ currents in response to blue light illumination in *amy3bam1* guard cell protoplasts could provide insights into the link between starch breakdown and the accumulation of K^+. If proton pump activity is inhibited in the *amy3bam1* double mutant, we would expect to observe also a reduction in the uptake of K^+ in response to blue light. This experiment might be complemented with direct measurements of malate and K^+ in epidermal peels of wild type and *amy3bam1* plants under different light conditions or using different buffers.

Furthermore, the manipulation of gene expression specifically in guard cells will advance our understanding of the role of guard cell metabolism. With the identification of promoter sequences that are specifically activated in guard cells such as the promoter of CYP86A2, MYB60 and GC1 (Francia et al., 2008; Galbiati et al., 2008; Cominelli et al., 2011; Yang et al., 2008), the generation of transgenic plants overexpressing genes in these cells as well as guard cell specific gene silencing are now feasible. For example, Kelly and colleagues investigated the role of HXK1 in stomatal regulation through its guard cell specific overexpression (Kelly et al., 2013; see Discussion in Chapter 5) and we were able to silence the *BAM1* gene specifically in guard cells of Arabidopsis using the CYP86A2 promoter region (see Chapter 1). Future analysis of plants overexpressing or silencing genes coding for enzymes of malate and sucrose metabolism as well as the downregulation of organic acid and sugar transporter in guard cells will provide valuable insights into the role of guard cell metabolism. Importantly, these approaches allow the analysis of changes in metbaolites specifically in these cells, without pleiotropic effects from changes in the overall metabolic state of plants. As discussed above (Chapter 5), the inhibition of stomatal opening in the *pgm* mutant could be due to changes in the overall metabolite levels during the day and the night, such as high sugar contents in the

light phase, which are rapidly metabolised during the initial hours of the night, followed by a starvation phase.

Target genes to include in the future, amongst others, are transporters and ion channels such as ALMT6 and related ALMTs, which could be important for malate import into the vacuole (Meyer et al., 2011) as well as members of the STP family of sugar transporters (Stadler et al., 2003). Finally, plants expressing silencing constructs against malate metabolism genes in guard cells will help to elucidate the exact pathway of guard cell malate synthesis, which was proposed to involve cytosolic MDH and PEPC (Chapter 1, Supplementary Data 1) as well as the role of malate metabolism during stomatal closure (Penfield et al., 2012). Similarly, manipulating the transcription of sucrose synthase as well as cell wall and cytosolic invertases (see Chapter 5) will greatly improve our limited understanding of the role of guard cell sucrose metabolism for the regulation of guard cell movement.

The pathway of guard cell starch synthesis only starts to emerge

Besides the reported progress in elucidating guard cell starch degradation, we began to investigate the pathway of starch synthesis in these cells (Chapter 5). From our preliminary results it seems that guard cell photosynthetic carbon assimilation contributes only a relatively small part to the sugars serving as substrate for the synthesis of ADP-Glc. The majority of sugars used for the synthesis of starch seem to be imported as Glc6P by GPT1, although the contribution of GPT2 and other sugar transporters cannot be rules out at the moment. Furthermore, a detailed analysis of the contribution of the different isoforms of SSs, BEs and DBEs, as well as the molecular characterisation of guard cell starch granule structure will be required in the future (see Discussion in Chapter 5). In order to investigate the structure of guard cell starch granules and for a better estimation of the amount of released maltose in the first hour of illumination, a focused ion beam set-up coupled with scanning electron microscopy (FIB-SEM) could yield interesting new results. This technique allows the 3-dimensional imaging of a single sample with the FIB used to remove the upper most layer after the imaging by SEM. A stack of images from a single sample obtained through FIB-SEM can be used for the 3-dimensional reconstruction and detailed analysis of cellular compartments, allowing the precise quantification of starch granule volumes.

Starch granules clearly re-appeared after 3 h of illumination and starch synthesis continued throughout the remainder of the day (Chapter 1). While we could show that

blue light induces the rapid starch degradation in the morning, nothing is known about the switch from net starch degradation to net synthesis. Judged from the rapid degradation, it seems unlikely that simultaneous breakdown and synthesis occurs, which results in a net accumulation of starch. Rather, it seems more feasible that starch breakdown is inhibited soon after the depletion of guard cell starch reserves, but how this is achieved remains unknown. A novel mutation found in the *BAM1* locus through a screen of EMS mutagenised Arabidopsis seeds in the laboratory of Prof. Alison Smith (John Innes Centre, Norwich, UK), seems to express a constitutively active version of the BAM1 protein. In this mutant almost no starch can be synthesised in guard cells throughout the day (data not shown), indicating that the inhibition of BAM1 activity is necessary for net starch accumulation in these cells. This mutant might provide further insights into the switch from net starch degradation to starch synthesis in guard cells.

Regulatory mechanisms controlling BAM1

Transcriptional regulation of BAM1

As discussed in the introduction, cell type-specific gene expression seems to be one factor important for the differences in starch metabolism between certain cell types. Genes coding for enzymes important for starch synthesis such as *PGM1*, *APS1*, *APL1* and *SS1* are transcriptionally active in starch containing cells (e.g. mesophyll cells and root cap cells), but inactive in starchless cell types (e.g. root cells other than the root cap) (Tsai et al., 2009). In the case of *BAM1*, gene expression prior to flowering is primarily active in guard cells and cells of the root tip, while the expression of *BAM3* is primarily restricted to leaf mesophyll cells (Valerio et al., 2011).

We therefore analysed the promoter regions of *BAM1* and *AMY3*, as well as the promoter of the *BAM3* gene, noticing the presence of several short (T/A)AAAG sequences (Figure 6.1 A and B), known as DOF binding elements. DOF (DNA-binding with one finger) proteins are a plant specific subclass of zinc finger transcription factors (Yanagisawa, 2004). DOF transcription factors are known to play important roles in processes such as tissue differentiation, seed development and regulation of metabolism and several members of the DOF family were shown to respond to light, phytohormones and the circadian clock (Noguero et al., 2013).

Several guard cell specific genes were shown to contain DOF elements in their promoter regions, necessary for their tissue specific expression. For example, the

potato DOF transcription factor StDOF1 was shown to bind to (T/A)AAAG elements in the promoter of the potato guard cell potassium channel *KST1*, conferring guard cell specific expression (Plesch et al., 2001). The *Arabidopsis* homologue of *KST1*, the K^+ channel encoding *KAT1* gene also contains several DOF elements (Galbiati et al., 2008). DOF-binding sites were furthermore found in the promoter of the *Arabidopsis thaliana MYB60* transcription factor gene, as well as in the *MYB60* ortholog of *Vitis vinifera* (Cominelli et al., 2005, 2011; Galbiati et al., 2011). Finally, the promoter of *PCK1*, which was shown to be important for the removal of malate during stomatal closure and which is highly expressed in Arabidopsis guard cells contains several DOF motifs (Penfield et al., 2012).

We therefore speculated that the DOF elements could be important for the tissue specific expression of BAM1 and other starch degrading enzymes. It should be noted that not every single element serves as a functional target site (Cominelli et al., 2011). It is rather known that clusters of at least three (T/A)AAAG elements within 100 to 120 bp enhance binding affinity of DOF transcription factors to target promoter regions (Galbiati et al., 2008). While the promoter of *BAM1* contained several DOF elements, which formed a total of three clusters satisfying these conditions, we also found one of these clusters in *AMY3* and surprisingly in *BAM3* as well (Figure 6.1. A and B). This could potentially be explained by the fact that DOF transcription factors can either activate or inhibit the expression of target genes, depending on the presence of other transcription factors with which they directly interact through their conserved, bifunctional DOF domain (Yanagisawa, 2004).

Interestingly, the promoter regions of *BAM1* and *AMY3* contain ABRE elements in the vicinity of the DOF clusters (Figure 6.1 A and Chapter 3). Because both BAM1 and AMY3 are involved in the response to osmotic stress in an ABA-dependent response (see Chapter 3), it is tempting to speculate that under normal growth conditions DOF transcription factors are involved in guard cell specific gene expression of starch degrading enzymes, while under stress conditions ABA responsive transcription factors induce BAM1 expression also in mesophyll cells through binding to the ABRE.

A

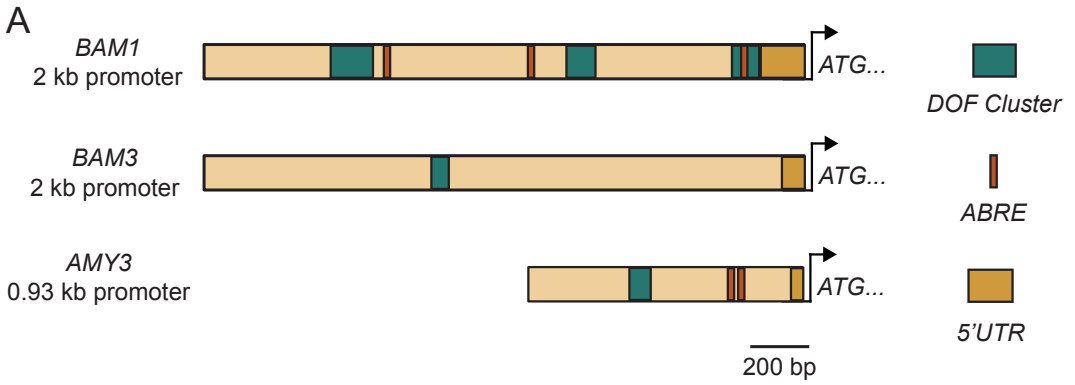

B

tgttccctcagctcccaaattcgaccctctagtagccacatctgctttattttatttatctttcagta
aatctgccccattaaaatgtccaataaaaaatcttccttacttcagggtagagattttgatatttaca
tatagttattcttattgtaccgattgtatcgaatatttatatacttggatatatctttgtacatcaaat
ggagtcaataataatatcaagaacggtgaagaaactgccagctagagggatgagattgattgatgcagt
tatcaaagtggattgcaacaactctttcatgtgaatgtgatcttaatatcatgtcacacaaatacataa
tctgtttctactaattgcgttttgtgtaaaagattaataatacttcacatcttaattactctttaaacg
aatcattgatctttcatgaaaggaaaagaaggttctagtctttgtcagaaatccataatccaatcttgt
aaaaggcaaacagtttttgtcctaaaagatttgacgagcaacgaatcggttcattcccagccgttggat
tgatttaaatactcaggaaaagtcatcccaaaaaggtgggaacttgccactccacatcaccatggcacg
tggtaagcttacagaggaaaacttcaatattggtttactttctccaccactcaacattttgtttgttcg
tgcatgttgttttgtgtccgtgtattatctattaatctatgttagacatttttttcttcttttttcgtc
aaggatattcctttttatgtttaaagtattgtgtacatatataaaaaaatattgcatattagattattg
acttgaatcgaaggatttttaaaaaaaaaaaaactgtttgtagagaagaaaaatcgaaaactacttgta
ttcatcagaattaaaaaaaaaaaagtcagtctaaaaatataccctaataaactgacatacctatttcaac
gatacaattctataatgagttattaaattgatttgatttcgtattctctaaaatatactcatagacata
gcagaaactagttaatttgcttatatgttcatattcttgtacatcatgtgatctcacgtggaataaaaa
taatgtgaccatctctaattctctacttcacttagtatctaagtatccactgtgataccttgttttctg
ctcaaagttgtacatgcgtagattaataaatacatttcacccttcaattgatcccaaaagcctctaca
agacagccaaaacaaatcaaggattgcgcaaagcattcaagtttcgaaacaataatttttttaatggtt
gacaaaaagcaataatttgtaaagcgattcataggtcagcttctaaatgttctcgaaataactcgaacc
aacacctaaaccatttgttctaacgataatagacgaacgtattagagactcgttaggaaaacactactt
gtatatattcactttacatacatatttgtttccttcatatatttatttatttacataacaaaccaata
tgaaaaacgtacgtttcatgaaagagaacgttgtagaacactatcaccgtttgcttgtaagaaaaagc
ttatctcacctataaactcgtgagtcatatttatactcttaacaataataaataaaataaaactctatt
ttggtaaccacaaaaaatattctgaggctaaaagcgcgtctgctggaaagttcacgcgctctgctaacc
ccaccgtccattctgactctttttagatcttaaccgtgtctttatccacatcatacgtttatacacgtgt
cacacgatcacctattctataaaaaacattattttaatcttatcctttttatgcttcccctataaatta
tcttctcttcctccttctccgatctctcctccgtcacacaaaacttccgatttcaaaaaaacaatttga
aatttgtcaaaaggaatattctgacgatcgattcttgattcgttttctcgcgtatagagagaaaaATG

Figure 6.1: Analysis of the promoter region of *BAM1*, *BAM3* and *AMY3*
(A) Graphical representation of the promoter regions of *BAM1*, *BAM3* and *AMY3* showing the positions of the DOF clusters, ABA-responsive elements (ABRE) and the 5' untranslated regions (5'UTR). (B) The sequence of the 2 kb BAM1 promoter region. Five base long single DOF binding elements are highlighted in red with clusters of at least three of these putative DOF elements within 100 to 120 bases being underlined. ABRE are shown in blue and grey bases indicate the 5' UTR with the translational start codon ATG in capital letters.

Recently, Negi and colleagues reported that the DOF transcription factor STOMATAL CARPENTER 1 (SCAP1), also referred to as AtDOF5.7, activates the expression of several guard cell specific genes, including *MYB60* and *GORK*, through the direct binding to their promoter regions (Negi et al., 2013). Similar to the *BAM1* promoter,

both *GORK* and *MYB60* promoter regions contain clusters of DOF binding elements. We therefore wondered if SCAP1 could be involved in the guard cell specific expression of *BAM1* under normal growth conditions, and if this could have an influence on guard cell starch degradation.

While wild-type guard cells degraded their starch as reported above, *scap1* mutant plants had an initially high starch content at the end of the night and showed severely impaired degradation within the first hour of illumination (Figure 6.2). Remarkably, this resembles the phenotype of the *bam1* mutant guard cells, suggesting an involvement of the SCAP1 transcription factor in the regulation of guard cell starch breakdown, possibly via transcriptional regulation of *BAM1*. It could furthermore explain the observation by Negi and colleagues who reported that guard cell protoplasts (GCPs) of *scap1* mutants do not accumulate malate in the light when compared to dark incubated GCPs, while malate levels increased in wild type GCPs (Negi et al., 2013).

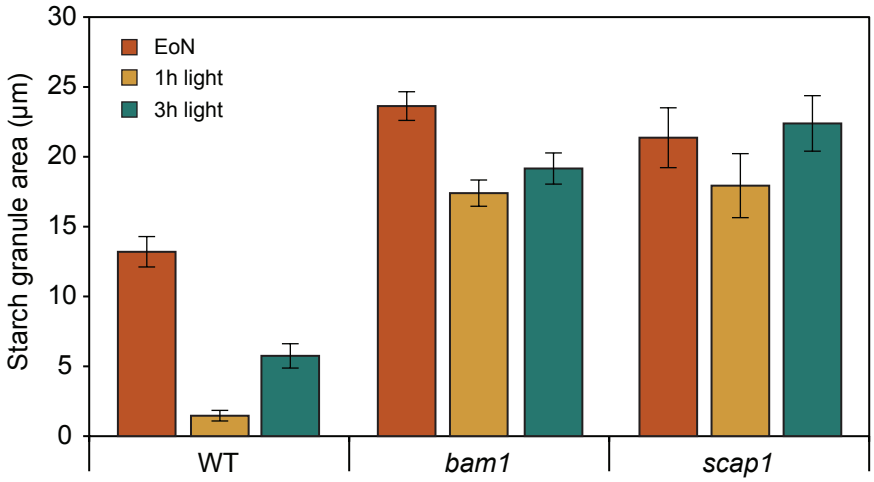

Figure 6.2: A possible role of SCAP1 in the transcriptional regulation of *BAM1*.
Epidermal peels were collected at the indicated time points from leaf 6 of 4-week-old soil grown WT (Col-0), *bam1* and *scap1* plants. Guard cell starch content was determined after PS-PI staining using confocal laser microscopy as described in Chapter 1. Each time point represents the average of at least 38 guard cells from four individual plants ± SE. EoN = end of night.

These preliminary results open an exciting possibility for further investigations into the differential regulation of carbon metabolism in guard and mesophyll cells. Initially, the transcript abundance of *BAM1* in epidermal peels of the *scap1* mutant will strengthen the link between SCAP1 and *BAM1* expression. Besides *BAM1*, also the expression levels of *AMY3*, *BAM3* and other genes thought to be important for guard cell carbon metabolism will shed some light on the role of SCAP1 in the control of guard cell specific gene regulation. Binding of SCAP1 to the *BAM1* promoter region

could have several consequences, potentially activating the gene expression in response to environmental conditions such as blue light illumination or altering the responsiveness towards ABA concentrations in guard cells. The possibility of detecting BAM1 protein with specific antibodies will further substantiate the influence of SCAP1 on *BAM1* transcription.

In a next step, the direct binding of the SCAP1 transcription factor to the DOF motifs in the *BAM1, AMY3* and *BAM3* genes could be investigated by transiently expressing SCAP1 together with a promoter-reporter gene construct in Arabidopsis protoplasts. This TEAMP system (*T*ransient *E*xpression in *A*rabidopsis *M*esophyll *P*rotoplasts) is an established method in our institute and would also allow the investigation of the binding sites through the analysis of the protein DNA interaction using mutagenized and truncated *BAM1* promoter versions. Alternatively, the physical interaction of SCAP1 and the BAM1 promoter can be investigated using the chromatin immunoprecipitation (ChIP) assay. Finally, this approach will be substantiated by the use of stable transformed Arabidopsis plants expressing BAM1 or BAM3 under their native or mutagenized promoters in the corresponding mutant background. This would also allow us to investigate if BAM3 is able to complement the guard cell *sex* phenotype of the *bam1* mutant if it is expressed under the *BAM1* promoter.

Protein phosphorylation

While *in vitro* we found good evidence for the phosphorylation of BAM1 at Ser^{59} through the activity of the GSK3-like kinase AtK4, phosphopeptides including this modification were also observed in the kinase mutant. It should be kept in mind that the phosphoproteomics approach employed here is only qualitative and not quantitative and that it is therefore possible that the overall extent of Ser^{59} phosphorylation is reduced in *atk4* plants.

To overcome this limitation, we will employ quantitative phosphoproteomics together with the FGCZ in order to investigate the extent to which Ser^{59} is phosphorylated in *atk4* plants compared to WT plants. This will also allow us to quantify the proportion of phosphorylation at Ser^{59} (as well as at Ser^{31} and Ser^{55} in response to different environmental conditions (e.g. in response to osmotic stress or to different light qualities).

The development of Selected Reaction Monitoring (SRM) based proteomics using triple quadruple mass spectrometers allows the targeted quantification of fragmentation ions of previously selected peptides and therefore the determination of

the abundance of specific proteins in a complex sample (Picotti and Aebersold, 2012). The use of synthetic heavy-isotope labelled peptides which resemble the native target peptides (including posttranslational modifications such as phosphorylation events) as standards allows the absolute quantification of pre-selected proteins or peptides and the comparison between different samples with high analytical precision (Gerber et al., 2003; Wolf-Yadlin et al., 2007). Here, the fragmentation ion patterns obtained from our initial experiment (Table 4.5) will be a valuable tool for setting up the precursor ion selection.

Using the combination of heavy isotope labelled standard peptides and SRM based detection methods, several groups demonstrated the efficient quantification of phosphopeptides in plant samples. For example, Haruta and colleagues were able to quantify differences in the phosphorylation pattern of the plasma membrane proton pumps AHA1 and AHA2 (Haruta et al., 2010). In another report, quantitative phosphoproteomics was used to investigate changes in the phosphorylation pattern of the Arabidopsis proteome upon ABA treatment in wild type and triple *snrk2.2/2.3/2.6* mutants (Wang et al., 2013a). SRM based proteomics will be key in the elucidation of the role of Ser^{55} and Ser^{59} phosphorylation in response to different environmental conditions and will reveal further insights into the roles of AtK4 and related GSK3/Shaggy-like kinases in the regulation of carbon metabolism upon stress conditions. Interestingly, an extensive bioinformatics analysis of BAM1-like proteins from 66 plant species, which are distinguished from BAM3-like β-amylases due to the sequence differences in the N-terminal domains, revealed that the (S/T)P-XX-(S/T)P motif is highly conserved among spermatophytes with the notable exception of grasses, where the putative GSK3 phosphorylation motif was most likely lost during evolution (M. Thalmann, unpublished results). This further suggests an important role of the phosphorylation motif in the regulation of BAM1 in many different species.

In order to investigate the role of BAM1 phosphorylation in guard cells using quantitative phosphoproteomics, a suitable material needs to be prepared in sufficient quantities with highly reproducible methods. This might involve the preparation of guard cell protoplasts using a large-scale material preparation protocol. Takemiya and colleagues showed recently that it is possible to extract up to 100 µg guard cell proteins from guard cell protoplasts and to use this material for phosphoproteomic analysis (Takemiya et al., 2013a). Unfortunately, this method requires the incubation of epidermal peels for a rather long time in a digestive solution with high osmolarity, which is able to induce osmotic stress responses as

can be observed in transcriptomic studies (Bates et al., 2012). This might make it difficult to actually distinguish between the guard cell response to changes in the environment (e.g. dark to light transition) and the responses to osmotic stress. It might be therefore better to rely on the rapid preparation of epidermal peels, as was previously used for microarray studies of gene expression (Bauer et al., 2013), although here the problem of relatively high contamination rates from mesophyll cells might influence the reliability of the experimental results obtained.

Redox-control of BAM1 activity

Besides a possible role for protein phosphorylation, it is well established that BAM1 and AMY3, but not BAM3 activity, is redox regulated (Sparla et al., 2006; Valerio et al., 2011; Seung et al., 2013). This fits with the observation that BAM1 is active in the light to degrade guard cell starch for stomatal opening (Chapter 1).
From our research it became clear that the reduction of the disulphide bridge in BAM1 is not sufficient to induce guard cell starch degradation as indicated by the fact that no starch breakdown occurred in illuminated guard cells treated with the PP1 inhibitor tautomycin (Chapter 1). Similarly, no starch breakdown occurred in *aha1* mutant guard cells under illumination, although the disulphide bridge of BAM1 should be reduced under this condition. It will be interesting to investigate whether guard cell starch degradation can be induced in the dark through fusicoccin treatment or if the light-dependent reduction through thioredoxins is a prerequisite for guard cell starch degradation. It should be noted that it is also possible that the BAM1 protein can be reduced in the dark through NADPH-thioredoxin reductase (NTRC) (Valerio et al., 2011). It might be therefore interesting to investigate guard cell starch degradation in plants expressing redox-insensitive mutant versions of BAM1 in the *bam1* mutant background. So far we obtained transgenic T1 plants in the Col-0 and *bam1* backgrounds, containing the *pDH54* construct, which allows the expression of the redox-insensitive BAM1 C73S C511S version from the *35S* promoter of the *pMDC83* vector (Curtis and Grossniklaus, 2003). It is possible that BAM1 redox-activation requires the prior phosphorylation of one or more serine residues, or that vice versa protein phosphorylation is influenced by the redox state of the protein. For example, as mentioned above, protein phosphorylation could control pre-dawn guard cell starch degradation, while the additional reduction of BAM1 would induce the rapid starch breakdown in response to illumination. This functional interaction of different post-translational modifications will be an interesting future research area.

Besides BAM1 and AMY3, several other enzymes associated with starch degradation were shown to be redox-regulated or sensitive to changes in the redox state of the plastidial stroma (Glaring et al., 2012; Santelia et al., 2015). For example, GWD can be activated by the reduction of a disulphide bridge through Trx *f* (Mikkelsen et al., 2005). Interestingly, it was recently suggested that GWD is not important for the adjustment of the starch degradation rates in mesophyll cells during the night (Skeffington et al., 2014). If this is also true in illuminated guard cells is not known, but it might be that the redox-regulation of GWD plays a role in controlling guard cell starch degradation through the phosphorylation of the glucan chains, thereby enabling the degradation of the starch granule through BAM1 and AMY3. Furthermore, SEX4, but not LSF2, activity is regulated by a disulphide bridge between Cys^{198} and Cys^{130} (Silver et al., 2013). Therefore, both a glucan, water dikinase and a phosphoglucan phosphatase, which are both required for proper starch degradation in Arabidopsis mesophyll cells during the night, could be active in the light in guard cells. Further research will be necessary in order to elucidate the early steps of starch breakdown, but redox-control could be one mechanism involved in regulating light-dependent guard cell starch degradation.

BIBLIOGRAPHY

Ache, P., Becker, D., Ivashikina, N., Dietrich, P., Roelfsema, M.R.G., and Hedrich, R. (2000). GORK, a delayed outward rectifier expressed in guard cells of *Arabidopsis thaliana*, is a K^+-selective, K^+-sensing ion channel. FEBS Lett. **486**: 93–98.

Allen, G.J., Chu, S.P., Schumacher, K., Shimazaki, C.T., Vafeados, D., Kemper, a, Hawke, S.D., Tallman, G., Tsien, R.Y., Harper, J.F., Chory, J., and Schroeder, J.I. (2000). Alteration of stimulus-specific guard cell calcium oscillations and stomatal closing in Arabidopsis *det3* mutant. Science **289**: 2338–2342.

Amodeo, G., Talbott, L.D., and Zeiger, E. (1996). Use of Potassium and Sucrose by Onion Guard Cells during a Daily Cycle of Osmoregulation. Plant Cell Physiol. **37**: 575–579.

Andersson, I. (2008). Catalysis and regulation in Rubisco. J Exp Bot **59**: 1555–1568.

Ando, E., Ohnishi, M., Wang, Y., Matsushita, T., Watanabe, A., Hayashi, Y., Fujii, M., Ma, J.F., Inoue, S., and Kinoshita, T. (2013). TWIN SISTER OF FT, GIGANTEA, and CONSTANS have a positive but indirect effect on blue light-induced stomatal opening in Arabidopsis. Plant Physiol. **162**: 1529–38.

De Angeli, A., Monachello, D., Ephritikhine, G., Frachisse, J.M., Thomine, S., Gambale, F., and Barbier-Brygoo, H. (2006). The nitrate/proton antiporter AtCLCa mediates nitrate accumulation in plant vacuoles. Nature **442**: 939–942.

De Angeli, A., Zhang, J., Meyer, S., and Martinoia, E. (2013). AtALMT9 is a malate-activated vacuolar chloride channel required for stomatal opening in Arabidopsis. Nat. Commun. **4**: 1804.

Anthon, G.E. and Barrett, D.M. (2002). Determination of reducing sugars with 3-methyl-2-benzothiazolinonehydrazone. Anal. Biochem. **305**: 287–289.

Antunes, W.C., Provart, N.J., Williams, T.C.R., and Loureiro, M.E. (2012). Changes in stomatal function and water use efficiency in potato plants with altered sucrolytic activity. Plant. Cell Environ. **35**: 747–759.

Arango, M., Gévaudant, F., Oufattole, M., and Boutry, M. (2003). The plasma membrane proton pump ATPase: the significance of gene subfamilies. Planta **216**: 355–65.

Asai, N., Nakajima, N., Tamaoki, M., Kamada, H., and Kondo, N. (2000). Role of Malate Synthesis Mediated by Phosphoenolpyruvate Carboxylase in Guard Cells in the Regulation of Stomatal Movement. Plant Cell Physiol. **41**: 10–15.

Assmann, S.M. (1988). Enhancement of the Stomatal Response to Blue Light by Red Light, Reduced Intercellular Concentrations of CO_2, and Low Vapor Pressure Differences. Plant Physiol. **87**: 226–231.

Assmann, S.M., Simoncini, L., and Schroeder, J.I. (1985). Blue light activates electrogenic ion pumping in guard cell protoplasts of *Vicia faba*. Nature **318**: 285–287.

Aylor, D.E., Parlange, J.-Y., and Krikorian, A.D. (1973). Stomatal Mechanics. Am. J. Bot. **60**: 163–171.

Baginsky, S. and Gruissem, W. (2009). The chloroplast kinase network: New insights from large-scale phosphoproteome profiling. Mol. Plant **2**: 1141–1153.

Ball, S., Colleoni, C., Cenci, U., Raj, J.N., and Tirtiaux, C. (2011). The evolution of glycogen and starch metabolism in eukaryotes gives molecular clues to understand the establishment of plastid endosymbiosis. J. Exp. Bot. **62**: 1775–1801.

Baroja-Fernandez, E., Munoz, F.J., Zandueta-Criado, A., Moran-Zorzano, M.T., Viale, A.M., Alonso-Casajus, N., and Pozueta-Romero, J. (2004). Most of ADP-glucose linked to starch biosynthesis occurs outside the chloroplast in source leaves. Proc. Natl.

Acad. Sci. U. S. A. **101**: 13080–13085.

Barragán, V., Leidi, E.O., Andrés, Z., Rubio, L., De Luca, A., Fernández, J.A., Cubero, B., and Pardo, J.M. (2012). Ion exchangers NHX1 and NHX2 mediate active potassium uptake into vacuoles to regulate cell turgor and stomatal function in Arabidopsis. Plant Cell **24**: 1127–42.

Bates, G.W., Rosenthal, D.M., Sun, J., Chattopadhyay, M., Peffer, E., Yang, J., Ort, D.R., and Jones, A.M. (2012). A Comparative Study of the *Arabidopsis thaliana* Guard-Cell Transcriptome and Its Modulation by Sucrose. PLoS One **7**: e49641.

Bauer, H. et al. (2013). The stomatal response to reduced relative humidity requires guard cell-autonomous ABA synthesis. Curr. Biol. **23**: 53–7.

Baunsgaard, L., Lütken, H., Mikkelsen, R., Glaring, M.A., Pham, T.T., and Blennow, A. (2005). A novel isoform of glucan, water dikinase phosphorylates pre-phosphorylated α-glucans and is involved in starch degradation in Arabidopsis. Plant J. **41**: 595–605.

Bayer, R.G., Stael, S., Rocha, A.G., Mair, A., Vothknecht, U.C., and Teige, M. (2012). Chloroplast-localized protein kinases: a step forward towards a complete inventory. J Exp Bot **63**: 1713–1723.

Blennow, A. and Engelsen, S.B. (2010). Helix-breaking news: fighting crystalline starch energy deposits in the cell. Trends Plant Sci. **15**: 236–40.

Boccalandro, H.E., Giordano, C. V., Ploschuk, E.L., Piccoli, P.N., Bottini, R., and Casal, J.J. (2012). Phototropins But Not Cryptochromes Mediate the Blue Light-Specific Promotion of Stomatal Conductance, While Both Enhance Photosynthesis and Transpiration under Full Sunlight. Plant Physiol. **158**: 1475–1484.

Boccalandro, H.E., Rugnone, M.L., Moreno, J.E., Ploschuk, E.L., Serna, L., Yanovsky, M.J., and Casal, J.J. (2009). Phytochrome B enhances photosynthesis at the expense of water-use efficiency in Arabidopsis. Plant Physiol. **150**: 1083–1092.

De Boer, A.H. and Leeuwen, I.J.D.V. Van (2012). Fusicoccanes: Diterpenes with surprising biological functions. Trends Plant Sci. **17**: 360–368.

Boller, T. and Felix, G. (2009). A Renaissance of Elicitors: Perception of Microbe-Associated Molecular Patterns and Danger Signals by Pattern-Recognition Receptors. Annu. Rev. Plant Biol. **60**: 379–406.

Bonardi, V., Pesaresi, P., Becker, T., Schleiff, E., Wagner, R., Pfannschmidt, T., Jahns, P., and Leister, D. (2005). Photosystem II core phosphorylation and photosynthetic acclimation require two different protein kinases. Nature **437**: 1179–1182.

Borchert, S., Große, H., and Heldt, H.W. (1989). Specific transport of inorganic phosphate, glucose 6-phosphate, dihydroxyacetone phosphate and 3-phosphoglycerate into amyloplasts from pea roots. FEBS Lett. **253**: 183–186.

Boyer, J.S. (1982). Plant productivity and environment. Science **218**: 443–448.

Brandt, B., Brodsky, D.E., Xue, S., Negi, J., Iba, K., Kangasjarvi, J., Ghassemian, M., Stephan, a. B., Hu, H., and Schroeder, J.I. (2012). Reconstitution of abscisic acid activation of SLAC1 anion channel by CPK6 and OST1 kinases and branched ABI1 PP2C phosphatase action. Proc. Natl. Acad. Sci. **109**: 10593–10598.

Brearley, J., Venis, M.A., and Blatt, M.R. (1997). The effect of elevated CO_2 concentrations on K^+ and anion channels of *Vicia faba* L. guard cells. Planta **203**: 145–154.

Briggs, W.R. et al. (2001). The phototropin family of photoreceptors. Plant Cell **13**: 993–997.

Briskin, D.P. and Reynolds-Niesman, I. (1991). Determination of H^+/ATP Stoichiometry for the Plasma Membrane H^+-ATPase from Red Beet (*Beta vulgaris* L.) Storage Tissue. Plant Physiol. **95**: 242–250.

Busch, F.A. (2014). Opinion: The red-light response of stomatal movement is sensed by the redox state of the photosynthetic electron transport chain. Photosynth. Res. **119**: 131–

140.

von Caemmerer, S., Lawson, T., Oxborough, K., Baker, N.R., Andrews, T.J., and Raines, C.A. (2004). Stomatal conductance does not correlate with photosynthetic capacity in transgenic tobacco with reduced amounts of Rubisco. J. Exp. Bot. **55**: 1157–1166.

Caird, M. a, Richards, J.H., and Donovan, L. a (2007). Nighttime stomatal conductance and transpiration in C3 and C4 plants. Plant Physiol. **143**: 4–10.

de Carbonnel, M., Davis, P., Roelfsema, M.R.G., Inoue, S.-I., Schepens, I., Lariguet, P., Geisler, M., Shimazaki, K.-I., Hangarter, R., and Fankhauser, C. (2010). The Arabidopsis PHYTOCHROME KINASE SUBSTRATE2 protein is a phototropin signaling element that regulates leaf flattening and leaf positioning. Plant Physiol. **152**: 1391–1405.

Caspar, T., Huber, S.C., and Somerville, C. (1985). Alterations in Growth, Photosynthesis, and Respiration in a Starchless Mutant of *Arabidopsis thaliana* (L.) Deficient in Chloroplast Phosphoglucomutase Activity. Plant Physiol. **79**: 11–17.

Casson, S. a., Franklin, K. a., Gray, J.E., Grierson, C.S., Whitelam, G.C., and Hetherington, A.M. (2009). phytochrome B and PIF4 Regulate Stomatal Development in Response to Light Quantity. Curr. Biol. **19**: 229–234.

Charrier, B., Champion, A., Henry, Y., and Kreis, M. (2002). Expression profiling of the whole Arabidopsis shaggy-like kinase multigene family by real-time reverse transcriptase-polymerase chain reaction. Plant Physiol. **130**: 577–590.

Chatterjee, M., Berbezy, P., Vyas, D., Coates, S., and Barsby, T. (2005). Reduced expression of a protein homologous to glycogenin leads to reduction of starch content in Arabidopsis leaves. Plant Sci. **168**: 501–509.

Cho, M.H., Lim, H., Shin, D.H., Jeon, J.S., Bhoo, S.H., Park, Y. Il, and Hahn, T.R. (2011). Role of the plastidic glucose translocator in the export of starch degradation products from the chloroplasts in *Arabidopsis thaliana*. New Phytol. **190**: 101–112.

Choi, K., Kim, J., Hwang, H.J., Kim, S., Park, C., Kim, S.Y., and Lee, I. (2011). The FRIGIDA complex activates transcription of *FLC*, a strong flowering repressor in Arabidopsis, by recruiting chromatin modification factors. Plant Cell **23**: 289–303.

Christie, J.M. (2007). Phototropin blue-light receptors. Annu. Rev. Plant Biol. **58**: 21–45.

Christie, J.M., Reymond, P., Powell, G.K., Bernasconi, P., Raibekas, a a, Liscum, E., and Briggs, W.R. (1998). Arabidopsis NPH1: a flavoprotein with the properties of a photoreceptor for phototropism. Science **282**: 1698–1701.

Christie, J.M., Salomon, M., Nozue, K., Wada, M., and Briggs, W.R. (1999). LOV (light, oxygen, or voltage) domains of the blue-light photoreceptor phototropin (nph1): binding sites for the chromophore flavin mononucleotide. Proc. Natl. Acad. Sci. U. S. A. **96**: 8779–8783.

Cohen, P. (2000). The regulation of protein function by multisite phosphorylation - a 25 year update. Trends Biochem. Sci. **25**: 596–601.

Cominelli, E., Galbiati, M., Albertini, A., Fornara, F., Conti, L., Coupland, G., and Tonelli, C. (2011). DOF-binding sites additively contribute to guard cell-specificity of *AtMYB60* promoter. BMC Plant Biol **11**: 162.

Cominelli, E., Galbiati, M., Vavasseur, A., Conti, L., Sala, T., Vuylsteke, M., Leonhardt, N., Dellaporta, S.L., and Tonelli, C. (2005). A guard-cell-specific MYB transcription factor regulates stomatal movements and plant drought tolerance. Curr Biol **15**: 1196–1200.

Comparot-Moss, S. et al. (2010). A putative phosphatase, LSF1, is required for normal starch turnover in Arabidopsis leaves. Plant Physiol. **152**: 685–697.

Corbesier, L., Vincent, C., Jang, S., Fornara, F., Fan, Q., Searle, I., Giakountis, A., Farrona, S., Gissot, L., Turnbull, C., and Coupland, G. (2007). FT protein movement

contributes to long-distance signaling in floral induction of Arabidopsis. Science. **316**: 1030–1033.

Costa, J.M., Monnet, F., Jannaud, D., Leonhardt, N., Ksas, B., Reiter, I.M., Pantin, F., and Genty, B. (2015). OPEN ALL NIGHT LONG: The Dark Side of Stomatal Control. Plant Physiol. **167**: 289–294.

Crevillén, P., Ballicora, M. a., Mérida, Á., Preiss, J., and Romero, J.M. (2003). The different large subunit isoforms of *Arabidopsis thaliana* ADP-glucose pyrophosphorylase confer distinct kinetic and regulatory properties to the heterotetrameric enzyme. J. Biol. Chem. **278**: 28508–28515.

Crevillen, P., Ventriglia, T., Pinto, F., Orea, A., Merida, A., and Romero, J.M. (2005). Differential Pattern of Expression and Sugar Regulation of *Arabidopsis thaliana* ADP-glucose Pyrophosphorylase-encoding Genes. J. Biol. Chem. **280**: 8143–8149.

Critchley, J.H., Zeeman, S.C., Takaha, T., Smith, A.M., and Smith, S.M. (2001). A critical role for disproportionating enzyme in starch breakdown is revealed by a knock-out mutation in Arabidopsis. Plant J. **26**: 89–100.

Crosson, S. and Moffat, K. (2001). Structure of a flavin-binding plant photoreceptor domain: insights into light-mediated signal transduction. Proc. Natl. Acad. Sci. U. S. A. **98**: 2995–3000.

Crumpton-Taylor, M., Grandison, S., Png, K.M., Bushby, A.J., and Smith, A.M. (2012). Control of starch granule numbers in Arabidopsis chloroplasts. Plant Physiol. **158**: 905–916.

Curtis, M.D. and Grossniklaus, U. (2003). A gateway cloning vector set for high-throughput functional analysis of genes in planta. Plant Physiol. **133**: 462–469.

Cutler, S.R., Rodriguez, P.L., Finkelstein, R.R., and Abrams, S.R. (2010). Abscisic Acid: Emergence of a Core Signaling Network. Annu. Rev. Plant Biol. **61**: 651–679

Dajani, R., Fraser, E., Roe, S.M., Young, N., Good, V., Dale, T.C., and Pearl, L.H. (2001). Crystal structure of glycogen synthase kinase 3 beta: structural basis for phosphate-primed substrate specificity and autoinhibition. Cell **105**: 721–732.

Dal Santo, S., Stampfl, H., Krasensky, J., Kempa, S., Gibon, Y., Petutschnig, E., Rozhon, W., Heuck, A., Clausen, T., and Jonak, C. (2012). Stress-Induced GSK3 Regulates the Redox Stress Response by Phosphorylating Glucose-6-Phosphate Dehydrogenase in Arabidopsis. Plant Cell **24**: 3380–3392.

Daloso, D.M., Antunes, W.C., Pinheiro, D.P., Waquim, J.P., Araújo, W.L., Loureiro, M.E., Fernie, A.R., and Williams, T.C.R. (2015). Tobacco guard cells fix CO_2 by both Rubisco and PEPcase while sucrose acts as a substrate during light-induced stomatal opening. Plant. Cell Environ. doi:10.1111/pce.12555 1–19.

Damour, G., Vandame, M., and Urban, L. (2008). Long-term drought modifies the fundamental relationships between light exposure, leaf nitrogen content and photosynthetic capacity in leaves of the lychee tree (*Litchi chinensis*). J Plant Physiol **165**: 1370–1378.

Darwin, F. (1898). Observations on Stomata. Proc. R. Soc. Lond. B **190**: 531–621.

Delatte, T., Trevisan, M., Parker, M., and Zeeman, S. (2005). Arabidopsis mutants *Atisa1* and *Atisa2* have identical phenotypes and lack the same multimeric isoamylase, which influences the branch point distribution of amylopectin during starch synthesis. Plant J. **41**: 815–830.

Delatte, T., Umhang, M., Trevisan, M., Eicke, S., Thorneycroft, D., Smith, S.M., and Zeeman, S.C. (2006). Evidence for distinct mechanisms of starch granule breakdown in plants. J. Biol. Chem. **281**: 12050–12059.

Delvallé, D., Dumez, S., Wattebled, F., Roldán, I., Planchot, V., Berbezy, P., Colonna, P., Vyas, D., Chatterjee, M., Ball, S., Mérida, Á., and D'Hulst, C. (2005). Soluble starch

synthase I: A major determinant for the synthesis of amylopectin in *Arabidopsis thaliana* leaves. Plant J. **43**: 398–412.

Denyer, K., Dunlap, F., Thorbjørnsen, T., Keeling, P., and Smith, a M. (1996). The major form of ADP-glucose pyrophosphorylase in maize endosperm is extra-plastidial. Plant Physiol. **112**: 779–785.

Denyer, K., Johnson, P., Zeeman, S., and Smith, A.M. (2001). The control of amylose synthesis. J. Plant Physiol. **158**: 479–487.

Denyer, K., Waite, D., Motawia, S., Møller, B.L., and Smith, A. M. (1999). Granule-bound starch synthase I in isolated starch granules elongates malto-oligosaccharides processively. Biochem. J. **340 (Pt 1**: 183–191.

Depège, N., Bellafiore, S., and Rochaix, J.-D. (2003). Role of chloroplast protein kinase Stt7 in LHCII phosphorylation and state transition in Chlamydomonas. Science **299**: 1572–1575.

Dodd, A., Jakobsen, M., Baker, A., Telzerow, A., Hou, S., Laplaze, L., Barrot, L., Poethig, R., Haseloff, J., and Webb, A. (2006). Time of day modulates low-temperature Ca^{2+} signals in Arabidopsis. Plant J. **48**: 962–973.

Dodd, A.N., Parkinson, K., and Webb, A.A.R. (2004). Independent circadian regulation of assimilation and stomatal conductance in the *ztl-1* mutant of Arabidopsis. New Phytol. **162**: 63–70.

Dodd, A.N., Salathia, N., Hall, A., Kévei, E., Tóth, R., Nagy, F., Hibberd, J.M., Millar, A.J., and Webb, A. a R. (2005). Plant circadian clocks increase photosynthesis, growth, survival, and competitive advantage. Science **309**: 630–633.

Doyle, E. a., Lane, A.M., Sides, J.M., Mudgett, M.B., and Monroe, J.D. (2007). An α-amylase (At4g25000) in Arabidopsis leaves is secreted and induced by biotic and abiotic stress. Plant. Cell Environ. **30**: 388–398.

Dumez, S., Wattebled, F., Dauvillee, D., Delvalle, D., Planchot, V., Ball, S.G., and D'Hulst, C. (2006). Mutants of Arabidopsis lacking starch branching enzyme II substitute plastidial starch synthesis by cytoplasmic maltose accumulation. Plant Cell **18**: 2694–709.

Edner, C., Li, J., Albrecht, T., Mahlow, S., Hejazi, M., Hussain, H., Kaplan, F., Guy, C., Smith, S.M., Steup, M., and Ritte, G. (2007). Glucan, water dikinase activity stimulates breakdown of starch granules by plastidial β-amylases. Plant Physiol. **145**: 17–28.

Edwards, D., Kerp, H., and Hass, H. (1998). Stomata in early land plants: an anatomical and ecophysiological approach. **49**: 255–278.

Eisenach, C., Chen, Z.-H., Grefen, C., and Blatt, M.R. (2012). The trafficking protein SYP121 of Arabidopsis connects programmed stomatal closure and K^+ channel activity with vegetative growth. Plant J. **69**: 241–51.

Ekberg, K., Palmgren, M.G., Veierskov, B., and Buch-Pedersen, M.J. (2010). A novel mechanism of P-type ATPase autoinhibition involving both termini of the protein. J. Biol. Chem. **285**: 7344–7350.

Facchinelli, F. and Weber, A.P.M. (2011). The Metabolite Transporters of the Plastid Envelope: An Update. Front. Plant Sci. **2**: 1–18.

Ferl, R.J. (2004). 14-3-3 proteins: regulation of signal-induced events. Physiol. Plant. **120**: 173–178.

Fettke, J., Albrecht, T., Hejazi, M., Mahlow, S., Nakamura, Y., and Steup, M. (2010). Glucose 1-phosphate is efficiently taken up by potato (*Solanum tuberosum*) tuber parenchyma cells and converted to reserve starch granules. New Phytol **185**: 663–675.

Fettke, J., Chia, T., Eckermann, N., Smith, A., and Steup, M. (2006). A transglucosidase necessary for starch degradation and maltose metabolism in leaves at night acts on cytosolic heteroglycans (SHG). Plant J. **46**: 668–84.

Fettke, J., Eckermann, N., Poeste, S., Pauly, M., and Steup, M. (2004). The glycan substrate of the cytosolic (Pho2) phosphorylase isozyme from *Pisum sativum* L.: identification, linkage analysis and subcellular localization. Plant J. **39**: 933–46.

Fettke, J., Malinova, I., Albrecht, T., Hejazi, M., and Steup, M. (2011). Glucose-1-phosphate transport into protoplasts and chloroplasts from leaves of Arabidopsis. Plant Physiol. **155**: 1723–1734.

Fincher, G.B. (1989). Molecular and Cellular Biology Associated With Endosperm Mobilization in Germinating Cereal Grains. Annu. Rev. Plant Physiol. Plant Mol. Biol. **40**: 305–346

Fischer, R.A. (1968). Stomatal opening: role of potassium uptake by guard cells. Science. **160**: 784–785.

Fischer, R.A. and Hsiao, T.C. (1968). Stomatal Opening in Isolated Epidermal Strips of *Vicia faba*. II. Responses to KCl Concentration and the Role of Potassium Absorption. Plant Physiol. **43**: 1953–1958.

Flügge, U.I. (1992). Reaction mechanism and asymmetric orientation of the reconstituted chloroplast phosphate translocator. Biochim. Biophys. Acta **1110**: 112–8.

Flügge, U.I., Häusler, R.E., Ludewig, F., and Gierth, M. (2011). The role of transporters in supplying energy to plant plastids. J. Exp. Bot. **62**: 2381–2392.

Folta, K.M. and Spalding, E.P. (2001). Unexpected roles for cryptochrome 2 and phototropin revealed by high-resolution analysis of blue light-mediated hypocotyl growth inhibition. Plant J. **26**: 471–478.

Food and Agricultural Organization of the United Nations (2013). The State of Food Insecurity in the World 2013.

Francia, P., Simoni, L., Cominelli, E., Tonelli, C., and Galbiati, M. (2008). Gene trap-based identification of a guard cell promoter in Arabidopsis. Plant Signal. Behav. **3**: 684–686.

Franks, P.J., Cowan, I.R., and Farquhar, G.D. (1998). A study of stomatal mechanics using the cell pressure probe. Plant. Cell Environ. **21**: 94–100.

Franks, P.J. and Farquhar, G.D. (2006). The Mechanical Diversity of Stomata and Its Significance in Gas-Exchange Control. Plant Physiol. **143**: 78–87.

Fu, Y., Ballicora, M. a., Leykam, J.F., and Preiss, J. (1998). Mechanism of reductive activation of potato tuber ADP-glucose pyrophosphorylase. J. Biol. Chem. **273**: 25045–25052.

Fuglsang, A.T., Guo, Y., Cuin, T.A., Qiu, Q., Song, C., Kristiansen, K.A., Bych, K., Schulz, A., Shabala, S., Schumaker, K.S., Palmgren, M.G., and Zhu, J.-K. (2007). Arabidopsis Protein Kinase PKS5 Inhibits the Plasma Membrane H^+-ATPase by Preventing Interaction with 14-3-3 Protein. Plant Cell **19**: 1617–1634.

Fuglsang, A.T., Visconti, S., Drumm, K., Jahn, T., Stensballe, A., Mattei, B., Jensen, O.N., Aducci, P., and Palmgren, M.G. (1999). Binding of 14-3-3 Protein to the Plasma Membrane H^+-ATPase AHA2 Involves the Three C-terminal Residues Tyr^{946}-Thr-Val and Requires Phosphorylation of Thr^{947}. J. Biol. Chem. **274**: 36774–36780.

Fujii, H. and Zhu, J.-K. (2009). Arabidopsis mutant deficient in 3 abscisic acid-activated protein kinases reveals critical roles in growth, reproduction, and stress. Proc. Natl. Acad. Sci. U. S. A. **106**: 8380–8385.

Fujita, Y. et al. (2009). Three SnRK2 protein kinases are the main positive regulators of abscisic acid signaling in response to water stress in Arabidopsis. Plant Cell Physiol. **50**: 2123–32.

Fulton, D.C. et al. (2008). β-AMYLASE4, a noncatalytic protein required for starch breakdown, acts upstream of three active β-amylases in Arabidopsis chloroplasts. Plant Cell **20**: 1040–1058.

Galbiati, M., Matus, J.T., Francia, P., Rusconi, F., Canon, P., Medina, C., Conti, L., Cominelli, E., Tonelli, C., and Arce-Johnson, P. (2011). The grapevine guard cell-related VvMYB60 transcription factor is involved in the regulation of stomatal activity and is differentially expressed in response to ABA and osmotic stress. BMC Plant Biol **11**: 142.

Galbiati, M., Simoni, L., Pavesi, G., Cominelli, E., Francia, P., Vavasseur, A., Nelson, T., Bevan, M., and Tonelli, C. (2008). Gene trap lines identify Arabidopsis genes expressed in stomatal guard cells. Plant J. **53**: 750–762.

Gallagher, S., Short, T.W., Ray, P.M., Pratt, L.H., and Briggs, W.R. (1988). Light-mediated changes in two proteins found associated with plasma membrane fractions from pea stem sections. Proc. Natl. Acad. Sci. U. S. A. **85**: 8003–8007.

Gao, X.-Q., Li, C.-G., Wei, P.-C., Zhang, X.-Y., Chen, J., and Wang, X.-C. (2005). The dynamic changes of tonoplasts in guard cells are important for stomatal movement in *Vicia faba*. Plant Physiol. **139**: 1207–1216.

Gautier, H., Vavasseur, a, Gans, P., and Lascève, G. (1991). Relationship between Respiration and Photosynthesis in Guard Cell and Mesophyll Cell Protoplasts of *Commelina communis* L. Plant Physiol. **95**: 636–41.

Gaxiola, R. a., Palmgren, M.G., and Schumacher, K. (2007). Plant proton pumps. FEBS Lett. **581**: 2204–2214.

Geiger, D., Maierhofer, T., Al-Rasheid, K. a S., Scherzer, S., Mumm, P., Liese, A., Ache, P., Wellmann, C., Marten, I., Grill, E., Romeis, T., and Hedrich, R. (2011). Stomatal closure by fast abscisic acid signaling is mediated by the guard cell anion channel SLAH3 and the receptor RCAR1. Sci. Signal. **4**: ra32.

Geiger, D., Scherzer, S., Mumm, P., Marten, I., Ache, P., Matschi, S., Liese, a, Wellmann, C., Al-Rasheid, K. a S., Grill, E., Romeis, T., and Hedrich, R. (2010). Guard cell anion channel SLAC1 is regulated by CDPK protein kinases with distinct Ca^{2+} affinities. Proc. Natl. Acad. Sci. U. S. A. **107**: 8023–8028.

Geiger, D., Scherzer, S., Mumm, P., Stange, A., Marten, I., Bauer, H., Ache, P., Matschi, S., Liese, A., Al-Rasheid, K.A.S., Romeis, T., and Hedrich, R. (2009). Activity of guard cell anion channel SLAC1 is controlled by drought-stress signaling kinase-phosphatase pair. Proc. Natl. Acad. Sci. U. S. A. **106**: 21425–30.

George, G.M., van der Merwe, M.J., Nunes-Nesi, A., Bauer, R., Fernie, A.R., Kossmann, J., and Lloyd, J.R. (2010). Virus-induced gene silencing of plastidial soluble inorganic pyrophosphatase impairs essential leaf anabolic pathways and reduces drought stress tolerance in *Nicotiana benthamiana*. Plant Physiol. **154**: 55–66.

Gerber, S. a, Rush, J., Stemman, O., Kirschner, M.W., and Gygi, S.P. (2003). Absolute quantification of proteins and phosphoproteins from cell lysates by tandem MS. Proc. Natl. Acad. Sci. U. S. A. **100**: 6940–6945.

Gibon, Y., Blasing, O.E., Palacios-Rojas, N., Pankovic, D., Hendriks, J.H., Fisahn, J., Hohne, M., Gunther, M., and Stitt, M. (2004). Adjustment of diurnal starch turnover to short days: depletion of sugar during the night leads to a temporary inhibition of carbohydrate utilization, accumulation of sugars and post-translational activation of ADP-glucose pyrophosphorylase in the followin. Plant J **39**: 847–862.

Gibon, Y., Pyl, E., Sulpice, R., Lunn, J., Hohne, M., Gunther, M., and Stitt, M. (2009). Adjustment of growth, starch turnover, protein content and central metabolism to a decrease of the carbon supply when Arabidopsis is grown in very short photoperiods. Plant Cell Environ. **32**: 859–874.

Gjetting, K.S.K., Ytting, C.K., Schulz, A., and Fuglsang, A.T. (2012). Live imaging of intra- and extracellular pH in plants using pHusion, a novel genetically encoded biosensor. J. Exp. Bot. **63**: 3207–18.

Glaring, M. a., Koch, C.B., and Blennow, A. (2006). Genotype-specific spatial distribution of starch molecules in the starch granule: A combined CLSM and SEM approach.

Biomacromolecules **7**: 2310–2320.

Glaring, M.A., Skryhan, K., Kotting, O., Zeeman, S.C., and Blennow, A. (2012). Comprehensive survey of redox sensitive starch metabolising enzymes in *Arabidopsis thaliana*. Plant Physiol Biochem **58**: 89–97.

Gobert, A., Isayenkov, S., Voelker, C., Czempinski, K., and Maathuis, F.J.M. (2007). The two-pore channel *TPK1* gene encodes the vacuolar K^+ conductance and plays a role in K^+ homeostasis. Proc. Natl. Acad. Sci. U. S. A. **104**: 10726–10731.

Godfray, H.C.J., Beddington, J.R., Crute, I.R., Haddad, L., Lawrence, D., Muir, J.F., Pretty, J., Robinson, S., Thomas, S.M., and Toulmin, C. (2010). Food security: the challenge of feeding 9 billion people. Science **327**: 812–818.

Goh, C.H., Kinoshita, T., Oku, T., and Shimazaki, K. (1996). Inhibition of Blue Light-Dependent H^+ Pumping by Abscisic Acid in Vicia Guard-Cell Protoplasts. Plant Physiol. **111**: 433–440.

González-Cruz, J. and Pastenes, C. (2012). Water-stress-induced thermotolerance of photosynthesis in bean (*Phaseolus vulgaris* L.) plants: The possible involvement of lipid composition and xanthophyll cycle pigments. Environ. Exp. Bot. **77**: 127–140.

Gorton, H.L., Williams, W.E., Binns, M.E., Gemmell, C.N., Leheny, E. a, and Shepherd, a C. (1989). Circadian Stomatal Rhythms in Epidermal Peels from *Vicia faba*. Plant Physiol. **90**: 1329–1334.

Gosti, F., Beaudoin, N., Serizet, C., Webb, a a, Vartanian, N., and Giraudat, J. (1999). ABI1 protein phosphatase 2C is a negative regulator of abscisic acid signaling. Plant Cell **11**: 1897–1910.

Gotow, K., Tanaka, K., Kondo, N., Kobayashi, K., and Syōno, K. (1985). Light Activation of NADP-Malate Dehydrogenase in Guard Cell Protoplasts from *Vicia faba* L. Plant Physiol **79**: 829–832.

Gotow, K., Taylor, S., and Zeiger, E. (1988). Photosynthetic Carbon Fixation in Guard Cell Protoplasts of *Vicia faba* L. : Evidence from Radiolabel Experiments. Plant Physiol. **86**: 700–5.

Graf, A., Schlereth, A., Stitt, M., and Smith, A.M. (2010). Circadian control of carbohydrate availability for growth in Arabidopsis plants at night. Proc Natl Acad Sci U S A **107**: 9458–9463.

Granot, D. (2008). Putting plant hexokinases in their proper place. Phytochemistry **69**: 2649–2654.

Guo, F.-Q., Young, J., and Crawford, N.M. (2003). The nitrate transporter AtNRT1.1 (CHL1) functions in stomatal opening and contributes to drought susceptibility in Arabidopsis. Plant Cell **15**: 107–117.

Guzel Deger, A., Scherzer, S., Nuhkat, M., Kedzierska, J., Kollist, H., Brosché, M., Unyayar, S., Boudsocq, M., Hedrich, R., and Roelfsema, M.R.G. (2015). Guard cell SLAC1-type anion channels mediate flagellin-induced stomatal closure. New Phytol. **208**: 162–173.

ter Haar, E., Coll, J.T., Austen, D. a, Hsiao, H.M., Swenson, L., and Jain, J. (2001). Structure of GSK3beta reveals a primed phosphorylation mechanism. Nat. Struct. Biol. **8**: 593–596.

Hanstein, S.M. and Felle, H.H. (2002). CO_2-triggered chloride release from guard cells in intact fava bean leaves. Kinetics of the onset of stomatal closure. Plant Physiol. **130**: 940–50.

Harmer, S.L. (2009). The circadian system in higher plants. Annu. Rev. Plant Biol. **60**: 357–377.

Harper, S.M., Neil, L.C., and Gardner, K.H. (2003). Structural basis of a phototropin light switch. Science **301**: 1541–1544.

Haruta, M., Burch, H.L., Nelson, R.B., Barrett-Wilt, G., Kline, K.G., Mohsin, S.B., Young, J.C., Otegui, M.S., and Sussman, M.R. (2010). Molecular characterization of mutant Arabidopsis plants with reduced plasma membrane proton pump activity. J. Biol. Chem. **285**: 17918–17929.

Hashimoto, M., Negi, J., Young, J., Israelsson, M., Schroeder, J.I., and Iba, K. (2006). Arabidopsis HT1 kinase controls stomatal movements in response to CO_2. Nat. Cell Biol. **8**: 391–397.

Hayashi, M., Inoue, S.-I., Takahashi, K., and Kinoshita, T. (2011). Immunohistochemical detection of blue light-induced phosphorylation of the plasma membrane H^+-ATPase in stomatal guard cells. Plant Cell Physiol. **52**: 1238–48.

Hayashi, M. and Kinoshita, T. (2011). Crosstalk between blue-light- and ABA-signaling pathways in stomatal guard cells. Plant Signal. Behav. **6**: 1662–1664.

Heazlewood, J.L., Durek, P., Hummel, J., Selbig, J., Weckwerth, W., Walther, D., and Schulze, W.X. (2008). PhosPhAt: a database of phosphorylation sites in *Arabidopsis thaliana* and a plant-specific phosphorylation site predictor. Nucleic Acids Res. **36**: D1015–21.

Heckwolf, M., Pater, D., Hanson, D.T., and Kaldenhoff, R. (2011). The *Arabidopsis thaliana* aquaporin AtPIP1;2 is a physiologically relevant CO_2 transport facilitator. Plant J. **67**: 795–804.

Hedrich, R. (2012). Ion Channels in Plants. Physiol. Rev. **92**: 1777–1811.

Hedrich, R., Marten, I., Lohse, G., Dietrich, P., Winter, H., Lohaus, G., and Heldt, H.-W. (1994). Malate-sensitive anion channels enable guard cells to sense changes in the ambient CO_2 concentration. Plant J. **6**: 741–748.

Hedrich, R., Neimanis, S., Savchenko, G., Felle, H.H., Kaiser, W.M., and Heber, U. (2001). Changes in apoplastic ph and membrane potential in leaves in relation to stomatal responses to CO_2, malate, abscisic acid or interruption of water supply. Planta **213**: 594–601.

Hejazi, M., Fettke, J., Kötting, O., Zeeman, S.C., and Steup, M. (2010). The Laforin-like dual-specificity phosphatase SEX4 from Arabidopsis hydrolyzes both C6- and C3-phosphate esters introduced by starch-related dikinases and thereby affects phase transition of α-glucans. Plant Physiol. **152**: 711–722.

Helliwell, C.A., Wood, C.C., Robertson, M., James Peacock, W., and Dennis, E.S. (2006). The Arabidopsis FLC protein interacts directly *in vivo* with SOC1 and FT chromatin and is part of a high-molecular-weight protein complex. Plant J. **46**: 183–192.

Hendriks, J.H.M., Kolbe, A., Gibon, Y., Stitt, M., and Geigenberger, P. (2003). ADP-glucose pyrophosphorylase is activated by posttranslational redox-modification in response to light and to sugars in leaves of Arabidopsis and other plant species. Plant Physiol. **133**: 838–849.

Hennen-Bierwagen, T.A., Liu, F., Marsh, R.S., Kim, S., Gan, Q., Tetlow, I.J., Emes, M.J., James, M.G., and Myers, A.M. (2008). Starch biosynthetic enzymes from developing maize endosperm associate in multisubunit complexes. Plant Physiol. **146**: 1892–908.

Hepworth, S.R., Valverde, F., Ravenscroft, D., Mouradov, A., and Coupland, G. (2002). Antagonistic regulation of flowering-time gene SOC1 by CONSTANS and FLC via separate promoter motifs. EMBO J. **21**: 4327–4337.

Hetherington, A. and Woodward, F. (2003). The role of stomata in sensing and driving environmental change. Nature **424**: 901–908.

Hills, A., Chen, Z.-H., Amtmann, A., Blatt, M.R., and Lew, V.L. (2012). OnGuard, a Computational Platform for Quantitative Kinetic Modeling of Guard Cell Physiology. Plant Physiol. **159**: 1026–1042.

Hite, D.R.C., Outlaw, W.H., and Tarczynski, M.C. (1993). Elevated Levels of Both Sucrose-

Phosphate Synthase and Sucrose Synthase in Vicia Guard Cells Indicate Cell-Specific Carbohydrate Interconversions. Plant Physiol. **101**: 1217–1221.

Hosy, E. et al. (2003). The Arabidopsis outward K^+ channel GORK is involved in regulation of stomatal movements and plant transpiration. Proc. Natl. Acad. Sci. U. S. A. **100**: 5549–5554.

Hu, H., Boisson-Dernier, A., Israelsson-Nordström, M., Böhmer, M., Xue, S., Ries, A., Godoski, J., Kuhn, J.M., and Schroeder, J.I. (2010). Carbonic anhydrases are upstream regulators of CO_2-controlled stomatal movements in guard cells. Nat. Cell Biol. **12**: 87–93

Hua, D., Wang, C., He, J., Liao, H., Duan, Y., Zhu, Z., Guo, Y., Chen, Z., and Gong, Z. (2012). A Plasma Membrane Receptor Kinase, GHR1, Mediates Abscisic Acid- and Hydrogen Peroxide-Regulated Stomatal Movement in Arabidopsis. Plant Cell **24**: 2546–2561.

Huala, E., Oeller, P.W., Liscum, E., Han, I.S., Larsen, E., and Briggs, W.R. (1997). Arabidopsis NPH1: a protein kinase with a putative redox-sensing domain. Science **278**: 2120–2123.

Humble, G.D. and Hsiao, T.C. (1969). Specific Requirement of Potassium for Light-Activated Opening of Stomata in Epidermal Strips. Plant Physiol. **44**: 230–234.

Humble, G.D. and Raschke, K. (1971). Stomatal opening quantitatively related to potassium transport: evidence from electron probe analysis. Plant Physiol. **48**: 447–53.

Iino, M., Ogawa, T., and Zeiger, E. (1985). Kinetic properties of the blue-light response of stomata. Proc. Natl. Acad. Sci. U. S. A. **82**: 8019–8023.

Imes, D., Mumm, P., Böhm, J., Al-Rasheid, K. a S., Marten, I., Geiger, D., and Hedrich, R. (2013). Open stomata 1 (OST1) kinase controls R-type anion channel QUAC1 in Arabidopsis guard cells. Plant J. **74**: 372–82.

Inoue, S.-I., Kinoshita, T., Matsumoto, M., Nakayama, K.I., Doi, M., and Shimazaki, K.-I. (2008). Blue light-induced autophosphorylation of phototropin is a primary step for signaling. Proc. Natl. Acad. Sci. U. S. A. **105**: 5626–5631.

Intergovernmental Panel on Climate Change (2007). Climate Change 2007: Synthesis Report (Intergovernmental Panel on Climate Change: IPCC Secretariat, Geneva, Switzerland).

Ivashikina, N., Deeken, R., Fischer, S., Ache, P., and Hedrich, R. (2005). AKT2/3 subunits render guard cell K^+ channels Ca^{2+} sensitive. J. Gen. Physiol. **125**: 483–492.

Jane, J.L., Kasemsuwan, T., Leas, S., Zobel, H., and Robyt, J.F. (1994). Anthology of Starch Granule Morphology by Scanning Electron Microscopy. Starch/Stärke **46**: 121–129.

Johanson, U., West, J., Lister, C., Michaels, S., Amasino, R., and Dean, C. (2000). Molecular analysis of FRIGIDA, a major determinant of natural variation in Arabidopsis flowering time. Science. **290**: 344–347.

Johansson, F., Sommarin, M., and Larsson, C. (1993). Fusicoccin Activates the Plasma Membrane H^+-ATPase by a Mechanism Involving the C-Terminal Inhibitory Domain. Plant Cell **5**: 321–327.

Jonak, C. and Hirt, H. (2002). Glycogen synthase kinase 3/SHAGGY-like kinases in plants: an emerging family with novel functions. Trends Plant Sci. **7**: 457–461.

Jones, R. and Mansfield, T. (1970). Suppression of stomatal opening in leaves treated with abscisic acid. J. Exp. Bot. **21**: 714–719.

Jossier, M., Kroniewicz, L., Dalmas, F., Le Thiec, D., Ephritikhine, G., Thomine, S., Barbier-Brygoo, H., Vavasseur, A., Filleur, S., and Leonhardt, N. (2010). The Arabidopsis vacuolar anion transporter, AtCLCc, is involved in the regulation of stomatal movements and contributes to salt tolerance. Plant J. **64**: 563–576.

Kagawa, T., Sakai, T., Suetsugu, N., Oikawa, K., Ishiguro, S., Kato, T., Tabata, S., Okada, K., and Wada, M. (2001). Arabidopsis NPL1: a phototropin homolog controlling the chloroplast high-light avoidance response. Science **291**: 2138–2141.

Kami, C., Lorrain, S., Hornitschek, P., and Fankhauser, C. (2010). Light-regulated plant growth and development. Curr. Top. Dev. Biol. **91**: 29–66.

Kammerer, B., Fischer, K., Hilpert, B., Schubert, S., Gutensohn, M., Weber, a, and Flügge, U.I. (1998). Molecular characterization of a carbon transporter in plastids from heterotrophic tissues: the glucose 6-phosphate/phosphate antiporter. Plant Cell **10**: 105–117.

Kanczewska, J., Marco, S., Vandermeeren, C., Maudoux, O., Rigaud, J.-L., and Boutry, M. (2005). Activation of the plant plasma membrane H^+-ATPase by phosphorylation and binding of 14-3-3 proteins converts a dimer into a hexamer. Proc. Natl. Acad. Sci. U. S. A. **102**: 11675–11680.

Kang, C.-Y., Lian, H.-L., Wang, F.-F., Huang, J.-R., and Yang, H.-Q. (2009). Cryptochromes, phytochromes, and COP1 regulate light-controlled stomatal development in Arabidopsis. Plant Cell **21**: 2624–2641.

Kang, Y., Outlaw Jr., W.H., Fiore, G.B., and Riddle, K.A. (2007). Guard cell apoplastic photosynthate accumulation corresponds to a phloem-loading mechanism. J. Exp. Bot. **58**: 4061–4070.

Kaplan, F. and Guy, C.L. (2005). RNA interference of Arabidopsis β-amylase8 prevents maltose accumulation upon cold shock and increases sensitivity of PSII photochemical efficiency to freezing stress. Plant J **44**: 730–743.

Keller, B., Hedrich, R., and Raschke, K. (1989). Voltage-dependent anion channels in the plasma membrane of guard cells. Nature **341**: 450–453.

Kelly, G., Moshelion, M., David-Schwartz, R., Halperin, O., Wallach, R., Attia, Z., Belausov, E., and Granot, D. (2013). Hexokinase mediates stomatal closure. Plant J. **75**: 977–988.

Kempa, S., Rozhon, W., Šamaj, J., Erban, A., Baluška, F., Becker, T., Haselmayer, J., Schleiff, E., Kopka, J., Hirt, H., and Jonak, C. (2007). A plastid-localized glycogen synthase kinase 3 modulates stress tolerance and carbohydrate metabolism. Plant J. **49**: 1076–1090.

Kim, W.-Y., Hicks, K.A., and Somers, D.E. (2005). Independent roles for EARLY FLOWERING 3 and ZEITLUPE in the control of circadian timing, hypocotyl length, and flowering time. Plant Physiol. **139**: 1557–69.

Kimura, Y., Aoki, S., Ando, E., Kitatsuji, A., Watanabe, A., Ohnishi, M., Takahashi, K., Inoue, S.-I., Nakamichi, N., Tamada, Y., and Kinoshita, T. (2015). A Flowering Integrator, SOC1, Affects Stomatal Opening in *Arabidopsis thaliana*. Plant Cell Physiol. **56**: 640–649.

Kinoshita, T., Ono, N., Hayashi, Y., Morimoto, S., Nakamura, S., Soda, M., Kato, Y., Ohnishi, M., Nakano, T., Inoue, S.I., and Shimazaki, K. I. (2011). FLOWERING LOCUS T regulates stomatal opening. Curr. Biol. **21**: 1232–1238.

Kinoshita, T., Doi, M., Suetsugu, N., Kagawa, T., Wada, M., and Shimazaki, K. (2001). phot1 and phot2 mediate blue light regulation of stomatal opening. Nature **414**: 656–660.

Kinoshita, T., Emi, T., Tominaga, M., Sakamoto, K., Shigenaga, A., Doi, M., and Shimazaki, K. (2003). Blue-light- and phosphorylation-dependent binding of a 14-3-3 protein to phototropins in stomatal guard cells of broad bean. Plant Physiol. **133**: 1453–1463.

Kinoshita, T. and Shimazaki, K. (2002). Biochemical evidence for the requirement of 14-3-3 protein binding in activation of the guard-cell plasma membrane H^+-ATPase by blue light. Plant Cell Physiol. **43**: 1359–1365.

Kinoshita, T. and Shimazaki, K.I. (1999). Blue light activates the plasma membrane H^+-ATPase by phosphorylation of the C-terminus in stomatal guard cells. EMBO J. **18**: 5548–5558.

Kirchberger, S., Leroch, M., Huynen, M. A., Wahl, M., Neuhaus, E. H., and Tjaden, J. (2007). Molecular and biochemical analysis of the plastidic ADP-glucose transporter (ZmBT1) from Zea mays. J. Biol. Chem. **282**: 22481–22491.

Kirchberger, S., Tjaden, J., and Neuhaus, E. H. (2008). Characterization of the Arabidopsis Brittle1 transport protein and impact of reduced activity on plant metabolism. Plant J. **56**: 51–63.

Van Kirk, C. A. and Raschke, K. (1978a). Presence of Chloride Reduces Malate Production in Epidermis during Stomatal Opening. Plant Physiol. **61**: 361–364.

Van Kirk, C. A. and Raschke, K. (1978b). Release of Malate from Epidermal Strips during Stomatal Closure. Plant Physiol. **61**: 474–5.

Knappe, S., Flügge, U.-I., and Fischer, K. (2003). Analysis of the plastidic phosphate translocator gene family in Arabidopsis and identification of new phosphate translocator-homologous transporters, classified by their putative substrate-binding site. Plant Physiol. **131**: 1178–1190.

Kolbe, A., Tiessen, A., Schluepmann, H., Paul, M., Ulrich, S., and Geigenberger, P. (2005). Trehalose 6-phosphate regulates starch synthesis via posttranslational redox activation of ADP-glucose pyrophosphorylase. Proc. Natl. Acad. Sci. U. S. A. **102**: 11118–11123.

Kölling, K., George, G.M., Künzli, R., Flütsch, P., and Zeeman, S.C. (2015). A whole-plant chamber system for parallel gas exchange measurements of Arabidopsis and other herbaceous species. Plant Methods **11**: 48.

Kollist, H., Jossier, M., Laanemets, K., and Thomine, S. (2011). Anion channels in plant cells. FEBS J. **278**: 4277–4292.

Kollist, H., Nuhkat, M., and Roelfsema, M.R.G. (2014). Closing gaps: Linking elements that control stomatal movement. New Phytol. **203**: 44–62.

Kollist, T., Moldau, H., Rasulov, B., Oja, V., Ramma, H., Huve, K., Jaspers, P., Kangasjarvi, J., and Kollist, H. (2007). A novel device detects a rapid ozone-induced transient stomatal closure in intact Arabidopsis and its absence in *abi2* mutant. Physiol. Plant. **129**: 796–803.

Koornneef, M., Blankestijn-de Vries, H., Hanhart, C., Soppe, W., and Peeters, T. (1994). The phenotype of some late-flowering mutants is enhanced by a locus on chromosome 5 that is not effective in the Landsberg erecta wild-type. Plant J. **6**: 911–919.

Korthout, H.A. and de Boer, A.H. (1994). A fusicoccin binding protein belongs to the family of 14-3-3 brain protein homologs. Plant Cell **6**: 1681–1692.

Kötting, O., Kossmann, J., Zeeman, S.C., and Lloyd, J.R. (2010). Regulation of starch metabolism: the age of enlightenment? Curr. Opin. Plant Biol. **13**: 320–328.

Kötting, O., Pusch, K., Tiessen, A., Geigenberger, P., Steup, M., and Ritte, G. (2005). Identification of a novel enzyme required for starch metabolism in Arabidopsis leaves. The phosphoglucan, water dikinase. Plant Physiol. **137**: 242–252.

Kötting, O., Santelia, D., Edner, C., Eicke, S., Marthaler, T., Gentry, M.S., Comparot-Moss, S., Chen, J., Smith, A.M., Steup, M., Ritte, G., and Zeeman, S.C. (2009). STARCH-EXCESS4 is a laforin-like Phosphoglucan phosphatase required for starch degradation in *Arabidopsis thaliana*. Plant Cell **21**: 334–346.

Kruger, N.J. and ap Rees, T. (1983). Properties of α-Glucan Phosphorylase from Pea-Chloroplasts. Phytochemistry **22**: 1891–1898.

Kumar, J.K., Tabor, S., and Richardson, C.C. (2004). Proteomic analysis of thioredoxin-targeted proteins in *Escherichia coli*. Proc. Natl. Acad. Sci. U. S. A. **101**: 3759–64.

Kunz, H.H., Häusler, R.E., Fettke, J., Herbst, K., Niewiadomski, P., Gierth, M., Bell, K., Steup, M., Flügge, U.I., and Schneider, A. (2010). The role of plastidial glucose-6-phosphate/phosphate translocators in vegetative tissues of *Arabidopsis thaliana* mutants impaired in starch biosynthesis. Plant Biol. **12**: 115–128.

Kwak, J.M., Murata, Y., Baizabal-Aguirre, V.M., Merrill, J., Wang, M., Kemper, A., Hawke, S.D., Tallman, G., and Schroeder, J.I. (2001). Dominant negative guard cell K^+ channel mutants reduce inward-rectifying K^+ currents and light-induced stomatal opening in Arabidopsis. Plant Physiol. **127**: 473–85.

de la Fuente van Bentem, S., Anrather, D., Dohnal, I., Roitinger, E., Csaszar, E., Joore, J., Buijnink, J., Carreri, A., Forzani, C., Lorkovic, Z.J., Barta, A., Lecourieux, D., Verhounig, A., Jonak, C., and Hirt, H. (2008). Site-specific phosphorylation profiling of Arabidopsis proteins by mass spectrometry and peptide chip analysis. J Proteome Res **7**: 2458–2470.

Laby, R.J., Kim, D., and Gibson, S.I. (2001). The *ram1* Mutant of Arabidopsis Exhibits Severely Decreased β-Amylase Activity. **127**: 1798–1807.

Lao, N.T., Schoneveld, O., Mould, R.M., Hibberd, J.M., Gray, J.C., and Kavanagh, T.A. (1999). An Arabidopsis gene encoding a chloroplast-targeted β-amylase. Plant J. **20**: 519–527.

Lasceve, G., Leymarie, J., and Vavasseur, A. (1997). Alterations in light-induced stomatal opening in a starch-deficient mutant of *Arabidopsis thaliana* L. deficient in chloroplast phosphoglucomutase activity. Plant. Cell Environ. **20**: 350–358.

Latz, A., Mehlmer, N., Zapf, S., Mueller, T.D., Wurzinger, B., Pfister, B., Csaszar, E., Hedrich, R., Teige, M., and Becker, D. (2013). Salt stress triggers phosphorylation of the Arabidopsis vacuolar K^+ channel TPK1 by calcium-dependent protein kinases (CDPKs). Mol. Plant **6**: 1274–89.

Lawson, T. (2009). Guard cell photosynthesis and stomatal function. New Phytol. **181**: 13–34.

Lawson, T. and Blatt, M.R. (2014). Stomatal Size, Speed, and Responsiveness Impact on Photosynthesis and Water Use Efficiency. Plant Physiol. **164**: 1556–1570.

Lawson, T., Simkin, A.J., Kelly, G., and Granot, D. (2014). Mesophyll photosynthesis and guard cell metabolism impacts on stomatal behaviour. New Phytol. **203**: 1064–1081.

Lawson, T. and Weyers, J. (1999). Spatial and temporal variation in gas exchange over the lower surface of *Phaseolus vulgaris* L. primary leaves. J. Exp. Bot. **50**: 1381–1391.

Lebaudy, A., Pascaud, F., Véry, A.A., Alcon, C., Dreyer, I., Thibaud, J.B., and Lacombe, B. (2010). Preferential KAT1-KAT2 heteromerization determines inward K^+ current properties in Arabidopsis guard cells. J. Biol. Chem. **285**: 6265–6274.

Lebaudy, A., Vavasseur, A., Hosy, E., Dreyer, I., Leonhardt, N., Thibaud, J.-B., Véry, A.-A., Simonneau, T., and Sentenac, H. (2008). Plant adaptation to fluctuating environment and biomass production are strongly dependent on guard cell potassium channels. Proc. Natl. Acad. Sci. U. S. A. **105**: 5271–5276.

Lee, I. and Amasino, R.M. (1995). Effect of Vernalization, Photoperiod, and Light Quality on the Flowering Phenotype of Arabidopsis Plants Containing the FRIGIDA Gene. Plant Physiol. **108**: 157–162.

Lee, M., Choi, Y., Burla, B., Kim, Y.-Y., Jeon, B., Maeshima, M., Yoo, J.-Y., Martinoia, E., and Lee, Y. (2008). The ABC transporter AtABCB14 is a malate importer and modulates stomatal response to CO_2. Nat. Cell Biol. **10**: 1217–1223.

Lee, S.C., Lan, W., Buchanan, B.B., and Luan, S. (2009). A protein kinase-phosphatase pair interacts with an ion channel to regulate ABA signaling in plant guard cells. Proc. Natl. Acad. Sci. U. S. A. **106**: 21419–24.

Lemaire, S.D., Michelet, L., Zaffagnini, M., Massot, V., and Issakidis-Bourguet, E. (2007).

Thioredoxins in chloroplasts. Curr. Genet. **51**: 343–365.

Leonhardt, N., Kwak, J.M., Robert, N., Waner, D., Leonhardt, G., and Schroeder, J.I. (2004). Microarray expression analyses of Arabidopsis guard cells and isolation of a recessive abscisic acid hypersensitive protein phosphatase 2C mutant. Plant Cell **16**: 596–615.

Leshem, Y. and Levine, A. (2013). Zooming into sub-organellar localization of reactive oxygen species in guard cell chloroplasts during abscisic acid and methyl jasmonate treatments. Plant Signal. Behav. **8**: 1–4.

Levchenko, V., Konrad, K.R., Dietrich, P., Roelfsema, M.R.G., and Hedrich, R. (2005). Cytosolic abscisic acid activates guard cell anion channels without preceding Ca^{2+} signals. Proc. Natl. Acad. Sci. U. S. A. **102**: 4203–4208.

Leymarie, J., Lasceve, G., and Vavasseur, A (1999). Elevated CO_2 enhances stomatal responses to osmotic stress and abscisic acid in Arabidopsis thaliana. Plant Cell Environ. **22**: 301–308.

Li, J., Li, J., Nam, K.H., and Nam, K.H. (2002). Regulation of Brassinosteroid Signaling by a GSK3/SHAGGY-Like Kinase. Science. **295**: 1299–1301.

Lin, T.P., Caspar, T., Somerville, C., and Preiss, J. (1988a). Isolation and Characterization of a Starchless Mutant of *Arabidopsis thaliana* (L.) Heynh Lacking ADPglucose Pyrophosphorylase Activity. Plant Physiol. **86**: 1131–1135.

Lin, T.P., Caspar, T., Somerville, C.R., and Preiss, J. (1988b). A Starch Deficient Mutant of *Arabidopsis thaliana* with Low ADPglucose Pyrophosphorylase Activity Lacks One of the Two Subunits of the Enzyme. Plant Physiol. **88**: 1175–1181.

Lind, C. et al. (2015). Stomatal Guard Cells Co-opted an Ancient ABA-Dependent Desiccation Survival System to Regulate Stomatal Closure. Curr. Biol. **25**: 928–935.

Linder, B. and Raschke, K. (1992). A slow anion channel in guard cells, activating at large hyperpolarization, may be principal for stomatal closing. FEBS Lett. **313**: 27–30.

Lisitsky, I. and Schuster, G. (1995). Phosphorylation of a chloroplast RNA-binding protein changes its affinity to RNA. Nucleic Acids Res **23**: 2506–11.

Liu, F., Makhmoudova, A., Lee, E. a., Wait, R., Emes, M.J., and Tetlow, I.J. (2009). The amylose extender mutant of maize conditions novel protein-protein interactions between starch biosynthetic enzymes in amyloplasts. J. Exp. Bot. **60**: 4423–4440.

Liu, L.J., Zhang, Y.C., Li, Q.H., Sang, Y., Mao, J., Lian, H.L., Wang, L., and Yang, H.Q. (2008). COP1-mediated ubiquitination of CONSTANS is implicated in cryptochrome regulation of flowering in Arabidopsis. Plant Cell **20**: 292–306.

Lloyd, F.E. (1908). The Physiology of Stomata (Carnegie Institution of Washington).

Lu, P., Outlaw Jr, W.H., Smith, B.G., and Freed, G. a. (1997). A New Mechanism for the Regulation of Stomatal Aperture Size in Intact Leaves (Accumulation of Mesophyll-Derived Sucrose in the Guard-Cell Wall of *Vicia faba*). Plant Physiol. **114**: 109–118.

Lu, P., Zhang, S.Q., Outlaw, W.H., and Riddle, K. a (1995). Sucrose: a solute that accumulates in the guard-cell apoplast and guard-cell symplast of open stomata. FEBS Lett. **362**: 180–184.

Lu, Y., Gehan, J.P., and Sharkey, T.D. (2005). Daylength and circadian effects on starch degradation and maltose metabolism. Plant Physiol. **138**: 2280–2291.

Lu, Y. and Sharkey, T.D. (2004). The role of amylomaltase in maltose metabolism in the cytosol of photosynthetic cells. Planta **218**: 466–473.

Lu, Y., Steichen, J.M., Yao, J., and Sharkey, T.D. (2006). The role of cytosolic α-glucan phosphorylase in maltose metabolism and the comparison of amylomaltase in Arabidopsis and *Escherichia coli*. Plant Physiol. **142**: 878–889.

Lüttge, U. (2002). CO_2-concentrating: consequences in crassulacean acid metabolism. J.

Exp. Bot. **53**: 2131–2142.

Ma, Y., Szostkiewicz, I., Korte, A., Moes, D., Yang, Y., Christmann, A., and Grill, E. (2009). Regulators of PP2C phosphatase activity function as abscisic acid sensors. Science. **324**: 1064–1068.

MacRobbie, E.A.C. and Lettau, J. (1980). Potassium content and aperture in "intact" stomatal and epidermal cells of *Commelina communis* L. J. Membr. Biol. **56**: 249–256.

Malinova, I., Mahlow, S., Alseekh, S., Orawetz, T., Fernie, A.R., Baumann, O., Steup, M., and Fettke, J. (2014). Double Knockout Mutants of Arabidopsis Grown under Normal Conditions Reveal that the Plastidial Phosphorylase Isozyme Participates in Transitory Starch Metabolism. Plant Physiol. **164**: 907–921.

Mao, J., Zhang, Y.-C., Sang, Y., Li, Q.-H., and Yang, H.-Q. (2005). A role for Arabidopsis cryptochromes and COP1 in the regulation of stomatal opening. Proc. Natl. Acad. Sci. U. S. A. **102**: 12270–12275.

Marra, M., Fullone, M.R., Fogliano, V., Pen, J., Mattei, M., Masi, S., and Aducci, P. (1994). The 30-kilodalton protein present in purified fusicoccin receptor preparations is a 14-3-3-like protein. Plant Physiol. **106**: 1497–1501.

Marre, E. (1979). Fusicoccin: A Tool in Plant Physiology. Annu. Rev. Plant Physiol. **30**: 273–288.

Marten, H., Hedrich, R., and Roelfsema, M.R.G. (2007). Blue light inhibits guard cell plasma membrane anion channels in a phototropin-dependent manner. Plant J. **50**: 29–39.

Marten, H., Hyun, T., Gomi, K., Seo, S., Hedrich, R., and Roelfsema, M.R.G. (2008). Silencing of NtMPK4 impairs CO_2-induced stomatal closure, activation of anion channels and cytosolic Ca^{2+} signals in *Nicotiana tabacum* guard cells. Plant J. **55**: 698–708.

Martin, E.S. and Meidner, H. (1971). Endogenous Stomatal Movements in *Tradescantia virginiana*. New Phytol. **70**: 923–928.

Martin, T., Sharma, R., Sippel, C., Waegemann, K., Soll, J., and Vothknecht, U.C. (2006). A protein kinase family in Arabidopsis phosphorylates chloroplast precursor proteins. J. Biol. Chem. **281**: 40216–4023.

Martinoia, E. and Rentsch, D. (1994). Malate compartmentation - Responses to a complex metabolism. Annu. Rev. Plant Physiol. Plant Mol. Biol. **45**: 447–467.

Mathieu, J., Warthmann, N., Küttner, F., and Schmid, M. (2007). Export of FT protein from phloem companion cells is sufficient for floral induction in Arabidopsis. Curr. Biol. **17**: 1055–1060.

Matsuoka, D. and Tokutomi, S. (2005). Blue light-regulated molecular switch of Ser/Thr kinase in phototropin. Proc. Natl. Acad. Sci. U. S. A. **102**: 13337–1342.

May, T. and Soll, J. (2000). 14-3-3 Proteins Form a Guidance Complex With Chloroplast Precursor Proteins in Plants. Plant Cell **12**: 53–64.

McAdam, S.A.M. and Brodribb, T.J. (2013). Ancestral stomatal control results in a canalization of fern and lycophyte adaptation to drought. New Phytol. **198**: 429–441

Meinhard, M. and Schnabl, H. (2001). Fusicoccin- and light-induced activation and *in vivo* phosphorylation of phosphoenolpyruvate carboxylase in Vicia guard cell protoplasts. Plant Sci. **160**: 635–646.

Merilo, E., Laanemets, K., Hu, H., Xue, S., Jakobson, L., Tulva, I., Gonzalez-Guzman, M., Rodriguez, P.L., Schroeder, J.I., Brosche, M., and Kollist, H. (2013). PYR/RCAR Receptors Contribute to Ozone-, Reduced Air Humidity-, Darkness-, and CO_2-Induced Stomatal Regulation. Plant Physiol. **162**: 1652–1668.

Merlot, S., Leonhardt, N., Fenzi, F., Valon, C., Costa, M., Piette, L., Vavasseur, A., Genty, B., Boivin, K., Müller, A., Giraudat, J., and Leung, J. (2007). Constitutive activation of

a plasma membrane H^+-ATPase prevents abscisic acid-mediated stomatal closure. EMBO J. **26**: 3216–26.

Merlot, S., Mustilli, A.-C., Genty, B., North, H., Lefebvre, V., Sotta, B., Vavasseur, A., and Giraudat, J. (2002). Use of infrared thermal imaging to isolate Arabidopsis mutants defective in stomatal regulation. Plant J. **30**: 601–9.

Messinger, S.M., Buckley, T.N., and Mott, K. a (2006). Evidence for involvement of photosynthetic processes in the stomatal response to CO_2. Plant Physiol. **140**: 771–778.

Meyer, S., Lauterbach, C., Niedermeier, M., Barth, I., Sjolund, R.D., and Sauer, N. (2004). Wounding enhances expression of AtSUC3, a sucrose transporter from Arabidopsis sieve elements and sink tissues. Plant Physiol. **134**: 684–693.

Meyer, S., Mumm, P., Imes, D., Endler, A., Weder, B., Al-Rasheid, K.A., Geiger, D., Marten, I., Martinoia, E., and Hedrich, R. (2010). AtALMT12 represents an R-type anion channel required for stomatal movement in Arabidopsis guard cells. Plant J **63**: 1054–1062.

Meyer, S., Scholz-Starke, J., De Angeli, A., Kovermann, P., Burla, B., Gambale, F., and Martinoia, E. (2011). Malate transport by the vacuolar AtALMT6 channel in guard cells is subject to multiple regulation. Plant J. **67**: 247–57.

Michaels, S.D., Himelblau, E., Kim, S.Y., Schomburg, F.M., and Amasino, R.M. (2005). Integration of flowering signals in winter-annual Arabidopsis. Plant Physiol. **137**: 149–156.

Michalska, J., Zauber, H., Buchanan, B.B., Cejudo, F.J., and Geigenberger, P. (2009). NTRC links built-in thioredoxin to light and sucrose in regulating starch synthesis in chloroplasts and amyloplasts. Proc. Natl. Acad. Sci. U. S. A. **106**: 9908–9913.

Mikkelsen, R., Mutenda, K.E., Mant, A., Schürmann, P., and Blennow, A. (2005). α-glucan, water dikinase (GWD): a plastidic enzyme with redox-regulated and coordinated catalytic activity and binding affinity. Proc. Natl. Acad. Sci. U. S. A. **102**: 1785–1790.

Mockler, T., Yang, H., Yu, X., Parikh, D., Cheng, Y., Dolan, S., and Lin, C. (2003). Regulation of photoperiodic flowering by Arabidopsis photoreceptors. Proc. Natl. Acad. Sci. U. S. A. **100**: 2140–2145.

von Mohl, H. (1856). Welche Ursachen bewirken die Erweiterung und Verengung der Spaltöffnungen? Bot. Zeitschrift **14**: 697 – 704.

Monroe, J.D., Storm, A.R., Badley, E.M., Lehman, M.D., Platt, S.M., Saunders, L.K., Schmitz, J.M., and Torres, C.E. (2014). β-AMYLASE1 and β-AMYLASE3 are Plastidic Starch Hydrolases in Arabidopsis that Appear to be Adapted for Different Thermal, pH, and Stress Conditions. Plant Physiol. **166**: 1748–1763

Montrichard, F., Alkhalfioui, F., Yano, H., Vensel, W.H., Hurkman, W.J., and Buchanan, B.B. (2009). Thioredoxin targets in plants: The first 30 years. J. Proteomics **72**: 452–474.

Morison, J.I.L., Baker, N.R., Mullineaux, P.M., and Davies, W.J. (2008). Improving water use in crop production. Philos. Trans. R. Soc. Lond. B. Biol. Sci. **363**: 639–58.

Morth, J.P., Pedersen, B.P., Buch-Pedersen, M.J., Andersen, J.P., Vilsen, B., Palmgren, M.G., and Nissen, P. (2011). A structural overview of the plasma membrane Na^+,K^+-ATPase and H^+-ATPase ion pumps. Nat. Rev. Mol. Cell Biol. **12**: 60–70.

Mott, K.A. (2009). Opinion: Stomatal responses to light and CO_2 depend on the mesophyll. Plant, Cell Environ. **32**: 1479–1486.

Mott, K.A. and Buckley, T.N. (2000). Patchy stomatal conductance: Emergent collective behaviour of stomata. Trends Plant Sci. **5**: 258–263.

Mott, K.A., Sibbernsen, E.D., and Shope, J.C. (2008). The role of the mesophyll in stomatal responses to light and CO_2. Plant. Cell Environ. **31**: 1299–1306.

Mugford, S.T., Fernandez, O., Brinton, J., Flis, A., Krohn, N., Encke, B., Feil, R., Sulpice, R., Lunn, J.E., Stitt, M., and Smith, A.M. (2014). Regulatory Properties of ADP Glucose Pyrophosphorylase Are Required for Adjustment of Leaf Starch Synthesis in Different Photoperiods. Plant Physiol. **166**: 1733–1747.

Müller-Röber, B., Ellenberg, J., Provart, N., Willmitzer, L., Busch, H., Becker, D., Dietrich, P., Hoth, S., and Hedrich, R. (1995). Cloning and electrophysiological analysis of KST1, an inward rectifying K^+ channel expressed in potato guard cells. EMBO J. **14**: 2409–2416.

Muñoz, F.J., Baroja-Fernández, E., Morán-Zorzano, M.T., Viale, A.M., Etxeberria, E., Alonso-Casajús, N., and Pozueta-Romero, J. (2005). Sucrose synthase controls both intracellular ADP glucose levels and transitory starch biosynthesis in source leaves. Plant Cell Physiol. **46**: 1366–1376.

Muñoz, F.J., Zorzano, M.T.M., Alonso-Casajús, N., Baroja-Fernández, E., Etxeberria, E., and Pozueta-Romero, J. (2006). New enzymes, new pathways and an alternative view on starch biosynthesis in both photosynthetic and heterotrophic tissues of plants. Biocatal. Biotransformation **24**: 63–76.

Mustilli, A.-C., Merlot, S., Vavasseur, A., Fenzi, F., and Giraudat, J. (2002). Arabidopsis OST1 protein kinase mediates the regulation of stomatal aperture by abscisic acid and acts upstream of reactive oxygen species production. Plant Cell **14**: 3089–3099.

Nakagami, H., Sugiyama, N., Mochida, K., Daudi, A., Yoshida, Y., Toyoda, T., Tomita, M., Ishihama, Y., and Shirasu, K. (2010). Large-scale comparative phosphoproteomics identifies conserved phosphorylation sites in plants. Plant Physiol. **153**: 1161–74.

Negi, J., Matsuda, O., Nagasawa, T., Oba, Y., Takahashi, H., Kawai-Yamada, M., Uchimiya, H., Hashimoto, M., and Iba, K. (2008). CO_2 regulator SLAC1 and its homologues are essential for anion homeostasis in plant cells. Nature **452**: 483–486.

Negi, J., Moriwaki, K., Konishi, M., Yokoyama, R., Nakano, T., Kusumi, K., Hashimoto-Sugimoto, M., Schroeder, J.I., Nishitani, K., Yanagisawa, S., and Iba, K. (2013). A Dof transcription factor, SCAP1, is essential for the development of functional stomata in Arabidopsis. Curr Biol **23**: 479–484.

Neuhaus, E.H., Häusler, R.E., and Sonnewald, U. (2005). No need to shift the paradigm on the metabolic pathway to transitory starch in leaves. Trends Plant Sci. **10**: 154–156.

Niewiadomski, P., Knappe, S., Geimer, S., Fischer, K., Schulz, B., Unte, U.S., Rosso, M.G., Ache, P., Flügge, U.-I., and Schneider, A. (2005). The Arabidopsis plastidic glucose 6-phosphate/phosphate translocator GPT1 is essential for pollen maturation and embryo sac development. Plant Cell **17**: 760–775.

Niittylä, T., Comparot-Moss, S., Lue, W.-L., Messerli, G., Trevisan, M., Seymour, M.D.J., Gatehouse, J. a, Villadsen, D., Smith, S.M., Chen, J., Zeeman, S.C., and Smith, A.M. (2006). Similar protein phosphatases control starch metabolism in plants and glycogen metabolism in mammals. J. Biol. Chem. **281**: 11815–8.

Niittylä, T., Fuglsang, A.T., Palmgren, M.G., Frommer, W.B., and Schulze, W.X. (2007). Temporal Analysis of Sucrose-induced Phosphorylation Changes in Plasma Membrane Proteins of Arabidopsis. Mol. Cell. Proteomics **6**: 1711–1726.

Niittyla, T., Messerli, G., Trevisan, M., Chen, J., Smith, A.M., and Zeeman, S.C. (2004). A previously unknown maltose transporter essential for starch degradation in leaves. Science. **303**: 87–89.

Nishimura, N., Sarkeshik, A., Nito, K., Park, S.Y., Wang, A., Carvalho, P.C., Lee, S., Caddell, D.F., Cutler, S.R., Chory, J., Yates, J.R., and Schroeder, J.I. (2010). PYR/PYL/RCAR family members are major *in-vivo* ABI1 protein phosphatase 2C-interacting proteins in Arabidopsis. Plant J. **61**: 290–299.

Noguero, M., Atif, R.M., Ochatt, S., and Thompson, R.D. (2013). The role of the DNA-binding One Zinc Finger (DOF) transcription factor family in plants. Plant Sci. **209**: 32–45.

Nühse, T.S., Stensballe, A., Jensen, O.N., and Peck, S.C. (2004). Phosphoproteomics of the Arabidopsis plasma membrane and a new phosphorylation site database. Plant Cell **16**: 2394–405.

O'Sullivan, A.C. and Perez, S. (1999). The relationship between internal chain length of amylopectin and crystallinity in starch. Biopolymers **50**: 381–90.

Oecking, C., Eckerskorn, C., and Weiler, E.W. (1994). The fusicoccin receptor of plants is a member of the 14-3-3 superfamily of eukaryotic regulatory proteins. FEBS Lett. **352**: 163–166.

Ogawa, T., Ishikawa, H., Shimada, K., and Shibata, K. (1978). Synergistic action of red and blue light and action spectra for malate formation in guard cells of *Vicia faba* L. Planta **142**: 61–65.

Ohgishi, M., Saji, K., Okada, K., and Sakai, T. (2004). Functional analysis of each blue light receptor, cry1, cry2, phot1, and phot2, by using combinatorial multiple mutants in Arabidopsis. Proc. Natl. Acad. Sci. U. S. A. **101**: 2223–2228.

Olsen, R.L., Pratt, R.B., Gump, P., Kemper, A., and Tallman, G. (2002). Red light activates a chloroplast-dependent ion uptake mechanism for stomatal opening under reduced CO_2 concentrations in Vicia spp. New Phytol. **153**: 497–508.

Oreña, S.J., Torchia, A.J., and Garofalo, R.S. (2000). Inhibition of glycogen-synthase kinase 3 stimulates glycogen synthase and glucose transport by distinct mechanisms in 3T3-L1 adipocytes. J. Biol. Chem. **275**: 15765–15772.

Osakabe, Y., Arinaga, N., Umezawa, T., Katsura, S., Nagamachi, K., Tanaka, H., Ohiraki, H., Yamada, K., Seo, S.-U., Abo, M., Yoshimura, E., Shinozaki, K., and Yamaguchi-Shinozaki, K. (2013). Osmotic stress responses and plant growth controlled by potassium transporters in Arabidopsis. Plant Cell **25**: 609–624.

Ottmann, C., Marco, S., Jaspert, N., Marcon, C., Schauer, N., Weyand, M., Vandermeeren, C., Duby, G., Boutry, M., Wittinghofer, A., Rigaud, J.-L., and Oecking, C. (2007). Structure of a 14-3-3 coordinated hexamer of the plant plasma membrane H^+-ATPase by combining X-ray crystallography and electron cryomicroscopy. Mol. Cell **25**: 427–40.

Outlaw, W.H., Du, Z., Meng, F.X., Aghoram, K., Riddle, K. a., and Chollet, R. (2002). Requirements for activation of the signal-transduction network that leads to regulatory phosphorylation of leaf guard-cell phosphoenolpyruvate carboxylase during fusicoccin-stimulated stomatal opening. Arch. Biochem. Biophys. **407**: 63–71.

Outlaw, W.H. and Kennedy, J. (1978). Enzymic and Substrate Basis for the Anaplerotic Step in Guard Cells. Plant Physiol **62**: 648–652.

Outlaw, W.H. and Lowry, O.H. (1977). Organic acid and potassium accumulation in guard cells during stomatal opening. Proc. Natl. Acad. Sci. U. S. A. **74**: 4434–8.

Outlaw, W.H. and Manchester, J. (1979). Guard cell starch concentration quantitatively related to stomatal aperture. Plant Physiol. **64**: 79–82.

Outlaw, W.H., Manchester, J., and Brown, P.H. (1981). High Levels of Malic Enzyme Activities in *Vicia faba* L. Epidermal Tissue. Plant Physiol **68**: 1047–1051.

Outlaw, W.H., Tarczynski, M.C., and Anderson, L.C. (1982). Taxonomic survey for the presence of Ribulose-1,5-Bisphosphate Carboxylase Activity in Guard Cells. Plant Physiol. **70**: 1218–1220.

Outlaw, Jr., W.H. (2003). Integration of Cellular and Physiological Functions of Guard Cells. Crit. Rev. Plant Sci. **22**: 503–529.

Ovecka, M., Bahaji, A., Munoz, F.J., Almagro, G., Ezquer, I., Baroja-Fernandez, E., Li, J., and Pozueta-Romero, J. (2012). A sensitive method for confocal fluorescence microscopic visualization of starch granules in iodine stained samples. Plant Signal Behav **7**: 1146–1150.

Overlach, S., Diekmann, W., and Raschke, K. (1993). Phosphate Translocator of Isolated Guard-Cell Chloroplasts. Plant Physiol. **101**: 1201–1207.

Palmgren, M.G. (2001). Plant Plasma Membrane H^+-ATPases: Powerhouses for Nutrient Uptake. Annu. Rev. Plant Physiol. Plant Mol. Biol. **52**: 817–845.

Palmgren, M.G., Sommarin, M., Serrano, R., and Larsson, C. (1991). Identification of an autoinhibitory domain in the C-terminal region of the plant plasma membrane H^+-ATPase. J. Biol. Chem. **266**: 20470–20475.

Pandey, S., Wang, R.-S., Wilson, L., Li, S., Zhao, Z., Gookin, T.E., Assmann, S.M., and Albert, R. (2010). Boolean modeling of transcriptome data reveals novel modes of heterotrimeric G-protein action. Mol. Syst. Biol. **6**: 372.

Pandey, S., Wang, X.-Q., Coursol, S.A., and Assmann, S.M. (2002). Preparation and Applications of Arabidopsis thaliana Guard Cell Protoplasts. New Phytol. **153**: 517–526.

Park, S.-Y., Fung, P., Nishimura, N., Jensen, D.R., Fujii, H., Zhao, Y., Lumba, S., Santiago, J., Rodrigues, A., Chow, T.-F., Alfred, S. E., Bonetta, D., Finkelstein, R., Provart, N. J., Desveaux, D., Rodriguez, P.L., McCourt, P., Zhu, J.-K., Schroeder, J.I., Volkman, B.F., and Cutler, S.R. (2009). Abscisic acid inhibits type 2C protein phosphatases via the PYR/PYL family of START proteins. Science. **324**: 1068–1071.

Pedersen, B.P., Buch-Pedersen, M.J., Morth, J.P., Palmgren, M.G., and Nissen, P. (2007). Crystal structure of the plasma membrane proton pump. Nature **450**: 1111–4.

Pei, Z.M., Murata, Y., Benning, G., Thomine, S., Klüsener, B., Allen, G.J., Grill, E., and Schroeder, J.I. (2000). Calcium channels activated by hydrogen peroxide mediate abscisic acid signalling in guard cells. Nature **406**: 731–734.

Penfield, S., Clements, S., Bailey, K.J., Gilday, A.D., Leegood, R.C., Gray, J.E., and Graham, I. a (2012). Expression and manipulation of phosphoenolpyruvate carboxykinase 1 identifies a role for malate metabolism in stomatal closure. Plant J. **69**: 679–88.

Peng, P., Zhao, J., Zhu, Y., Asami, T., and Li, J. (2010). A Direct Docking Mechanism for a Plant GSK3-like Kinase to Phosphorylate Its Substrates. J. Biol. Chem. **285**: 24646–24653.

Pérez, S. and Bertoft, E. (2010). The molecular structures of starch components and their contribution to the architecture of starch granules: A comprehensive review. Starch/Stärke **62**: 389–420.

Picotti, P. and Aebersold, R. (2012). Selected reaction monitoring–based proteomics: workflows, potential, pitfalls and future directions. Nat. Methods **9**: 555–566.

Pillitteri, L.J. and Dong, J. (2013). Stomatal development in Arabidopsis. Arabidopsis Book **11**: e0162.

Plesch, G., Ehrhardt, T., and Mueller-Roeber, B. (2001). Involvement of TAAAG elements suggests a role for Dof transcription factors in guard cell-specific gene expression. Plant J. **28**: 455–464.

Poffenroth, M., Green, D.B., and Tallman, G. (1992). Sugar Concentrations in Guard Cells of *Vicia faba* Illuminated with Red or Blue Light : Analysis by High Performance Liquid Chromatography. Plant Physiol. **98**: 1460–1471.

Prasch, C.M., Ott, K.V., Bauer, H., Ache, P., Hedrich, R., and Sonnewald, U. (2015). ß-amylase1 mutant Arabidopsis plants show improved drought tolerance due to reduced starch breakdown in guard cells. J. Exp. Bot. **66**: 6059–6067.

Prasch, C.M. and Sonnewald, U. (2013). Simultaneous application of heat, drought, and virus to Arabidopsis plants reveals significant shifts in signaling networks. Plant Physiol. **162**: 1849–66.

Price, G.D., von Caemmerer, S., Evans, J.R., Siebke, K., Anderson, J.M., and Badger, M.R. (1998). Photosynthesis is strongly reduced by antisense suppression of

chloroplastic cytochrome bf complex in transgenic tobacco. Aust. J. Plant Physiol. **25**: 445–452.

Ramon, M., Rolland, F., and Sheen, J. (2008). Sugar Sensing and Signaling. Arab. B. **6**: e0117.

Raschke, K. and Humble, G.D. (1973). No uptake of anions required by opening stomata of *Vicia faba*: Guard cells release hydrogen ions. Planta **115**: 47–57.

Raschke, K. and Schnabl, H. (1978). Availability of Chloride Affects the Balance between Potassium Chloride and Potassium Malate in Guard Cells of *Vicia faba* L. Plant Physiol. **62**: 84–87.

Rathore, R.S., Garg, N., Garg, S., and Kumar, A. (2009). Starch phosphorylase: role in starch metabolism and biotechnological applications. Crit Rev Biotechnol **29**: 214–224.

Rayapuram, N., Bonhomme, L., Bigeard, J., Haddadou, K., Przybylski, C., Hirt, H., and Pflieger, D. (2014). Identification of Novel PAMP-Triggered Phosphorylation and Dephosphorylation Events in *Arabidopsis thaliana* by Quantitative Phosphoproteomic Analysis. J. Proteome Res. **13**: 2137–2151.

Reckmann, U., Scheibe, R., and Raschke, K. (1990). Rubisco activity in guard cells compared with the solute requirement for stomatal opening. Plant Physiol. **92**: 246–53.

Reddy, A.R. and Das, V.S.R. (1986). Stomatal Movement and Sucrose Uptake by Guard Cell Protoplasts of *Commelina benghalensis* L . Plant Cell Physiol. **27**: 1565–1570.

Reiland, S., Messerli, G., Baerenfaller, K., Gerrits, B., Endler, A., Grossmann, J., Gruissem, W., and Baginsky, S. (2009). Large-scale Arabidopsis phosphoproteome profiling reveals novel chloroplast kinase substrates and phosphorylation networks. Plant Physiol **150**: 889–903.

Reinhold, H., Soyk, S., Simkova, K., Hostettler, C., Marafino, J., Mainiero, S., Vaughan, C.K., Monroe, J.D., and Zeeman, S.C. (2011). β-amylase-like proteins function as transcription factors in Arabidopsis, controlling shoot growth and development. Plant Cell **23**: 1391–1403.

Richard, O., Paquet, N., Haudecoeur, E., and Charrier, B. (2005). Organization and expression of the GSK3/shaggy kinase gene family in the moss *Physcomitrella patens* suggest early gene multiplication in land plants and an ancestral response to osmotic stress. J. Mol. Evol. **61**: 99–113.

Rienmüller, F., Dreyer, I., Schönknecht, G., Schulz, A., Schumacher, K., Nagy, R., Martinoia, E., Marten, I., and Hedrich, R. (2012). Luminal and cytosolic pH feedback on proton pump activity and ATP affinity of V-type ATPase from Arabidopsis. J. Biol. Chem. **287**: 8986–8993.

Ritte, G., Heydenreich, M., Mahlow, S., Haebel, S., Kötting, O., and Steup, M. (2006). Phosphorylation of C6- and C3-positions of glucosyl residues in starch is catalysed by distinct dikinases. FEBS Lett. **580**: 4872–6.

Ritte, G., Lloyd, J.R., Eckermann, N., Rottmann, A., Kossmann, J., and Steup, M. (2002). The starch-related R1 protein is an α-glucan, water dikinase. Proc. Natl. Acad. Sci. U. S. A. **99**: 7166–71.

Ritte, G. and Raschke, K. (2003). Metabolite export of isolated guard cell chloroplasts of *Vicia faba*. New Phytol. **159**: 195–202.

Ritte, G., Rosenfeld, J., Rohrig, K., and Raschke, K. (1999). Rates of Sugar Uptake by Guard Cell Protoplasts of *Pisum sativum* L. Related to the Solute Requirement for Stomatal Opening. Plant Physiol. **121**: 647–656.

Rizhsky, L., Liang, H., Shuman, J., Shulaev, V., Davletova, S., Mittler, R., Rizhsky L., Liang H., Shuman J., Shulaev V., Davletova S., and R., M. (2004). When Defense Pathways Collide. The Response of Arabidopsis to a Combination of Drought and Heat Stress. Plant Physiol. **134**: 1683–1696.

Robinson, N. and Preiss, J. (1985). Biochemical phenomena associated with stomatal function. Physiol. Plant. **64**: 141–146.

Roelfsema, M.R., Konrad, K.R., Marten, H., Psaras, G.K., Hartung, W., and Hedrich, R. (2006). Guard cells in albino leaf patches do not respond to photosynthetically active radiation, but are sensitive to blue light, CO_2 and abscisic acid. Plant. Cell Environ. **29**: 1595–1605.

Roelfsema, M.R., Steinmeyer, R., Staal, M., and Hedrich, R. (2001). Single guard cell recordings in intact plants: light-induced hyperpolarization of the plasma membrane. Plant J. **26**: 1–13.

Roelfsema, M.R.G., Hanstein, S., Felle, H.H., and Hedrich, R. (2002). CO_2 provides an intermediate link in the red light response of guard cells. Plant J. **32**: 65–75.

Roelfsema, M.R.G., Hedrich, R., and Geiger, D. (2012). Anion channels: Master switches of stress responses. Trends Plant Sci. **17**: 221–229.

Roelfsema, M.R.G., Levchenko, V., and Hedrich, R. (2004). ABA depolarizes guard cells in intact plants, through a transient activation of R- and S-type anion channels. Plant J. **37**: 578–588.

Roitinger, E., Hofer, M., Köcher, T., Pichler, P., Novatchkova, M., Yang, J., Schlögelhofer, P., and Mechtler, K. (2015). Quantitative Phosphoproteomics of the ATM and ATR dependent DNA damage response in *Arabidopsis thaliana*. Mol. Cell. Proteomics **14**: 556–571.

Roldán, I., Wattebled, F., Mercedes Lucas, M., Delvallé, D., Planchot, V., Jiménez, S., Pérez, R., Ball, S., D'Hulst, C., and Mérida, Á. (2007). The phenotype of soluble starch synthase IV defective mutants of *Arabidopsis thaliana* suggests a novel function of elongation enzymes in the control of starch granule formation. Plant J. **49**: 492–504.

Rubio, S., Rodrigues, A., Saez, A., Dizon, M.B., Galle, A., Kim, T.-H., Santiago, J., Flexas, J., Schroeder, J.I., and Rodriguez, P.L. (2009). Triple loss of function of protein phosphatases type 2C leads to partial constitutive response to endogenous abscisic acid. Plant Physiol. **150**: 1345–1355.

Sakai, T., Kagawa, T., Kasahara, M., Swartz, T.E., Christie, J.M., Briggs, W.R., Wada, M., and Okada, K. (2001). Arabidopsis nph1 and npl1: blue light receptors that mediate both phototropism and chloroplast relocation. Proc. Natl. Acad. Sci. U. S. A. **98**: 6969–74.

Sakai, T., Wada, T., Ishiguro, S., and Okada, K. (2000). RPT2. A signal transducer of the phototropic response in Arabidopsis. Plant Cell **12**: 225–236.

Sakamoto, K. and Briggs, W.R. (2002). Cellular and subcellular localization of phototropin 1. Plant Cell **14**: 1723–1735.

Salinas, P., Fuentes, D., Vidal, E., Jordana, X., Echeverria, M., and Holuigue, L. (2006). An extensive survey of CK2 alpha and beta subunits in Arabidopsis: Multiple isoforms exhibit differential subcellular localization. Plant Cell Physiol. **47**: 1295–1308.

Salomon, M., Christie, J.M., Knieb, E., Lempert, U., and Briggs, W.R. (2000). Photochemical and mutational analysis of the FMN-binding domains of the plant blue light receptor, phototropin. Biochemistry **39**: 9401–9410.

Salomon, M., Knieb, E., Von Zeppelin, T., and Rüdiger, W. (2003). Mapping of low- and high-fluence autophosphorylation sites in phototropin 1. Biochemistry **42**: 4217–4225.

Santelia, D., Kotting, O., Seung, D., Schubert, M., Thalmann, M., Bischof, S., Meekins, D.A., Lutz, A., Patron, N., Gentry, M.S., Allain, F.H., and Zeeman, S.C. (2011). The phosphoglucan phosphatase like sex four2 dephosphorylates starch at the C3-position in Arabidopsis. Plant Cell **23**: 4096–4111.

Santelia, D., Trost, P., and Sparla, F. (2015). New insights into redox control of starch degradation. Curr. Opin. Plant Biol. **25**: 1–9.

Santelia, D. and Zeeman, S.C. (2011). Progress in Arabidopsis starch research and potential biotechnological applications. Curr. Opin. Biotechnol. **22**: 271–280.

Santiago, J., Rodrigues, A., Saez, A., Rubio, S., Antoni, R., Dupeux, F., Park, S.Y., Márquez, J.A., Cutler, S.R., and Rodriguez, P.L. (2009). Modulation of drought resistance by the abscisic acid receptor PYL5 through inhibition of clade A PP2Cs. Plant J. **60**: 575–588.

Sato, A., Sato, Y., Fukao, Y., Fujiwara, M., Umezawa, T., Shinozaki, K., Hibi, T., Taniguchi, M., Miyake, H., Goto, D.B., and Uozumi, N. (2009). Threonine at position 306 of the KAT1 potassium channel is essential for channel activity and is a target site for ABA-activated SnRK2/OST1/SnRK2.6 protein kinase. Biochem. J. **424**: 439–448.

Satoh, H., Shibahara, K., Tokunaga, T., Nishi, A., Tasaki, M., Hwang, S. K., Okita, T. W., Kaneko, N., Fujita, N., Yoshida, M., Hosaka, Y., Sato, A., Utsumi, Y., Ohdan, T. and Nakamura, Y. (2008). Mutation of the plastidial α-glucan phosphorylase gene in rice affects the synthesis and structure of starch in the endosperm. Plant Cell **20**: 1833–1849.

Schachtman, D.P., Schroeder, J.I., Lucas, W.J., Anderson, J.A., and Gaber, R.F. (1992). Expression of an inward-rectifying potassium channel by the Arabidopsis KAT1 cDNA. Science **258**: 1654–1658.

Scheibe, R., Reckmann, U., Hedrich, R., and Raschke, K. (1990). Malate Dehydrogenases in Guard Cells of *Pisum sativum*. Plant Physiol. **93**: 1358–64.

Schleiff, E., Soll, J., Sveshnikova, N., Tien, R., Wright, S., Dabney-Smith, C., Subramanian, C., and Bruce, B.D. (2002). Structural and guanosine triphosphate/diphosphate requirements for transit peptide recognition by the cytosolic domain of the chloroplast outer envelope receptor, Toc34. Biochemistry **41**: 1934–46.

Schnabl, H. (1980). CO_2 and malate metabolism in starch-containing and starch-lacking guard-cell protoplasts. Planta **149**: 52–58.

Schnabl, H. and Raschke, K. (1980). Potassium Chloride as Stomatal Osmoticum in *Allium cepa* L., a Species Devoid of Starch in Guard Cells. Plant Physiol. **65**: 88–93.

Schneider, A., Häusler, R.E., Kolukisaoglu, Ü., Kunze, R., Van der Graaff, E., Schwacke, R., Catoni, E., Desimone, M., and Flügge, U.I. (2002). An *Arabidopsis thaliana* knock-out mutant of the chloroplast triose phosphate/phosphate translocator is severely compromised only when starch synthesis, but not starch mobilisation is abolished. Plant J. **32**: 685–699.

Schroeder, J.I., Allen, G.J., Hugouvieux, V., Kwak, J.M., and Waner, D. (2001a). Guard cell signal transduction. Annu. Rev. Plant Physiol. Plant Mol. Biol. **52**: 627–658.

Schroeder, J.I., Hedrich, R., and Fernandez, J.M. (1984). Potassium-selective single channels in guard cell protoplasts of *Vicia faba*. Nature **312**: 361–362.

Schroeder, J.I., Kwak, J.M., and Allen, G.J. (2001b). Guard cell abscisic acid signalling and engineering drought hardiness in plants. Nature **410**: 327–330.

Schroeder, J.I., Raschke, K., and Neher, E. (1987). Voltage dependence of K^+ channels in guard-cell protoplasts. Proc. Natl. Acad. Sci. U. S. A. **84**: 4108–4112.

Schulze, E.D., Lange, O.L., Kappen, L., Buschbom, U., and Evenari, M. (1973). Stomatal responses to changes in temperature at increasing water stress. Planta **110**: 29–42.

Schumacher, K. and Krebs, M. (2010). The V-ATPase: Small cargo, large effects. Curr. Opin. Plant Biol. **13**: 724–730.

Schwartz, A. and Zeiger, E. (1984). Metabolic energy for stomatal opening. Roles of photophosphorylation and oxidative phosphorylation. Planta **161**: 129–136.

Scialdone, A., Mugford, S.T., Feike, D., Skeffington, A., Borrill, P., Graf, A., Smith, A.M., and Howard, M. (2013). Arabidopsis plants perform arithmetic division to prevent starvation at night. Elife **2**: e00669.

Serrano, E.E., Zeiger, E., and Hagiwara, S. (1988). Red light stimulates an electrogenic proton pump in Vicia guard cell protoplasts. Proc. Natl. Acad. Sci. U. S. A. **85**: 436–440.

Serrato, A.J., Pérez-Ruiz, J.M., Spínola, M.C., and Cejudo, F.J. (2004). A novel NADPH thioredoxin reductase, localized in the chloroplast, which deficiency causes hypersensitivity to abiotic stress in Arabidopsis thaliana. J. Biol. Chem. **279**: 43821–43827.

Seung, D., Soyk, S., Coiro, M., Maier, B. a., Eicke, S., and Zeeman, S.C. (2015). PROTEIN TARGETING TO STARCH Is Required for Localising GRANULE-BOUND STARCH SYNTHASE to Starch Granules and for Normal Amylose Synthesis in Arabidopsis. PLOS Biol. **13**: e1002080.

Seung, D., Thalmann, M., Sparla, F., Abou Hachem, M., Lee, S.K., Issakidis-Bourguet, E., Svensson, B., Zeeman, S.C., and Santelia, D. (2013). Arabidopsis thaliana AMY3 Is a Unique Redox-regulated Chloroplastic α-Amylase. J. Biol. Chem. **288**: 33620–33633.

Sharkey, T.D. and Raschke, K. (1981). Effect of Light Quality on Stomatal Opening in Leaves of *Xanthium strumarium* L. Plant Physiol. **68**: 1170–1174.

Sherson, S.M., Alford, H.L., Forbes, S.M., Wallace, G., and Smith, S.M. (2003). Roles of cell-wall invertases and monosaccharide transporters in the growth and development of Arabidopsis. J. Exp. Bot. **54**: 525–531.

Shimazaki, K., Doi, M., Assmann, S.M., and Kinoshita, T. (2007). Light regulation of stomatal movement. Annu. Rev. Plant Biol. **58**: 219–47.

Shimazaki, K., Iino, M., and Zeiger, E. (1986). Blue light-dependent proton extrusion by guard-cell protoplasts of *Vicia faba*. Nature **319**: 324–326.

Shimazaki, K., Terada, J., Tanaka, K., and Kondo, N. (1989). Calvin-Benson Cycle Enzymes in Guard-Cell Protoplasts from *Vicia faba* L. Plant Physiol. **90**: 1057–1064.

Shimazaki, K.-I. (1989). Ribulosebisphosphate Carboxylase Activity and Photosynthetic O_2 Evolution Rate in Vicia Guard-Cell Protoplasts. Plant Physiol **91**: 459–463.

Shimazaki, K.-I. and Zeiger, E. (1985). Cyclic and noncyclic photophosphorylation in isolated guard cell chloroplasts of *Vicia faba* L. Plant Physiol. **78**: 211–214.

Shope, J.C., DeWald, D.B., and Mott, K.A. (2003). Changes in surface area of intact guard cells are correlated with membrane internalization. Plant Physiol. **133**: 1314–21.

Siegfried, E., Chou, T.B., and Perrimon, N. (1992). Wingless signaling acts through zeste-white 3, the Drosophila homolog of glycogen synthase kinase-3, to regulate engrailed and establish cell fate. Cell **71**: 1167–1179.

Silver, D.M., Silva, L.P., Issakidis-Bourguet, E., Glaring, M. a., Schriemer, D.C., and Moorhead, G.B.G. (2013). Insight into the redox regulation of the phosphoglucan phosphatase SEX4 involved in starch degradation. FEBS J. **280**: 538–48.

Sirichandra, C., Gu, D., Hu, H.-C., Davanture, M., Lee, S., Djaoui, M., Valot, B., Zivy, M., Leung, J., Merlot, S., and Kwak, J.M. (2009). Phosphorylation of the Arabidopsis AtrbohF NADPH oxidase by OST1 protein kinase. FEBS Lett. **583**: 2982–6.

Skeffington, A.W., Graf, A., Duxbury, Z., Gruissem, W., and Smith, A.M. (2014). Glucan, Water Dikinase Exerts Little Control over Starch Degradation in Arabidopsis Leaves at Night. Plant Physiol. **165**: 866–879.

Smart, R.E. and Bingham, G. (1974). Rapid estimates of relative water content. Plant Physiol. **53**: 258–260.

Smith, A.M. and Zeeman, S.C. (2006). Quantification of starch in plant tissues. Nat. Protoc. **1**: 1342–1345.

Smith, A.M., Zeeman, S.C., and Smith, S.M. (2005). Starch Degradation. Annu. Rev. Plant Biol. **56**: 73–98.

Smith, S.M., Fulton, D.C., Chia, T., Thorneycroft, D., Chapple, A., Dunstan, H., Hylton, C., Zeeman, S.C., and Smith, A.M. (2004). Diurnal Changes in the Transcriptome Encoding Enzymes of Starch Metabolism Provide Evidence for Both Transcriptional and Posttranscriptional Regulation of Starch Metabolism in Arabidopsis Leaves. Plant Physiol. **136**: 2687–2699.

Somers, D.E., Webb, A.A., Pearson, M., and Kay, S.A. (1998). The short-period mutant, *toc1-1*, alters circadian clock regulation of multiple outputs throughout development in *Arabidopsis thaliana*. Development **125**: 485–494.

Song, Y., Miao, Y., and Song, C.P. (2014). Behind the scenes: The roles of reactive oxygen species in guard cells. New Phytol. **201**: 1121–1140.

Soyk, S., Imkova, K., Zurcher, E., Luginbuhl, L., Brand, L.H., Vaughan, C.K., Wanke, D., and Zeeman, S.C. (2014). The Enzyme-Like Domain of Arabidopsis Nuclear β-Amylases Is Critical for DNA Sequence Recognition and Transcriptional Activation. Plant Cell **26**: 1746–1763.

Sparla, F., Costa, A., Lo Schiavo, F., Pupillo, P., and Trost, P. (2006). Redox regulation of a novel plastid-targeted β-amylase of Arabidopsis. Plant Physiol. **141**: 840–850.

Srikanth, A. and Schmid, M. (2011). Regulation of flowering time: all roads lead to Rome. Cell. Mol. Life Sci. **68**: 2013–2037.

Stadler, R., Buttner, M., Ache, P., Hedrich, R., Ivashikina, N., Melzer, M., Shearson, S.M., Smith, S.M., and Sauer, N. (2003). Diurnal and light-regulated expression of AtSTP1 in guard cells of Arabidopsis. Plant Physiol **133**: 528–537.

Staehelin, L. A and Arntzen, C.J. (1983). Regulation of chloroplast membrane function: protein phosphorylation changes the spatial organization of membrane components. J. Cell Biol. **97**: 1327–1337.

Stanley, D., Fitzgerald, A., Farnden, K., and McRae, E. (2002). Characterization of putative amylases from apple (*Malus domestica*) and *Arabidopsis thaliana*. Biologia. **57**: 137.

Stitt, M. and Zeeman, S.C. (2012). Starch turnover: pathways, regulation and role in growth. Curr. Opin. Plant Biol. **15**: 282–292.

Streb, S., Delatte, T., Umhang, M., Eicke, S., Schorderet, M., Reinhardt, D., and Zeeman, S.C. (2008). Starch granule biosynthesis in Arabidopsis is abolished by removal of all debranching enzymes but restored by the subsequent removal of an endoamylase. Plant Cell **20**: 3448–3466.

Streb, S., Egli, B., Eicke, S., and Zeeman, S.C. (2009). The debate on the pathway of starch synthesis: a closer look at low-starch mutants lacking plastidial phosphoglucomutase supports the chloroplast-localized pathway. Plant Physiol. **151**: 1769–72.

Streb, S., Eicke, S., and Zeeman, S.C. (2012). The Simultaneous Abolition of Three Starch Hydrolases Blocks Transient Starch Breakdown in Arabidopsis. J. Biol. Chem. **287**: 41745–41756.

Streb, S. and Zeeman, S.C. (2012). Starch metabolism in Arabidopsis. Arab. B. **10**: e0160.

Suetsugu, N., Takami, T., Ebisu, Y., Watanabe, H., Iiboshi, C., Doi, M., and Shimazaki, K. (2014). Guard cell chloroplasts are essential for blue light-dependent stomatal opening in Arabidopsis. PLoS One **9**: e108374.

Sugiyama, N., Nakagami, H., Mochida, K., Daudi, A., Tomita, M., Shirasu, K., and Ishihama, Y. (2008). Large-scale phosphorylation mapping reveals the extent of tyrosine phosphorylation in Arabidopsis. Mol. Syst. Biol. **4**: 193.

Sullivan, S., Thomson, C.E., Kaiserli, E., and Christie, J.M. (2009). Interaction specificity of Arabidopsis 14-3-3 proteins with phototropin receptor kinases. FEBS Lett. **583**: 2187–2193.

Sundberg, M., Pfister, B., Fulton, D., Bischof, S., Delatte, T., Eicke, S., Stettler, M.,

Smith, S.M., Streb, S., and Zeeman, S.C. (2013). The Heteromultimeric Debranching Enzyme Involved in Starch Synthesis in Arabidopsis Requires Both Isoamylase1 and Isoamylase2 Subunits for Complex Stability and Activity. PLoS One **8**: e75223..

Sung, S. and Amasino, R.M. (2005). Remembering winter: toward a molecular understanding of vernalization. Annu. Rev. Plant Biol. **56**: 491–508.

Svennelid, F., Olsson, a, Piotrowski, M., Rosenquist, M., Ottman, C., Larsson, C., Oecking, C., and Sommarin, M. (1999). Phosphorylation of Thr-948 at the C terminus of the plasma membrane H^+-ATPase creates a binding site for the regulatory 14-3-3 protein. Plant Cell **11**: 2379–2391.

Szydlowski, N., Ragel, P., Raynaud, S., Lucas, M.M., Roldan, I., Montero, M., Munoz, F.J., Ovecka, M., Bahaji, A., Planchot, V., Pozueta-Romero, J., D'Hulst, C., and Merida, A. (2009). Starch Granule Initiation in Arabidopsis Requires the Presence of Either Class IV or Class III Starch Synthases. Plant Cell **21**: 2443–2457.

Szydlowski, N., Ragel, P., Hennen-Bierwagen, T.A., Planchot, V., Myers, A.M., Merida, A., d'Hulst, C., and Wattebled, F. (2011). Integrated functions among multiple starch synthases determine both amylopectin chain length and branch linkage location in Arabidopsis leaf starch. J. Exp. Bot. **62**: 4547–4559.

Szyroki, a, Ivashikina, N., Dietrich, P., Roelfsema, M.R., Ache, P., Reintanz, B., Deeken, R., Godde, M., Felle, H., Steinmeyer, R., Palme, K., and Hedrich, R. (2001). KAT1 is not essential for stomatal opening. Proc. Natl. Acad. Sci. U. S. A. **98**: 2917–2921.

Takeda, Y. and Hizukuri, S. (1981). Re-examination of the action of sweet-potato β-amylase on phosphorylated (1→4)-α-D-glucan. Carbohydr. Res. **89**: 174–178.

Takemiya, A., Inoue, S., and Doi, M. (2005). Phototropins promote plant growth in response to blue light in low light environments. Plant Cell **17**: 1120–1127.

Takemiya, A., Kinoshita, T., Asanuma, M., and Shimazaki, K.-I. (2006). Protein phosphatase 1 positively regulates stomatal opening in response to blue light in *Vicia faba*. Proc. Natl. Acad. Sci. U. S. A. **103**: 13549–54.

Takemiya, A. and Shimazaki, K. (2010). Phosphatidic acid inhibits blue light-induced stomatal opening via inhibition of protein phosphatase 1. Plant Physiol. **153**: 1555–1562.

Takemiya, A., Sugiyama, N., Fujimoto, H., Tsutsumi, T., Yamauchi, S., Hiyama, A., Tada, Y., Christie, J.M., and Shimazaki, K.-I. (2013a). Phosphorylation of BLUS1 kinase by phototropins is a primary step in stomatal opening. Nat. Commun. **4**: 2094.

Takemiya, A., Yamauchi, S., Yano, T., Ariyoshi, C., and Shimazaki, K.-I. (2013b). Identification of a Regulatory Subunit of Protein Phosphatase 1 Which Mediates Blue Light Signaling for Stomatal Opening. Plant Cell Physiol. **54**: 24–35.

Talbott, L. and Zeiger, E. (1998). The role of sucrose in guard cell osmoregulation. J. Exp. Bot. **49**: 329–337.

Talbott, L.D., Shmayevich, I.J., Chung, Y., Hammad, J.W., and Zeiger, E. (2003). Blue light and phytochrome-mediated stomatal opening in the *npq1* and *phot1 phot2* mutants of Arabidopsis. Plant Physiol. **133**: 1522–1529.

Talbott, L.D. and Zeiger, E. (1996). Central Roles for Potassium and Sucrose in Guard-Cell Osmoregulation. Plant Physiol. **111**: 1051–1057.

Talbott, L.D. and Zeiger, E. (1993). Sugar and Organic Acid Accumulation in Guard Cells of *Vicia faba* in Response to Red and Blue Light. Plant Physiol. **102**: 1163–1169.

Tallman, G. and Zeiger, E. (1988). Light quality and osmoregulation in Vicia guard cells: evidence for involvement of three metabolic pathways. Plant Physiol **88**: 887–895.

Taoka, K.-I., Ohki, I., Tsuji, H., Furuita, K., Hayashi, K., Yanase, T., Yamaguchi, M., Nakashima, C., Purwestri, Yekti A., Tamaki, S., Ogaki, Y., Shimada, C., Nakagawa, A., Kojima, C., and Shimamoto, K. (2011). 14-3-3 proteins act as intracellular receptors for rice Hd3a florigen. Nature. **476**: 332–335.

Tarczynski, M.C., Outlaw, W.H., Arold, N., Neuhoff, V., and Hampp, R. (1989). Electrophoretic Assay for Ribulose 1,5-Bisphosphate Carboxylase/Oxygenase in Guard Cells and Other Leaf Cells of *Vicia faba* L. Plant Physiol. **89**: 1088–93.

Tatge, H., Marshall, J., Martin, C., Edwards, E.A., and Smith, A.M. (1999). Evidence that amylose synthesis occurs within the matrix of the starch granule in potato tubers. Plant. Cell Environ. **22**: 543–550.

Taylor, A.R. and Assmann, S.M. (2001). Apparent absence of a redox requirement for blue light activation of pump current in broad bean guard cells. Plant Physiol. **125**: 329–338.

Tetlow, I.J., Beisel, K.G., Cameron, S., Makhmoudova, A., Liu, F., Bresolin, N.S., Wait, R., Morell, M.K., and Emes, M.J. (2008). Analysis of protein complexes in wheat amyloplasts reveals functional interactions among starch biosynthetic enzymes. Plant Physiol. **146**: 1878–1891.

Tetlow, I.J., Wait, R., Lu, Z., Akkasaeng, R., Bowsher, C.G., Esposito, S., Kosar-Hashemi, B., Morell, M.K., and Emes, M.J. (2004). Protein phosphorylation in amyloplasts regulates starch branching enzyme activity and protein-protein interactions. Plant Cell **16**: 694–708.

Thormählen, I., Ruber, J., von Roepenack-Lahaye, E., Ehrlich, S.-M., Massot, V., Hümmer, C., Tezycka, J., Issakidis-Bourguet, E., and Geigenberger, P. (2013). Inactivation of thioredoxin f1 leads to decreased light activation of ADP-glucose pyrophosphorylase and altered diurnal starch turnover in leaves of Arabidopsis plants. Plant. Cell Environ. **36**: 16–29.

Tian, W., Hou, C., Ren, Z., Pan, Y., Jia, J., Zhang, H., Bai, F., Zhang, P., Zhu, H., He, Y., Luo, S., Li, L., and Luan, S. (2015). A molecular pathway for CO_2 response in Arabidopsis guard cells. Nat. Commun. **2**: 1–10.

Tickle, P., Burrell, M.M., Coates, S.A., Emes, M.J., Tetlow, I.J., and Bowsher, C.G. (2009). Characterization of plastidial starch phosphorylase in *Triticum aestivum* L. endosperm. J Plant Physiol **166**: 1465–1478.

Tiessen, A., Hendriks, J.H.M., Stitt, M., Branscheid, A., Gibon, Y., Farré, E.M., and Geigenberger, P. (2002). Starch synthesis in potato tubers is regulated by post-translational redox modification of ADP-glucose pyrophosphorylase: a novel regulatory mechanism linking starch synthesis to the sucrose supply. Plant Cell **14**: 2191–2213.

Tiessen, A., Prescha, K., Branscheid, A., Palacios, N., McKibbin, R., Halford, N.G., and Geigenberger, P. (2003). Evidence that SNF1-related kinase and hexokinase are involved in separate sugar-signalling pathways modulating post-translational redox activation of ADP-glucose pyrophosphorylase in potato tubers. Plant J. **35**: 490–500.

Tominaga, M., Kinoshita, T., and Shimazaki, K. (2001). Guard-cell chloroplasts provide ATP required for H^+ pumping in the plasma membrane and stomatal opening. Plant Cell Physiol. **42**: 795–802.

Truernit, E., Bauby, H., Dubreucq, B., Grandjean, O., Runions, J., Barthelemy, J., and Palauqui, J.C. (2008). High-resolution whole-mount imaging of three-dimensional tissue organization and gene expression enables the study of Phloem development and structure in Arabidopsis. Plant Cell **20**: 1494–1503.

Tsai, H.L., Lue, W.L., Lu, K.J., Hsieh, M.H., Wang, S.M., and Chen, J. (2009). Starch synthesis in Arabidopsis is achieved by spatial cotranscription of core starch metabolism genes. Plant Physiol. **151**: 1582–1595.

Tseng, T.-S. and Briggs, W.R. (2010). The Arabidopsis *rcn1-1* mutation impairs dephosphorylation of Phot2, resulting in enhanced blue light responses. Plant Cell **22**: 392–402.

Tseng, T.-S., Whippo, C., Hangarter, R.P., and Briggs, W.R. (2012). The Role of a 14-3-3 Protein in Stomatal Opening Mediated by PHOT2 in Arabidopsis. Plant Cell **24**: 1114–1126.

Tsutsumi, T., Takemiya, A., Harada, A., and Shimazaki, K.I. (2013). Disruption of ROOT PHOTOTROPISM2 gene does not affect phototropin-mediated stomatal opening. Plant Sci. **201-202**: 93–97.

Turck, F., Fornara, F., and Coupland, G. (2008). Regulation and identity of florigen: FLOWERING LOCUS T moves center stage. Annu. Rev. Plant Biol. **59**: 573–594.

Uehlein, N., Lovisolo, C., Siefritz, F., and Kaldenhoff, R. (2003). The tobacco aquaporin NtAQP1 is a membrane CO_2 pore with physiological functions. Nature **425**: 734–737.

Ueno, K., Kinoshita, T., Inoue, S.I., Emi, T., and Shimazaki, K.I. (2005). Biochemical characterization of plasma membrane H^+-ATPase activation in guard cell protoplasts of *Arabidopsis thaliana* in response to blue light. Plant Cell Physiol. **46**: 955–963.

Umezawa, T., Sugiyama, N., Mizoguchi, M., Hayashi, S., Myouga, F., Yamaguchi-Shinozaki, K., Ishihama, Y., Hirayama, T., and Shinozaki, K. (2009). Type 2C protein phosphatases directly regulate abscisic acid-activated protein kinases in Arabidopsis. Proc. Natl. Acad. Sci. U. S. A. **106**: 17588–17593.

Umezawa, T., Sugiyama, N., Takahashi, F., Anderson, J.C., Ishihama, Y., Peck, S.C., and Shinozaki, K. (2013). Genetics and phosphoproteomics reveal a protein phosphorylation network in the abscisic acid signaling pathway in *Arabidopsis thaliana*. Sci. Signal. **6**: rs8.

Vahisalu, T., Puzõrjova, I., Brosché, M., Valk, E., Lepiku, M., Moldau, H., Pechter, P., Wang, Y.-S., Lindgren, O., Salojärvi, J., Loog, M., Kangasjärvi, J., and Kollist, H. (2010). Ozone-triggered rapid stomatal response involves the production of reactive oxygen species, and is controlled by SLAC1 and OST1. Plant J. **62**: 442–453.

Vahisalu, T., Kollist, H., Wang, Y.-F., Nishimura, N., Chan, W.-Y., Valerio, G., Lamminmäki, A., Brosché, M., Moldau, H., Desikan, R., Schroeder, J.I., and Kangasjärvi, J. (2008). SLAC1 is required for plant guard cell S-type anion channel function in stomatal signalling. Nature **452**: 487–491.

Valerio, C., Costa, A., Marri, L., Issakidis-Bourguet, E., Pupillo, P., Trost, P., and Sparla, F. (2011). Thioredoxin-regulated β-amylase (BAM1) triggers diurnal starch degradation in guard cells, and in mesophyll cells under osmotic stress. J. Exp. Bot. **62**: 545–555.

Vatén, A. and Bergmann, D.C. (2013). Mechanisms of stomatal development: an evolutionary view. Evodevo **4**: 11.

Vaughn, K.C. and Outlaw, W.H. (1983). Cytochemical and cytofluorometric evidence for guard cell photosystems. Plant Physiol. **71**: 420–424.

Vavasseur, A. and Raghavendra, A.S. (2005). Guard cell metabolism and CO_2 sensing. New Phytol. **165**: 665–682.

Venema, K., Quintero, F.J., Pardo, J.M., and Donaire, J.P. (2002). The Arabidopsis Na^+/H^+ exchanger AtNHX1 catalyzes low affinity Na^+ and K^+ transport in reconstituted liposomes. J. Biol. Chem. **277**: 2413–2418.

Ventriglia, T., Kuhn, M.L., Ruiz, M.T., Ribeiro-Pedro, M., Valverde, F., Ballicora, M.A., Preiss, J., and Romero, J.M. (2008). Two Arabidopsis ADP-glucose pyrophosphorylase large subunits (APL1 and APL2) are catalytic. Plant Physiol. **148**: 65–76.

Vlad, F., Rubio, S., Rodrigues, A., Sirichandra, C., Belin, C., Robert, N., Leung, J., Rodriguez, P.L., Laurière, C., and Merlot, S. (2009). Protein phosphatases 2C regulate the activation of the Snf1-related kinase OST1 by abscisic acid in Arabidopsis. Plant Cell **21**: 3170–3184.

Voelker, C., Gomez-Porras, J.L., Becker, D., Hamamoto, S., Uozumi, N., Gambale, F., Mueller-Roeber, B., Czempinski, K., and Dreyer, I. (2010). Roles of tandem-pore K^+ channels in plants - a puzzle still to be solved. Plant Biol. **12**: 56–63.

Voelker, C., Schmidt, D., Mueller-Roeber, B., and Czempinski, K. (2006). Members of the

Arabidopsis AtTPK/KCO family form homomeric vacuolar channels in planta. Plant J. **48**: 296–306.

Walker, D.J., Leigh, R.A., and Miller, A.J. (1996). Potassium homeostasis in vacuolate plant cells. Proc. Natl. Acad. Sci. U. S. A. **93**: 10510–10514.

Wang, F.F., Lian, H.L., Kang, C.Y., and Yang, H.Q. (2010a). Phytochrome B is involved in mediating red light-induced stomatal opening in *Arabidopsis thaliana*. Mol. Plant **3**: 246–259.

Wang, H. and Wang, H. (2015). Phytochrome Signaling: Time to Tighten up the Loose Ends. Mol. Plant **8**: 540–551.

Wang, P., Xue, L., Batelli, G., Lee, S., Hou, Y.-J., Van Oosten, M.J., Zhang, H., Tao, W.A., and Zhu, J.-K. (2013a). Quantitative phosphoproteomics identifies SnRK2 protein kinase substrates and reveals the effectors of abscisic acid action. Proc. Natl. Acad. Sci. U. S. A. **110**: 11205–10.

Wang, X., Bian, Y., Cheng, K., Gu, L.-F., Ye, M., Zou, H., Sun, S.S.-M., and He, J.-X. (2013b). A large-scale protein phosphorylation analysis reveals novel phosphorylation motifs and phosphoregulatory networks in Arabidopsis. J. Proteomics **78**: 486–98.

Wang, X., Xue, L., Sun, J., and Zuo, J. (2010b). The Arabidopsis BE1 gene, encoding a putative glycoside hydrolase localized in plastids, plays crucial roles during embryogenesis and carbohydrate metabolism. J. Integr. Plant Biol. **52**: 273–288.

Wattebled, F., Dong, Y., Dumez, S., Delvallé, D., Planchot, V., Berbezy, P., Vyas, D., Colonna, P., Chatterjee, M., Ball, S., and D'Hulst, C. (2005). Mutants of Arabidopsis lacking a chloroplastic isoamylase accumulate phytoglycogen and an abnormal form of amylopectin. Plant Physiol. **138**: 184–195.

Way, D.A. and Pearcy, R.W. (2012). Sunflecks in trees and forests: From photosynthetic physiology to global change biology. Tree Physiol. **32**: 1066–1081.

Webb, A.A.R. (2003). The physiology of circadian rhythms in plants. New Phytol. **160**: 281–303.

Webster, M.T., Rozycka, M., Sara, E., Davis, E., Smalley, M., Young, N., Dale, T.C., and Wooster, R. (2000). Sequence variants of the Axin gene in breast, colon, and other cancers: An analysis of mutations that interfere with GSK3 binding. Genes Chromosom. Cancer **28**: 443–453.

Wheeler, M.C.G., Tronconi, M.A., Drincovich, M.F., Andreo, C.S., Flügge, U.-I., and Maurino, V.G. (2005). A comprehensive analysis of the NADP-malic enzyme gene family of Arabidopsis. Plant Physiol. **139**: 39–51.

Wiśniewski, J.R., Zougman, A., Nagaraj, N., and Mann, M. (2009). Universal sample preparation method for proteome analysis. Nat. Methods **6**: 359–362.

Wolf-Yadlin, A., Hautaniemi, S., Lauffenburger, D.A., and White, F.M. (2007). Multiple reaction monitoring for robust quantitative proteomic analysis of cellular signaling networks. Proc. Natl. Acad. Sci. U. S. A. **104**: 5860–5865.

World Bank (2008). World Development Report 2008: Agriculture for Development.

Würtele, M., Jelich-Ottmann, C., Wittinghofer, A., and Oecking, C. (2003). Structural view of a fungal toxin acting on a 14-3-3 regulatory complex. EMBO J. **22**: 987–94.

Xie, T., Ren, R., Zhang, Y.-Y., Pang, Y., Yan, C., Gong, X., He, Y., Li, W., Miao, D., Hao, Q., Deng, H., Wang, Z., Wu, J.-W., and Yan, N. (2012). Molecular Mechanism for Inhibition of a Critical Component in the *Arabidopsis thaliana* Abscisic Acid Signal Transduction Pathways, SnRK2.6, by Protein Phosphatase ABI1. J. Biol. Chem. **287**: 794–802.

Xue, L., Wang, P., Wang, L., Renzi, E., Radivojac, P., Tang, H., Arnold, R., Zhu, J.-K., and Tao, W.A. (2013). Quantitative measurement of phosphoproteome response to osmotic stress in Arabidopsis based on Library-Assisted eXtracted Ion Chromatogram

(LAXIC). Mol. Cell. Proteomics **53**: 1–39.

Xue, S., Hu, H., Ries, A., Merilo, E., Kollist, H., and Schroeder, J.I. (2011). Central functions of bicarbonate in S-type anion channel activation and OST1 protein kinase in CO_2 signal transduction in guard cell. EMBO J. **30**: 1645–1658.

Yaffe, M.B., Rittinger, K., Volinia, S., Caron, P.R., Aitken, A., Leffers, H., Gamblin, S.J., Smerdon, S.J., and Cantley, L.C. (1997). The Structural Basis for 14-3-3:Phosphopeptide Binding Specificity. Cell **91**: 961–971.

Yamaguchi, A., Kobayashi, Y., Goto, K., Abe, M., and Araki, T. (2005). TWIN SISTER of FT (TSF) acts as a floral pathway integrator redundantly with FT. Plant Cell Physiol. **46**: 1175–1189.

Yanagisawa, S. (2004). Dof Domain Proteins: Plant-Specific Transcription Factors Associated with Diverse Phenomena Unique to Plants. Plant Cell Physiol. **45**: 386–391.

Yang, Y., Costa, A., Leonhardt, N., Siegel, R.S., and Schroeder, J.I. (2008). Isolation of a strong Arabidopsis guard cell promoter and its potential as a research tool. Plant Methods **4**: 6.

Yang, Z., Guo, G., Zhang, M., Liu, C.Y., Hu, Q., Lam, H., Cheng, H., Xue, Y., Li, J., and Li, N. (2013). Stable isotope metabolic labeling-based quantitative phosphoproteomic analysis of Arabidopsis mutants reveals ethylene-regulated time-dependent phosphoproteins and putative substrates of constitutive triple response 1 kinase. Mol. Cell. Proteomics **12**: 3559–3582.

Ye, W., Adachi, Y., Munemasa, S., Nakamura, Y., Mori, I.C., and Murata, Y. (2015). Open Stomata 1 Kinase is Essential for Yeast Elicitor-Induced Stomatal Closure in Arabidopsis. Plant Cell Physiol. **56**: 1239–1248.

Yu, J.-W., Rubio, V., Lee, N.-Y., Bai, S., Lee, S.-Y., Kim, S.-S., Liu, L., Zhang, Y., Irigoyen, M.L., Sullivan, J.A., Zhang, Y., Lee, I., Xie, Q., Paek, N.-C., and Deng, X.W. (2008). COP1 and ELF3 control circadian function and photoperiodic flowering by regulating GI stability. Mol. Cell **32**: 617–630.

Yu, T.S., Zeeman, S.C., Thorneycroft, D., Fulton, D.C., Dunstan, H., Lue, W.L., Hegemann, B., Tung, S.Y., Umemoto, T., Chapple, A., Tsai, D.L., Wang, S.M., Smith, A.M., Chen, J., and Smith, S.M. (2005). α-Amylase is not required for breakdown of transitory starch in Arabidopsis leaves. J. Biol. Chem. **280**: 9773–9779.

Yu, T.S., Kofler, H., Häusler, R.E., Hille, D., Flügge, U.I., Zeeman, S.C., Smith, A.M., Kossmann, J., Lloyd, J., Ritte, G., Steup, M., Lue, W.L., Chen, J., and Weber, A. (2001). The Arabidopsis *sex1* mutant is defective in the R1 protein, a general regulator of starch degradation in plants, and not in the chloroplast hexose transporter. Plant Cell **13**: 1907–1918.

Yu, T.S., Lue, W.L., Wang, S.M., and Chen, J. (2000). Mutation of Arabidopsis plastid phosphoglucose isomerase affects leaf starch synthesis and floral initiation. Plant Physiol. **123**: 319–326.

Zeeman, S.C. and Ap Rees, T. (1999). Changes in carbohydrate metabolism and assimilate export in starch-excess mutants of Arabidopsis. Plant. Cell Environ. **22**: 1445–1453.

Zeeman, S.C., Northrop, F., Smith, A.M., and Rees, T. (1998). A starch-accumulating mutant of *Arabidopsis thaliana* deficient in a chloroplastic starch-hydrolysing enzyme. Plant J **15**: 357–365.

Zeeman, S.C., Thorneycroft, D., Schupp, N., Chapple, A., Weck, M., Dunstan, H., Haldimann, P., Bechtold, N., Smith, A.M., and Smith, S.M. (2004). Plastidial α-glucan phosphorylase is not required for starch degradation in Arabidopsis leaves but has a role in the tolerance of abiotic stress. Plant Physiol. **135**: 849–858.

Zeeman, S.C., Tiessen, A., Pilling, E., Kato, K.L., Donald, A.M., and Smith, A.M. (2002). Starch synthesis in Arabidopsis. Granule synthesis, composition, and structure. Plant Physiol. **129**: 516–529.

Zeiger, E., Assmann, S.M., and Meioner, H. (1983). The photobiology of Paphiopedilum stomata - opening under blue but not red light. Photochem. Photobiol. **38**: 627–630.

Zeiger, E. and Field, C. (1982). Photocontrol of the Functional Coupling between Photosynthesis and Stomatal Conductance in the Intact Leaf: Blue Light and Par-Dependent Photosystems in Guard Cells. Plant Physiol. **70**: 370–375.

Zemel, E. and Gepstein, S. (1985). Immunological Evidence for the Presence of Ribulose Bisphosphate Carboxylase in Guard Cell Chloroplasts. Plant Physiol. **78**: 586–590.

Zhang, H., Zhou, H., Berke, L., Heck, A.J.R., Mohammed, S., Scheres, B., and Menke, F.L.H. (2013). Quantitative Phosphoproteomics after Auxin-stimulated Lateral Root Induction Identifies an SNX1 Protein Phosphorylation Site Required for Growth. Mol. Cell. Proteomics **12**: 1158–1169.

Zhang, X., Szydlowski, N., Delvalle, D., D'Hulst, C., James, M.G., and Myers, A.M. (2008). Overlapping functions of the starch synthases SSII and SSIII in amylopectin biosynthesis in Arabidopsis. BMC Plant Biol **8**: 96.

Zhang, X., Wang, H., Takemiya, A., Song, C., Kinoshita, T., and Shimazaki, K. (2004). Inhibition of blue light-dependent H^+ pumping by abscisic acid through hydrogen peroxide-induced dephosphorylation of the plasma membrane H^+-ATPase in guard cell protoplasts. Plant Physiol. **136**: 4150–8.

Ziegler, P. (1999). Cereal β-amylases. J. Cereal Sci. **29**: 195–204.

ACKNOWLEDGEMENTS

First of all, I want to thank my supervisor Dr. Diana Santelia for the possibility to work on this exciting new topic and for her continuous support of my PhD work. Thank you for all the discussions and guidance throughout the last years.

Most of the scientific freedom we had over the last couple of years was due to the support we got from Prof. Enrico Martinoia. Thank you Enrico for always being approachable and supportive, for creating a nice working atmosphere and for chairing my thesis committee.
I have to thank the other members of my thesis committee, Prof. Sam Zeeman (ETH Zürich) and Prof. Beat Keller for their support of my PhD project through many interesting discussions and for all their suggestions, which significantly improved this work. Furthermore I want to thank Prof. Francesca Sparla (University of Bologna) for the discussions about BAM1 and for agreeing to evaluate my thesis.

Of course there were many more people who contributed important ideas, suggestions and critical discussions concerning our different projects. I want to thank especially Prof. Tracy Lawson (University of Essex) and Prof. Mike Blatt (University of Glasgow) for discussing guard cell science with starch people. Dr. Peter Gehrig (Functional Genomics Centre Zürich) for his introduction into the world of (phospho)proteomics and especially for his help with data analysis. Dr. Claudia Jonak and Dr. Julia Krasensky (Gregor Mendel Institute, Vienna) for their help with the BAM1 phosphorylation project and the great collaboration.

Of course this thesis would not have been possible without the tremendous help from colleagues, fellow students and friends. Foremost, I have to thank Sabrina Flütsch for her incredible commitment during her Master studies and for contributing what is perhaps the most interesting finding of this entire thesis. Furthermore, thank you for trying to improve my Swiss German, I'm not sure if it helped, but I will try to work on it!

The other members of our little starch group and of course everybody in the department made important contributions to the project, but it will be impossible to list everyone and everything they did over the last years in order to help me preparing this thesis. I hope all the important scientific contributions are listed above, but besides those, I was also lucky to meet amazing people during the last four years. Given the length of the thesis, I can only list a few and apologize to everybody else. I didn't forget you and I will always appreciate your help and friendships over the last years!

Some special thank you notes: I want to thank Rike for always being around to chat, to have a coffee with or a beer on occasion. Without you the last four years would have been much harder. Same goes for Arianna, thanks for being around, even when I got a bit grumpy in the lab sometimes. I hope there will be many more skiing days in the future! Matthias, thank you for being my personal Wikipedia, not only regarding my Chemistry questions, but also for explaining everything related to Swiss politics. Also thanks to Tiago for a detailed description of Swiss football, one of the few areas where Matthias was not much of a help. Last but not least in our little group: Thank you "lab" Diana for actually running and organizing the lab on top of doing all the qPCRs and the numerous other experiments! And we are sorry that we created such a mess while you were gone.

Without many “little helpers” it would not be possible to conduct any research in the Institute and therefore I want to thank the technical and IT staff, the gardeners and the administration. Honorable mentions go to Sascha Weinert for constantly trying to keep our growth chambers alive, to Daniel Bollier for his magic work with our lab equipment and to Kari Huwiler for keeping the pathogens in check.

Outside of our nice little garden I have to give a big thank you to the Plant Biochemistry group at ETH Zürich for accepting me into the starch family as kind of their weird cousin. Of course a big thank you to one of the nicest and kindest persons I have ever met. Yes, that would be you Dave. Obviously. Thank you for showing me most of the methods regarding starch, for always happily sharing your tremendous knowledge and just for being such a nice person to hang out with. And then of course I have to thank Mario Coiro for kick-starting the whole guard cell project through his suggestion of trying the PS-PI staining.

Zum Schluss will ich natürlich auch noch meiner ganzen Familie danken, allen voran meinen Eltern. Danke für die Unterstützung über die mittlerweile schon zahlreichen Jahre des Studiums! Vielleicht bekomme ich ja doch noch einen “richtigen” Job.

Ohne Judith wären die letzten Jahre so viel schwieriger gewesen. Danke für Alles!

CURRICULUM VITAE

HORRER, Daniel

born August 17th, 1986
German nationality

EDUCATION

1998 - 2006	Abitur, Hans Purrmann Gymnasium Speyer, Germany
2006 – 2012	**Studies in Biology**, Eberhard Karls Universität Tübingen, Germany Diploma degree awarded 01.03.2012 Diploma thesis at the Max Planck Institut for Developmental Biology under the supervision of Dr. Markus Schmid Title: "Role of Gibberellic acid in flowering time regulation in *Arabidopsis thaliana*"
since 04 / 2012	**PhD thesis**, Institute of Plant Biology, University of Zurich, Switzerland Dissertation under the supervision of Dr. Diana Santelia Title: "Starch metabolism in guard cells of *Arabidopsis thaliana*"

SCHOLARSHIPS

PhD Scholarship	awarded by the "Studienstiftung des deutschen Volkes" 2013 - 2015
Scholarship	awarded by the "Studienstiftung des deutschen Volkes" 2009 - 2012

PUBLICATIONS

Horrer, D., Flütsch, S, Pazmino, D., Matthews, J.S.A., Thalmann, M., Nigro, A., Leonhardt, N., Lawson, T., and Santelia, D. (2015)
Blue light induces a distinct starch degradation pathway in guard cells for stomatal opening. Current Biology, *accepted*.

Galvão, V.C., Collani, S., Horrer, D., and Schmid, M. (2015)
Gibberellic acid signaling is required for ambient temperature-mediated induction of flowering in *Arabidopsis thaliana*. Plant J.: doi: 10.1111/tpj.13051.

Galvão, V.C., Horrer, D., Küttner, F., and Schmid, M. (2012)
Spatial control of flowering by DELLA proteins in *Arabidopsis thaliana*. Development 139: 4072–4082.

Yu, S., Galvão, V.C., Zhang, Y.-C.C., Horrer, D., Zhang, T.-Q.Q., Hao, Y.-H.H., Feng, Y.-Q.Q., Wang, S., Schmid, M., and Wang, J.-W.W. (2012).
Gibberellin Regulates the Arabidopsis Floral Transition through miR156-Targeted SQUAMOSA PROMOTER BINDING-LIKE Transcription Factors. Plant Cell 24: 3320–3332.